TECTONICS OF THE WESTERN MEDITERRANEAN

Marc Helman

Wolfson College
University of Oxford

Trinity, 1989



Marc Helman
Wolfson College

Doctor of Philosophy
Trinity, 1989

TECTONICS OF THE WESTERN MEDITERRANEAN

ABSTRACT

The evolution of the Western Mediterranean takes place between the converging African and Eurasian plates, therefore the motion between them cannot be determined directly. The motion between them is the finite difference between the independent seafloor spreading systems in the Central and North Atlantic Oceans.

Primary magnetic anomaly data from the North and Central Atlantic was reexamined. All Late Cretaceous and Cenozoic anomalies (Anomaly 34 - Anomaly 2) were remapped. Fracture zones were remapped using bathymetic maps, topographic profiles from ship tracks, SEASAT altimetry (geoid deflection) data, and SEASAT derived gravity images. Fracture zones were used as the primary control for the determination of rotation parameters.

Finite difference solutions were computed between matched anomalies using the newly determined rotation parameters for each ocean with parameters of Pindell et al. (1988) used for Early Cretaceous and Jurassic spreading in the Central Atlantic. The product was a kinematic model describing the motion of Africa with respect to Europe from 175 Ma to the present.

The motion of Africa was seen to be much smoother and not marked by the sharp, unusual direction changes that characterized previous work. On a gross scale the motion could be divided into phases that correlated with major geological events, but on a smaller scale it was clear that relative motion between Africa and Eurasia did little more than set very broad boundary conditions within which a variety of geological events occurred.

Africa's motion is divisible into several distince phases. From the Jurassic start of seafloor spreading until the Late Cretaceous Quiet Zone (KQZ) the motion between the plates was sinistral strike-slip. During the KQZ, but prior to Anomaly 34 (84 Ma, Campanian) Africa's motion changed to northeasterly directed compression. Shortly after Anomaly 30 (68 Ma), close to the Cretaceous-Tertiary boundary, until after Anomaly 24 (55 Ma, mid-Eocene) there was a period of little relative motion between the two plates.

After Anomaly 24 strong relative motion recommenced between Africa and Eurasia. Africa continued on a trajectory between N and NNE until the Middle Miocene (Anomalies 5A - 5D) when motion became directed to the NW.

Within the relative motion framework a model for the geological evolution of the Western Mediterranean Sea is evolved. Although the Western Mediterranean is a Neogene phenomena the history of the region prior to this time is also examined, albeit in less detail. Among the major problems for which solutions are suggested is the convergence direction of Iberia with respect to Europe and the reason extension initiated in the Tyrrhenian Sea.

LONG ABSTRACT

The evolution of the Neogene Western Mediterranean Sea takes place between the converging African and Eurasian plates. The motion between them cannot be determined directly because the magnetic anomalies and fractures which hold that data have been subducted. The motion between these plates is determined by computing the finite difference between the independent seafloor spreading systems in the Central and North Atlantic Oceans.

Magnetic anomalies from the North and Central Atlantic were reexamined using data supplied by the Lamont-Doherty Geological Observatory of Columbia University, New York. The data includes all magnetic data collected by Lamont-Doherty's research vessels, R.V. Vema and R.V. Conrad, and data collected by other research vessels or aeromagnetic survey that is available to Lamont-Doherty by contract with the National Geophysical Data Center in Boulder, Colorado. All Late Cretaceous and Cenozoic anomalies (Anomaly 34 - Anomaly 2) were reexamined, reprocessed to remove the ambient field when necessary, and remapped. The work was done independently of previous mapping so that the results could be compared independently and also to ensure that the work would be internally consistent.

Fracture zones were remapped using bathymetic maps of various, topographic profiles from ship tracks, gravity data collected on research cruises, and SEASAT altimetry data, specifically deflection from the geoid data, as well as SEASAT-derived gravity

images. Fracture zones were used as a primary control during the determination of rotation parameters and comparison of the kinematic model with to older models.

This was the first work to incorporate use of all anomalies and not just anomalies that are easily identifiable or thought to correspond to tectonic events, changes in spreading rate, or changes in spreading direction. A procedure was defined to determine the rotation parameters of "non-standard" anomalies that involved testing "standard" anomaly rotation parameters, determining the set that worked best, and using this as a basis for determining rotation parameters for non-standard anomalies. Final testing involved comparing synthetic fracture zone traces to real fracture zones to determine if the rotation parameters were acceptable.

The Charlie-Gibbs Fracture Zone is the only major, well-defined fracture zone in the North Atlantic Ocean, i.e., north of the Azores-Gibraltar Fracture Zone. It is, therefore, the only feature that holds a complete record of seafloor spreading in this ocean. Special importance was placed upon its role in determining rotation parameters. The question of whether or not long offset, slow-spreading transform faults accurately show past seafloor spreading directions is examined. Spreading rate is suggested as the critical variable in resolving this question. Both the North and Central Atlantic spread slowly and have narrow principal deformation zones. Spreading faster than a critical velocity (suggested to be > 4 cm/yr) would enlarge the principal

transform deformation zone. The narrow deformation zone is critical to preserving data on spreading direction.

The rotation parameters for both parts of the Atlantic were compared to other models using the technique of generating synthetic fracture zones and comparing them to fracture zones. Using all available anomalies is shown to produce a much better fit than models that use only a few anomalies. This is particularly true of the North Atlantic because the very slow spreading rate and complex physiography make identification of anomalies difficult.

An important result of this study was to suggest that changes in the pole of rotation do not always occur at the times that have been previously suggested. This suggests that matching anomalies may not be the best way to define the spreading history of oceans. A suggestion for future kinematic studies based on detailed analysis of structural features in fracture zones and transform faults is presented.

The Central Atlantic is simpler to analyze, largely because of the presence of several well defined, large offset fracture zones and a somewhat faster spreading rate. The spreading rate is not sufficiently fast to exceed the critical spreading velocity that would render the fracture zones unsuitable for analyzing seafloor spreading directions. Because of the greater simplicity of the Central Atlantic many of the rotation parameters for standard anomalies are the same as, or differ only slightly from, those in the most recent study. However, use of all anomalies is shown to

produce a better fit to fracture zone traces.

Changes in Central Atlantic poles of rotation were found to occur at other than the standard anomalies, as was also the case in the North Atlantic. Comparison of the timing of pole changes with a recently published curve of coastal onlap showed that these pole changes commonly occurred 1 - 3 million years prior to stratigraphic sequence boundaries. This is the amount of time necessary for in-plane stresses to build up prior to their propagation. The correlation indicates that some relative sea level changes may be due to varying in-plane stress produced by changes in plate boundary configuration and indicated by changing poles of rotation. An example from the North Sea is presented to show this relationship.

Finite difference solutions were computed between matched anomalies using the newly determined rotation parameters in each ocean. The parameters of Pindell et al. (1988) were used for Early Cretaceous and Jurassic spreading in the Central Atlantic. The product was a kinematic model describing the motion of Africa with respect to Europe from 175 Ma to the present.

The motion of Africa was seen to be much smoother and not marked by the sharp, unusual direction changes that characterized previous work. The major older models of Africa-Europe relative motion were compared to this work and a general trend towards a smoother path was noted in each work. On a gross scale the motion could be divided into phases that correlated with major geological events, but on a smaller scale it was clear that

relative motion between Africa and Eurasia did little more than set very broad boundary conditions within which a variety of geological events occurred.

From the Jurassic start of seafloor spreading until the Late Cretaceous Quiet Zone (KQZ) the motion between the plates was sinistral strike-slip. This correlates with the formation of the Neo-Tethyan Ocean and the development of passive margins in southern Europe and North Africa. During the KQZ Africa's motion changed to one of northeasterly directed compression. The exact time of this change cannot be determined because of the lack of large scale magnetic reversals in the KQZ. The change generally coincides with the initiation of seafloor spreading north of the modern Azores-Gibraltar Fracture Zone, which was accompanied by the rotation of Iberia away from the Amorican margin of France to open the Bay of Biscay. Suggested times for the change in Africa's motion are investigated, but none of the proposed models offers an unambiguous solution. Spreading stopped in Biscay just after Anomaly 34 (84 Ma, Campanian).

After Anomaly 30 (67 Ma), close to the time of the Cretaceous-Tertiary boundary, until after Anomaly 24 (mid-Eocene) there was a period of relatively little motion between the two plates. This correlates with reorganizations of seafloor spreading in the North Atlantic that are denoted by changes in the orientation of the Charlie-Gibbs Fracture Zone. It also correlates with a period in Alpine history known as the Paleocene Restoration, a time in which there was little orogenic activity.

After Anomaly 24 (55 Ma, Middle Eocene), when spreading began in the Norwegian-Greenland Sea, strong relative motion between Africa and Eurasia recommenced. Africa moved on a trajectory that varied between N and NNE until Middle Miocene time (Anomalies 5D - 5A) when the motion became directed to the NW. This change is viewed as the reason for the initiation of back-arc extension in the Tyrrhenian Sea. This change brought the downgoing slab into parallelism with the motion vector. Changes of this type have been shown to initiate back-arc spreading in regions behind Pacific island arcs.

The framework provided by this new kinematic model was used to derive a new model for the evolution of the Western Mediterranean Sea. Although the Western Mediterranean is a Neogene phenomena the history of the region prior to this time is also examined, albeit in less detail. A major feature of the evolution of the region is that, for most the Neogene Western Mediterranean tectonic events were not directly controlled by the interaction of Africa and Europe. Vector triangles that were plotted on reconstructions show that only in post-Anomaly 5 time did the major blocks and Africa have the same motion vector. Prior to this time many blocks and microcontinents in the region moved to the ESE and SE as Africa moved to the N and NNE.

In a similar vein it is noted that kinematic indicators from the Alpine arc do not reflect the pattern of Africa's motion. The implication of this is that Adria ceased to be a promontory of Africa at some time in the Cretaceous.

TABLE OF CONTENTS

ABSTRACT Page i
LONG ABSTRACT Page ii
TABLE OF CONTENTS Page viii
LIST OF FIGURES Page xii
LIST OF TABLES Page xv
ACKNOWLEDGMENTS Page xvi

CHAPTER 1 INTRODUCTION
1.1 Previous Work in Kinematic Modeling Page 1-2
1.2 Poles of Rotation Page 1-6
1.3 Organization of This Work Page 1-8

CHAPTER 2 KINEMATIC MODEL FOR THE OPENING OF THE NORTH ATLANTIC OCEAN
2.1 Introduction Page 2-1
2.2 Sources of Data Page 2-3
2.2.1 Magnetic Anomaly Data Page 2-3
2.2.2 Fracture Zone Data Page 2-4
2.3 Methodology Page 2-4
2.3.1 Anomaly Characteristics Page 2-5
2.3.1a Anomalies 2 - 4A Page 2-5
2.3.1b Anomalies 5 - 6C Page 2-6
2.3.1c Anomalies 7 - 19 Page 2-7
2.3.1d Anomalies 20 - 29 Page 2-8
2.3.1e Anomalies 30 - 34 Page 2-9
2.3.2 Determination of Rotation Parameters Page 2-9
2.4 Major Features of the North Atlantic Ocean Page 2-12
2.4.1 Fracture Zones Page 2-12
2.4.1a The Charlie-Gibbs Fracture Zone Page 2-12
2.4.1b The Azores-Gibraltar Plate Boundary Page 2-13
2.4.1c Other Fracture Zones Page 2-15
2.4.2 Mid-Plate Swells and Anomalous Deeps Page 2-16
2.4.2a The East and West Thulean Rises Page 2-16
2.4.2b The Azores-Biscay Rise Page 2-17
2.4.2c The King's Trough Page 2-18
2.4.2d The Madiera-Tore Rise Page 2-20
2.4.3 Seamounts Page 2-21
2.4.3a The Charcot Seamounts Page 2-21
2.4.3b The Newfoundland Seamounts Page 2-21
2.4.3c The Horseshoe Seamounts Page 2-22
2.4.4 Continental Fragments (Microcontinents) Page 2-22
2.4.4a The Eastern North Atlantic Page 2-22
2.4.4b The Western North Atlantic Page 2-23
2.5 Kinematic Model Page 2-24
2.5.1 Rotation Parameters Page 2-24
2.5.2 Flow Lines Page 2-25
2.5.3 Comparison With Other Models Page 2-29
2.5.3a Pitman and Talwani's Model (1972) Page 2-31
2.5.3b Philips and Forsyth's Model (1972) Page 2-32
2.5.3c Sclater,Hellinger and Tapscott's Model

(1977) Page 2-33
2.5.3d Savostin's Model (1981) Page 2-33
2.5.3e Olivet, Bonnin, Beuzart, and Auzende's Model (1984) Page 2-34
2.5.3f Livermore and Smith's Model (1985) Page 2-34
2.5.3g Bott's Model (1985) Page 2-35
2.5.3h Savostin, Sibuet, Zonenshain, LePichon, and Roulet's Model (1986) Page 2-35
2.5.3i Srivastava and Tapscott's Model (1986) Page 2-36
2.5.3j Discussion Page 2-39
2.6 Discussion of the Kinematic Model Page 2-40

CHAPTER 3 KINEMATIC MODEL FOR THE OPENING OF THE CENTRAL ATLANTIC OCEAN
3.1 Introduction Page 3-1
3.2 Major Features of the Central Atlantic Ocean Page 3-2
3.2.1 Fracture Zones Page 3-2
3.2.2 Mid-Plate Swells and Anomalous Deeps Page 3-2
3.2.2a The Madiera-Tore Rise Page 3-2
3.2.2b The Bermuda Rise Page 3-3
3.2.3 Seamounts Page 3-4
3.2.3a The New England Seamounts Page 3-4
3.2.3b The Corner Ridge Seamounts Page 3-4
3.2.3c Eastern Central Atlantic Seamounts Page 3-6
3.2.4 Continental Fragments (Microcontinents) Page 3-7
3.2.4a The Blake Plateau Page 3-8
3.2.4b The Bahama Platform Page 3-8
3.2.4c The Mazagan Plateau Page 3-9
3.2.5 Other Features Page 3-9
3.2.5a The Canary and Cape Verde Islands Page 3-10
3.2.5b Asymmetry of the Central Atlantic Page 3-10
3.3 Kinematic Model Page 3-11
3.3.1 Rotation Parameters Page 3-11
3.3.2 Flow Lines Page 3-12
3.3.3 Comparison With Other Models Page 3-12
3.3.3a Pitman and Talwani's Model (1972) Page 3-13
3.3.3b Philips and Forsyth's Model (1972) Page 3-13
3.3.3c Sclater,Hellinger and Tapscott's Model (1977) Page 3-14
3.3.3d Olivet, Bonnin, Beuzart, and Auzende's Model (1984) Page 3-14
3.3.3e Savostin, Sibuet, Zonenshain, LePichon, and Roulet's Model (1986) Page 3-15
3.3.3f Klitgord and Schouten's Model (1986) Page 3-15
3.3.3g Pindell, Cande, Pitman, Rowley, Dewey, LaBreque, and Haxby's Model (1988) Page 3-15
3.3.3h Discussion Page 3-16
3.4 Discussion of the Kinematic Model Page 3-16

CHAPTER 4 THE MOTION OF AFRICA RELATIVE TO EUROPE
4.1 Introduction Page 4-1

4.2 Finite Difference Solutions Page 4-1
4.3 Kinematic Model Page 4-4
4.3.1 Rotation Parameters Page 4-4
4.3.2 Presentation of Africa's Motion Page 4-4
4.3.3 Africa's Motion Page 4-5
4.3.4 Comparison with Other Models Page 4-9
4.3.4a Dewey, Pitman, Ryan, and Bonnin's Model (1973) Page 4-11
4.3.4b Biju-Duval, Dercourt, and LePichon's Model (1977) Page 4-12
4.3.4c Olivet, Bonnin, Beuzart, and Auzende's Model (1984) Page 4-12
4.3.4d Livermore and Smith's Model (1985) Page 4-13
4.3.4e Savostin, Sibuet, Zonenshain, Le Pichon, and Roulet's Model (1986) Page 4-14
4.3.4f Sclater, Hellinger, and Tapscott's Model (1977) Page 4-15
4.3.4g DNAG Model (1986) Page 4-15
4.3.4h Discussion Page 4-17
4.4 Discussion of the Kinematic Model Page 4-19

CHAPTER 5 REGIONAL GEOLOGY
5.1 Introduction Page 5-1
5.2 Mountain Ranges and Associated Basins Page 5-1
5.2.1 Betic Cordillera and Guadilquivir Basin Page 5-2
5.2.2 Rif, Tell, and Associated Basins Page 5-5
5.2.3 Apennines, Po Basin, and Apenninic Foredeep Page 5-12
5.2.4 Southern Alps and Po Basin Page 5-16
5.2.5 Alps and Molasse Basin Page 5-18
5.2.6 Pyrennes, Ebro Basin, and Aquitaine Basin Page 5-21
5.2.7 Atlas Chain (North Africa) Page 5-25
5.3 Western Mediterranean Sea Page 5-27
5.3.1 Alboran Sea Page 5-27
5.3.2 Gulf of Valencia Page 5-32
5.3.3 Western Mediterranean Sea Page 5-34
5.3.4 Tyrrhenian Sea Page 5-36

CHAPTER 6 GEOLOGICAL MODEL OF WESTERN MEDITERRANEAN EVOLUTION
6.1 Introduction Page 6-1
6.2 Pre-Seafloor Spreading (Late Permian-Early Jurassic) Page 6-1
6.3 Start of Seafloor Spreading (Early and Middle Jurassic) Page 6-2
6.3.1 Early Jurassic Reconstruction Page 6-4
6.3.1a Rockall Trough Page 6-4
6.3.1b Labrador Sea Page 6-5
6.3.1c Bay of Biscay and Rotation of Iberia Page 6-6
6.3.1d Other Aspects of the Reconstruction Page 6-7
6.4 Seafloor Spreading and Adria's Detachment (Oxfordian-Albian) Page 6-7

6.5 Early Alpine Orogenesis (Late Cretaceous) Page 6-10
6.6 Meso-Alpine Orogenesis (Paleocene-Eocene) Page 6-11
6.6.1 Polarity of subduction Page 6-15
6.7 Evolution of the Western Mediterranean (Oligocene-Present) Page 6-18
6.7.1 Latest Eocene-Priabonian 38 Ma Page 6-18
6.7.2 Earliest Miocene-Aquitanian 23 Ma Page 6-21
6.7.3 Early Miocene-Burdigalian 18 Ma Page 6-25
6.7.4 Late Miocene-Tortonian 9 Ma Page 6-26
6.7.4a Extension in the Tyrrhenian Sea Page 6-28
6.7.5 Late Miocene-Tortonian 7 Ma Page 6-29
6.7.6 Earliest Pliocene-Zanclean 5 Ma Page 6-30
6.7.7 Late Pliocene-Piacenzian 3 Ma Page 6-31
6.7.8 Piacenzian to Holocene 3 Ma to Present Page 6-32

CHAPTER 7 DISCUSSION AND CONCLUSIONS Page 7-1

CHAPTER 8 REFERENCES Page 8-1

APPENDIX A List of Shiptracks and Aeromagnetic Surveys Used in This Study Page A-1

APPENDIX B Listings of Computer Programs Used in This Study
Rotations.For (computes rotations) Page B1-1
Rofn3.For (computes finite difference) Page B2-1
Plots.For (plots maps) Page B3-1
Stagepoles.For (computes stagepoles) Page B4-1
Synfzplot.For (generates synthetic fracture zone) Page B5-1
Rate.For (computes spreading rate) Page B6-1
Plotrate.For (plots spreading rate) Page B7-1
Incdec.For (computes inclination and declination of magnetic field) Page B8-1
Model2.For (models magnetic anomalies) Page B9-1

APPENDIX C Timescale Used for Magnetic Anomalies Page C-1

LIST OF FIGURES

		following
CHAPTER 1		
Figure 1.1	Finite and Stage Poles of Rotation	Page 1-7
CHAPTER 2		
Figure 2.1	Magnetic Anomaly Profile Models	Page 2-5
Figure 2.2	SEASAT Deflection From the Geoid Data for the North Atlantic	Page 2-11
Figure 2.3	Simplified Tectonic Element Map of the North Atlantic	Page 2-12
Figure 2.4	Kinematic Model Synthetic Fracture Zone	Page 2-25
Figure 2.5	Synthetic Fracture Zone Model (Pitman and Talwani, 1972)	Page 2-31
Figure 2.6	Synthetic Fracture Zone Model (Philips and Forsyth, 1972)	Page 2-32
Figure 2.7	Synthetic Fracture Zone Model (Sclater et al., 1977)	Page 2-33
Figure 2.8	Synthetic Fracture Zone Model (Savostin, 1981)	Page 2-33
Figure 2.9	Synthetic Fracture Zone Model (Olivet et al., 1984)	Page 2-34
Figure 2.10	Synthetic Fracture Zone Model (Livermore and Smith, 1985)	Page 2-34
Figure 2.11	Synthetic Fracture Zone Model (Bott, 1985)	Page 2-35
Figure 2.12	Synthetic Fracture Zone Model (Savostin et al., 1986)	Page 2-35
Figure 2.13	Synthetic Fracture Zone Model (Srivastava and Tapscott, 1986)	Page 2-36
Figure 2.14	Boundaries of the Porcupine Plate	Page 2-37
Figure 2.15	Changes in Pole of Finite Rotation: North Atlantic Ocean	Page 2-41
Figure 2.16	Variation in Spreading Rate in a Small Region of the Northeast Atlantic	Page 2-41
CHAPTER 3		
Figure 3.1	Simplified Tectonic Element Map of the Central Atlantic	Page 3-1
Figure 3.2	SEASAT Deflection From the Geoid Data for the Central Atlantic	Page 3-1
Figure 3.3	Kinematic Model Synthetic Fracture Zone	Page 3-12
Figure 3.4	Synthetic Fracture Zone Model (Pitman and Talwani, 1972)	Page 3-13
Figure 3.5	Synthetic Fracture Zone Model (Philips and Forsyth, 1972)	Page 3-13
Figure 3.6	Synthetic Fracture Zone Model (Sclater et al., 1977)	Page 3-14
Figure 3.7	Synthetic Fracture Zone Model (Olivet et al., 1984)	Page 3-14
Figure 3.8	Synthetic Fracture Zone Model (Savostin	

et al., 1984) Page 3-14
Figure 3.8 Synthetic Fracture Zone Model (Savostin et al., 1986) Page 3-15
Figure 3.9 Synthetic Fracture Zone Model (Klitgord and Schouten, 1986) Page 3-15
Figure 3.10 Synthetic Fracture Zone Model (Pindell et al., 1988) Page 3-16
Figure 3.11 Changes in Pole of Finite Rotation: Central Atlantic Ocean Page 3-18

Chapter 4 RELATIVE MOTION OF AFRICA WITH RESPECT TO EUROPE
Figure 4.1 Euler Construction Page 4-2
Figure 4.2 Finite Difference Solution: Africa's Motion With Respect to Europe Page 4-3
Figure 4.3 Kinematic Model: Reconstructed Positions of Africa Page 4-5
Figure 4.4 Kinematic Model: Africa's Path of Relative Motion Page 4-5
Figure 4.5 Cretaceous Quiet Zone Reconstructions Page 4-6
Figure 4.6 Dewey et al. (1973): Africa-Europe Reconstructions Page 4-11
Figure 4.7 Biju-Duval et al. (1977): Africa-Europe Reconstructions Page 4-12
Figure 4.8 Olivet et al. (1984): Africa-Europe Reconstructions Page 4-12
Figure 4.9 Livermore and Smith (1985): Africa-Europe Reconstructions Page 4-13
Figure 4.10 Savostin et al. (1986): Africa-Europe Reconstructions Page 4-14
Figure 4.11 Atlantic Spreading Rates: Recent Models Page 4-14
Figure 4.12 Sclater et al. (1977): Africa-Europe Reconstructions Page 4-15
Figure 4.13 Decade of North American Geology (DNAG) (1986): Africa-Europe Reconstructions Page 4-16

Chapter 5 REGIONAL GEOLOGY
Figure 5.1 Tectonic Sketch Map: Western Mediterranean Sea and Surrounding Region Page 5-1
Figure 5.2 DSDP and ODP Drilling Sites: Locations and Stratigraphy Page 5-27
Figure 5.3 Simplified Bathymetric Map of the Western Mediterranean Sea Page 5-28

Chapter 6 GEOLOGICAL MODEL OF WESTERN MEDITERRANEAN EVOLUTION
Figure 6.1 Early Jurassic Atlantic Reconstruction Page 6-4
Figure 6.2 Latest Eocene - Priabonian (38 Ma) Reconstruction Page 6-18
Figure 6.3 Earliest Miocene - Aquitanian (23 Ma) Reconstruction Page 6-20
Figure 6.4 Early Miocene - Burdigalian (18 Ma) Reconstruction Page 6-23
Figure 6.5 Late Miocene - Tortonian (9 Ma)

Reconstruction Page 6-26
Figure 6.6 Africa's Path of Relative Motion South of the Tyrrhenian Sea (Late Cenozoic) Page 6-28
Figure 6.7 Late Miocene - Tortonian (7 Ma) Reconstruction Page 6-29
Figure 6.8 Earliest Pliocene - Zanclean (5 Ma) Reconstruction Page 6-30
Figure 6.9 Late Pliocene - Piacenzian (3 Ma) Reconstruction Page 6-31
Figure 6.10 Piacenzian to Holocene (3 Ma to the Present) Reconstruction Page 6-32

Chapter 7 DISCUSSION AND CONCLUSIONS
Figure 7.1 Relationship Between Kinematics and Structure Page 7-3

LIST OF TABLES

	following
Chapter 1	
Table 1.1 Comparison of Geochronologic Timescales for Selected Marine Magnetic Anomalies	Page 1-5
Chapter 2	
Table 2.1 Distribution of Magnetic Anomaly Profiles by Latitude	Page 2-3
Table 2.2 Published Finite Pole Rotation Parameters for the North Atlantic	Page 2-10
Table 2.3 Finite Pole Rotation Parameters for the North Atlantic: Europe-North America Separation	Page 2-25
Table 2.4 Stage Pole Rotation Parameters for the North Atlantic	Page 2-25
Table 2.5 Comparison of Kinematic Models: North and Central Atlantic Oceans	Page 2-30
Chapter 3	
Table 3.1 Published Finite Pole Rotation Parameters for the Central Atlantic	Page 3-11
Table 3.2 Finite Pole Rotation Parameters for the Central Atlantic: Africa-North America Separation	Page 3-12
Table 3.3 Stage Pole Rotation Parameters for the Central Atlantic	Page 3-12
Table 3.4 M-Series Finite Pole Rotation Parameters for the Central Atlantic	Page 3-12
Table 3.5 M-Series Stage Pole Rotation Parameters for the Central Atlantic	Page 3-12
Chapter 4	
Table 4.1 Finite Pole Rotation Parameters for the Motion of Africa With Respect to Europe	Page 4-4
Table 4.2 Published Finite Pole Rotation Parameters for the Motion of Africa With Respect to Europe	Page 4-4
Table 4.3 Interpolated Rotation Parameters for Africa's Motion During the Cretaceous Quiet Zone	Page 4-6
Table 4.4 Finite Pole Rotation Parameters for the Motion of Africa With Respect to Europe (Sclater, Hellinger, and Tapscott, 1977)	Page 4-15
Table 4.5 Finite Pole Rotation Parameters for the Motion of Africa With Respect to Europe and the Porcupine Plate (Klitgord and Schouten, 1986; Srivastava and Tapscott, 1986)	Page 4-16
Chapter 5	
Table 5.1 Tectonic Units of the Apennines	Page 5-12
Chapter 6	
Table 6.1 Finite Pole Rotation Parameters for the Motion of Iberia With Respect to Europe	Page 6-7

ACKNOWLEDGEMENTS

Writing acknowledgements may be at once the most enjoyable and the most distressing part of writing a thesis. They are usually the last thing, hence it feels good to be doing it. They also evoke memories, both good and bad, of the preceeding few years that stream by in rapid succession, leaving the author dazed and wondering how it all came to pass. But because most of the good memories involve the people you've met along the way writing acknowledgements becomes rather enjoyable.

I'd like to start by thanking my advisor, Professor John F. Dewey, for his encouragement and support. John threw me into the sea of Mediterranean tectonics but was always there to pull me up just when I felt like I was going down for the third time. Among other things, John provided grammar a lesson that focused on the proper use of that and which, which I will never forget. John and his wife, Molly, were gracious hosts at many meals and, occasionally, provided a place to sleep.

Aside from your advisor perhaps the most important people you deal with while working on a thesis are fellow students. At the University of Durham, where this all started, I shared an office with two exceptional people, Jim Pindell and Kevin Brown (both students of John Dewey). They made me feel welcome when I first arrived without warning from New York, helped get me acquainted with the university and the rest of the department, and, perhaps most importantly, introduced me to Exhibition and Castle Eden (two of the finest beers I've ever enjoyed). Jim also assisted me greatly when I was working on the Atlantic magnetic anomaly data at Lamont-Doherty by introducing me to the computer system and showing me how to pick magnetic anomalies.

At Oxford, I was also fortunate enough to share an office with two other John Dewey students, Webster Mohriak and Paul Dailly, who also transferred from Durham. I've always wondered if Paul found my New York accent as hard to understand as I did his Scottish accent. Webster was especially kind in helping me to write or alter some of the computer programs I used.

Fellow students at Oxford really kept me going. Sriyanee De Silva introduced me to various restaurants and to "Croissante Amande", Joe Cartwright introduced me to things I can't mention in print, and Steve Knott and Simon Wallis were constant aids in helping to understand what I was doing. Clive, Mike, Angela, Chris, Peter W., Peter C., Hugh, Bails, Mark B., Mark W., Dave, Rhoda, Ros, Beth, and many others made Oxford most enjoyable. Dr. C. Ashley Price (sometimes known as "Stormin' Norman"), John Dewey's post-doc, was like a fellow student. Perhaps it was the common Durham heritage that we shared. Ashley was always there when a problem arose or when a drinking companion was needed. It is utterly impossible for me to express in words just how much these people mean to me. I only hope that they know.

Faculty and staff at both Durham and Oxford were exceptionally kind to me. At Durham, Drs. Donny Hutton, Rob Butler, and Garry

Karner spent incredible amounts of time discussing various aspects of geology and geophysics with me, thus giving me needed background from which to progress. Garry and his wife, Lois, also provided a needed refuge, complete with games of Trivial Pursuit, on many occasions. At Oxford, Drs. Phil Allen, Keith Cox, Phil England, Simon Harley, Stuart McKerrow, John Platt, Harold Reading, and Paul Taylor always seemed to have the time to discuss something that was confusing or interesting.

Part of my time was spent at the Lamont-Doherty Geological Observatory of Columbia University in Palisades, New York working on magnetic anomalies in the Atlantic. Drs. Steve Cande and Walter Pitman made the original suggestion to use all of the magnetic anomalies in the Atlantic and not just the standard anomalies. They graciously provided computer time, assistance, advice, and encouragement. Dr. Kim Kastens showed me the cores drilled on ODP Leg 107 in the Tyrrhenian Sea shortly after they arrived at core storage facility at Lamont-Doherty. She also discussed many aspects of Mediterranean geology with me. Dr. Charlotte Schreiber, of Queens College (C.U.N.Y.) and Lamont-Doherty, encouraged me to do a D. Phil., introduced me to the wonderful world of evaporites, and introduced me to John Dewey. She is largely the reason I undertook a project centered on the Mediterranean Sea.

Staff at both Durham and Oxford were always helpful. In particular, Sally Thompson, Professor Dewey's overworked and underpaid secretary, always seemed to help me get things that I needed. Similarly, the guys in the shop, Derek Prescott and Don Trafford were very helpful in supplying tools for fixing up my office. Claire Carlton and Julia York, drafting technicians, were very helpful showing me how to improve my drafting (not that it could have gotten worse) and Richard McAvoy always seemed to be able to produce slides or photos on short notice if I needed them.

In addition to people connected with institutions involved there are many others, not directly involved, who should be thanked. Jayne Worthington was a great friend in New York and a needed familiar face when I first came to Britain. John and Jean Cooper made me feel at home in their house my first year in Durham. Glenn, Wayne, and Maria were ideal roommates at Wolfson College. Our area was probably the most international in the college with four countries (America, Australia, New Zealand, Portugal). Finally, back in the U.S. my mom and dad provided a constant supply of letters to keep me informed on family matters and to let me know that I wasn't forgotten.

Finally, because in the end everything costs, I acknowledge the Committee of Vice-Chancellors and Principals of the Universities of the United Kingdom who provided partial tuition assistance through an Overseas Research Student Award. I also thank the Burdette-Coutts Fund, Department of Earth Sciences, for financial aid. Funds to present results of this work at conferences were provided by the Edward P. Abraham Ceppalosporin Fund, the Committee on Graduate Studies, and Wolfson College.

CHAPTER 1

INTRODUCTION

The Western Mediterranean is one of the most studied and, at the same time, one of the least understood regions in the world. It was only within the last 20 years, as a consequence of widespread acceptance of the plate tectonic model, that the general outlines of tectonic evolution in this region were agreed upon. The details of this evolution are, however, far from agreed upon. Indeed it is the uncertainty of these details that makes the region such an interesting area of study.

Many of the concepts of plate tectonics do not seem to be immediately applicable to the present-day Western Mediterranean. The structures (spreading ridges, subduction zones, transform faults) commonly used to define plate boundaries are not obvious, yet this region contains a major plate boundary. Seismicity and deformation are diffuse, occurring over a large area rather than being concentrated in the narrow zones which define most plate margins.

Despite this, it is the application of plate tectonic concepts that allows the kinematic and geologic evolution of this region to be unraveled. Plate tectonics follows rigid geometric constraints (see Cox, 1973; Cox and Hart, 1987; LePichon et al., 1973; Bird, 1980 for relevant papers and discussion). By working within these constraints the kinematic evolution of an area can

be studied. Plate kinematics provide the basis from which testable geological hypotheses can formulated, i.e. they provide the framework within which geological data must be explained.

1.1 Previous Work in Kinematic Modeling

Kinematic models of Alpine-Mediterranean tectonics are based largely upon age calibrated magnetic anomalies and fracture zone traces from the North and Central Atlantic Oceans. The relative motion of Africa with respect to Europe can be computed because of the differential motion between the two independent Atlantic spreading systems. The geometry which enables this to be done is discussed in Chapter 4.

The earliest attempt to model the development of the Alpine system using rigid body rotations was that of Smith (1971) who used the Bullard *et al.* (1965) Pangea reconstruction of the continents as a starting point and extended it to include continental fragments around the Mediterranean (see his Fig. 4). Employing the simplifying assumptions of a fixed pole opening model for the Atlantic and a single, although irregular, plate boundary between Europe and Africa Smith was able to account for many geological features in the circum-Mediterranean region.

A more rigorous model for the opening of the Atlantic was published less than a year after Smith's synthesis. Pitman and Talwani (1972) deduced the opening history of the Atlantic mainly from studies of marine magnetic anomalies. They gave this

history "...in terms of a time sequence of poles and angles of rotation..." which described the Europe-North America and Africa-North America seafloor spreading histories. A set of isochrons and synthetic fracture zones was derived from the model and found to be in accord with the ages of oceanic basement and the trends of fracture zones, as known at that time.

This Atlantic opening model provided the kinematic basis for the first major plate tectonic synthesis of Alpine evolution (Dewey et al., 1973). The motion of Africa with respect to Europe was determined by the finite difference method using the motions: Africa with respect to North America, North America with respect to Europe. Dewey et al. (1973) rejected the idea of a single plate boundary between Europe and Africa. They noted the numerous microplates and continental blocks between the two continents and suggested that this situation has probably existed, in various forms, throughout the history of Tethys. By using geological structures, facies relations, and paleomagnetic data in conjunction with their kinematic model old plates and their boundaries in the Tethyan-Alpine-Mediterranean system were reconstructed for the past 200 million years.

The next major advances in kinematic modeling came in 1977 and 1978. Prior to 1977 the most commonly used continental reconstruction was that of Bullard et al (1965) which was a least squares best fit of various bathymetric contours. LePichon et al. (1977) made a major adjustment to this reconstruction by utilizing fracture zone data from near the continents and

matching geological features on opposing continental margins. Sclater et al. (1977) studied the paleobathymetric evolution of the Atlantic, while Cande and Kristoffersen (1977) reidentified magnetic anomalies in the North Atlantic providing new insight into the timing of separation. Seafloor spreading in the Laborador and Norwegian Seas and its relation to North Atlantic evolution was discussed by Kristoffersen and Talwani (1977), Talwani and Eldholm (1977), and Srivastava (1978).

At the Split, Yugoslavia meeting on the structural history of the Mediterranean a new plate tectonic model for the evolution of the Western Alpine System was presented (Biju-Duval et al., 1977). This kinematic model varied from Dewey et al. (1973) in that it considered only three microplates to have been involved in Alpine-Mediterranean evolution. This new model was presented as a series of palinspastic reconstructions which attempted to show the relations between the various plates and microplates through Mesozoic and Cenozoic time. The basis and methods for restoring various units to their original size and shape was not explained.

The question of microplates has resulted in a variety of models. Some of these models, especially those limited areally and temporally, are qualitative in nature (e.g. Alvarez et al., 1974; Alvarez, 1976). Others attempt to be more quantitative and define which microplates have rotated and by how much (e.g. Channell and Horvath, 1976; Channell et al., 1979; Laubscher and Bernoulli, 1976). The problem of how various microplates and

blocks fit into a Pangea reconstruction still remains.

Recent kinematic models for Africa-Europe relative motion (Olivet et al., 1984; Livermore and Smith, 1985; Savostin et al., 1986) have used somewhat newer, published and unpublished, data (Savostin, 1981; Klitgord and Schouten, 1982; Olivet et al., 1984) but also incorporated older data. Both Livermore and Smith (1985) and Savostin et al. (1986) rely entirely on identification and mapping of anomalies done by others and generally have used published poles or interpolations from published poles; in neither study was any original data reexamined. Thus their work is not as current as it seems (Livermore and Smith's work was first presented at a NATO/ARI Conference in 1982 but it was not published until late 1985).

All published Atlantic kinematic models have used the same few marine magnetic anomalies as the basis for reconstructions. For Tertiary and Late Cretaceous time these are Anomalies 5, 13, 24 or 25, 30, 33, and M0, although some studies also use 6, 21, and 34. The correspondence of these marine magnetic anomalies to various geochronological timescales is shown in Table 1.1. For the earlier part of the Cretaceous and the Jurassic the choice of anomalies has been more varied. The reasons for initially using these anomalies were that they were 1) easily identifiable and 2) thought to correspond in time to important tectonic events or to plate reorganizations. As a first approximation the rotation parameters used to bring anomaly pairs into coincidence were considered adequate to describe the relative motion path between

TABLE 1.1A

COMPARISON OF GEOCHRONOLOGIC TIMESCALES

FOR SELECTED MARINE MAGNETIC ANOMALIES

ANOMALY	BKFVC85+ KG85*	HCLPSW82	NLC80+ VH76*	LKC77+ LH75*	HDHPL68+ LP72*
5	8.92 Tortonian	8.85 Tortonian	8.34 L. Miocene	8.79 Tortonian	8.80 Miocene
6	19.35 Burdigal.	19.41 Aquitanian	19.45 E. Miocene	18.95 Burdigal.	20.19 Miocene
13	35.29 Rupelian	36.73 Rupelian	34.75 E. Olig.	35.26 Rupelian	37.61 Oligocene
21	48.75 Lutetian	47.64 Lutetian	47.60 M. Eocene	49.04 Lutetian-Ypresian	52.41 Eocene
24	55.14 Ypresian	52.36 Ypresian	54.65 E. Eocene-L. Paleo.	55.58 Thanetian	59.43 Paleocene
25	58.64 Selandian	55.60 Thanetian	57.60 L. Paleo.	58.67 Montian	62.75 Paleocene
30	66.74 Maestrich.	65.39 Maestrich.	67.05 Maestrich.	65.37 Maestrich.	69.93 Maestrich-Campanian
32	71.37 Maestrich.	69.48 Maestrich.	72.15 Maestrich-Campanian	69.20 Maestrich.	74.17 Campanian-Santonian
33	74.91 Maestrich-Campanian	72.06 Maestrich-Campanian	75.35 Campanian	71.62 Maestrich-Campanian	77.20 Santonian
34	84.00 Campanian-Santonian	82.93 Campanian-Santonian	85.90 Santonian	79.65 Campanian-Santonian	79.80 Coniacian

NOTES: At end of Table 1.1B

TABLE 1.1B

COMPARISON OF GEOCHRONOLOGIC TIMESCALES

FOR SELECTED MARINE MAGNETIC ANOMALIES

ANOMALY	BKFVC85+ KG85*	HCLPSW82	NLC80+ VH76*	LKC77+ LH75*	HDHPL68+ LP72*
M-0	118.70 Aptian-Barremian	118.21 Aptian-Barremian	107.95 Albian-Aptian	107.90 Aptian	a
M-4	126.46 Hauteriv.	126.42 Hauteriv.	123.75 Hauteriv.	116.50 Barremian	115.90 Barremian
M-10N	131.65 Hauteriv-Valangin.	133.11 Valangin.	126.60 Valangin.	123.35 Hauteriv-Valangin.	a
M-16	141.85 Berriasian	144.08 Berrias-Tithonian	132.60 Berriasian	134.90 Berrias-Tithonian	133.15 Berriasian
M-25	156.55 Oxfordian-Kimmeridg.	160.90 Oxfordian	145.50 Oxfordian	152.75 Oxfordian	a
M-29	160.33 Oxfordian	164.82 Callovian	a	a	a

NOTES: BKFVC85 = Berggren et al., 1985.
KG85 = Kent and Gradstein, 1985.
HCLPSW82 = Harland et al., 1982
NCL80 = Ness et al., 1980.
LKC77 = LaBreque et al., 1977.
VH76 = Van Hinte, 1976a,b.
LH75 = Larson and Hilde, 1975.
LP72 = Larson and Pitman, 1972.
HDHPL68 = Heirtzler et al., 1968.

\+ Timescale for Cenozoic time and/or Anomalies 1 - 34.
* Timescale for Mesozoic time and/or Keathley Anomalies.
a Anomaly was not known when timescale was published.

various plates (see McKenzie and Parker, 1967; Morgan, 1968; LePichon, 1968; Pitman and Talwani, 1972; Dewey et al., 1973 for justification of this idea).

1.2 Poles of Rotation

Although a detailed consideration of the geometry of plate tectonics is beyond the scope of this thesis an understanding of the concepts of poles of rotation is necessary and important to understanding of the material discussed in Chapters 2, 3, and 4. These chapters deal, respectively, with the kinematics of North Atlantic seafloor spreading, Central Atlantic seafloor spreading, and the motion of Africa relative to Europe. The mathematical, geometric, and theoretical concepts and the terminology of poles of rotation have been treated variously by different authors (cf., McKenzie and Parker, 1967; Harrison, 1972; LePichon et al., 1973; Dewey, 1975).

The terminology used in this work is an amalgam taken from these works and other sources (S. Cande, J. Pindell, personal communications, 1985-86). Rotation parameters, quantitative descriptions of these motions, consist of a set of latitude-longitude coordinates (pole of rotation) and the angle through which a point or plate is rotated. Expressed somewhat differently, a pole of rotation (regardless of type) is an axis originating at the center of the earth and intersecting its surface at a specified latitude and longitude. The term is

sometimes taken to include the angle of rotation.

Two types of poles are distinguished in this work, finite (or reconstruction) poles and stage (or finite-difference) poles (Fig. 1.1). The first specifies the rotation parameters necessary reconstruct past plate positions by rotating points on one or more plates into coincidence with points on another. The reference frame is fixed with regard to that plate which is not being rotated. The reference frame may be altered by changing the sign of the rotation angle.

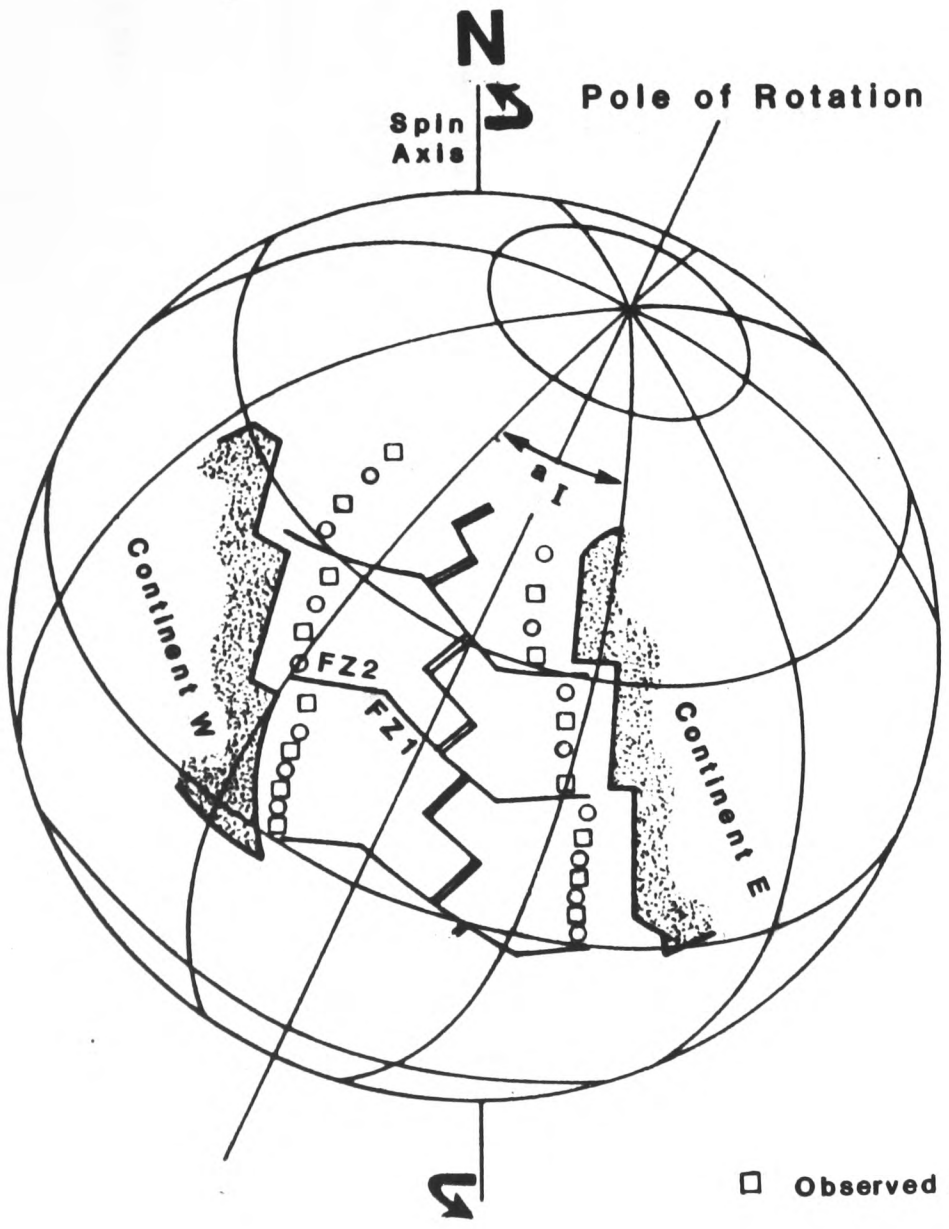
The important point concerning finite (or reconstruction) poles is that they <u>do not</u> necessarily describe the path of relative motion. They only describe the rotation necessary to bring sets of magnetic anomaly pairs, fracture zones, or matching geological features into coincidence. The singular case for which erroneous results will not be forthcoming is that in which it can be demonstrated that the pole of rotation did not move in the time interval involved.

Stage (finite-difference) poles are the rotation parameters which describe the motion between two sets of finite rotation parameters. For each plate in a spreading ocean there is stage pole for any particular interval, i.e., stage poles describe motion within a plate, hence the frame of reference for a stage pole is the plate itself and there are separate stage poles for each plate. The set of stage poles for any plate can be summed to give the finite pole for any time. It is because stage poles describe the actual motion of a plate for a specified time

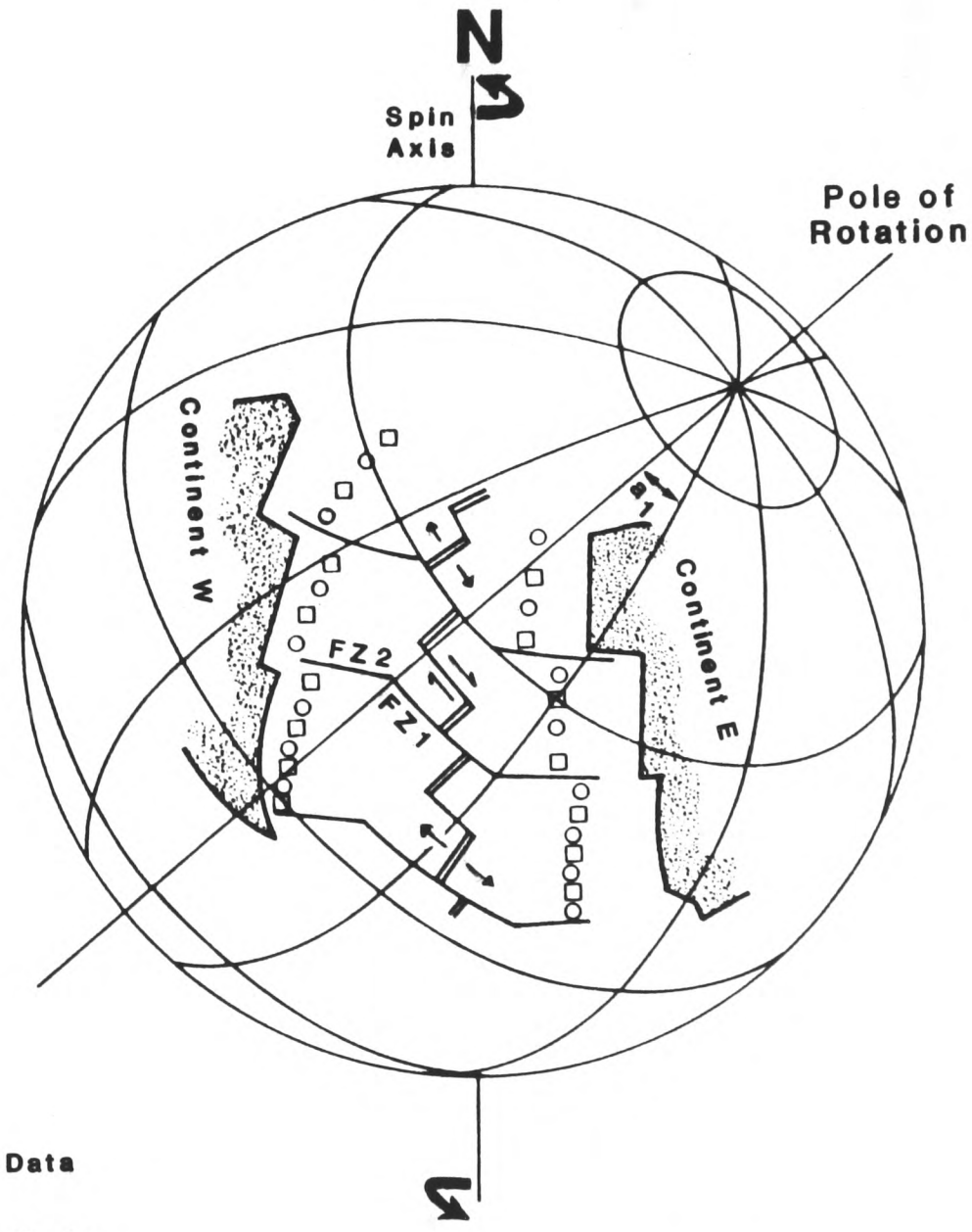
Figure 1.1: Finite and Stage Poles of Rotation

The two types of rotation poles for spreading oceans are illustrated. Finite poles (reconstruction poles) give reconstructed positions of plates at a specific time (i.e., an isochron). They do not show the path of relative motion. Stage poles (finite-difference poles) describe the path of relative motion for a specific time interval (i.e., time 2 - time 1). See text (section 1.2) for complete discussion.

FINITE POLE
ISOCHRON I



STAGE POLE
TIME T1 – T2



□ Observed Anomaly Data

○ Rotated Anomaly Data

// Spreading Ridge

Fracture Zone (FZ)

(modified from Klitgord and Schouten, 1986)

interval that they are used in the construction of flow lines or synthetic fracture zones and ideally there should be a one to one correspondence.

1.3 Organization of This Work

The organization of this work is to first establish rotation parameters that describe the kinematic evolution of the North and Central Atlantic Oceans (Chapters 2 and 3, respectively). The Central Atlantic was the first to open, and logically should be studied first. However, because of its greater complexity the North Atlantic is discussed first. The methods used and much of the rationale behind it was worked out dealing with the North Atlantic. In these chapters geological and physiographic features of these oceans are also discussed.

In addition, the new model for each ocean is compared to existing models. This is used by comparing synthetic fracture zone traces for each model to fracture zones in each ocean that were remapped as part of this work. Some implications of the models are also discussed.

Chapter 4 is the lynchpin of this work. In this chapter the finite difference solution between the Central and North Atlantic rotation parameters is determined and a kinematic model for the motion of Africa with respect to Europe is presented. As in the previous two chapters this model is compared with other models. The technique of matching synthetic fracture zones to actual

fracture zones cannot be used because the motion between Africa and Europe is convergent. The models are compared with respect the smoothness of their trajectories in light of the available data on Atlantic magnetic anomalies and fracture zones.

In Chapter 5 the geology of the Western Mediterranean region is reviewed. Much of the discussion forms the basis for the model that is presented in the ensuing chapter. Chapter 6 presents a model for the evolution of the Western Mediterranean. Although the Western Mediterranean Sea has developed only since the Oligocene the older evolution of the region is examined also, as is the evolution of the Atlantic.

Chapter 7 is a brief review and discussion of the preceeding chapters. References cited in the text or used in compiling tables, figures, or maps are given in Chapter 8. There are also 3 appendices. Appendix A is a list of scientific cruises and aeromagnetic track lines used in the study of Atlantic anomalies. Appendix B is a series of computer programs utilized in various phases of this work. Appendix C is the Anomaly timescale used.

CHAPTER 2

KINEMATIC MODEL FOR THE OPENING OF THE NORTH ATLANTIC OCEAN

2.1 Introduction

The development of rigid body rotation models to explain the kinematics of oceans that are currently undergoing seafloor spreading is based primarily on two types of data: magnetic anomalies and fracture zones. Magnetic anomalies are treated as isochrons because they have been age-calibrated (Harland et al., 1982; Berggren et al., 1985; Kent and Gradstein, 1985); hence they define the rate of seafloor spreading. Fracture zones are treated as flow lines, which define the direction of seafloor spreading. Hence, any rigid body rotation model is constrained to be internally consistent. Second order oceanic features such as mid-plate swells, anomalous deeps, ocean island or seamount chains may provide additional constraints once the first order motions are sufficiently known.

Such a kinematic model can be integrated then with geological and geophysical data to produce a model that describes the overall geologic evolution of a particular region. Discrepancies between the geological and kinematic model point out potential areas for future investigation, particularly geological fieldwork that will resolve the conflict.

In this and the next chapter, new models of the opening of the North Atlantic Ocean and Central Atlantic Ocean are

presented. The purpose of this is three-fold. First, it is a process-oriented approach to understanding the geology of the North Atlantic. Second, it is the initial step in a reconstruction of the continents that surrounded the Tethyan domain prior to the breakup of Pangea. Third, it provides the kinematic basis by which we study the evolution of the Tethyan-Alpine-Mediterranean system; that is, it is the framework within which the complex geology of this region must be understood. As explained in Chapter 1, the motion of Africa with respect to Europe is a consequence of the differential motions of Africa and Europe as they independently separated from North America during the Mesozoic and Cenozoic.

An essential part of this project was the identification of all anomalies within the standard magnetic anomaly sequence (Heirtzler et al., 1968) and determination of rotation parameters for each. Previous studies identified only selected anomalies that were easily identifiable or thought to correspond with times of important tectonic events or plate reorganization. The approach employed here seeks to impose tighter control on the interpreted motion path, especially in light of the paucity of fracture zones in the North Atlantic, by using all available data. A more detailed motion path allows greater correlation between plate kinematics and the evolution of geological features.

Finally, many previous workers have failed to present any error analysis of their work. Such an analysis is essential if

kinematic studies are to move beyond modeling and into the realm of quantitative science. This work will include a discussion of possible sources of error, attempt to quantify them, and present a realistic numerical estimate of the total error involved.

2.2 Sources of Data

2.2.1 Magnetic Anomaly Data

All magnetic anomaly profiles used in this study were obtained from the data banks of the Lamont-Doherty Geological Observatory (Columbia University). Profiles were plotted on Mercator projections at a horizontal scale of 2 inches per degree of longitude and a vertical scale of 500 gammas per inch. These profiles were then examined to determine whether additional processing to remove regional magnetic field effects was necessary. Nearly 20% of all profiles were reprocessed and replotted. Areas that had a great density of data were replotted at a scale of 4 inches per degree of longitude and 1,000 gammas per inch for greater clarity and resolution.

Several hundred shipboard and airborne anomaly profiles were examined. The density of coverage was very variable. Only 68 surveys were available for the region from 54°N to 60° between 10°W and 50°W, whereas immediately to the north (60°N to 66°N), across the Rekyjanes Ridge, over 150 surveys were available. On average for a given 10° latitudinal range, more than 110 surveys were examined (Table 2.1).

TABLE 2.1

DISTRIBUTION OF MAGNETIC ANOMALY PROFILES BY LATITUDE

LATITUDE	LAMONT DATA	NON-LAMONT DATA	TOTAL PROFILES
60-66	20	>130	>150
54-60	21	47	68
44-54	18	66	84
33-45	25	101	126
20-34	39	80	119
12-21	56	77	113
10 degree average	30	>83	>113

2.2.2 Fracture Zone Data

Fracture zone data was obtained from published bathymetric maps (Laughton et al., 1975; Laughton and Monahan, 1978; Searle et al., 1982), bathymetric profiles from ship tracks, and SEASAT altimetry data. The last two were obtained from Lamont-Doherty's data bank. Bathymetric profiles were plotted at 2 inches per degree of longitude. SEASAT data was plotted at both 2 inches per degree of longitude and at 0.4375 inches per degree of longitude. The latter is equivalent to the 1:10,000,000 scale used on GEBCO maps and facilitated comparison.

2.3 Methodology

The practice followed in identifying anomalies was to identify the youngest part of the anomaly, i.e. the point of polarity change as shown by the point of inflection or slope change of each anomaly along the profile. Some previous workers have chosen to correlate the center of anomalies (e.g. Ladd, 1974, 1976; Cande and Schouten, unpublished data). More commonly the part of the anomaly being correlated is left unspecified.

Identification of anomalies was aided by the preparation of model magnetic anomaly profiles. These models were prepared at 10° latitudinal intervals. In constructing the models, several parameters were varied including, but not limited to, strength of magnetization, thickness of the magnetized layer, spreading rate(s), phase shift (skewness), and remnant magnetization to

produce models that closely approximated the actual anomaly profiles. These profiles were especially helpful in identifying the same part of each anomaly because the source block from which the anomaly arose was shown as part of the model (Fig. 2.1).

2.3.1 Anomaly Characteristics

Magnetic anomalies are identified by the manner in which they occur within a sequence and by individual characteristics. As with any wave form, amplitude and wavelength interact to determine the shape of the anomaly. In the marine magnetic anomaly sequence, wavelength is mostly a function of polarity interval duration and amplitude of geomagnetic field intensity. Secular variation in field intensity, latitude of formation, changes in how the magnetism is carried (CRM vs. TRM), and interference from adjacent polarity zones all influence the form and skewness (shape asymmetry) of the anomaly. More simply, it may be said that the shape of marine magnetic anomalies depends upon the horizontal and vertical variations in magnetization of the oceanic crust.

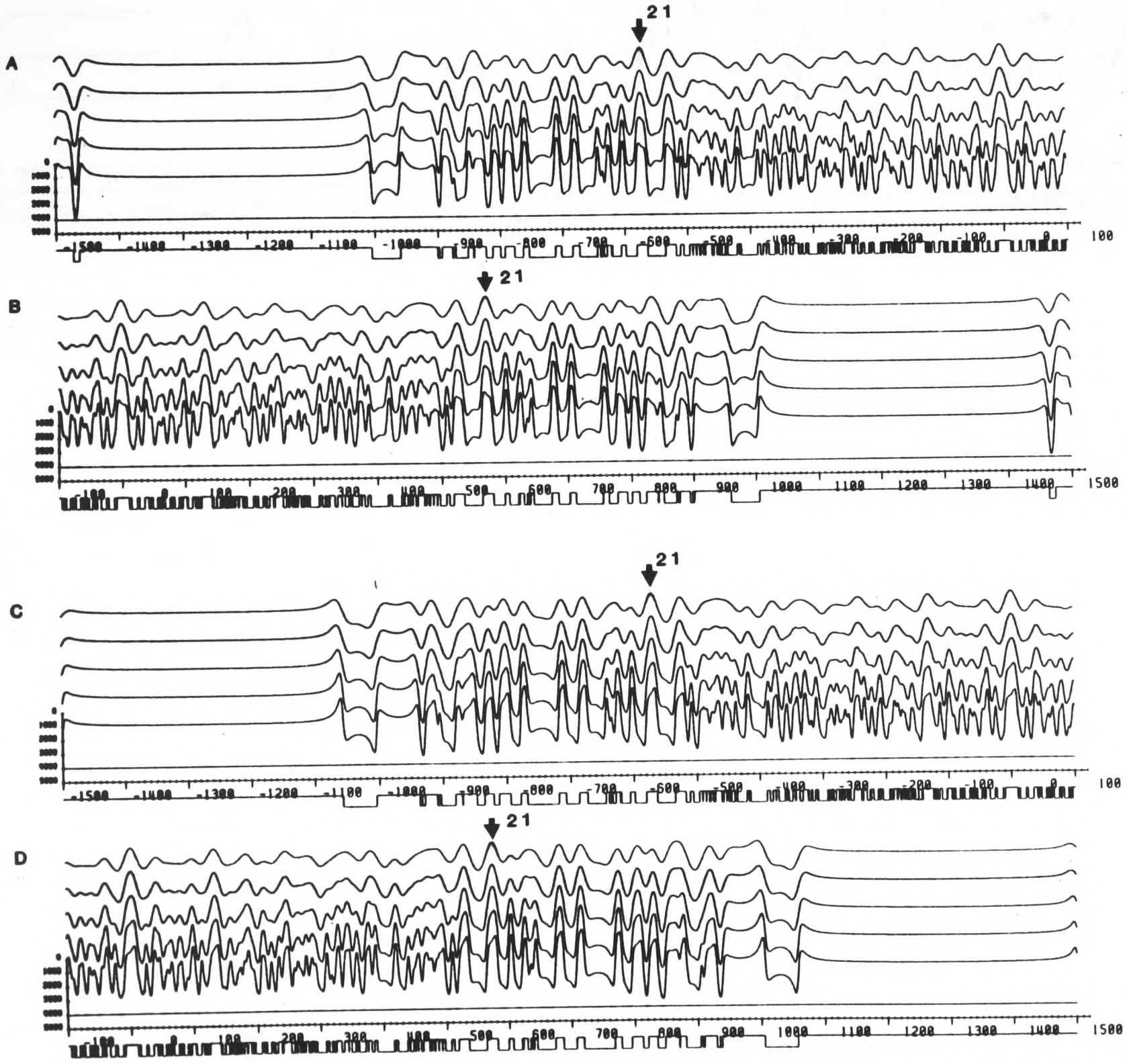
In this section, the characteristics of anomalies identified and mapped in this study are presented. The characteristics of the normally magnetized part of the anomaly are described with reference to the model anomaly profile(s) in Figure 2.1.

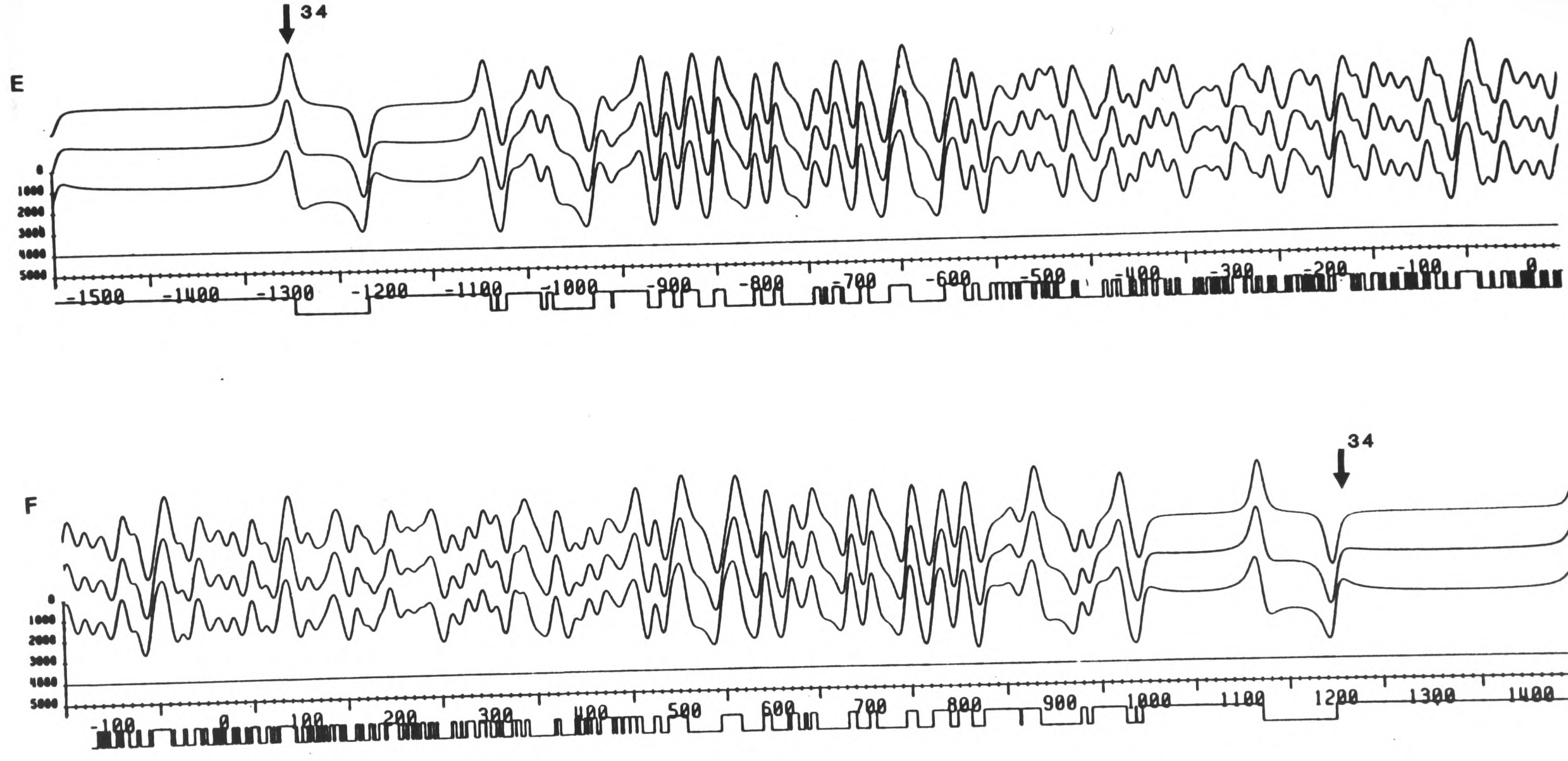
2.3.1a Anomalies 2 - 4A

In general, there is a decay of magnetization with age. The greatest amount occurs in the first 10 million years via crustal alteration due to hydrothermal circulation of seawater (Cande and

Figure 2.1: Magnetic Anomaly Profile Models

Models of magnetic anomaly profiles used to help make magnetic anomaly picks. Models A and B are projected along 50°N Latitude west and east of the Mid-Atlantic Ridge, respectively. Both have half-Gaussian filters to depths of 10 km to simulate the effect of overlapping lava flows during differing polarity epochs. Profiles C and D are projected along 40°N, again west and east, respectively. Note the variations that occur in the shape of the same anomaly om profiles; e.g. Anomaly 21 (shown by arrow). Profiles E and F, from the Central Atlantic are projected west and east along 25°N. They illustrate how models may be varied for skewness (shape asymmetry) by phase shifting. In this model, magnetization vectors have been varied by 30°, 60°, and 90°. The effects of this variation are seen most clearly by comparing Anomaly 34 (shown by arrow) on the western profile with its counterpart on the eastern profile. Recognition of the skewing effects of non-vertical magnetization vectors enabled Cande and Kristoffersen (1977) to identify clearly Anomalies 33 and 34 in the North Atlantic.


A
21
-1500
-1400
-1300
-1200
-1100
-1000
-900
-800
-700
-600
-500
-400
-300
-200
-100
0
100
B
21
-100
0
100
200
300
400
500
600
700
800
900
1000
1100
1200
1300
1400
1500
C
21
-1500
-1400
-1300
-1200
-1100
-1000
-900
-800
-700
-600
-500
-400
-300
-200
-100
0
100
D
21
-100
0
100
200
300
400
500
600
700
800
900
1000
1100
1200
1300
1400
1500


E
34
0
1000
2000
3000
4000
5000
-1500
-1400
-1300
-1200
-1100
-1000
-900
-800
-700
-600
-500
-400
-300
-200
-100
0
F
34
0
1000
2000
3000
4000
5000
-100
0
100
200
300
400
500
600
700
800
900
1000
1100
1200
1300
1400

Kent, 1976; Raymond and LaBreque, 1987). Anomalies less than 10 million years old should, theoretically, be easily identifiable. Because the Atlantic is a slow-spreading ocean, intrusion and extrusion events at the spreading ridge may mix magnetic components of differing polarity. The shape variation of anomalies due to these varying sources is modeled by applying a half-Gaussian filter (S. Cande, pers. comm., 1986).

The shape of Anomaly 2 is sharp but low in amplitude easily differentiated from the central anomaly and Anomaly 2a which is a high amplitude, broad, and characterized by a "double hump" which is most prominent on the young side. Anomalies 3 and 3A also have a "double hump", most prominently on the old side. Anomaly 4 has the highest amplitude of any in this sequence and is slightly skewed toward its young edge. This skewness is probably due to a short reversal prior to the start of the anomaly. 4A has a short wavelength and is often poorly developed.

2.3.1b Anomalies 5 - 6C

The time period of these anomalies is characterized by many reversals of varying duration. Berggren et al. (1985) show 16 chrons for this interval. Because of the slow rate of Atlantic spreading, the identification of anomalies in this work does not correspond directly to that shown on that geomagnetic timescale.

Anomaly 5 is a broad, high amplitude anomaly whose upper surface commonly dips to the west. Anomaly 5A is more symmetric with one-third the wavelength and two-thirds the amplitude of 5. As defined in this work, Anomaly 5B includes the oldest part of

Chron C5A, and Chrons C5AA, C5AB, C5AC, C5AD, as well as C5B. Even when well formed, the reversals do not form a discrete series but rather a wide multipeaked hump. The point of inflection or slope break identified on profiles appears to correspond to the young edge of Chron C5AB or C5AC of Berggren et al. (1985).

Anomalies 5C and 5D are more easily distinguished because of long periods of reverse polarity that separate them from 5B and 5C. 5E is separated also from 5D by a long reversed interval but not from Anomaly 6. Very slow North Atlantic spreading makes distinguishing 5E from 6 virtually impossible, hence it was not identified. In the Central Atlantic, 5E appears as a "blip" just before Anomaly 6.

2.3.1c Anomalies 7 - 19

The frequency of magnetic reversals begins to decrease sharply from Anomaly 7 time. This is probably because most secondary components of magnetization, particularly CRM, have been acquired by this time and distortion of the original TRM component is completed (Raymond and LaBreque, 1987). This, and the effect of sediment cover, can result in a loss of resolution for short period reversals.

Anomaly 7 appears as a symmetric, moderate amplitude, short wavelength anomaly surrounded by longer negatives. Anomaly 7A is of such low amplitude that it is swamped by the older negative and has not been mapped. Anomalies 8, 9, and 10 are nearly equal in amplitude and wavelength and form a triumverate that tends to

be readily identifiable. Anomalies 11 and 12 have similar amplitude, although 11 is slightly broader, are separated by a short negative, and commonly appear as a double humped arch.

Anomaly 13 is narrow, strong positive separated by long negatives. The sequence of 15, 16, 17, and 18 occurs in an interval of overwhelming normal polarity broken by short periods of reverse polarity. The wavelength and amplitude of each of these anomalies is greater than the previous. Anomaly 19 is a short, low amplitude anomaly within a moderately long negative interval. It is commonly poorly developed and hard to identify.

2.3.1d Anomalies 20 - 29

This group consists of some of the most easily identifiable anomalies because they tend to be high in amplitude and separated from each other by relatively long periods of reversed polarity. Anomaly 20 commonly stands out because of the poor development of 19 and the long negative between it and 21. Anomaly 21 is one of the highest amplitude anomalies in the entire sequence and is skewed slightly toward the west. Anomaly 22 is only slightly lower in amplitude but is much narrower.

Both 23 and 24 consist of two normal polarity intervals separated by a short reversal which is more pronounced for 24. The reversed interval separating these anomalies is also of short duration. Despite this, these anomalies are usually well defined and readily identifiable. Anomalies 25 and 26 may be the most easily identified of all anomalies. They are short, normal polarity events in the midst of a long reversed interval and have

the appearance of a set of "rabbit ears". Anomalies 27, 28, and 29 are usually poorly formed but are identified by their long wavelength.

2.3.1e Anomalies 30 - 34

The slow spreading rate of the Atlantic makes Anomalies 30 and 31 virtually indistinguishable because the reverse polarity interval separating them is extremely short (100,000 years). They often appear as a broad, moderate amplitude anomaly but, when distinguishable, 31 is higher in amplitude and is shorter in wavelength. Anomaly 32 consists of positive and negative of equal, although short, duration followed by a long positive and short negative. The amplitude of the long positive is more than twice that of the short positive and is slanted to the west.

Anomalies 33 and 34 are sometimes difficult to identify because of their skewness (shape asymmetry). This is ascribed to anomalous behavior of the paleomagnetic field (Cande, 1978). The sequence is best identified by looking for a long positive followed by a negative of slightly shorter duration, which is itself followed by a very long positive. This marks the end of the Cretaceous Quiet Zone.

2.3.2 Determination of Rotation Parameters

In all, nearly 3000 individual anomaly identifications were made in the North Atlantic. Each of these anomaly picks was then digitized. All previously published poles for the separation of Europe and North America were tested to see how well they fit the data. A compilation of the rotation poles that were tested is

given in Table 2.2. In a few cases, only a very minor modification to a published pole gave an excellent fit to the data. This was particularly true for Anomaly 5. Pitman and Talwani's (1972) pole fits the data with only a 0.09 degree change in rotation angle. Other poles for various anomalies were found to be unsatisfactory necessitating the determination of new ones. Thus the first results were obtained for "standard anomalies", i.e. those commonly used in previous studies (usually anomalies 5, 6, 13, 21, 24, 25, 30, 33, and 34).

To determine poles of rotation for all other anomalies a simple procedure, based on the assumption that poles of rotation (both finite and finite-difference) tend to remain relatively stable in the frame of reference of the two plates, was adopted. First a "standard anomaly" and its pole were chosen. The latitude and longitude of the pole were maintained but the rotation angle varied to obtain the best possible fit for the next younger or older anomaly. For example, anomaly 13 has a rotation pole of 62.50°N, 138.50°E, 7.30°. Anomalies 12 and 15 have rotation angles of 6.83° and 7.55° respectively but the same latitude and longitude (Table 2.3). This process was continued using the next younger or older anomaly, 11 and 16 in this example, until it was evident that the latitude-longitude coordinates being used could not produce a satisfactory fit. The coordinates of the next younger (or older) "standard anomaly" were then tested to see whether a satisfactory fit could be obtained. In this example, a change to the latitude-longitude

TABLE 2.2

PUBLISHED FINITE ROTATION PARAMETERS FOR THE NORTH ATLANTIC

SEPARATION OF EUROPE AND NORTH AMERICA

ANOMALY	LATITUDE	LONGITUDE	ROTATION	REFERENCE
5	68.00	137.00	2.50	(1)
5	73.00	96.50	3.00	(2)a
5	65.50	139.50	-----	(3)*d
5	63.10	142.10	1.91	(4)
5	59.50	141.20	2.00	(5)*c
5	62.30	134.60	2.30	(6)*d
6	63.10	142.10	4.00	(4)
6	64.50	136.50	3.80	(5)*+
6	68.00	138.20	4.75	(7)
13	65.00	133.00	7.60	(1)
13	73.00	96.50	11.50	(2)e
13	63.10	142.10	7.24	(4)
13	68.00	129.90	7.78	(8)
13	73.00	133.00	8.70	(5)*+
13	68.10	138.20	7.80	(9)
21	56.00	144.00	9.90	(1)
21	55.70	141.70	9.92	(10)
21	57.60	141.50	10.10	(9)*f
21	67.12	137.28	10.94	(7)
21	43.30	144.40	9.60	(6)*d
22	57.40	150.20	10.00	(4)
23	56.80	144.10	11.41	(10)
24	57.20	144.90	12.00	(11)
24	64.10	137.80	13.00	(5)*+
24	61.10	143.00	12.30	(9)
24	62.28	140.37	12.68	(7)
24	63.20	139.10	12.50	(12)*
25	63.00	157.00	14.00	(1)
25	40.80	144.30	12.70	(6)*d
25	63.25	143.89	14.15	(7)
28R	85.30	86.50	28.70	(2)g
29	70.90	144.40	16.00	(4)
30	69.82	145.61	17.10	(7)
30	74.00	142.60	17.00	(13)h
31	70.66	145.91	17.59	(7)
33	77.00	160.00	20.50	(1)i
33	68.00	147.20	18.95	(11)
33	69.50	147.00	19.30	(9)
33	74.52	147.69	20.30	(7)
34	79.50	145.60	22.50	(4)
34	69.30	147.60	20.48	(11)
34	81.60	150.30	23.80	(9)
34	76.23	148.80	21.83	(7)
34	88.80	-14.60	36.00	(2)j

REFERENCES CITED:
(1)Pitman and Talwani, 1972; (2)Phillips and Forsyth, 1972;
(3)Karasik, 1974; (4)Sclater *et al.*, 1977; (5)Savostin, 1981;
(6)Klitgord and Schouten, 1986; (7)Srivastava and Tapscott, 1986;
(8)Talwani and Eldholm, 1977; (9)Olivet *et al.*, 1984;
(10)Kristoffersen and Talwani, 1977; (11)Kristoffersen, 1978;
(12)Savostin, in prep.; (13)Savostin *et al.*, 1986;

NOTES:

(*)Rotation parameters are from Tables 2 and 3 of Savostin *et al.* (1986) and reference is from their listing. Where possible the original reference was checked to insure accuracy [See notes (d) and (f)].

(+)Errors of =or- 0.4°, 0.5°, and 0.7° are given for the rotation angles of anomalies 6, 13, and 24 respectively.

(a)Rotation parameters are for 10Ma, which is approximately the age of Anomaly 5.

(b)No rotation angle is cited in Savostin *et al.* (1986). I have been unable to obtain a copy of the original reference to check.

(c)Rotation parameters are interpolated from Savostin and Karasik (1981).

(d)Rotation parameters are cited in Savostin *et al.* (1986) as those of Klitgord and Schouten (1986). However, Klitgord and Schouten's paper deals with the kinematics of the Central Atlantic. I was unable to locate the parameters that Savostin *et al.* cite in this publication.

(e)Rotation parameters are for 35Ma, which is approximately the age of Anomaly 13.

(f)Rotation parameters are cited in Savostin *et al.* (1986) as those of Olivet *et al.* (1984). However, I was unable to find these rotation parameters listed in Olivet *et al.* (1984). Olivet *et al.* (1984) only give rotation parameters for Anomalies 13, 24, 33, and pre-34 but not Anomaly 21.

(g)Rotation parameters are for 65Ma, which is approximately the age of Anomaly 28R.

(h)Rotation parameters are noted as being found by interpolation.

(i)Originally identified as Anomaly 31 but subsequently reidentified as Anomaly 33 by Kristoffersen and Cande (1978).

(j)Rotation parameters are for 105Ma, which is within the Cretaceous Quiet Zone. 105Ma is within the Albian stage.

All anomaly ages are referred to the Berggren *et al.* (1985) and Kent and Gradstein (1985) time scales.

coordinates of Anomaly 6 was made after Anomaly 9 (Table 2.3).

In some cases, this procedure was unsuccessful and an independent search was made for the best fit pole. The coordinates of such an pole were found usually to be intermediate between those of the adjacent "standard anomaly" poles. The latitude-longitude coordinates used in the rotation parameters of anomlies 22 and 23 are a good example (Table 2.3).

Finally, the difference between each pair of rotation parameters was computed to determine the stage poles of rotation. The stage pole rotation parameters are presented in Table 2.4.

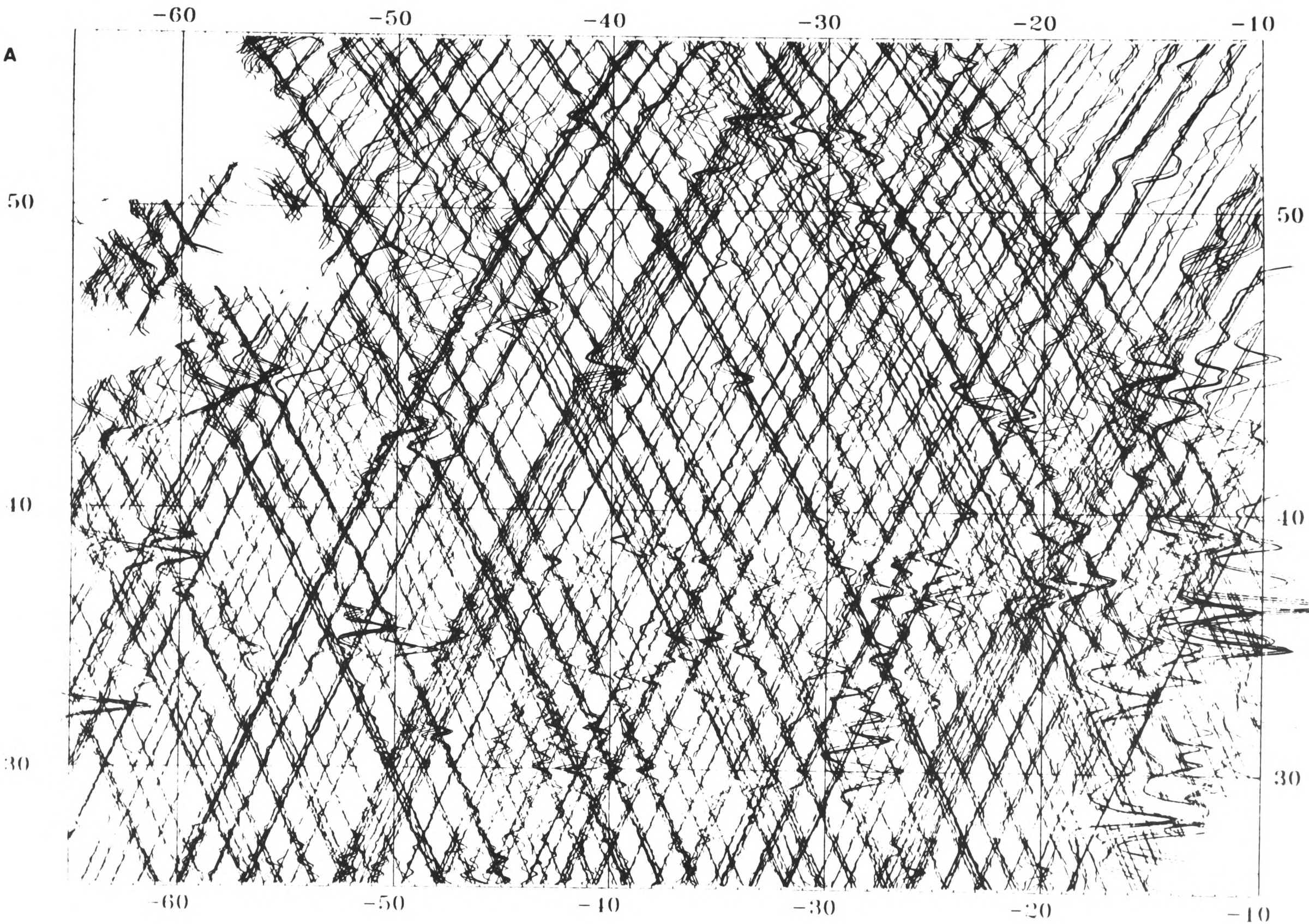
Fracture zones were defined on the basis of bathymetry and SEASAT altimetry data. SEASAT data was projected east-west (i.e. roughly perpendicular to the strike of the Mid-Atlantic Ridge) rather than perpendicular to the satellite path in order to give a better indication of fracture zone locations (Fig. 2.2). The first mapping was done using SEASAT deflection from the geoid data and bathymetric profiles compiled along ship tracks to define potential fracture zone locations. This was supplemented by gravity data derived from SEASAT altimetry (Haxby, 1985). These maps were compared with bathymetric maps published at various scales to best define the trends of fracture zones.

Synthetic fracture zone traces were constructed using stage pole rotation parameters. The traces of synthetic fracture zones were overlaid on the mapped fracture zone traces to check their correspondence. In the case of a mismatch, all the data was reexamined to determine the source of the discrepancy.

Figure 2.2: SEASAT Deflection from Geoid Data

SEASAT data was utilized in conjuction with bathymetric maps, topographic profiles along ship tracks, and SEASAT derived gravity data to remap fracture zones. In A, the raw data showing deflection from the geoid projected at an azimuth of 090°, the general trend of fracture zones in all parts of the Atlantic, is presented. In B, the trace of the Charlie-Gibbs Fracture Zone is overlain on this data and is labeled CGFZ.

A



B

−60 −50 −40 −30 −20 −10

50

40

30

CGFZ

2.4 Major Features of the North Atlantic Ocean

The North Atlantic Ocean has within its confines a variety of structural features, which have been interpreted in various ways. In this section, the major aspects of these features are briefly described and the manner(s) in which they have previously been interpreted noted. These features are shown in Figure 2.3 and Plate I; any model that seeks to describe the evolution of the North Atlantic must account for them.

2.4.1 Fracture Zones

There are 2 major fracture zones in the North Atlantic; Charlie-Gibbs and East Azores. The latter forms one part of the Europe-Africa plate boundary and is discussed in the context of this boundary. Other fracture zones in the North Atlantic are not well developed and/or are of small offset. They are only briefly discussed.

2.4.1a The Charlie-Gibbs Fracture Zone

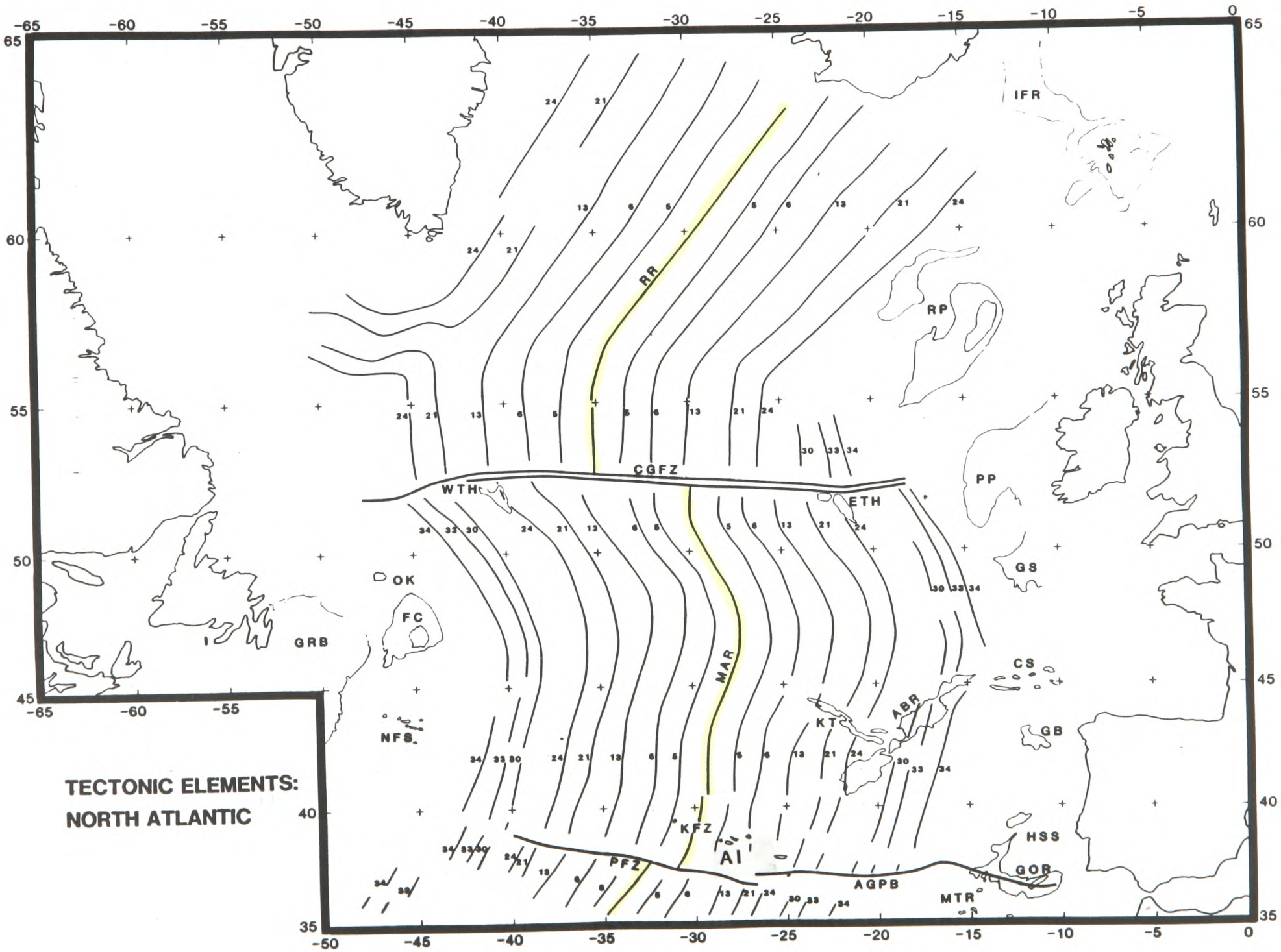
The most important feature of the North Atlantic Ocean, in terms of kinematic models, is the Charlie-Gibbs Fracture Zone. It is the only well-developed, major offset fracture zone in the Atlantic between Iceland and the Azores. It is, therefore, the major constraint on flowlines for reconstructions of the North Atlantic (see 2.5.2 below).

Charlie-Gibbs extends from the eastern margin of Labrador to the Rockall Trough, just west of the Porcupine Bank, between the latitudes of 52°N and 53°N. As such, it is one of the few

Figure 2.3: Simplified Tectonic Element Map: North Atlantic

Major features and locations mentioned in text are shown, along with general position of selected magnetic anomaly lineations. A more complete version of this map is to be found as Plate I. Locations of magnetic anomaly picks are presented in Plate II.
Legend: MAR = Mid-Atlantic Ridge; RR = Reykjanes Ridge; 5, 6, 13, 21, 24, 30, 33, 34 = Magnetic Anomalies; CGFZ = Charlie-Gibbs Fracture Zone; AGPB = Azores-Gibraltar Plate Boundary; PFZ = Pico Fracture Zone; KFZ = Kurchatov Fracture Zone; IFR = Iceland-Faeroe Ridge; ETH, WTH = East (West) Thulean Rise; ABR = Azores-Biscay Rise; AI = Azores Islands; KT = King's Trough; MTR = Madiera-Tore Rise; CS = Charcot Seamounts; HSS = Horseshoe Seamounts; NFS = Newfoundland Seamounts; RP = Rockall Plateau; PP = Porcupine Plateau; GS = Goban Spur; GB = Galicia Bank; GOR = Gorringe Bank; GB = Grand Banks; OK = Orphan Knoll; FC = Flemish Cap.

MAR and RR are highlighted for clarity



TECTONIC ELEMENTS:
NORTH ATLANTIC

fracture zones to have been shown to exist from one continental margin to another. It has a left-lateral, double transform fault consisting of a northern and a southern trough separated by a transverse median ridge. The transform fault offsets the Mid-Atlantic Ridge by 350 kilometers. The seismically active part of the fracture zone is between 30°W and 35°W and includes a small spreading center at 32.75°W. Fault plane solutions on the transform segments are indicative of E-W dextral shear, consistent with the sinistral offset of the ridge (Fleming et al., 1970; Vogt and Avery 1974; Olivet et al., 1974; Einarsson, 1979; Searle, 1981; Whitmarsh and Calvert, 1986).

2.4.1b The Azores-Gibraltar Plate Boundary

On the east side of the Mid-Atlantic Ridge, a zone of complex topography, structure, and seismicity marks the boundary between the African and Eurasian plates. This boundary, referred to here as the Azores-Gibraltar Plate Boundary, shows a progressive west to east change from accretion to translation to convergence within the oceanic realm. Further east, beyond the Iberian and Moroccan continental margins, this boundary becomes a zone of continental collision. Only the absence of a well developed subduction zone prevents this region from exhibiting all the classical boundaries associated with the plate tectonic paradigm. This boundary results from the differential motion of Africa with respect to Europe as these plates independently separate from North America.

The zone extends from 39°N to 35°N and from 30°W to 10°W where it crosses the continental margins. Laughton and Whitmarsh (1974) divided the boundary into 3 sections: the Azores section (30°W-24°W), the central section (24°W-16°W), and the eastern section (16°W-10°W). These sections were delineated on the basis of morphology. More recent work by Grimison and Chen (1986) shows a strong correlation between the pattern of seismicity and this morphological zonation.

The Azores section is characterized by normal and strike-slip faults associated with the Azores Triple Junction and the Terciera Rift. The detailed structure of this, and the westernmost central region, was mapped by Searle (1980) using Gloria side-scan sonar data. The Azores section shows fault scarps, linear volcanic ridges, and other tectonic lineaments which trend 120°-300°.

The western extremity of the Gloria Fault marks the start of the central zone. This fault is considered the "...presently active transform fault bounding the European and African plates east of the Azores..." (Searle, 1980) and is part of the East Azores Fracture Zone, which continues to south of the Terciera Rift and intersects the Mid-Atlantic Ridge. The central section is relatively inactive seismically (Einarrson, 1986; Grimison and Chen, Fig. 2, 1986). However, where solutions have been presented, they show clear dextral motion along east-west trending fault planes (Udias et al., 1976).

Upon entering the eastern section, the topography changes

drastically. The zone is dominated by a series of ridges and seamounts (the northern end of the Madeira-Tore Rise, Horseshoe Seamounts, Gorringe and Hirondelle Bank) and the East Azores Fracture Zone is not really discernible (see Searle et al., 1982). Seismicity is scattered over a much wider area and shows "...a combination of strike-slip and thrust faulting without an apparent pattern..." except for a consistent P-axis orientation between NNW and NW (Grimison and Chen, 1986).

The exact position of the plate boundary within the eastern zone and as it crosses the continental boundary (assuming there are no intervening microplates) is difficult to ascertain. Seismicity, generally the best indicator, is widespread, diffuse, and offers little help. However, gravity data derived from SEASAT altimeter measurements suggest that the oceanic lithosphere in the eastern zone is fractured and may have been obducted in the area of Gorringe Bank (Karner et al., 1985). The association of ophiolitic oceanic and upper mantle rocks and silica deficient alkaline rocks found by dredging and drilling in this area is typical of subduction zones (Gavasci et al., 1973).

2.4.1c Other Fracture Zones

The Kurchatov Fracture Zone is the most commonly noted of the other fracture zones in the North Atlantic. Only three other fracture zones, Maxwell, Faraday, and Bight, are commonly named on bathymetric maps of the North Atlantic south of Iceland. Of these only the Kurchatov has been studied (Searle, 1979).

The Kurchatov Fracture Zone is characterized by a transform valley that is oblique to the spreading direction and a fracture valley that does not follow a small circle. Oblique transform valleys are characteristic of fracture zones with offsets of less than 20 km, as in the FAMOUS area (Searle, 1979).

2.4.2 Mid-Plate Swells and Anomalous Deeps

Mid-plate swells and anomalous deeps are intra-oceanic regions whose depths are either much less than, or much more than, that predicted by the age-depth relationship for oceanic crust (Parsons and Sclater, 1977). The origin of such features may be tectonic or related to the input of heat into the crust.

2.4.2a The East and West Thulean Rises

The East and West Thulean Rises are enigmatic features clearly visible on the GEBCO and IOS bathymetric maps (Laughton et al., 1975; Searle and Monahan, 1978). They are elongate features trending NW-SE symmetrically disposed about the Mid-Atlantic Ridge just south of the Charlie-Gibbs Fracture Zone. Their location is correlative with Anomalies 24 and 25 and with a change in trend of Charlie-Gibbs.

The rises were named by Vogt and Avery (1974) and were independently noted by Laughton (1971), Vogt et al. (1971a), and Olivet et al. (1974). These authors noted the coincidence of the rises with a change in seafloor spreading direction. In addition, both Laughton (1971) and Olivet et al. (1974) noted the presence of a similarly oriented basement high north of Charlie-Gibbs and offset to the west.

The Thulean Rises, although little explored, have been interpreted in various ways. Vogt (1971) regarded them as the product of a hot spot plume whose basaltic component was progressively depleted as indicated by the decline in elevation of the ridges from North to South. Laughton (1971) regarded them as the counterpart of the basement high noted to NW of Charlie-Gibbs and thought it part of an extinct spreading system.

2.4.2b The Azores-Biscay Rise

The Azores-Biscay Rise is a northeast-southwest trending aseismic ridge 650 kilometers long. The rise stands up to 3 kilometers above the surrounding seafloor and rises to less than 2 kilometers below the sea surface (Whitmarsh et al., 1982). It has been implicated in various hypotheses concerning the tectonics of the North Atlantic and Western Tethyan regions.

Seismic reflection profiles show that the basic morphology of the rise is that of a broad arch. There is no evidence of fault scarps or faulted sedimentary cover on the rise despite the fact that on its southeastern side it is bordered by a series of 5 deep sedimentary basins, collectively known as the Mirrol Trough (Addy and Kagami, 1979). On its northwestern side, the rise intersects the southeastern ends of the Peake and Freen Deeps which are part of the Kings Trough complex (Matthews et al., 1969; Searle and Whitmarsh, 1978; Kidd et al, 1982).

The rise is thought to be a volcanic construct related to excessive volcanic activity and/or hotspot activity along the Mid-Atlantic Ridge based on seismic refraction, gravity,

bathymetric, and GLORIA sonar data (Whitmarsh et al., 1982). Hypotheses that suggest this feature has been a locus of transform or strike-slip motion (Matthews et al., 1969; LePichon and Sibuet, 1971) or of compression (Grimaud et al., 1982) during the Pyrenean orogenesis are not in accord with the available geophysical and geological data. Magnetic anomalies are not offset as they should be if the Azores-Biscay Rise was a transform fault for all or part of its history (Verhoef et al., 1986). Nor, as previously noted, is there evidence of faulting or folding as would be expected in a compressional setting. Moreover, the rise seems to have formed prior to the Pyrenean Orogeny, unless the younger age suggested by Mattauer and Henry (1974) for the formation of the Pyrenees is accepted.

2.4.2c The King's Trough

The King's Trough is the main basin in a 450 km long complex of basins, ridges, and seamounts which trend 120°-300° on the eastern flank of the Mid-Atlantic Ridge. As with its eastern neighbor, the Azores-Biscay Rise, the King's Trough complex has had various origins suggested for it and has also been suggested as a locus of intraplate tectonism during the Cenozoic.

The morphology of the King's Trough Complex (here taken to include Palmer Ridge and the Peake and Freen Deeps) is quite complex. Kings Trough itself is approximately 200 km in length and reaches a depth of more than 4 km. It is bounded by ridges that stand nearly 3 km above the basin floor (Searle and Whitmarsh, 1978). These flanking ridges are fault bounded on

their inner sides but not their outer sides and show extensive outcrops of volcanic rock. The faults are stepped and show features typical of normal faults (Kidd et al., 1982). Subsidiary basins within the complex show the same features.

The Peake and Freen Deeps are found on the eastern extremity of the King's Trough Complex and have a more easterly trend. These deeps are 80 km long, subparallel to each other, fault bounded, more than 5 km deep, and separated by the Palmer Ridge which rises 2 km above them.

Rock samples from various parts of the complex are mostly of igneous origin, both plutonic and volcanic (Stebbins and Thompson, 1978; Kidd et al., 1982). These rocks include typical oceanic tholeiites, intra-oceanic alkaline basalts, as well as tuffs, trachytes, diorites, hyaloclastites, and serpentinites. Kidd et al. (1982) conclude on the basis of "...highly-vesiculated glasses...present in both tuffs and ashes..." and the presence of "...traces of foraminifera and diatoms and of rounded glauconite grains..." that the tuffs were erupted in shallow marine waters...up to 200m water depth..." and possibly subaerially. The tuffs postdate trachytes that have been dated as 32-34 Ma (lower Oligocene) (Kidd et al., 1982).

Tectonic models for the genesis of the King's Trough are varied. Matthews et al. (1969) and LePichon and Sibuet (1971) suggested it was a compressive plate boundary, whereas Grimaud et al. (1982) cite it as a locus of strike-slip motion. The rather small offset of magnetic anomalies across the trough suggests

that any strike-slip motion will be minor (less than 30-40 km). Such an offset may be related to minor extension rather than strike-slip. Similarly, the presence of stepped, normal faults within the basin suggests extension rather than compression.

More recent hypotheses suggest an origin related to mantle plume discharge in a triple junction or hot spot (Searle and Whitmarsh, 1978; Kidd et al., 1982). This is supported by Cann (1971) who found evidence of a 27 Ma (late Oligocene) metamorphic event and by Stebbins and Thompson (1978). These latter authors reported "...unusual petrographic, mineralogical, and chemical features..." in the rocks and suggested an off-ridge, intra-plate tectonic environment for their formation. This data is in accord with evidence of Miocene faulting and an Eocene-Oligocene hiatus found during drilling on DSDP Leg 94 (Shipboard Scientific Party, 1987). Taken together, the stratigraphic data and the small offset of magnetic anomalies suggest that the King's Trough formed in Oligocene-Miocene time due to reheating, thinning, and extension of previously formed oceanic crust.

2.4.2d The Madiera-Tore Rise

The northernmost part of the Madiera-Tore Rise forms part of the North Atlantic. The rise, 1,000 km in length, trends NNE-SSW across the Europe-Africa plate boundary (see 2.4.1b). The Tore Seamount, which marks the northern terminus, is circular and encloses a 1800 m deep. The deep is considered to be either a caldera (Tucholke and Ludwig, 1982) or the product of intersecting tectonic trends (Laughton et al., 1975). The rise is also discussed in Chapter 3.

2.4.3 Seamounts

Seamounts are distinguished from mid-plate swells largely on the basis of size and depth. Seamounts rise at least 1,000 m above their surroundings and have a limited extent across their summit. They are highly varied in shape and composition.

2.4.3a The Charcot Seamounts

The Charcot Seamounts form two E-W trending ridges separated by a valley. In the west, the ridges merge into the Azores-Biscay Rise (see 2.4.2b) whereas to the east they lose height and become covered by sediment. As with most of the features of the North Atlantic, multiple origins have been suggested for the seamounts.

Because of their orientation and location, Williams (1975) considered these seamounts an extinct spreading center, related to the opening of the Bay of Biscay. This is disputed by Keen et al. (1977) who see them as the eastern end of a seamount chain that crosses the Mid-Atlantic Ridge, thus imputing a hot spot origin. Moreover, other extinct spreading centers of similar age (Rockall Trough, Laborador Sea) have no physiographic expression. A final model invokes uplift due to the Pyrenean Orogen for their origin (Laughton et al., 1975).

2.4.3b The Newfoundland Seamounts

The Newfoundland Seamounts are an E-W trending chain, 400 km in length, which lie off the central Newfoundland Coast. These seamounts have ages of approximately 100 Ma +/- 5 based on radiometric age dates and ages of sediments. The most probable origin is either as a leaky transform fault or a transverse

volcanic lineament that was activated as a result of changing spreading geometry during the Cretaceous Quiet Zone (Sullivan, 1983).

2.4.3c The Horseshoe Seamounts

The Horseshoe Seamounts form the southern, eastern, and part of the northern border of the Horseshoe Abyssal Plain. The seamounts are part of the zone of complex topography that forms the eastern portion of the Azores-Gibraltar plate boundary (see 2.4.1b). The origin of this topography has been ascribed to underthrusting in this region (Purdy, 1975).

2.4.4 Continental Fragments (Microcontinents)

Continental fragments are subsided areas whose geophysical and/or lithological signatures are anomalous with respect to the surrounding oceanic crust. Microcontinents or continental fragments are generally formed by rifting of long, thin strips of crust away from a major continental mass. Locally, such crust may remain attached to the continent through an area of more highly attenuated crust. Continental fragments are buoyed by their low density, thus allowing them to rise to anomalous depths within the oceans.

2.4.4a Eastern North Atlantic

In the eastern North Atlantic, the Rockall Plateau (including both Hatton and Rockall Banks), the Porcupine Plateau, the Goban Spur, and Galicia Bank are the most prominent continental fragments. All have been intensively studied.

Typical continental rocks have been dredged or drilled from all these areas except the Porcupine Plateau. Pre-Cambrian granulites have been recovered from the Rockall Plateau (Roberts et al., 1975), Paleozoic quartzites, arkosic sandstone, and black shale from Goban Spur (Lefort et al., 1985), and Pre-Cambrian or Paleozoic schist, gneiss, and phyllite from Galicia Bank (Group Galice, 1979). Although Porcupine Plateau has not been directly sampled, extensive geophysical surveying has established the continental nature of this location and allowed correlation with the rocks of southwest Ireland (Bott and Watts, 1971).

2.4.4b Western North Atlantic

Suspected continental fragments near the North American continental margin are more problematic. Orphan Knoll and Flemish Cap are undoubtedly of continental origin. Pelletier (1971) reported granodiorite from a drill core on Flemish Cap. On Orphan Knoll, DSDP Leg 12 drilled unfossiliferous, crossbedded sandstone containing anthracite fragments over black shales. Ruffman and Van Hinte (1973) interpreted this as a channel deposit from an alluvial or nearshore fluvial environment. In addition, these same authors reported on samples of Devonian limestone dredged from the same locality.

Two other prominent features, the Southeast Newfoundland Ridge and the J-Anomaly Ridge, have been suggested as being partly formed of continental crust. Similar histories for these ridges and the margins of the Grand Banks have been inferred on the basis of borehole and seismic reflection data (Gradstein et

al., 1977). This has been disputed by Rabinowitz et al. (1978) who propose a geomagnetic model based on correlation of the J-Anomaly Ridge with seafloor spreading anomalies M-0 to M-4 and drilling results of DSDP Leg 43 at Site 384. The J-Anomaly Ridge has been suggested as a correlative feature fo the Madiera-Tore Rise (see 2.4.2d). In this model, the Southeast Newfoundland Ridge is the trace of an old transform fault.

2.5 Kinematic Model

2.5.1 Rotation Parameters

The separation of North America and Europe is quite complex and diachronous along the length of the North Atlantic Ocean. In the southernmost North Atlantic, separation of Iberia from North America probably began just prior to Anomaly M-0 (118.0 Ma) (Group Galice, 1979). This anomaly has not been well mapped in the western North Atlantic although Sullivan (1983) notes a correspondence in position with a proposed northward extension of the J-Anomaly. In the Norwegian and Greenland Seas, spreading did not begin until Anomaly 24 (55.1 Ma) (Talwani and Eldholm, 1977). Spreading stopped in the Bay of Biscay shortly after Anomaly 34 (84.0 Ma) (Masson and Miles, 1984) and prior to Anomaly 13 (35.3 Ma) in the Laborador Sea (Kristoffersen and Talwani, 1977).

The most complete recording of North Atlantic seafloor spreading history is found in the trace of the Charlie-Gibbs

Fracture Zone. Rotation parameters were developed using the trace of this fracture zone as a major constraint (see 2.3 and 2.5.2).

Charlie-Gibbs shows two major changes in trend along its length. The first is best seen on the western side. Between 45°W and 46°W (approximately Anomaly 27 [63.0 Ma]), the trend changes from E-W to ENE-WSW. This change is not seen clearly on bathymetric maps but shows up very well on SEASAT altimetry data (Fig. 2.2) and SEASAT-derived gravity images (Haxby, 1985).

The second change is more gradual. It commences at Anomaly 24 or 25 time (55.1 - 58.6 Ma). The present orientation (098°-278°) is achieved by approximately Anomaly 20 (44.7 Ma). This change is seen easily on the east and west sides of Charlie-Gibbs.

Complete finite and stage pole rotation parameters are given in Tables 2.3 and 2.4 respectively. The changes in Charlie-Gibbs orientation are reflected in changes of both finite and stage poles. In Figure 2.4, the trace of the Charlie-Gibbs Fracture Zone is overlain by synthetic fracture zones constructed using stagepole parameters. In Plates II and III unrotated and rotated magnetic anomaly picks are presented.

2.5.2 Flow Lines

The importance of the Charlie-Gibbs Fracture Zone to this model has been alluded to several times. Because of the importance attached to it, understanding the rationale that

TABLE 2.3

FINITE POLE ROTATION PARAMETERS FOR THE NORTH ATLANTIC

SEPARATION OF EUROPE AND NORTH AMERICA

ANOMALY	LATITUDE	LONGITUDE	ROTATION
2	68.00	137.00	0.41
2A	68.00	137.00	0.62
3	68.00	137.00	0.98
3A	68.00	137.00	1.40
4	68.00	137.00	1.74
4A	68.00	137.00	2.09
5	68.00	137.00	2.41
5A	68.00	137.00	3.01
5B	66.85	135.46	3.17
5C	66.85	135.46	4.01
5D	66.85	135.46	4.35
6	66.85	135.46	4.55
6A	66.85	135.46	5.06
6B	66.85	135.46	5.34
7	66.85	135.46	5.86
8	66.85	135.46	5.97
9	62.50	138.50	6.04
10	62.50	138.50	6.34
11	62.50	138.50	6.61
12	62.50	138.50	6.83
13	62.50	138.50	7.30
15	62.50	138.50	7.55
16	62.50	138.50	7.68
17	62.50	138.50	7.83
18	62.50	141.50	8.39
19	62.50	141.50	8.99
20	62.50	141.50	9.29
21	55.70	143.25	9.81
22	55.70	144.90	10.64
23	55.70	144.90	11.21
24	61.10	144.90	12.04
25	66.00	148.75	13.64
26	66.00	148.75	14.12
27	66.80	152.50	15.45
28	66.80	152.50	15.90
29	66.80	152.50	16.22
30	66.80	152.50	16.54
31	68.10	153.50	16.90
32	68.10	152.00	17.35
33	69.50	152.00	18.10
33R	71.50	152.50	19.69
34	75.00	152.50	21.20

TABLE 2.4A

STAGE POLE ROTATION PARAMETERS -- NORTH ATLANTIC

MOTION OF EUROPE WITH RESPECT TO NORTH AMERICA

ANOMALY	LATITUDE	LONGITUDE	ROTATION
2 - 1	68.00	137.00	-0.41
2A - 2	66.04	137.00	-0.21
3 - 2A	67.00	137.00	-0.36
3A - 3	67.81	137.00	-0.42
4 - 3A	67.86	137.00	-0.34
4A - 4	68.23	137.00	-0.35
5 - 4A	69.62	137.00	-0.32
5A - 5	69.62	137.00	-0.59
5B - 5A	45.31	120.59	-0.18
5C - 5B	66.96	135.46	-0.84
5D - 5C	66.57	135.46	-0.34
6 - 5D	65.72	135.46	-0.20
6A - 6	67.32	135.46	-0.51
6B - 6A	68.37	135.46	-0.28
7 - 6B	66.75	135.46	-0.52
8 - 7	75.07	135.46	-0.10
9 - 8	15.70	-29.01	0.48
10 - 9	62.98	138.50	-0.30
11 - 10	62.00	138.50	-0.27
12 - 11	63.52	138.50	-0.21
13 - 12	62.17	138.50	-0.48
15 - 13	62.40	138.50	-0.25
16 - 15	57.28	138.50	-0.14
17 - 16	60.26	138.50	-0.15
18 - 17	55.71	175.82	-0.59
19 - 18	62.26	141.50	-0.60
20 - 19	62.02	141.50	-0.30
21 - 20	6.41	-35.08	1.25
22 - 21	53.13	163.06	-0.85
23 - 22	55.61	144.90	-0.57
24 - 23	68.42	-47.75	-1.37
25 - 24	73.95	-99.03	-1.97
26 - 25	65.65	148.75	-0.48
27 - 26	66.17	-163.05	-1.40
28 - 27	67.52	152.50	-0.45
29 - 28	67.23	152.50	-0.32
30 - 29	67.23	152.50	-0.32
31 - 30	61.93	-67.66	-0.53
32 - 31	63.28	104.07	-0.48
33 - 32	80.22	-55.76	-0.87
33R - 33	84.08	-93.91	-1.72
34 - 33R	66.87	-44.15	-1.95

TABLE 2.4B

STAGE POLE ROTATION PARAMETERS -- NORTH ATLANTIC

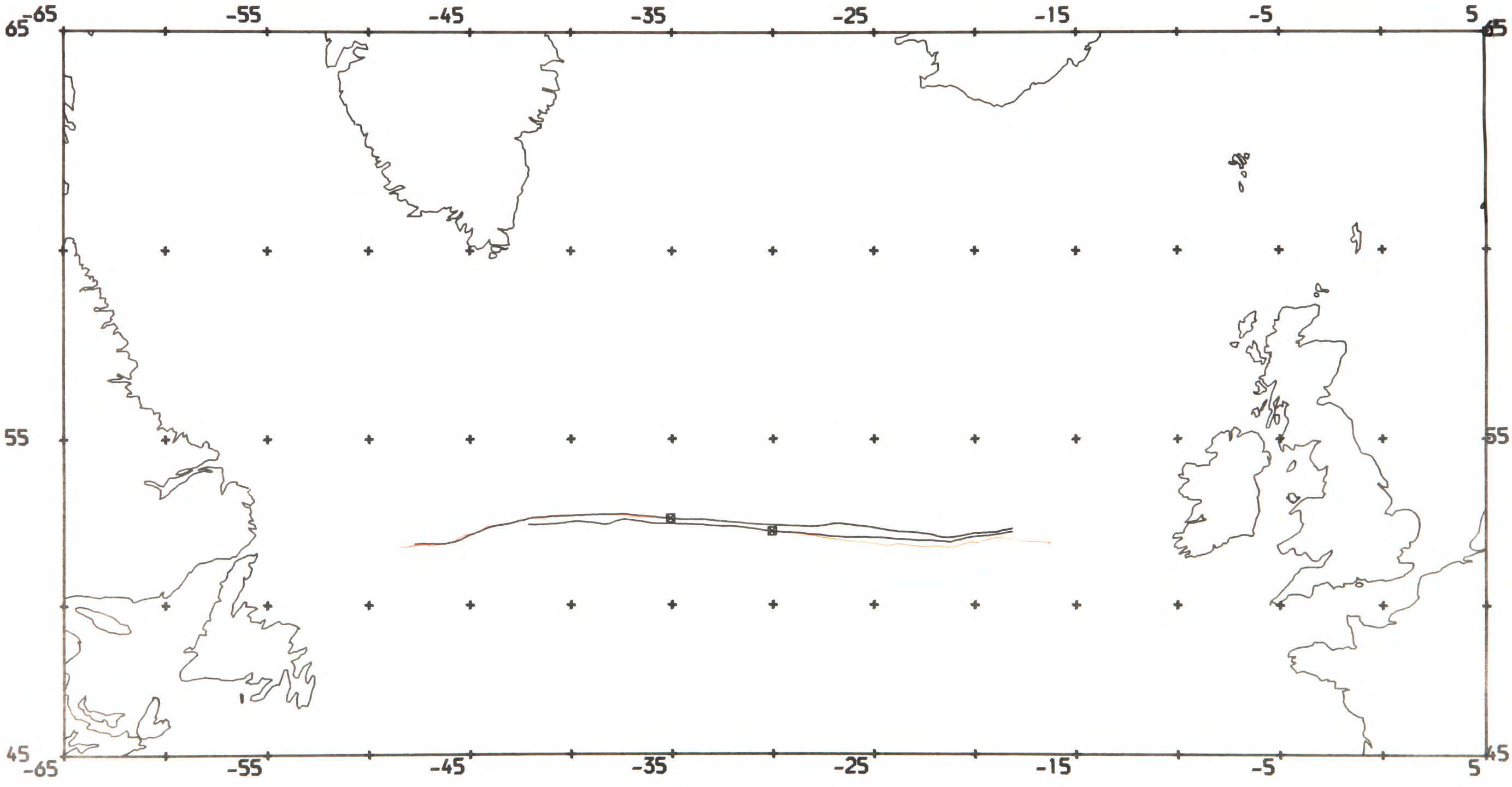
MOTION OF NORTH AMERICA WITH RESPECT TO EUROPE

ANOMALY	LATITUDE	LONGITUDE	ROTATION
2 - 1	68.00	137.00	0.41
2A - 2	66.04	137.00	0.21
3 - 2A	67.00	137.00	0.36
3A - 3	67.81	137.00	0.42
4 - 3A	67.86	137.00	0.34
4A - 4	68.23	137.00	0.35
5 - 4A	69.62	137.00	0.32
5A - 5	69.62	137.00	0.59
5B - 5A	45.02	122.25	0.18
5C - 5B	66.96	135.46	0.84
5D - 5C	66.56	135.46	0.34
6 - 5D	65.72	135.46	0.20
6A - 6	67.32	135.46	0.51
6B - 6A	68.37	135.46	0.28
7 - 6B	66.75	135.46	0.52
8 - 7	75.06	135.46	0.10
9 - 8	14.95	-22.92	0.48
10 - 9	62.98	138.50	0.30
11 - 10	62.00	138.50	0.27
12 - 11	63.52	138.50	0.21
13 - 12	62.17	138.50	0.48
15 - 13	62.40	138.50	0.25
16 - 15	57.28	138.50	0.14
17 - 16	60.26	138.50	0.15
18 - 17	57.97	178.44	0.59
19 - 18	62.26	141.50	0.60
20 - 19	62.02	141.50	0.30
21 - 20	5.83	-26.38	-1.25
22 - 21	55.04	163.99	0.85
23 - 22	55.61	144.90	0.57
24 - 23	68.42	22.45	1.37
25 - 24	78.54	-73.67	1.97
26 - 25	65.65	148.75	0.48
27 - 26	70.58	-159.44	1.40
28 - 27	67.52	152.50	0.45
29 - 28	67.23	152.50	0.32
30 - 29	67.23	152.50	0.32
31 - 30	64.92	-40.98	0.53
32 - 31	58.65	111.95	0.48
33 - 32	80.22	-0.24	0.87
33R - 33	86.50	-3.53	1.72
34 - 33R	66.87	-10.85	1.95

Figure 2.4 Kinematic Model: Synthetic Fracture Zone

A: Synthetic fracture zone (red) constructed from rotation parameters determined in this study (Tables 2.3 and 2.4). Overlain on the actual trace of the Charlie-Gibbs Fracture Zone (black) for comparison. Ridge positions are show by squares with x in center (black). The northern fracture valley trace is utilized on the west side and the southern fracture valley trace on the east side.
B: Same as A but with addition of anomaly positions shown by squares with + sign in center (blue).

A



B

65 -65 -55 -45 -35 -25 -15 -5 5 65

55

45 -65 -55 -45 -35 -25 -15 -5 5 45

justifies its use as the prime determinant of seafloor spreading directions in the North Atlantic is necessary. This section explains that rationale.

Two characteristics of the North Atlantic are the small offsets of ridge segments and the very slow spreading rate. The present rate of seafloor spreading in the North Atlantic, as well as for most of its history, is between 2 and 3 cm/yr. One consequence of slow spreading is variablity in the shape of magnetic anomalies due to the contamination of polarity blocks by dikes of different polarity. Another, is a thinner crust due to the solidification of magma at greater axial depths.

Side-scan sonar studies of fracture zones have shown that transform segments of small offset fracture zones have oblique rather than orthogonal geometries. The Kurchatov Fracture Zone is a good North Atlantic example, as is the FAMOUS area in the Central Atlantic (Searle, 1979). Motion in such segments is by oblique or asymmetric spreading rather than by transcurrent faulting. This seems to be a consequence of a thinned, weakened crust. In contrast, Charlie-Gibbs, which has the same spreading rate but a large offset, has an orthogonal ridge-transform-ridge geometry.

A different interpretation of the Kurchatov and FAMOUS area geometries is that they result from changes in plate boundaries. Reorganization of plate boundaries will commonly cause compression and extension across different areas of transform faults and fracture zones (Dewey, 1975). The Kurchatov Fracture

Zone and the FAMOUS area lie immediately north and south, respectively, of the western end of the Europe-Africa plate boundary, the Azores Triple Junction. Searle (1980) has suggested that this triple junction originally had an unstable ridge-transform-transform configuration for most of its history and only recently evolved to a stable ridge-ridge-ridge geomety. Movement of the triple junction could result in a reorientation of fault traces.

Which, if either, interpretation truly explains the lack of orthogonal geometry is unimportant in this instance. What is important is recognizing that the orientation of these small offset transforms and fracture zones is not indicative of the actual sea floor spreading direction.

Other considerations also bear on the reliance placed upon Charlie-Gibbs. These are the mode of deformation in fracture zones, the permanence of fracture zones, and the sediment thickness in the North Atlantic. Mapping fracture zones by their topographic expression becomes nearly impossible more than 700 - 800 km from the ridge crest because of the thick sediment wedge that covers the flanks of the Mid-Atlantic Ridge (Ewing et al., 1964). Locally, this sediment blanket is several kilometers thick (Emery and Uchupi, 1984, Chart VIA).

Near the Reykjanes Ridge, Vogt and Avery (1974), using detailed aeromagnetic data, recorded the presence of small offset transforms that seemed to form for a short period of time and then disappear. Their observation regarding the potential

ephemeral nature of transform faults and fracture zones is strongly opposed by Schouten and Klitgord (1982). In the Central Atlantic, also using a dense aeromagnetic survey, they were able to define Mesozoic sea floor spreading lineations. The frequent offset of the lineations was the basis for mapping fracture zones and assserting that present day plate boundary geometry (i.e. transform segmented) is inherited. In areas of insufficient magnetics coverage and thick sediment cover, offsets were mapped using seismic reflection data. The stronger relief of fracture zone basement strongly contrasts with that of normal ocean floor. Although neither the magnetic nor the seismic coverage of the North Atlantic is sufficient to resolve this controversy, a detailed survey in a small area (50 km^2) supports the latter view (White and Matthews, 1980).

The controlling influence of offset length and spreading rate on the mode of deformation was suggested by Fox and Gallo (1984). Large-offset fracture zones associated with slow spreading ridge systems, such as Charlie-Gibbs, have narrow, highly strained principal deformation zones. Faster spreading produces a more unstable principal deformation zone and, consequently, the plate boundary migrates. The difference is a product of interactions at the ridge-transform intersection.

The wedge of lithosphere created at an accretion axis proximal to a fracture zone forms a weld with the older, colder lithosphere across the ridge-transform interface. The strike-slip motion in the transform zone creates a shear couple across

this weld. The strength of the weld is predominantly a function of the thickness of the newly formed lithospheric wedge. The strength is greatest at slow-spreading ridges, especially those with large offsets. The stress induced by the transform motion needs to be greater and more localized to exceed the strength of the rocks. The result is that the deformation is confined to a narrow, well defined zone.

In summary, the North Atlantic lacks fracture zones that are easily mappable due to thick sediment cover, small offset between ridge segments, and possible disappearance with time. Detailed magnetic and seismic reflection data necessary to map possible continuations of offsets seen at the Mid-Atlantic Ridge are not currently available. Therefore, flow lines for any model of North Atlantic sea floor spreading must match the trace of the Charlie-Gibbs Fracture Zone.

2.5.3 Comparison With Other Models

There is a plethora of models for the kinematic and tectonic evolution of the Atlantic Ocean, particularly the North Atlantic. The earliest major study was that of Pitman and Talwani (1972), which employed the technique of matching pairs of magnetic anomalies from opposite sides of the ocean to recreate the positions of the continents at that particular time. Their results were presented as a set of (finite) poles and angles of rotation, which gave past continental positions and a further set of (stage or finite-difference) poles and angles, which gave the

path of relative continental motion.

Most ensuing work utilized a similar methodology and/or presented their results in a similar fashion. A generalized, rudimentary comparison of the most important of these studies is presented in Table 2.5.

Sclater et al. (1977) recognized the relationship between the age of oceanic lithosphere and its depth below sea level and used this relationship to reconstruct the spreading history of the Atlantic. Their reconstructions were presented graphically and by a series of poles and angles. They concluded that the age/depth relationship of ocean floors was sufficiently well defined to allow paleodepth contours to be used as isochrons. The importance of this study was that it provided future workers with an additional basis with which to evaluate their reconstructions, as well as providing a second quantitative dimension to constrain reconstructions.

The different evolution and kinematics of the South Atlantic (Africa-South America separation), Central Atlantic (Africa-North America separation), and North Atlantic (Europe-North America separation) was recogized early on. The South and Central Atlantic are relatively straight-forward and the most recent studies have achieved remarkably similar results (compare Klitgord and Schouten's (1986) rotation parameters with those of Pindell et al. (1988) for the Central Atlantic).

North Atlantic kinematics, in contrast, are quite complex and have been studied regionally (e.g. Kristoffersen and Talwani,

TABLE 1 COMPARISON OF KINEMATIC MODELS: NORTH AND CENTRAL ATLANTIC OCEAN

STUDY	METHODS AND DATA USED IN STUDY	REGIONS STUDIED * C.A.	N.A.	Arctic	Other	PRESENTATION OF DATA AND RESULTS Poles!	Anomalies/Age	Other Methods	COMMENTS
Williams & McKenzie (1971)	Magnetic anomalies, Seafloor features: Kings Trough, Peake and Freen Deeps	No	Yes, NE Atl. only	No	BOB	No	2,5,6,11,13, 20,21,24,25, 29,30,31-32	Lineation map, Reconstructions, Spreading Rates	Numbers anomalies 1-32, but notes uncertainty. Bay of Biscay thought to be older than 125 Ma. J Anomaly tentatively identified near Iberia. Discusses Kings Trough in relation to seafloor spreading.
Pitman & Talwani (1972)	Matching magnetic anomaly pairs with some fracture zone control	Yes	Yes	Yes, GRN EUR BS	BOB IBE	F&D	N.A. 5,13,21, 25,31*, 81Ma, plus KQZ & 155Ma in C.A.	Anomaly profiles, Spread-rates, Reconstructions	Anomaly 31 later reidentified as Anomaly 33 by Cande and Kristoffersen (1978). Starts from Bullard et al. (1965) fit. Fracture zones used to determine Anomaly 5 pole. Uses Heirtzler et al. (1968) timescale.
Phillips & Forsyth (1972)	Spreading rates from magnetic profiles, Paleomagnetic data	Yes	Yes	Yes, GRN LB SEA	S.A. BOB MED SEA CARIB	F&D	N.A. given in Ma 10,35,65, 105 plus 130, 150, & 200 in the C.A.	Reconstructions with paleolatitude, Polar wander paths	Starts from Bullard et al. (1965) fit. Assumes constant spreading rates and tries to hold pole positions steady. Poles are far different from most other studies of the Atlantic.
Williams (1975)	Magnetic anomalies, Seafloor features: North Spanish Trough, Biscay Seamounts	No	Yes, NE Atl.	No	BOB is objective of study.	No	2,5,6,13,18, 20,21,24,26, 27,31-32,32, 33,34	Lineation and contour maps of anomalies, Reconstructions	Suggests three-fold history for Biscay: NW-SE sinistral strikeslip (130-113 Ma), seafloor spreading (130-113 Ma) in Biscay with triple junction (80-73 Ma) and Biscay Seamounts as former ridge site, and northward compression (45-20 Ma).
Sclater et al. (1977)	Magnetic anomaly matching, Age-depth relationship and DSDP drilling data	Yes	Yes	Yes, LB SEA NO-GRN SEA	S.A. IBE CARIB	F&D	N.A. given in Ma 10,21,38, 53,80,95 plus 110,125,140 & 165 in C.A.	Paleobathymetric maps, Reconstructions	Tectonic history related to bathymetry of Atlantic. Bathymetry to provide framework for study of oceanic sedimentation. Starts from LePichon et al. (1977 fit with some modification. Uses Sclater et al. (1974) and Van Hinte (1976) time scales.
Kristoffersen & Talwani (1977)	Magnetic anomaly matching, Bathymetry, Gravity, Seismic reflection data	No	Yes	Yes LB SEA CAN AR	None	F&D	13, 21, 23	Lineation map, Reconstructions	Study of extinct triple junction south of Greenland. Incorporates varied geophysical data. Study is more limited in areal extent than others cited. Uses the Heirtzler et al. (1968) timescale.
Talwani & Eldholm (1977)	Magnetic anomalies, Bathymetry, Reflection and refraction seismic, Gravity, Fracture zones	No	Yes	Yes NO-GRN SEA	None	F&D	5,13,21,23, & initial opening between 24 and 25	Lineation map, Reconstructions, Spreading rates	Study of kinematic evolution of a small ocean basin. Matches ocean-continent boundaries to make initial reconstruction, but notes discrepancy between real and synthetic fracture zone traces. Notes Heirtzler et al. (1968) ages may be 5 - 10 m.y. too great.
Kristoffersen (1978)	Magnetic anomaly matching, Paleomagnetic data, Gravity data	No	Yes	Yes LB SEA NO-GRN SEA	BOB	F&D	24,33,34, & initial opening (pre-34)	Lineation map, Reconstructions	Discusses Charlie-Gibbs Fracture Zone and Rockall Trough. No J Anomaly near Newfoundland or Iberia. Notes Anomaly 33 mismatch near Iberia. Uses Larson & Pitman (1972) timescale and his own reconstruction.
Srivastava (1978)	Magnetic anomalies, Seismic reflection, Gravity, Seafloor features	No	Yes	Yes LB SEA NO-GRN SEA	None	F&D	21,24,25,28, 31,32,33	Lineation map, Anomaly profiles, Reconstructions	Study of kinematic evolution of a small ocean basin. Uses Heirtzler et al. (1968) timescale.
Olivet et al. (1984)	Magnetic anomaly matching, Seafloor features: Charlie-Gibbs, Rockall	Yes	Yes	Yes LB SEA	BOB IBE	F	N.A. 13,24, 33,pre-34,100 Ma, 110Ma and M22 in C.A.	Lineation map, Reconstructions	Study not available for complete review.
Bott (1985)	Magnetic anomaly matching, Gravity data	No	Yes	Yes NO-GRN SEA		F&D	26Ma 44Ma & 54Ma	Reconstructions	Study of the evolution of the Icelandic Transverse Ridge. Jan Mayen block moves independently from 44-26 Ma. Modifies Nunns (1983) rotation poles.
Klitgord & Schouten (1986)	Magnetic anomaly matching, Fracture zones, Seismic reflection and gravity data	Yes	No	No	S.A.	F&D	5,6,13,21,25, 30,32,33,33R, 34,92Ma,M0,M4 M10N,M16,M21, M25, and BSMA	Lineation map, Reconstructions, Fracture zones, Spreading rates	Presents various closure poles, including their own Detailed use of seismic reflection data to map positions of fracture zones near continental margins. Rotation poles provide basis for hypothesis that Iberia remains attached to Africa until Anomaly 10.
Srivastava & Tapscott (1986)	Magnetic anomaly matching, Seismic reflection data,	No	Yes	Yes LB SEA NO-GRN SEA	BOB IBE AFRICA	F&D	5,6,13,21,24, 25,30,31,33, 34,LB SEA fit Rockall fit	Lineation map, Reconstructions, Spreading rates	Presents hypothesis of short-lived "Porcupine Plate" to explain mismatch between anomalies in the Arctic and those near Iberia. Iberia as part of the African plate until Anomaly 10 time.

NOTES: *C.A.=Central Atlantic, N.A.=North Atlantic, S.A.=South Atlantic, GRN=Greenland, EUR BS=Eurasian Basin, LB SEA=Labrador Sea, NO-GRN SEA=Norwegian-Greenland Sea, CAN AR=Canadian Arctic, BOB=Bay of Biscay, IBE=Iberia, MED SEA=Mediterranean Sea, CARIB=Caribbean Sea, AFRICA=Africa
!F=Poles of finite rotation (reconstruction poles), D=Poles of finite-difference rotation (stage poles)

1977; Talwani and Eldholm, 1977; Srivastava, 1978; Bott, 1985), as well as with a more general perspective (e.g. Olivet et al., 1984; Srivastava and Tapscott, 1986). This complexity has lead to novel hypotheses being suggested to explain various aspects of North Atlantic evolution. These include the Porcupine Plate of Srivastava and Tapscott (1986) and connecting Iberia to Africa until post-Eocene time (Schouten et al., unpub. mans.).

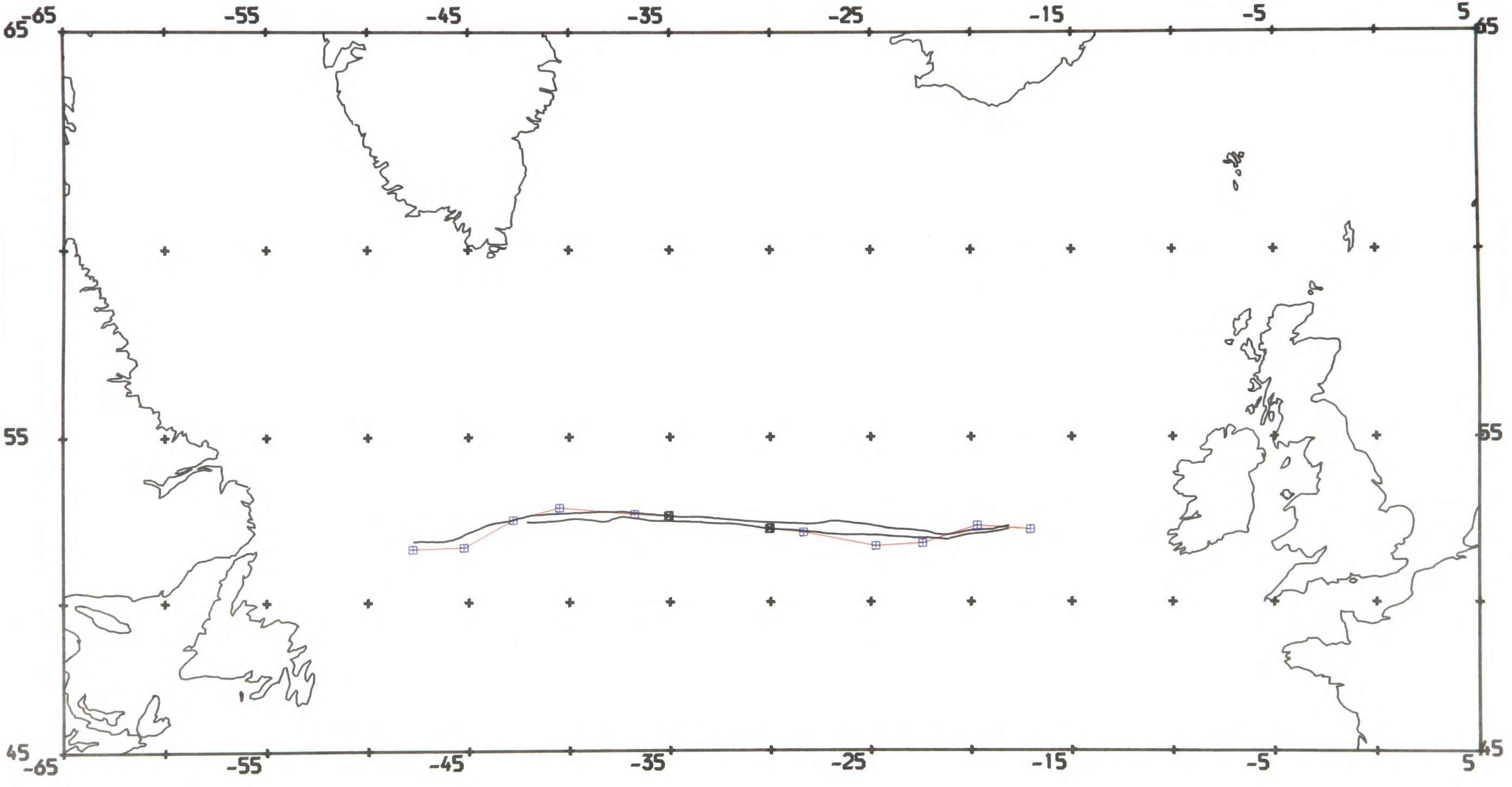
The Charlie-Gibbs Fracture Zone and the importance attached to it (see 2.5.2 above) provides a basis for comparison between models that is independent of all other considerations. The finite poles given in the various models (Tables 2.2 and 2.5) were used to compute stagepole parameters, which, in turn, were used to construct synthetic fracture zone traces. These were then plotted using the ridge positions adjacent to Charlie-Gibbs as starting points and overlain on the trace of the fracture zone. Because Charlie-Gibbs is a double fracture zone, the northern fracture valley was used to compare the fit west of the Mid-Atlantic Ridge and the southern fracture valley the fit on the eastern side. The results, shown in Figures 2.5 to 2.13, are discussed below.

2.5.3a Pitman and Talwani's Model (1972)

This was the first kinematic model to use the technique of matching magnetic anomalies from opposite sides of an ocean to make continental reconstructions. Given the relatively small amount of data available at the time, the model was immensely successful. The synthetic fracture zone derived from the model

Figure 2.5 Pitman and Talwani (1972): Synthetic Fracture Zone

Synthetic fracture zone (red) contructed from the published rotation parameters of Pitman and Talwani (1972), overlain on the Charlie-Gibbs Fracture Zone (black) for comparison. Anomaly positions are shown by squares with + in center (blue) and ridge positions by squares with x in center (black). Anomalies used are 5, 13, 21, 25, 33 (originally identified as 31).


-65
-55
-45
-35
-25
-15
-5
5
65
55
45

nearly parallels the shape of Charlie-Gibbs, with Anomaly 5 falling directly on its trace and Anomaly 21 nearly so (Figure 2.5). The finite pole position for Anomaly 5 used in this study and by Srivastava and Tapscott (1986) is the same as in this model. Similarly, the rotation parameter for Anomaly 21 in this study is modified by less than 1° from that of Pitman and Talwani and many other models use a pole with approximately the same coordinates (Table 2.2).

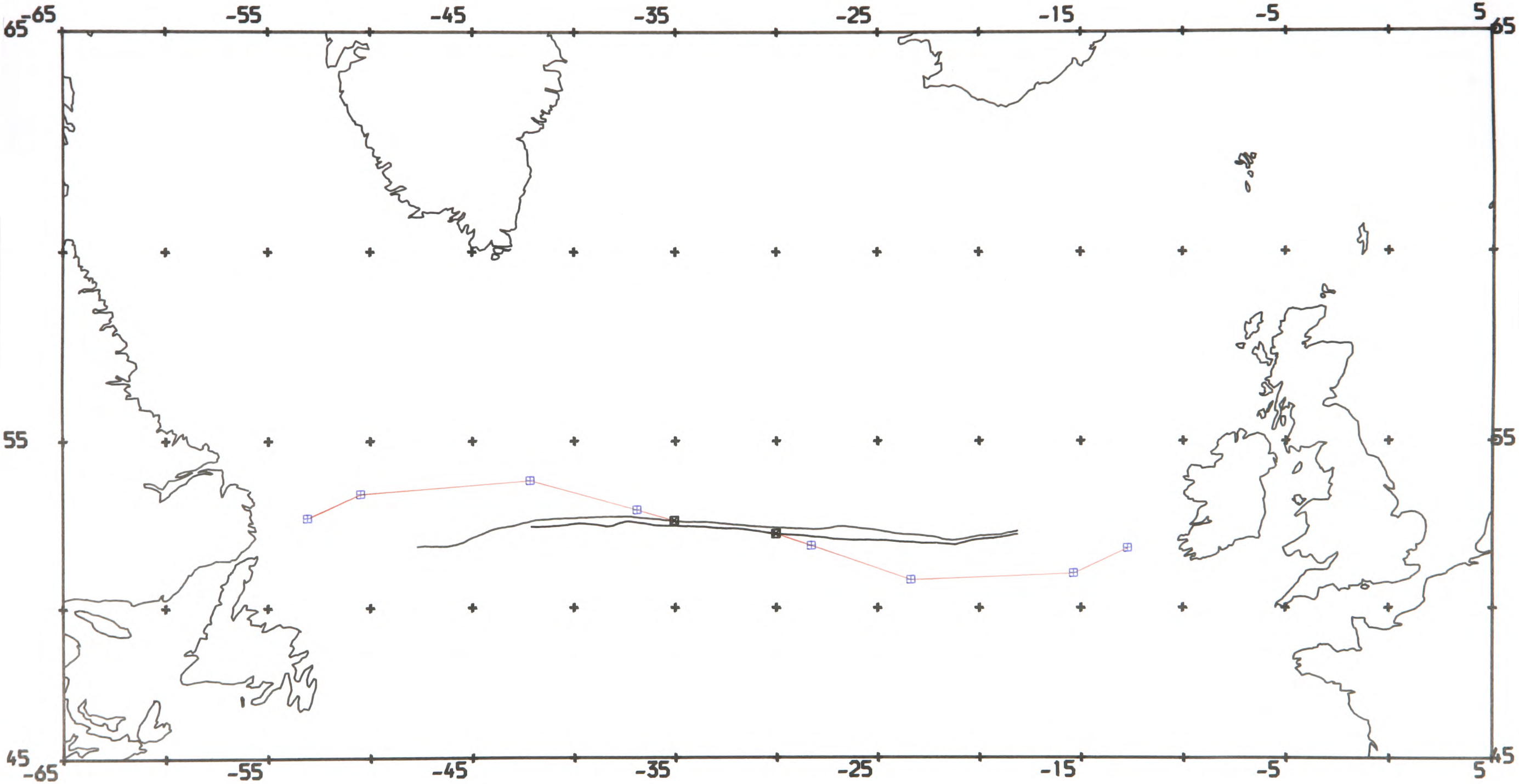
The amount of displacement from Charlie-Gibbs for Anomalies 13, 25, and 33 (originally identified as 31) is on the order of 50 to 75 km. The fit on the western side is generally better than on the eastern side. This is true of all models tested, including this study. Thick sediment cover, rifted continental crust of Rockall Bank, and the possibility of an older spreading center in the region of Rockall Trough complicate the bathymetry, making the eastern portion of the fracture zone difficult to map.

2.5.3b Philips and Forsyth's Model (1972)

This model used available magnetic anomaly data to work out spreading rates and supplemented this with paleomagnetic data to work out continental positions at various times. The poles used were derived starting from Bullard et al.'s (1965) pole of total average motion. It is immediately apparent from Figure 2.6 that the positions and flow lines of the continents are seriously misrepresented. The synthetic fracture zone traces are misplaced from Charlie-Gibbs by up to 400 km (Anomaly 28R).

Figure 2.6 Philips and Forsyth (1972): Synthetic Fracture Zone

Synthetic fracture zone (red) contructed from the published rotation parameters of Philips and Forsyth (1972), overlain on the Charlie-Gibbs Fracture Zone (black) for comparison. Anomaly positions are shown by squares with + in center (blue) and ridge positions by squares with x in center (black). Anomalies used are 5, 13, 28R, and 105 Ma.


65
-65
-55
-45
-35
-25
-15
-5
5
55
45

Philips and Forsyth's paper was published three months after Pitman and Talwani (1972), in the same journal, but is rarely cited. Given the results shown here, it is understandable why this is so. It is included here for the sake of completeness and as an example of the attempt to merge the paleomagnetic and magnetic anomaly data bases, as they existed at that time.

2.5.3c Sclater, Hellinger, and Tapscott's Model (1977)

As noted above, this model added another dimension to kinematic modeling by using the age/depth relationship for the ocean floors to assist in making the reconstructions. The Mid-Atlantic Ridge was rotated to determine isochrons and paleobathymetric contours rather than matching magnetic anomalies directly. The fit of the synthetic fracture zone to Charlie-Gibbs shows an improvement on Pitman and Talwani's pole for Anomaly 13 but not for any other anomalies (Fig 2.7). In general, the shape of the synthetic fracture zone shows less parallelism with Charlie-Gibbs than that of Pitman and Talwani (1972).

2.5.3d Savostin's Model (1981)

The data on which this comparison is based was taken from Tables 1 and 3 Savostin et al. (1986), although the rotation parameters are from Savostin's thesis. The rotation angles for Anomalies 6, 13, and 24 are given with error bars but none are given for Anomaly 5. A second Anomaly 24 pole from work in preparation is also given. Synthetic fracture zone traces using both Anomaly 24 poles are presented in Figure 2.8.

It is evident from Figure 2.8 that, except for Anomalies 5 and

Figure 2.7 Sclater et al. (1977): Synthetic Fracture Zone

Synthetic fracture zone (red) contructed from the published rotation parameters of Sclater et al. (1977), overlain on the Charlie-Gibbs Fracture Zone (black) for comparison. Anomaly positions are shown by squares with + in center (blue) and ridge positions by squares with x in center (black). Anomalies used are 5, 6, 13, 22, 29, and 34.

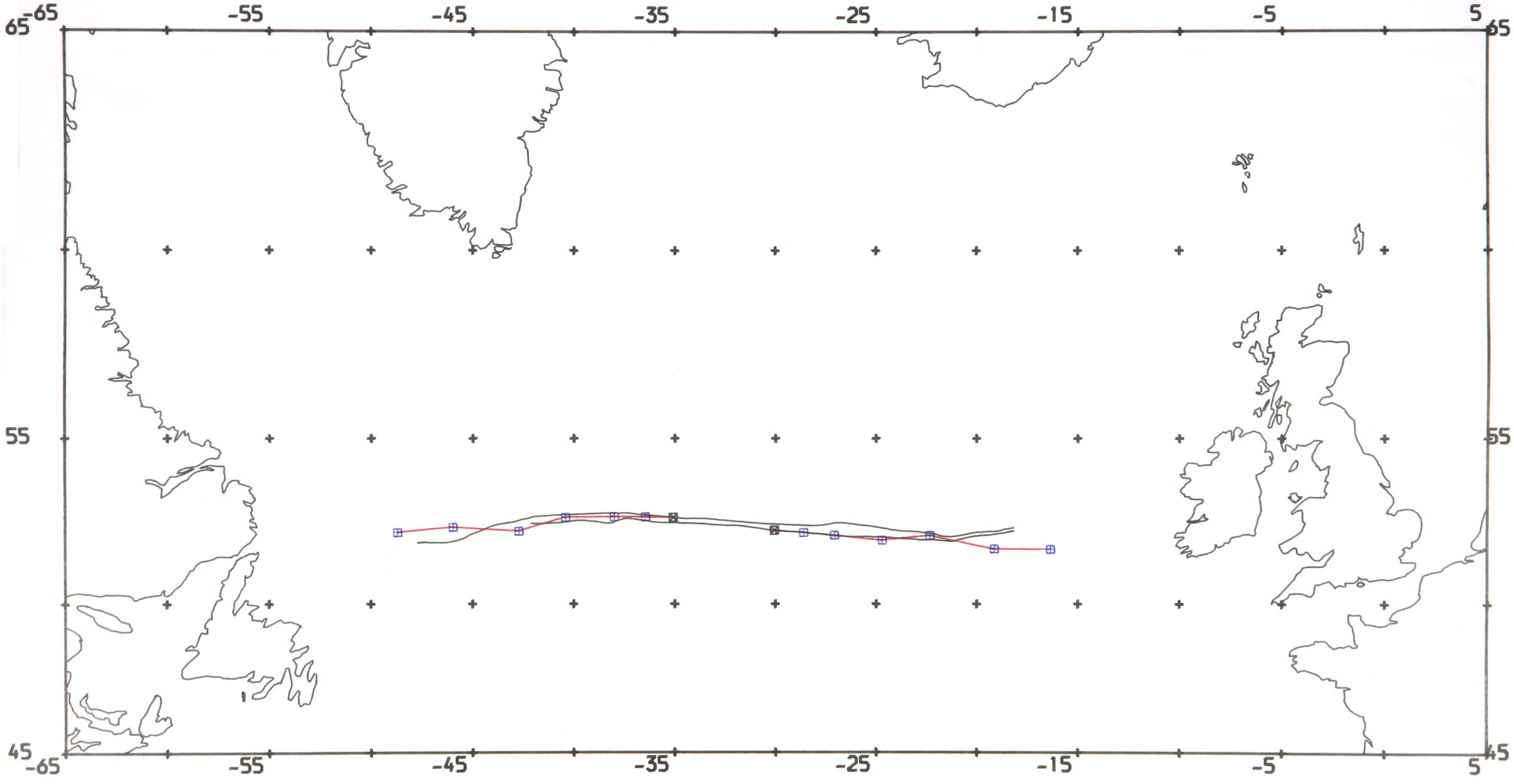

65
-65
-55
-45
-35
-25
-15
-5
5
55
45

Figure 2.8 Savostin (1981): Synthetic Fracture Zones

Synthetic fracture zones (red) contructed from the published rotation parameters of Savostin (1981), overlain on the Charlie-Gibbs Fracture Zone (black) for comparison. Anomaly positions are shown by squares with + in center (blue) and ridge positions by squares with x in center (black). Anomalies used are 5, 6, 13, and 24 for which 2 poles given (see Table 2.2). The different poles for Anomaly 24 are shown in A and B. Note that there is very little difference between the positions.

A

65 -65 -55 -45 -35 -25 -15 -5 5 65

55

45 -65 -55 -45 -35 -25 -15 -5 5 45

B

65 -65 -55 -45 -35 -25 -15 -5 5 65

55

45 -65 -55 -45 -35 -25 -15 -5 5 45

6, the poles used by Savostin do not produce an acceptable solution. The synthetic fracture zone trace is a nearly straight line that trends 100°-280°. The tendency to produce solutions that diverge increasingly from Charlie-Gibbs seems to be typical of models that rely predominantly on data from the Arctic (see 2.5.3g below). It also points out a problem inherent in North Atlantic kinematic models, namely the relationship between the Arctic, where seafloor spreading commenced in the Eocene (Anomaly 24), and the area to the south where seafloor spreading began in the Cretaceous.

2.5.3e Olivet, Bonnin, Beuzart, and Auzende's Model (1984)

The synthetic fracture zone for this model is shown in Figure 2.9. The poles given in the model are augmented by a pole for Anomaly 21 attributed by Savostin et al. (1986) to Olivet et al. (1984) (see Table 2.2, Note f). The fit of Anomaly 13 to Charlie-Gibbs is excellent althought the trace between it and the ridge crest is not aligned with the fracture zone. This could be remedied easily by using additional anomalies. Beyond Anomaly 13, the fit becomes less satisfactory, with the synthetic traces lying north and south of the actual fracture zone and not reflecting its changes in orientation.

2.5.3f Livermore and Smith's Model (1985)

This model is a compilation of rotation parameters taken from Talwani and Eldholm (1977), Kristoffersen and Talwani (1977), and Kristoffersen (1978) and given in Livermore and Smith (1985, Table 5.2). The parameters are examined here because of the close relationship between the workers who determined them and

Figure 2.9 Olivet et al. (1984): Synthetic Fracture Zone

Synthetic fracture zone (red) contructed from the published rotation parameters of Olivet et al. (1984), overlain on the Charlie-Gibbs Fracture Zone (black) for comparison. Anomaly positions are shown by squares with + in center (blue) and ridge positions by squares with x in center (black). Anomalies used are 13, 21*, 24, 33, and 34. *See Table 2.2, Note d, concerning the rotation parameters for this anomaly.

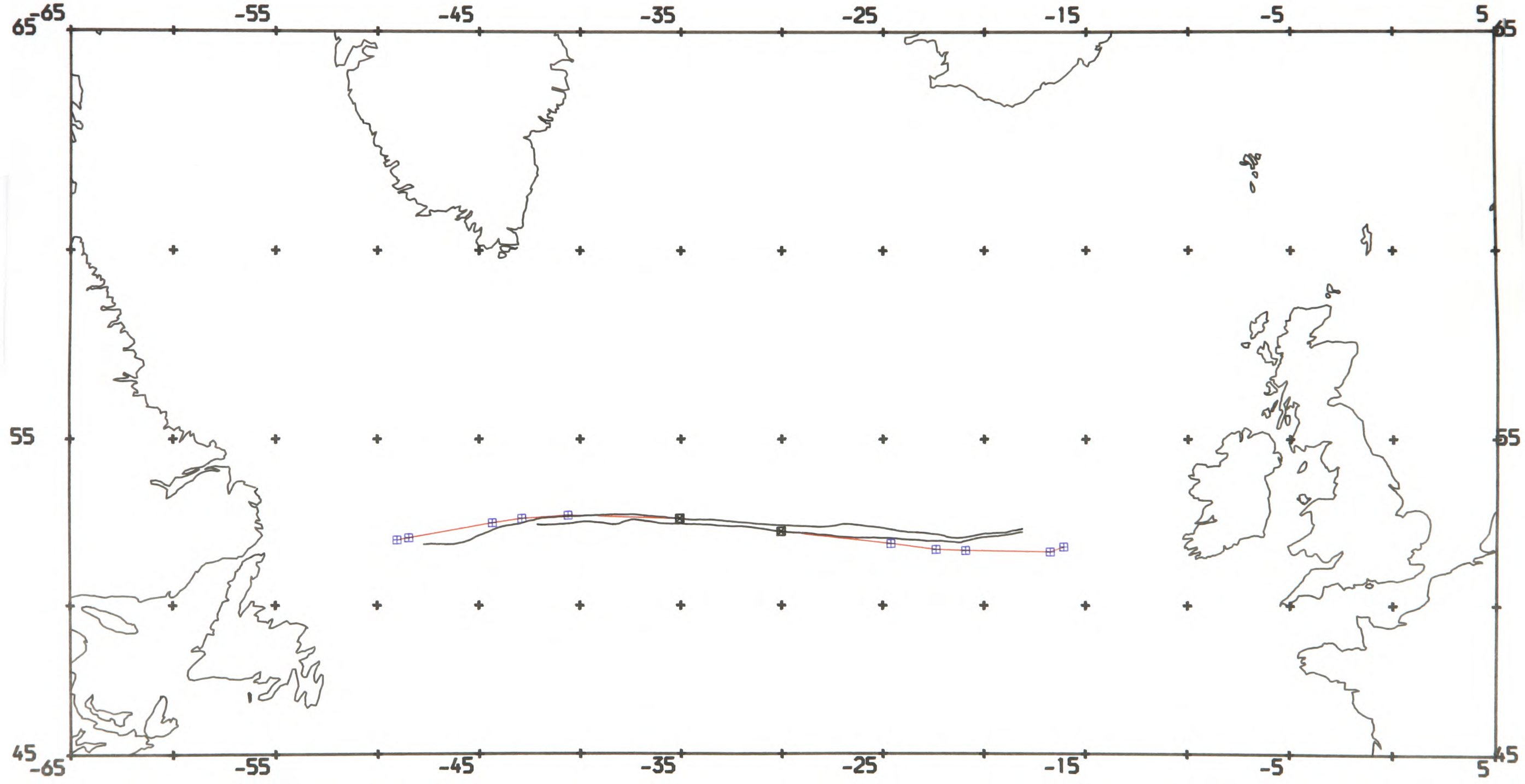
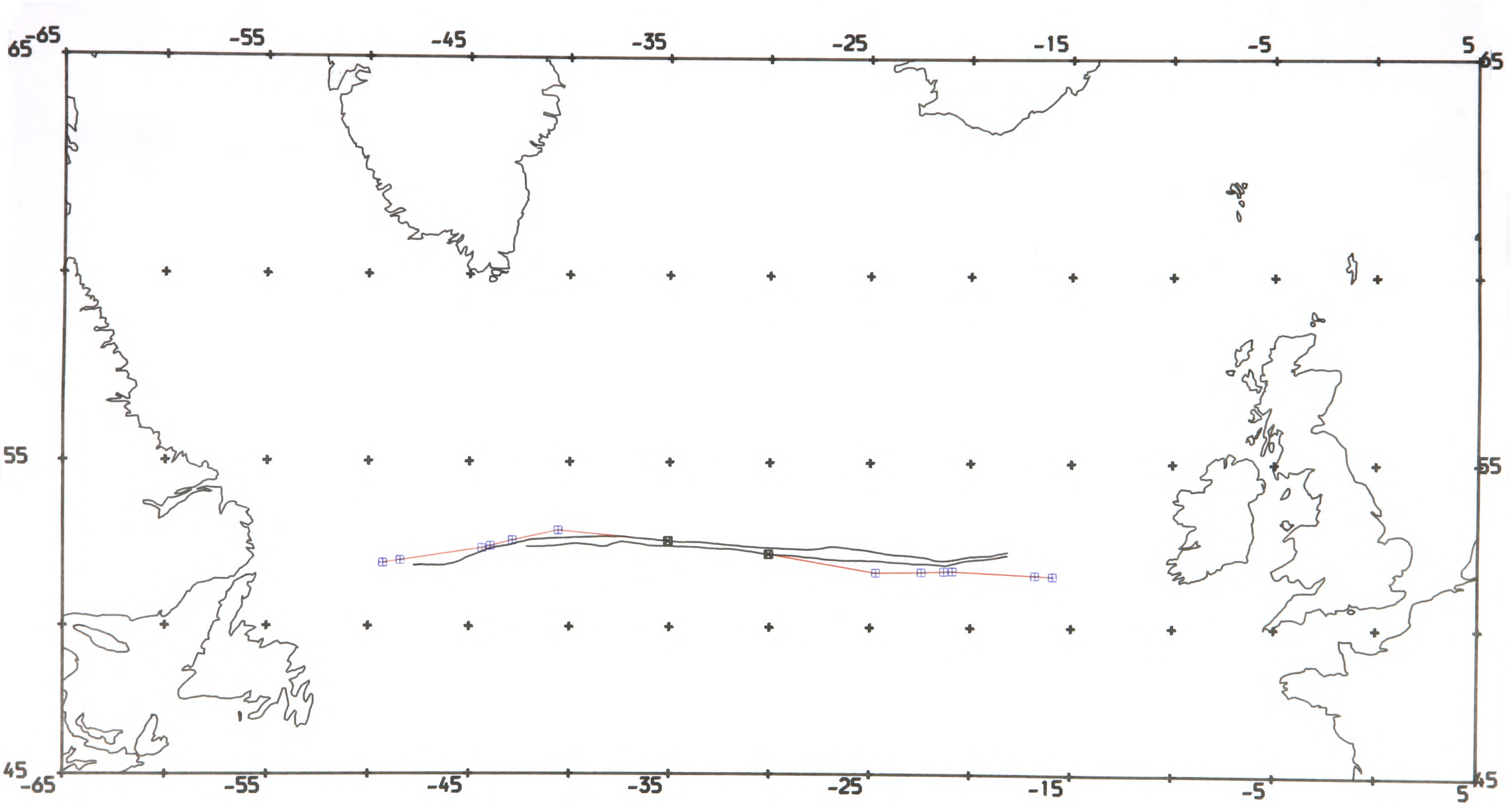

65
-65
-55
-45
-35
-25
-15
-5
5
55
45

Figure 2.10 Livermore and Smith (1985): Synthetic Fracture Zone

Synthetic fracture zone (red) contructed from the published rotation parameters of Livermore and Smith (1985), overlain on the Charlie-Gibbs Fracture Zone (black) for comparison. Anomaly positions are shown by squares with + in center (blue) and ridge positions by squares with x in center (black). Anomalies used are 13 (Talwani and Eldholm, 1977), 21, 23 (Kristoffersen and Talwani, 1977), 24, 33, and 34 (Kristoffersen, 1978).


65
-65
-55
-45
-35
-25
-15
-5
5
55
45

because Livermore and Smith used them in deriving a relative motion path for Africa with respect to Europe.

The synthetic fracture zone trace parallels the northern fracture valley of Charlie-Gibbs for a short distance west of the ridge crest and for a shorter distance on the eastern segment of the southern fracture valley (Fig. 2.10). Beyond this point, the synthetic fracture zone falls north (west side) or south (east side) of Charlie-Gibbs. However, it is noted that Anomalies 21, 23, and 24 are not displaced nearly as much as Anomalies 33 and 34, especially on the western side. The fit for Anomaly 13 is poorer than that of many of the models discussed previously with the exception of Philips and Forsyth (1972). When evaluating Livermore and Smith's model for Africa's motion with respect to Europe (see 4.3.4) the generally better fit at Anomalies 21, 23, and 24 than at 33 and 34 should be kept in mind.

2.5.3g Bott's Model (1985)

This model deals with the limited region of the Iceland Transverse Ridge and attempts to explain the evolution of this feature and that of the region immediately to the north in which the Jan Mayen microcontinent is located. As with Savostin (1981), the pattern of the synthetic fracture zone is one of increasing displacement with age from Charlie-Gibbs (Fig. 2.11).

2.5.3h Savostin, Sibuet, Zonenshain, Le Pichon, and Roulet's Model (1986)

This model is also a compilation of rotation parameters from various sources, some but not all from Savostin (1981). They are published in Table 3 of Savostin et al. (1986). The results are

Figure 2.11 Bott (1985): Synthetic Fracture Zone

Synthetic fracture zone (red) contructed from the published rotation parameters of Bott (1985), overlain on the Charlie-Gibbs Fracture Zone (black) for comparison. Anomaly positions are shown by squares with + in center (blue) and ridge positions by squares with x in center (black). Anomalies used are 7, 20, and 24.

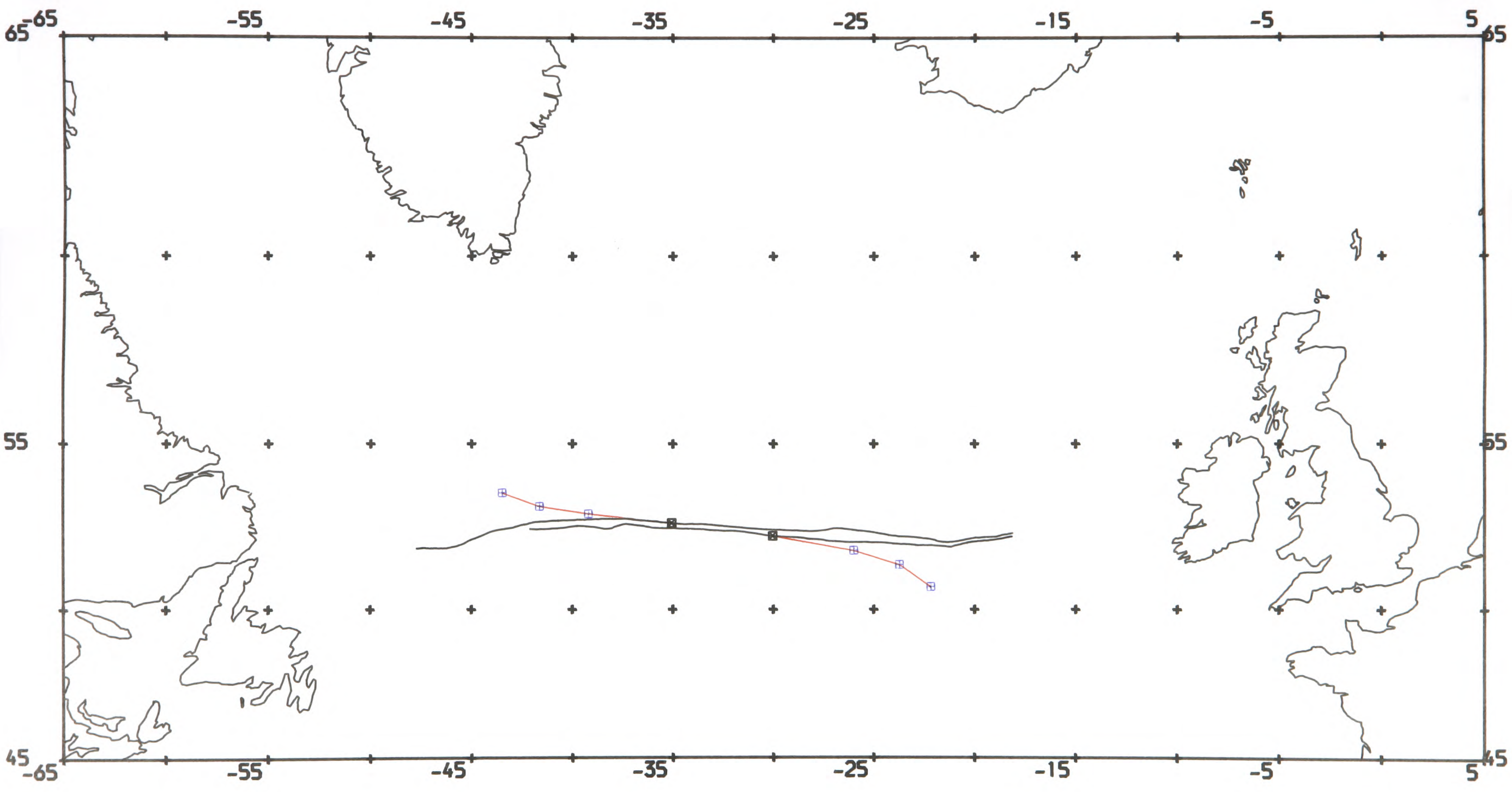
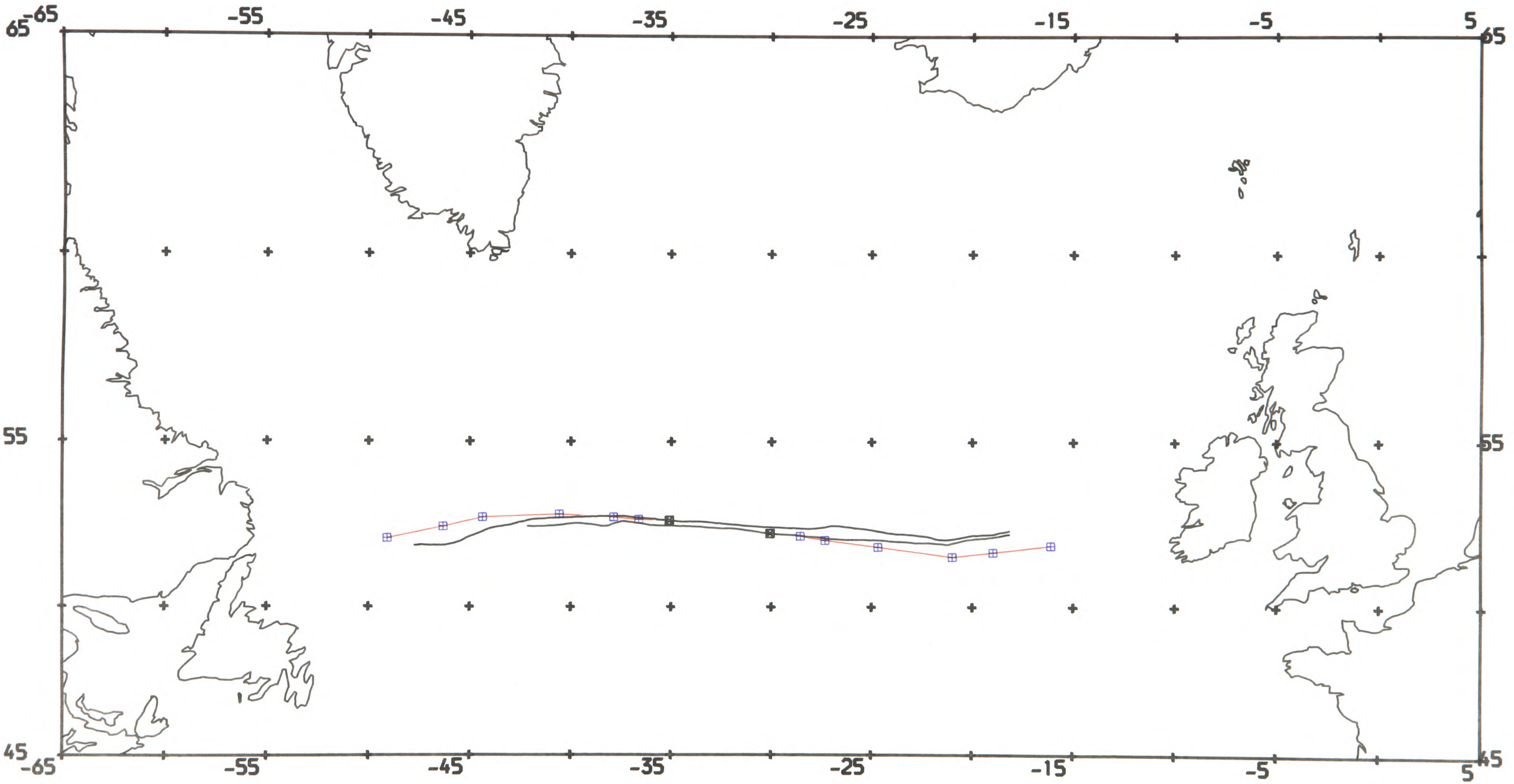

65
-65
-55
-45
-35
-25
-15
-5
5
55
45

Figure 2.12 Savostin et al. (1986): Synthetic Fracture Zone

Synthetic fracture zone (red) contructed from the published rotation parameters of Savostin et al. (1986), overlain on the Charlie-Gibbs Fracture Zone (black) for comparison. Anomaly positions are shown by squares with + in center (blue) and ridge positions by squares with x in center (black). Anomalies used are 5, 6, 13, 24, 30, and 34.


65
-65
-55
-45
-35
-25
-15
-5
5
55
45

analyzed here because these parameters, and a similar compilation for the Central Atlantic, were used to determine Africa's motion with respect to Europe.

The synthetic fracture zone trace for this model, shown in Figure 2.12, is similar to that for the Savostin (1981) model (2.5.3d) although the use of different poles for Anomalies 13 and 24 changes their positions slightly. The trend of the synthetic fracture zone changes at Anomaly 24 to a trend of 078°-258°. The anomalies from 24 to 34 are strongly displaced from the synthetic fracture zone.

2.5.3i Srivastava and Tapscott's Model (1986)

This model is predicated upon a mismatch of the magnetic anomalies off the coast of Iberia that occurs if anomalies are matched from the Eurasian Basin to the Azores-Gibraltar Plate Boundary and on the close relationship between the motions of Iberia and Africa prior to Anomaly 10 (Schouten et al., unpub. ms.). Specifically, Iberia is treated as a part of Africa from the Triassic until Anomaly 10. The mismatch of anomalies is indirectly attributed to intraplate deformation (or deformation at previously existing boundaries) and a novel hypothesis involving the creation of a new, entirely oceanic microplate by a finite difference rotation, is used to resolve the difficulty. This new microplate is called the Porcupine Plate because it lies near the Porcupine Bank to the southwest of the British Isles. The Porcupine Plate is considered to have come into existence sometime between Anomaly 25 and Anomaly 21 (Srivastava and

Figure 2.13 Srivastava and Tapscott (1986): Synthetic Fracture Zones

Synthetic fracture zones (red) contructed from the published rotation parameters of Srivastava and Tapscott (1986) for the Eurasian Plate (A) and the Porcupine Plate (B) (see text for explanation), overlain on the Charlie-Gibbs Fracture Zone (black) for comparison. Anomaly positions are shown by squares with + in center (blue) and ridge positions by squares with x in center (black). Anomalies used are 5, 6, 13, 21, 24, 25, 30, 31, 33 and 34.

B

-65 -55 -45 -35 -25 -15 -5 5

65

55

45

B

65 -65 -55 -45 -35 -25 -15 -5 5 65

55

45 -65 -55 -45 -35 -25 -15 -5 5 45



Tapscott, 1986).

A mismatch of magnetic anomalies near Iberia was first noted by Kristoffersen (1978) in making his reconstruction for Anomaly 33. He ascribed the cause of this offset to a subsequent rotation of Iberia, probably related to the Pyrenean Orogeny. Significantly, neither in his reconstruction for Anomaly 34 nor in his discussion of the poles and reconstructions for Anomaly 24 is there any further mention of this problem.

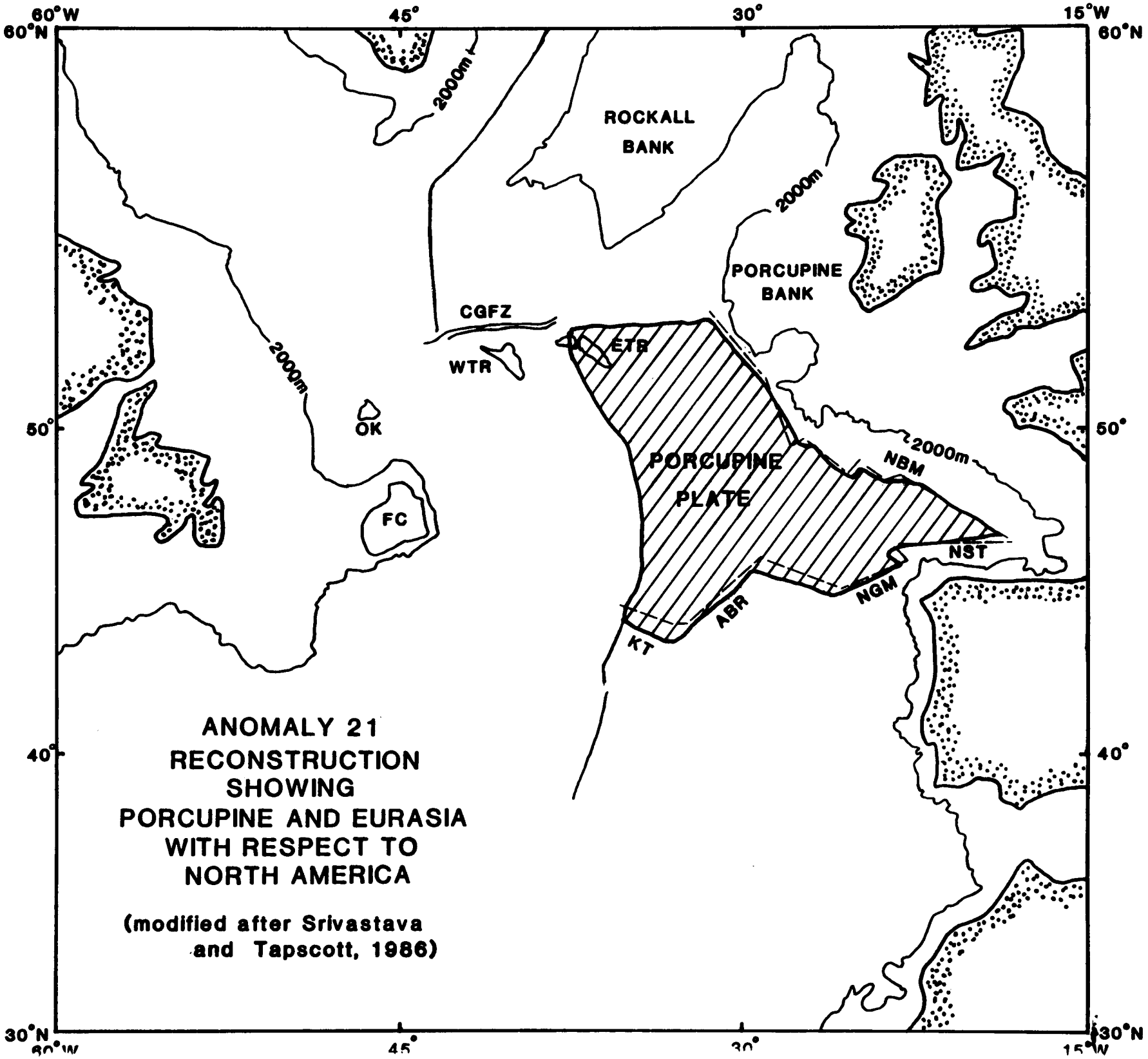
The Porcupine Plate solution imposes a finite difference rotation on all anomalies older than Anomaly 13 (35 Ma) to correct this misalignment. The finite difference between the rotation of Eurasia with respect to North America and North America with respect to Porcupine is a rotation of 1.15° about a pole at 57.1°N, 5.3°E for Anomaly 21 and 1.8° about a pole at 56.2°N, 8.6°E for anomalies older than 21.

Synthetic fracture zones were constructed using the poles given for each (Fig. 2.13). It is clear from this figure that the fit of the Porcupine Plate poles to Charlie-Gibbs is far better than those for the Eurasian Plate. The anomaly positions lie close to, and the general shape of the synthetic fracture zone is very similar to, the fracture zone. The questions that must be answered are: what is the exact nature of the Porcupine Plate and what is the evidence for it?

Figure 2.14 shows Srivastava and Tapscott's (1986) Anomaly 21 reconstruction, with the Porcupine Plate and its boundaries highlighted. What is of particular importance about this figure

Figure 2.14 Boundaries of the Porcupine Plate

Reconstruction showing the boundaries of the Porcupine Plate as reconstructed at Anomaly 21 using rotation parameters of Srivastava and Tapscott (1986). Note that eastern boundary is continental margin on the northern edge of the Bay of Biscay. Difference in position when Eurasian Plate parameters are used implies extension across King's Trough and compression along the North Biscay margin. However, although evidence for the latter may exist (Montadert et al., 1979) currently available data suggests that the main events in the formation of King's Trough are Miocene in age (Shipboard Scientific Party, 1987; Kidd and Ramsay, 1987).
Legend: Heavy black line = boundary of Porcupine Plate rotated to North American frame of reference; Thin dashed line = boundary of Porcupine Plate rotated to North American frame of reference with parameters for Eurasia; CGFZ = Charlie-Gibbs Fracture Zone; WTR = West Thulean Rise; ETR = East Thulean Rise; OK = Orphan Knoll; FC = Flemish Cap; NBM = North Biscay Margin; NST = North Spanish Trough; NGM = North Galicia Margin; ABR = Azores-Biscay Rise; KT = King's Trough; Rockall Bank, Porcupine Bank, and 2000m isobath as shown.



ANOMALY 21
RECONSTRUCTION
SHOWING
PORCUPINE AND EURASIA
WITH RESPECT TO
NORTH AMERICA

(modified after Srivastava
and Tapscott, 1986)

is the location and nature of the plate boundaries. The western and northern boundaries are formed by the Mid-Atlantic Ridge and the Charlie-Gibbs Fracture Zone, respectively. These correspond to present day boundaries and pose no problem. However, the eastern and southern boundaries are more problematic as they are not the typical boundaries described in the plate tectonic model.

The eastern boundary coincides with the northern margin of the Bay of Biscay, a passive continental margin formed in the early Cretaceous (Montadert et al., 1979). The southern margin is complex and consists of the King's Trough, the Azores-Biscay Rise, the North Galicia Margin, and the North Spanish Trough. The difference in the positions of the Porcupine and Eurasian Plates in Srivastava and Tapscott's Anomaly 21 reconstruction (Fig. 2.14) implies varying amounts of extension, strike-slip and compression along the North Biscay margin. Evidence for Eocene compression and strike-slip are mostly present along the Trevelyan Escarpment, but this model predicts the greatest compression to the east. Post-Aptian subsidence in Biscay is thermally driven, with no new extensional faults or fault reactivation (Montadert et al., 1979) as the model predicts.

Along the southern boundary, the difference in positions implies extension across King's Trough, although stratigraphic evidence suggests that the major tectonic events involved in its formation were younger (Shipboard Scientific Party, 1987). Transtensional motion is predicted along the Azores-Biscay Rise, although there is no evidence to support this (see 2.4.2b).

In summary, the Porcupine Plate model seems to present as many problems as it attempts to solve despite a reasonably good fit of these parameters to Charlie-Gibbs because there is little geological evidence for Iberia remaining attached to Africa from the Jurassic until Anomaly 10. The collapsed continental margin (Mesozoic) of the Betic Cordillera in southern Spain includes metabasites whose geochemistry is typical of ophiolitic suites found in oceanic fracture zones (Bodinier et al., 1987) and Atlantic Triassic fauna in Alpujarride carbonates (Martin and Braga, 1987). These are only two of the lines of evidence that argue against this hypothesis (see 6.3).

2.5.3j Discussion

It is clear from the variations in models for the kinematic evolution of the North Atlantic that no unique solution exists, or is likely to exist, without a much larger data base. As suggested by Srivastava and Tapscott (1986), the question, at present, is where to locate present or past plate boundaries or zones of intra-plate deformation to account for the inability to match magnetic anomalies from the Eurasian Basin to the Azores-Gibraltar Plate Boundary, while satisfactorily explaining the evolution of the North Atantic.

Examination of the synthetic fracture zones for Bott's (1985) model (Fig. 2.11) and Savostin's (1981) models (Fig. 2.8), the fanning magnetic anomaly pattern observed in the Jan Mayen region (Nunns, 1982; Nunns and Peacock, 1982), and fracture zone orientations, particularly the East Jan Mayen Fracture Zone,

north of Iceland (Laughton and Monahan, 1978) combine to suggest a plate boundary in this region. The Jan Mayen Fracture Zone itself is a possible boundary because fault plane solutions for the Mohns Ridge to the north and the Kolbeinsey Ridge to the south differ (Savostin and Karasik, 1981). The search for such a boundary is, however, beyond the scope of this work.

2.6 Discussion of the Kinematic Model

One of the major differences between this study and others is the use of nearly all Late Cretaceous and Tertiary magnetic anomalies to define the kinematics of the North Atlantic. The advantage of reducing the time interval between poles of rotation is that it permits greater control of rotation parameters by assuring that they follow the direction of seafloor spreading; i.e., that flow lines are parallel to fracture zones. This advantage is clearly seen by comparing Figure 2.4 with Figures 2.5 - 2.13. Although it is preferable to have several large-offset, slow-slipping fracture zones to act as guides (see 2.5.2), this is not the situation in the North Atlantic. Just how much the use of more anomalies compensates for the absence of fracture zones is uncertain.

The use of magnetic anomalies not generally considered points out that one of the assumptions upon which many models are based can be called into question. The assumption referred to holds that pole changes and changes in rate of seafloor spreading occur

at the anomalies used in the study. The timing of pole changes in this work suggests that this is not the case (Table 2.3, Fig. 2.15).

Furthermore, detailed study of fracture zones using SEABEAM, GLORIA and data gathered from submersibles calls into question the practice of defining pole changes at anomalies. The complex structure and morphology exhibited by some fracture zones, particulary alternating nodal basins and ridges within the main transform tectonized zone, reflects changing amounts of ridge volcanism and very slight changes in spreading orientation (B. Tucholke, pers. comm.). It might be better to look carefully at orientation changes in structural features to determine when pole changes occur. The alternating nodal basins and ridges can be indirectly interpreted as changes in rates of seafloor spreading.

Spreading rates are generally calculated along, or parallel to, a magnetic anomaly line with time plotted against distance. Average spreading rates are calculated from the slope of lines connecting various segments. However, the solutions are not always unique (Srivastava and Tapscott, 1986, Fig. 3). This lack of uniqueness may be partly due to lack of fracture zones so that spreading rate is not calculated parallel to spreading direction.

Another reason for apparent lack of uniqueness, even when there is good fracture zone control, is different spreading rates on opposite sides of a fracture zone. Figure 2.16a presents detailed magnetic data from a survey of a small region in the eastern North Atlantic in which an unknown fracture zone was

Figure 2.15 Changes in Pole of Rotation: North Atlantic Ocean

Pole changes in the North Atlantic are shown plotted on the geological time scale. The Berggren et al. (1985) timescale is used for the Cenozoic and the Kent and Gradstein (1985) timescale for the Mesozoic. Also shown is the curve of coastal onlap of Haq et al. (1987) and the correlation between pole changes and sequence boundaries.

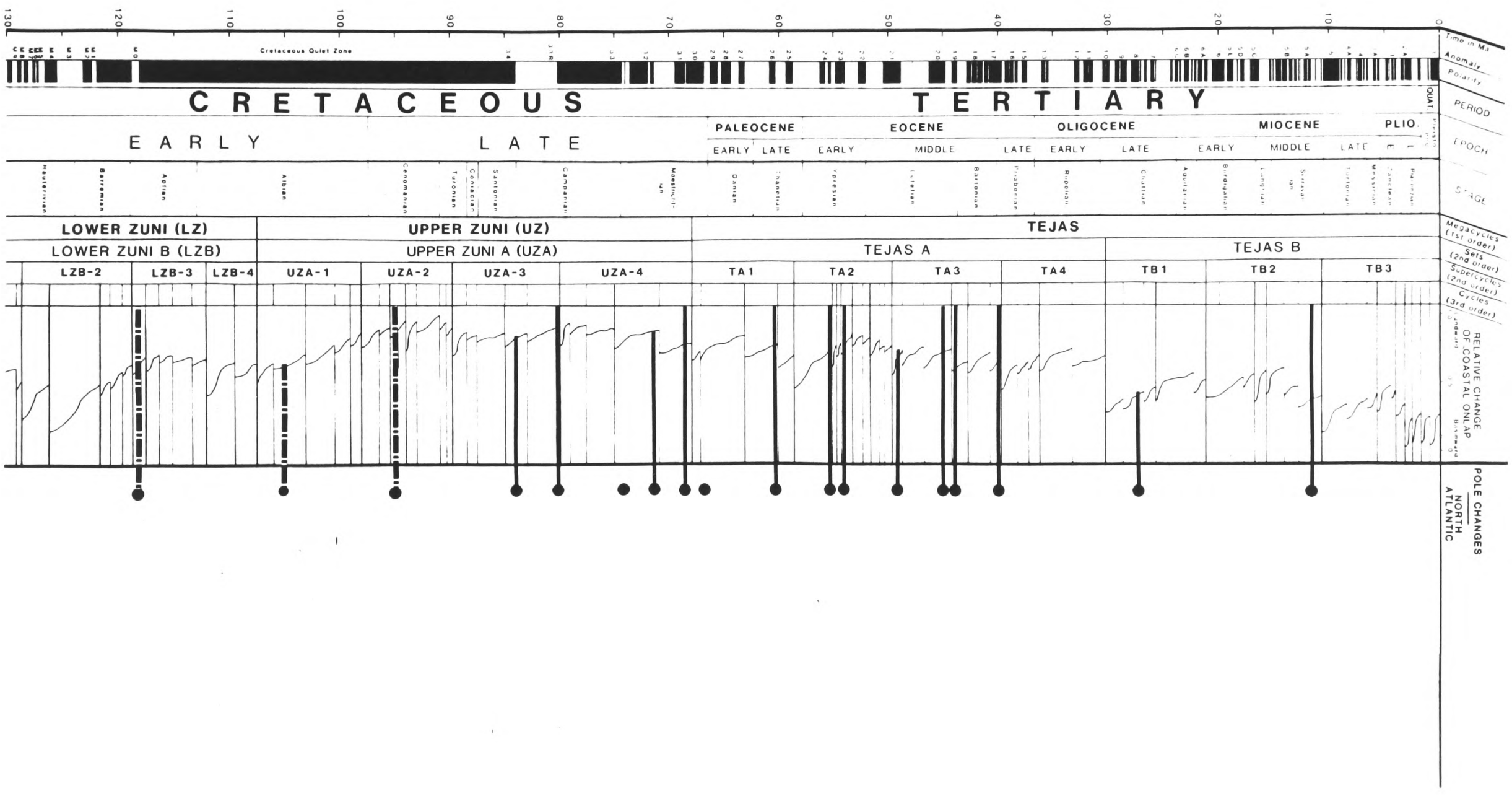
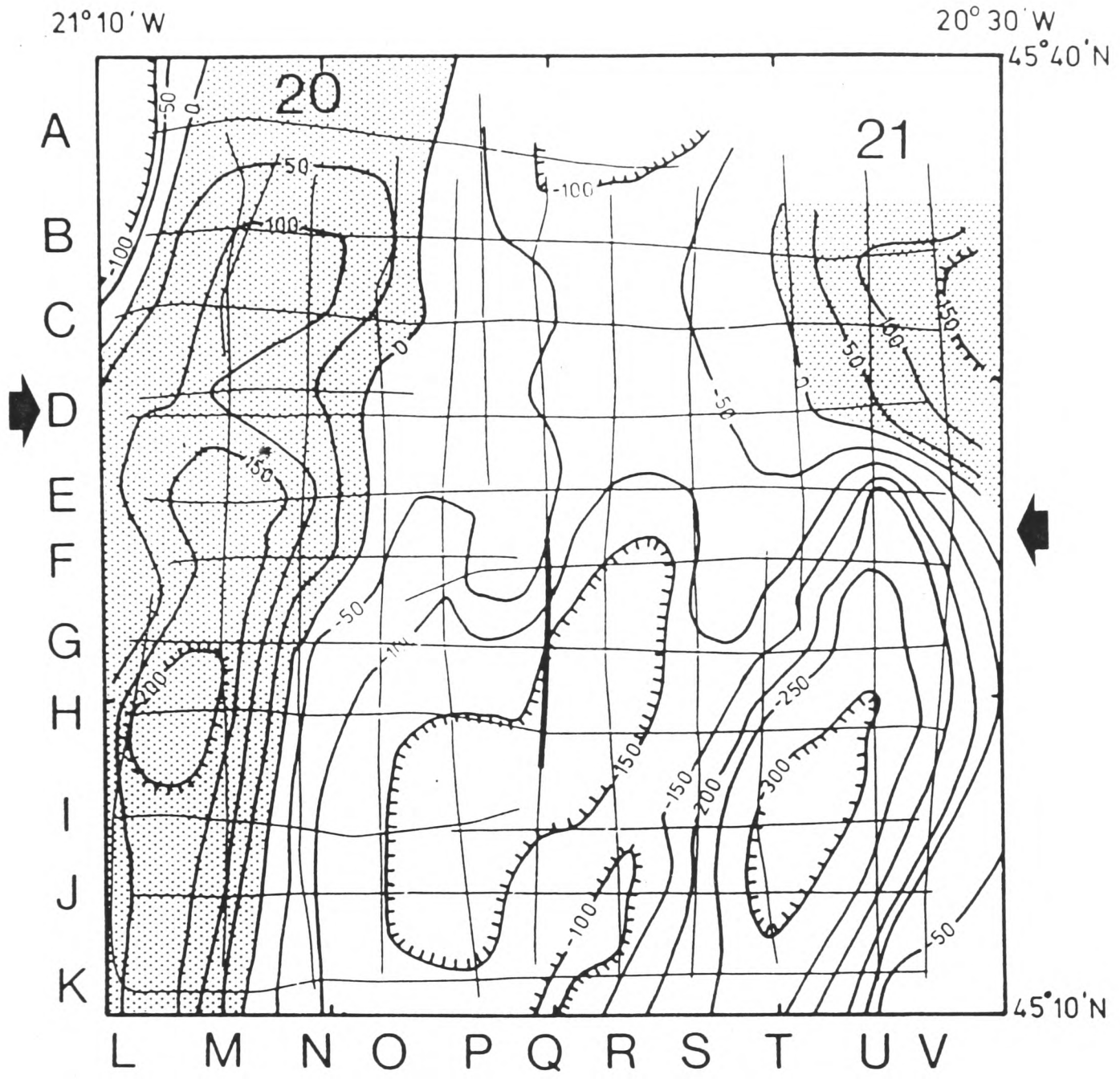

Time in Ma
Anomaly
Polarity
Cretaceous Quiet Zone
PERIOD
EPOCH
STAGE
CRETACEOUS
TERTIARY
QUAT.
EARLY
LATE
PALEOCENE
EOCENE
OLIGOCENE
MIOCENE
PLIO.
EARLY
LATE
MIDDLE
Hauterivian
Barremian
Aptian
Albian
Cenomanian
Turonian
Coniacian
Santonian
Campanian
Maestrichtian
Danian
Thanetian
Ypresian
Lutetian
Bartonian
Priabonian
Rupelian
Chattian
Aquitanian
Burdigalian
Langhian
Serravallian
Tortonian
Messinian
Zanclean
Piacenzian
LOWER ZUNI (LZ)
LOWER ZUNI B (LZB)
UPPER ZUNI (UZ)
UPPER ZUNI A (UZA)
TEJAS
TEJAS A
TEJAS B
LZB-2
LZB-3
LZB-4
UZA-1
UZA-2
UZA-3
UZA-4
TA1
TA2
TA3
TA4
TB1
TB2
TB3
Megacycles (1st order)
Sets (2nd order)
Supercycles (2nd order)
Cycles (3rd order)
RELATIVE CHANGE OF COASTAL ONLAP
POLE CHANGES
NORTH ATLANTIC

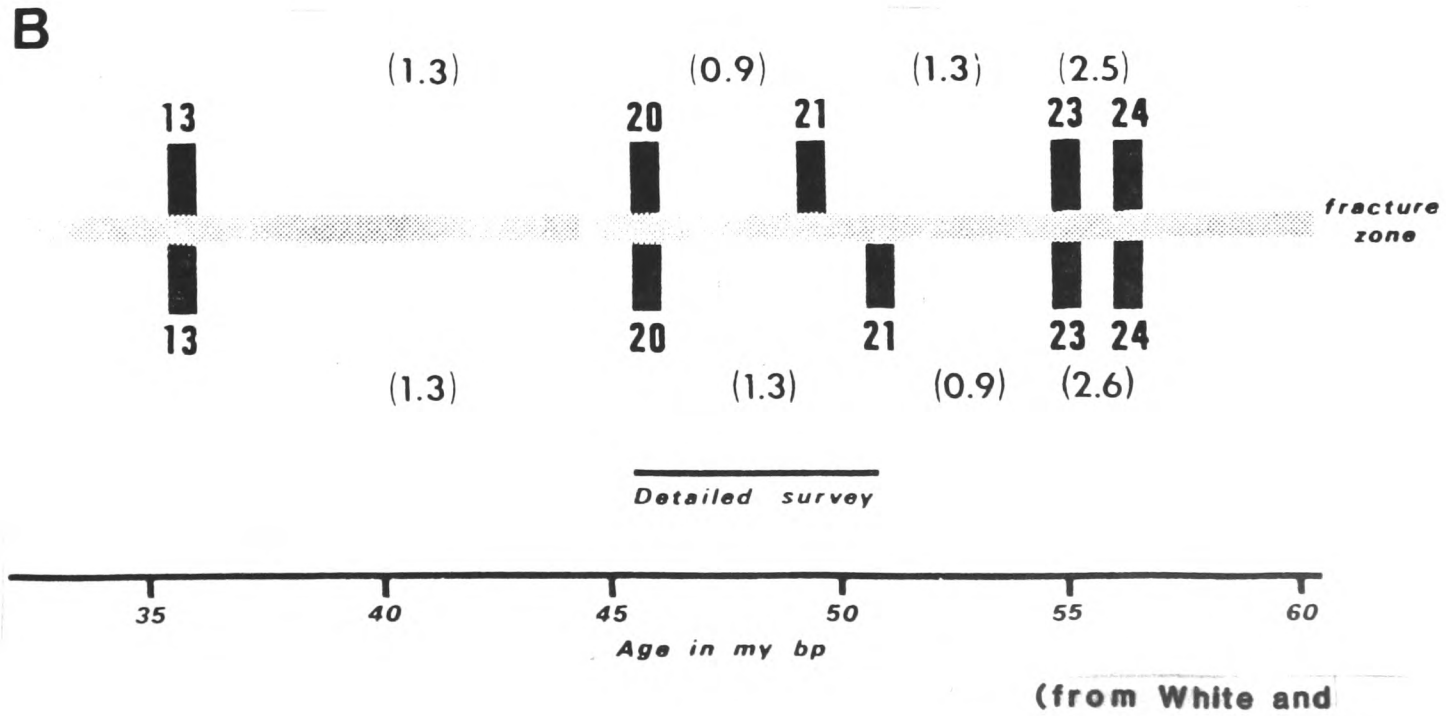
Figure 2.16 Variation in Spreading Rate in a Small Area of the Northeast Atlantic

A: Contour map of magnetic anomalies from a detailed survey in a 20 minute by 30 minute section of the Atlantic. Lines A to V show the survey grid. Note the variation in width of Anomaly 21R north and south of a previously unknown fracture zone shown by arrows.
B: Schematic drawing showing variation in spreading rate for Anomaly 20 - 21 time on either side of the fracture zone. In a slow spreading ocean like the North Atlantic a 0.4 cm/year difference between segments is the equivalent of a 30% difference. Ages used for anomalies are from LaBreque et al. (1977) which vary by less than 2.5% from those used in this study.

A



B



(from White and Matthews, 1980)

discovered (White and Matthews, 1980). Figure 2.16b is a schematic drawing of that data demonstrating the variation in spreading rate across a fracture zone. Similar variations in width of anomaly bands, implying different spreading rates across fracture zones are also known from the Central Atlantic (Klitgord and Schouten, 1986, Fig. 4b).

Variation in spreading rates, particularly when combined with irregular distribution of fracture zone and anomaly data, makes matching of isochrons very difficult. The degree of acceptability for non-exact matching cannot be judged with any precision between regions.

CHAPTER 3

KINEMATIC MODEL FOR THE OPENING OF THE CENTRAL ATLANTIC OCEAN

3.1 Introduction

The separation of North America and Africa, with the subsequent formation of the Central Atlantic Ocean, is rather simple compared with the complex history of the North Atlantic Ocean. This is reflected in the simpler physiography of this ocean basin (Fig. 3.1, Plate IV).

The major features of the Central Atlantic are a series of well-developed, large-offset transform faults and associated fracture zones. The fracture zones are picked out easily on bathymetric maps (Searle et al., 1982) and on SEASAT altimetry data (Fig. 3.2). The ridge crest and transform faults are seismically well-defined between the Fifteen-Twenty Fracture Zone and Azores-Gibraltar Plate Boundary (Einarsson, 1986), which mark the southern and northern limits of the Central Atlantic.

The most noteable features of the Central Atlantic seafloor, in addition to the transform faults and fracture zones, are two groups of volcanic islands (Canary Islands and Cape Verde Islands), a seamount chain (New England Seamounts), and two mid-plate swells (Madiera-Tore Rise, Bermuda Rise) (Fig. 3.1, Plate IV). There are no anomalous deeps, such as the King's Trough, or symmetrically disposed ridges, such as the Thulean Rises.

Figure 3.1: Simplified Tectonic Element Map: Central Atlantic

Major features and locations mentioned in text are shown, along with general position of selected magnetic anomaly lineations. A more complete version of this map is shown as Plate IV. Locations of magnetic anomaly picks are presented in Plate V.
Legend: MAR = Mid-Atlantic Ridge; 5, 6, 13, 21, 24, 30, 33, 34 = Magnetic Anomalies; AGPB = Azores-Gibraltar Plate Boundary; AFZ = Atlantis Fracture Zone; FTFZ = Fifteen-Twenty Fracture Zone; HFZ = Hayes Fracture Zone; KFZ = Kane Fracture Zone; OFZ = Oceanographer Fracture Zone; PFZ = Pico Fracture Zone; VFZ = Vema Fracture Zone; AI = Azores Islands; BB = Bahama Bank; BI = Bermuda Island; BR = Bermuda Rise; BE = Blake Escarpment; BP = Blake Plateau; BS = Blake Spur; CI = Canary Islands; CVI = Cape Verde Islands; CVP = Cape Verde Plateau; FC = Flemish Cap; GOR = Gorringe Bank; GRB = Grand Banks; JAR = J-Anomaly Ridge; MI = Madiera Islands; MTR = Madiera-Tore Rise; MP = Mazagan Plateau; OK = Orphan Knoll; SENR = Southeast Newfoundland Ridge; AS = Atlantis Seamount; CRS = Corner Ridge Seamounts; CS = Cruiser Seamount; DS = Dacia Seamount; GMS = Great Meteor Seamount; HS = Hyeres Seamount; HSS = Horseshoe Seamounts; IS = Irving Seamount; NES = New England (Kelvin) Seamounts; NFS = Newfoundland Seamounts; PS = Plato Seamount; SS = Saharan Seamounts; TS = Tropic Seamount.

MAR is highlighted for clarity.

TECTONIC ELEMENTS: CENTRAL ATLANTIC

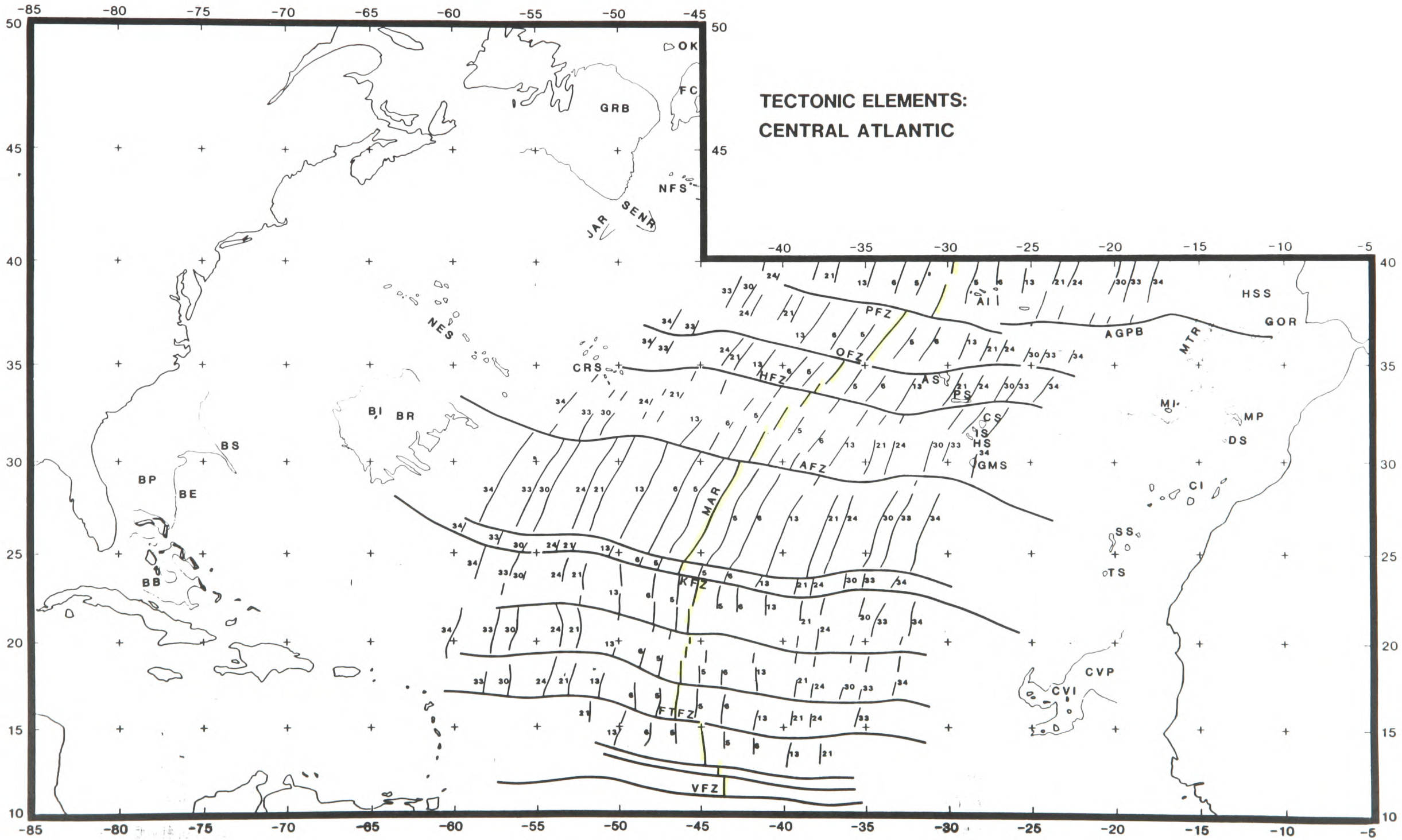
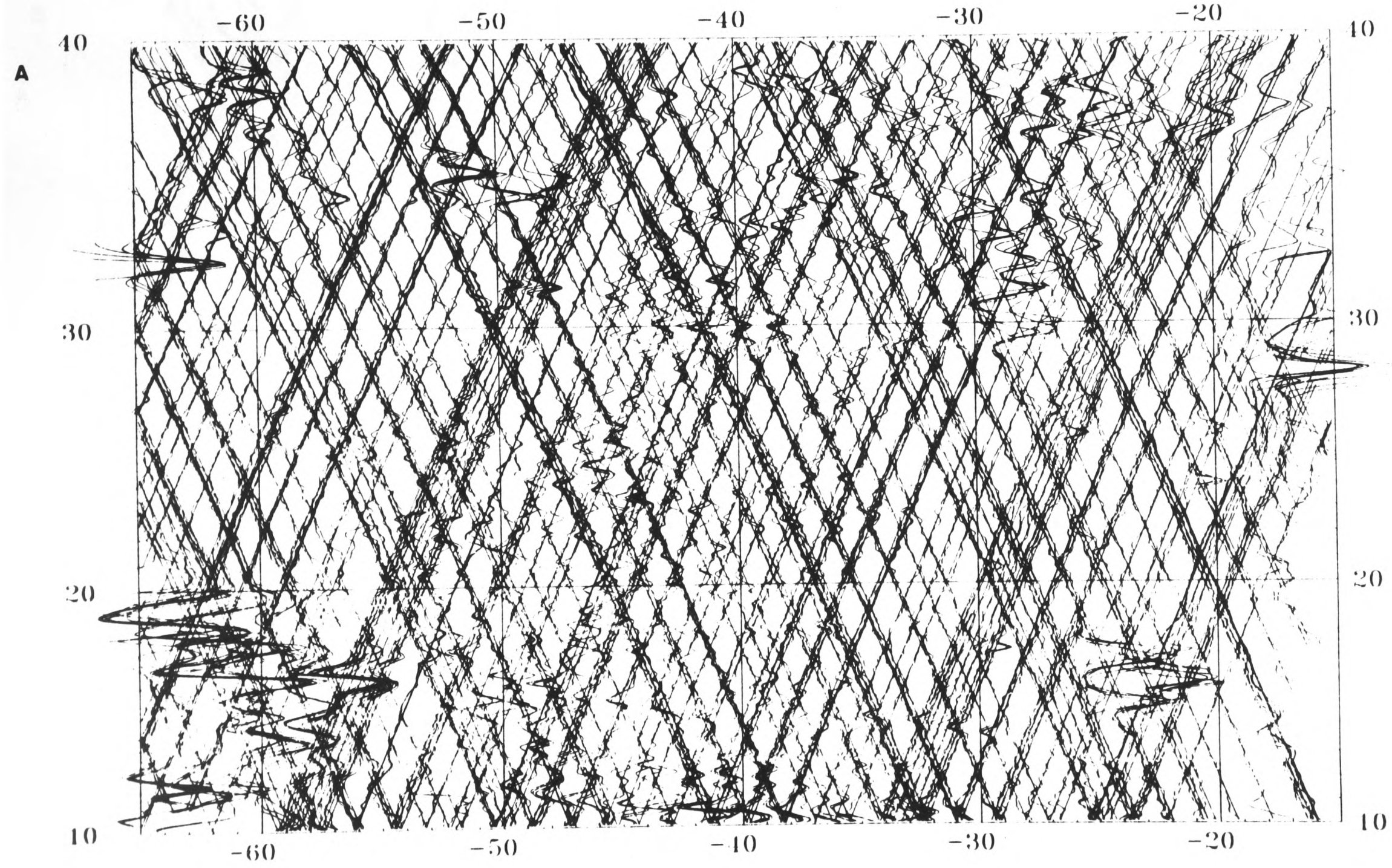
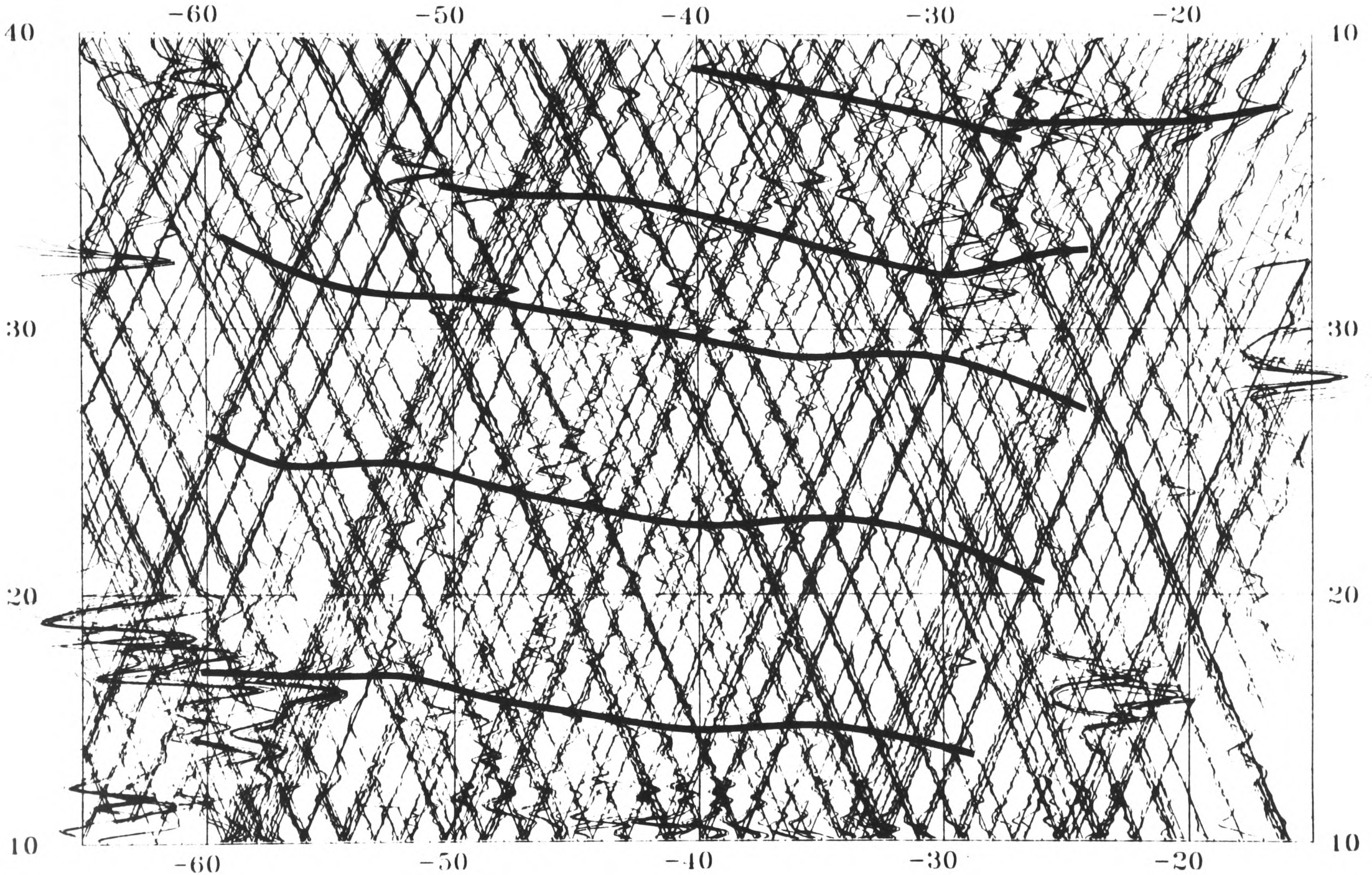


Figure 3.2: SEASAT Deflection from Geoid Data

SEASAT data was utilized in conjuction with bathymetric maps, topographic profiles along ship tracks, and SEASAT derived gravity data to remap fracture zones. In A, the raw data showing deflection from the geoid projected at an azimuth of 090°, the general trend of fracture zones in the Atlantic, is presented. In B, the traces of the Atlantis, Fifteen-Twenty, Hayes, and Kane Fracture Zones are overlain on this data.


A
−60
−50
−40
−30
−20
40
30
20
10

B



3.2 Major Features of the Central Atlantic Ocean

3.2.1 Fracture Zones

There are 5 major, large offset-fracture zones in the Central Atlantic Ocean (Atlantis, Fifteen-Twenty, Hayes, Kane, and Oceanographer). As noted above all are well-defined, both seismically and topographically, and display pronounced changes of direction similar to those observed in the Charlie-Gibbs Fracture Zone in the North Atlantic. These changes occur at Anomaly 22 (52.0 Ma) and, approximately, at Anomaly 34 (84.0 Ma).

In addition to these well-known, well-studied fracture zones, there are many other, smaller-offset fracture zones, such as Transforms A and B in the FAMOUS area (Searle et al., 1982). Many of these fracture zones are known to extend from continental margin to continental margin based on mapping using closely-spaced magnetic surveys and seismic reflection data (Schouten and Klitgord, 1982; Roeser, 1982).

3.2.2 Mid-Plate Swells and Anomalous Deeps

The Central Atlantic contains 2 prominent mid-plate swells, the Bermuda Rise and the Madiera-Tore Rise. These are located on the west and east sides of the ocean, respectively, but are not complementary features.

3.2.2a The Madiera-Tore Rise

The greater part of the Madiera-Tore Rise is located south of the Azores-Gibraltar Plate Boundary Zone. Over most of its length, it has over 2 km of relief and rises above sea level at

Madiera Island, the southern end of the rise. Madiera Island is built of Miocene volcanics, both andesite and basalt, on a basement of typical oceanic crust (Emery and Uchupi, 1984).

The Madiera-Tore Rise has been suggested to be the conjugate of the J-Anomaly Ridge (Rabinowitz et al., 1978; 2.4.4b). However, there is no offset of the rise where it crosses the Azores-Gibraltar Plate Boundary and the J-Anomaly Ridge does not extend north of the Southeast Newfoundland Ridge, unless it is considered coincident with the Grand Banks shelfbreak. Moreover, the nature of the J-Anomaly Ridge (continental crust vs. oceanic crust) has been questioned (Gradstein et al., 1977; 2.4.4b).

3.2.2b The Bermuda Rise

The Bermuda Rise is a broad feature that is a mid-plate swell in the strict sense. The island of Bermuda is only the tip of a much broader feature that trends NE-SW, is nearly 900 km in length, and almost 600 km in width. On average, the Bermuda Rise stands more than 0.5 km above the expected depth for sea floor of comparable age (B. Parsons, pers. comm.) and has a maximum depth anomaly of 1,000 m (Sclater and Wixon, 1986).

Drilling results on Bermuda (Project Deep Drill, 1972) and in adjacent waters (Sites 386 and 387 of DSDP Leg 43) show that uplift of the rise began in the Upper Eocene and was associated with a Lower Oligocene volcanic event, as indicated by a 33 Ma K-Ar date on lamprophyric sills (Reynolds and Aumento, 1974), and with termination of turbiditic sedimentation east of the rise (Tucholke and Vogt, 1979). Similar results were obtained in an

earlier study (Pirsson, 1914), which gave an Eocene or Lower Oligocene age for sediments overlying volcanics and, therefore, an Eocene or older age for the volcanism.

3.2.3 Seamounts

3.2.3a New England Seamounts

The New England Seamounts, also known as the Kelvin Seamounts, are a linear chain that trends NE-SW for nearly 1,300 km. More than 20 individual volcanic edifices have been mapped. Two hypotheses have been proposed to explain the origin of the New England Seamounts.

The first holds that the seamounts formed as the North American plate passed over a hotspot that was fixed relative to an asthenospheric reference frame. The major prediction of this hypothesis is that seamount ages would decrease from NW to SE. Furthermore, this pattern could be projected onshore for the plutons of New England and Quebec. Crough (1981) suggested, on the basis of apatite fission-track ages, paleotemperatures from conodonts, and isopach and lithofacies relations, that the hotspot formed a broad swell that tracked across eastern North America prior to the time of seamount formation. Continued plate motion then carried the ocean over the hotspot resulting in seamount formation. Crough (1981) further suggested that the present location of the hotspot is beneath, or close to, the Great Meteor Seamount.

The second hypothesis holds that the seamounts formed along a leaky transform fault, a propagating fracture system, or

volcanic lineament that may have been related to an older, continental line of weakness. McHone (1978), using orientations of Mesozoic dikes and plutons in New England, and Foland and Faul (1977), using age dates from these same rocks, showed that the hot spot hypothesis was unlikely. They suggested, seperately, that the intrusions were probably related to an older, reactivated fracture zone. Fletcher et al. (1978) showed that the Boston-Ottawa Seismic Zone was "...nearly spatially coincident..." with these plutons. The New England Seamounts were interpreted as a major transform fault that, together with the Boston-Ottawa Seismic Zone, formed a major tectonic zone more than 2,000 km in length.

Vogt and Tucholke (1979) reviewed both hypotheses based on drilling results from Leg 43 (Sites 382 and 385). They concluded that the range and uncertainty of ages at these sites precluded discrimination between the hot spot, propagating fracture, and leaky transform hypotheses. They also noted that inclusion of data from the White Mountain Igneous Province (New England) and the Corner Ridge Seamounts, which lie to the east, do not give definitive answers. However, including data from these other localities produces results that show general west to east trend of decreasing age of volcanism.

3.2.3b The Corner Ridge Seamounts

The Corner Ridge Seamounts are so named because they consist of two linear trends which intersect at a 90° angle. One segment trends 065° (ENE-WSW) and the other 335° (NNW-SSE). As they are

mostly flat-topped, they should be referred to as guyots.

The seamounts (or guyots) were formed as a result of shallow water, explosive volcanic activity of probable Campanian age. At DSDP Site 10 (Leg 2) a large increase in volcanic material was noted in Campanian age sediments (Peterson, Edgar, et al., 1970). This activity may have continued into the Tertiary, maintaining the anomalous height with respect to the ocean floor. Dredge samples from one of the guyots show shallow water reef algae in association with Eocene foraminifera (McGregor et al., 1973).

The origin of this seamount group has been ascribed to the interaction of a hot spot and the Mid-Atlantic Ridge, with a change in plate motion being the consequence of this interaction (McGregor and Krause, 1972). They suggested 4 possible models, including a leaky transform fault, based on characteristics of volcanism found throughout the world's ocean, but felt that the hot spot model provided the best fit to the available data. An interesting corollary of their model is that it predicts that the 065° trend of the Corner Ridge Seamounts and the trend of the Great Meteor, Cruiser, and Plato Seamounts in the eastern Central Atlantic should be symmetrical (see 3.2.3a and 3.2.3c).

3.2.3c Eastern Central Atlantic Seamounts

There are several large seamounts in the eastern portion of the Central Atlantic. These include, but are not limited to, the Atlantis, Cruiser, Great Meteor, Hyeres, Irving, and Plato Seamounts. The Atlantis Seamount is the furthest north and its northern edge is truncated by the Oceanographer Fracture Zone.

The Great Meteor Seamount is actually a guyot sitting astride an unnamed fracture zone north of the Atlantis Fracture Zone. Similarly, the Plato Seamount sits astride the Hayes Fracture Zone.

All these seamounts, with the exception of the Atlantis Seamount, are on oceanic crust that is Late Cretaceous or Early Tertiary in age. The Atlantis Seamount is on crust that was formed between Anomaly 15 and Anomaly 19. All these seamounts form a roughly NNW-SSE trend except for the Cruiser Seamount, which lies further east.

Of these seamounts only the Great Meteor has been studied in any detail. Pratt (1963) found that Great Meteor Seamount, in addition to a flat top, has benches at 330, 450, and 580 m depths along its sides. The top of the guyot is covered by an indurated pteropod ooze of Miocene age. This data weakens the suggestion of Crough (1981) that the hot spot, which may have formed the White Mountain Magma Series as well as the New England and Corner Ridge Seamount chains, is presently located beneath the Great Meteor Seamount, unless the hot spot is inactive (see 3.2.3a). Similarly, the preferred model of McGregor and Krause (1972), which predicts symmetry between this group of seamounts and the 065° trend of the Corner Ridge Seamounts, is also weakened.

3.2.4 Continental Fragments (Microcontinents)

There are 2 major areas of continental fragments or extensions on the west side of the Central Atlantic. These are

the Blake Plateau and the Bahama Platform. On the east side of the ocean, the Mazagan Plateau is the only major continental fragment.

3.2.4a The Blake Plateau

The Blake Plateau is a large basin, 400 km long, 250 km wide, with an average depth of nearly 800 m off the southeast coast of the United States. It is bounded on the west by the Florida-Hatteras Slope, on the south by the Bahama Platform, and on the east by the Blake Escarpment and Blake Spur. The Plateau narrows rapidly north of the Blake Spur, passing into the continental rise near the Hatteras Canyon.

Extensive geophysical (magnetic, gravity, seismic) surveys combined with drilling, dredging, and onshore geologic data show that the plateau is underlain by thinned continental crust (Dillon et al., 1979). A sedimentary sequence, consisting of thick Jurassic and Cretaceous but thin Tertiary successions, sits upon a Triassic unconformity that is overlain by an Early Jurassic volcanic layer. This sequence is up to 10 km thick on the southern part of the plateau.

3.2.4b The Bahama Platform

The Bahama Platform is one of the most studied regions in the Atlantic Ocean. Although much of the research has dealt with the carbonate sedimentology of the Bahama Bank, there is a large body of geophysical and well data that can be used to study its crustal underpinnings. One model suggests that the arrangement of shallow banks and deep basins on the platform reflects the underlying horst and graben topography of thinned continental

crust (Mullins and Lynts, 1977). The other model suggests that the platform was part of a large "megabank" that stretched from Texas to Georgia whose present topography reflects erosional and depositional processes (Schlager and Ginsburg, 1981).

Within the 10 km thick post-rift sediment sequence, a mid-Cretaceous unconformity was drilled on ODP Leg 101 (Austin, Schlager, Palmer, et al., 1986). This unconformity is thought to record the drowning of the "megabank", which was locally reestablished in the Late Cretaceous. Also, recently published seismic data (Ladd and Sheridan, 1987) suggests that the platform is built on thinned continental crust as far east as the Tongue of the Ocean and on oceanic crust to the Bahama Escarpment.

3.2.4c The Mazagan Plateau

The Mazagan Plateau lies off Morocco and is an offshore extension of the Moroccan Meseta. The plateau is cored by Paleozoic granite, in a thrust-faulted basement ridge. The granite outcrops along the base of the escarpment that bounds the plateau (Wissmann and von Rad, 1979).

3.2.5 Other Features

In addition to those discussed above, there are 3 other features of the Central Atlantic that have a bearing on its tectonic evolution. These are the Canary Islands, the Cape Verde Islands, and the observed asymmetry between the eastern and western sides of the ocean.

3.2.5a The Canary and Cape Verde Islands

The Canary and Cape Verde Islands are products of volcanic activity (Dillon and Sougy, 1974). The Canary Islands consist mostly of Miocene volcanics erupted through older (Jurassic) oceanic crust. However, the easternmost islands (Feurteventura and Lanzarote) may be underlain by thinned continental crust. Evidence for this has been put forth by Ibarrola (1970) on petrologic grounds, by Oversby et al. (1971) on isotopic grounds, and by Bosshard and MacFarlane (1970) on geophysical grounds.

There are, however, grounds for suggesting that the entire Canary Island chain is underlain by oceanic crust. Evidence for this view, based on sedimentological, borehole and geophysical data has been presented by Uchupi et al., (1976) and by Emery and Uchupi (1984).

The Cape Verde Islands are also the product of Miocene volcanism. Unlike the Canary Islands, there is no doubt that they are built entirely on oceanic crust. Linear magnetic anomalies were mapped there by Rona et al. (1970). These islands are associated with the Cape Verde Plateau, which is 900 km wide, 600 km long, with an average depth of 3,500 m. The plateau was uplifted in the Miocene after volcanism had begun (Lancelot and Siebold, 1977). The Cape Verde Plateau might reasonably be called a mid-plate swell.

3.2.5b Asymmetry of the Central Atlantic

The final "feature" of the Central Atlantic is only visible when the ocean is viewed as a whole. If ocean crust is generated symmetrically about a mid-ocean ridge, it is readily apparent

that something is "radically wrong" with the Central Atlantic. The western part of the ocean is much wider than the part east of the Mid-Atlantic Ridge. This asymmetry is in the width of the Jurassic Quiet Zone, located near the African and North American coasts.

Two explanations have been suggested to account for the asymmetry. Klitgord and Schouten (1986) proposed that an eastward jump in ridge position occurred at approximately 165 Ma. Emery and Uchupi (1984) question the need for a ridge jump. They state "...the asymmetry...probably reflects variation in the extent of the 7-km/second layer...that may be of continental origin". Hence, the difference merely reflects the width of attenuated continental crust off the North American coast. Varying widths of continental margins have implications for models of continental extension and basin formation and, ultimately, for continental reconstructions that take account of the amount of extension that occurs when continents rift and oceans form.

3.3 Kinematic Model

3.3.1 Rotation Parameters

Rotation parameters for the Central Atlantic were developed using the same data sources and methodology that was presented in Chapter 2 (2.2 and 2.3). Published rotation parameters that were tested are given in Table 3.1. Finite and stagepole rotation

TABLE 3.1

PUBLISHED ROTATION PARAMETERS FOR THE CENTRAL ATLANTIC SEPARATION OF AFRICA AND NORTH AMERICA

ANOMALY	LATITUDE	LONGITUDE	ROTATION	REFERENCE
5	69.70	-33.40	3.60	(1)
5	67.60	-14.00	3.10	(2)a
5	70.59	-18.70	2.70	(3)
5	78.00	11.50	2.70	(4)b
5	79.08	77.95	2.41	(5)
5	79.50	55.55	2.29	(6)
6	70.50	-18.70	5.70	(3)
6	78.00	-11.50	5.40	(4)b
6	79.57	37.84	5.29	(5)
6	80.61	36.37	5.22	(6)
13	79.00	13.00	9.75	(1)
13	67.60	-14.00	10.90	(2)c
13	70.50	-18.70	10.40	(7)
13	78.00	11.50	9.50	(8)
13	76.41	7.12	9.81	(5)
13	74.40	-4.06	10.15	(6)
21	77.00	15.00	13.90	(1)
21	74.51	-4.83	15.32	(5)
21	76.43	3.64	14.59	(6)
22	70.90	-13.10	16.40	(3)
24	79.40	3.20	17.00	(8)
24	77.78	0.36	16.84	(6)
25	75.00	15.00	17.00	(1)
25	80.60	-0.50	18.07	(5)
25	79.20	-1.41	18.36	(6)
28R	67.60	-14.00	20.20	(2)d
29	70.90	-10.90	21.20	(3)
30	75.90	-17.40	24.10	(4)
30	83.86	1.28	20.87	(5)
30	81.27	-5.84	21.29	(6)
32	81.35	-9.15	22.87	(5)
32	81.47	-8.14	23.70	(6)
33	71.00	-10.00	24.00	(1)e
33	78.20	-16.50	26.70	(8)
33	80.76	-11.76	23.91	(5)
33	81.57	-8.14	23.70	(6)
33R	78.30	-18.35	27.06	(5)
33R	77.50	-21.04	27.48	(6)
34	67.60	-14.00	34.70	(2)f
34	79.10	-15.70	30.30	(3)
34	72.90	26.10	33.90	(8)g
34	76.55	-20.73	29.60	(5)
34	77.03	-20.74	29.54	(6)

REFERENCES CITED:
(1)Pitman and Talwani, 1972; (2)Phillips and Forsyth, 1972; (3)Sclater *et al.*, 1977; (4)Savostin *et al.*, 1986; (5)Klitgord and Schouten, 1986; (6)Pindell *et al.*, 1988; (7)Franchteau, 1973; (8)Olivet *et al.*, 1984.

NOTES:
(a)Rotation parameters are given for 10Ma which is approximately the age of Anomaly 5.

(b)Rotation parameters are noted as being found by interpolation.

(c)Rotation parameters are given for 35Ma which is approximately the age of Anomaly 13.

(d)Rotation parameters are given for 65Ma which is approximately the age of Anomaly 28R.

(e)Originally as Anomaly 31 but subsequently reidentified as Anomaly 33 by Kristoffersen and Cande (1978).

(f)Rotation parameters are given for 105Ma (within the Cretaceous Quiet Zone). This can be considered part of Anomaly 34.

(g)The rotation angle is cited in Savostin *et al.* as 26.10°, but in Olivet *et al.* (1984) the rotation angle is that shown in the table. The rotation parameters are denoted as pre-Anomaly 34.

All anomaly ages are referred the Berggren *et al.* (1985) and the Kent and Gradstein (1985) timescales.

parameters determined in this study for anomalies 2 - 34 are given in Tables 3.2 and 3.3, respectively. Rotation parameters for the Keathley or M-Series anomalies, taken from Pindell et al. (1988), are given in Tables 3.4 and 3.5.

3.3.2 Flowlines

In the North Atlantic, only the Charlie-Gibbs Fracture Zone is useful for constraining the fit of magnetic anomalies. In the Central Atlantic, there are several well-developed, large-offset fracture zones to constrain magnetic anomaly fitting and act as flowlines. Four of these (Atlantis, Fifteen-Twenty, Hayes, Kane) have been remapped using bathymetric maps and SEASAT altimetry data (Fig. 3.2). In Figure 3.3 the traces of these fracture zones are overlain by synthetic fracture zones constructed using stagepole parameters. Plates V and VI show the unrotated and rotated picks for anomalies 2 - 34.

3.3.3 Comparison With Other Models

As with the North Atlantic, there have been many models suggested for the evolution of the Central Atlantic (Table 2.5). However, these models, particularly those that have dealt with the kinematic evolution of this ocean, show far less variation than those for the North Atlantic. A less complex evolutionary history, faster spreading rate, better-developed fracture zones, and larger data base have contributed to producing a consensus for models of Central Atlantic evolution.

The method used to compare various North Atlantic kinematic

TABLE 3.2

FINITE POLE ROTATION PARAMETERS FOR THE CENTRAL ATLANTIC SEPARATION OF AFRICA AND NORTH AMERICA

ANOMALY	LATITUDE	LONGITUDE	ROTATION
2	79.50	55.55	0.38
2A	79.50	55.55	0.59
3	79.50	55.55	1.00
3A	79.50	55.55	1.39
4	79.50	55.55	1.77
4A	79.50	55.55	1.95
5	79.50	55.55	2.29
5A	79.50	55.55	2.98
5B	79.50	55.55	3.40
5C	80.06	36.37	4.15
5D	80.06	36.37	4.65
5E	80.06	36.37	4.93
6	80.06	36.37	5.22
6A	80.06	36.37	5.78
6B	80.06	36.37	6.23
6C	80.06	36.37	6.58
7	80.06	36.37	6.93
8	80.06	36.37	7.28
9	74.40	-4.06	8.47
10	74.40	-4.06	8.93
11	74.40	-4.06	9.25
12	74.40	-4.06	9.69
13	74.40	-4.06	10.15
15	74.40	-4.06	10.81
16	74.40	-4.06	11.19
17	74.40	-4.06	11.76
18	74.40	-4.06	12.35
19	75.36	1.68	12.88
20	75.36	1.68	13.35
21	76.43	3.64	14.59
22	76.43	3.64	15.58
23	77.78	0.36	16.37
24	77.78	0.36	16.91
25	80.60	-0.50	18.18
26	80.60	-0.50	18.79
27	80.60	-0.50	19.90
28	81.27	-5.84	20.61
29	81.27	-5.84	21.05
30	81.27	-5.84	21.44
31	81.27	-5.84	22.10
32	81.57	-9.15	22.87
33	81.57	-8.14	23.70
33R	78.30	-18.35	27.17
34	77.07	-20.74	29.62

TABLE 3.3A

STAGE POLE ROTATION PARAMETERS -- CENTRAL ATLANTIC

MOTION OF AFRICA WITH RESPECT TO NORTH AMERICA

ANOMALY	LATITUDE	LONGITUDE	ROTATION
2 - 1	79.50	55.55	-0.38
2A - 2	80.49	55.55	-0.21
3 - 2A	79.37	55.55	-0.41
3A - 3	80.60	55.55	-0.39
4 - 3A	77.72	55.55	-0.38
4A - 4	77.14	55.55	-0.19
5 - 4A	80.09	55.55	-0.33
5A - 5	79.79	55.55	-0.69
5B - 5A	79.08	55.55	-0.42
5C - 5B	72.23	-22.34	-0.78
5D - 5C	79.77	36.37	-0.50
5E - 5D	81.18	36.37	-0.27
6 - 5E	81.14	36.37	-0.30
6A - 6	80.37	36.37	-0.55
6B - 6A	79.29	36.37	-0.45
6C - 6B	80.61	36.37	-0.35
7 - 6C	80.61	36.37	-0.35
8 - 7	80.61	36.37	-0.35
9 - 8	33.11	-39.18	-1.84
10 - 9	74.53	-4.06	-0.46
11 - 10	73.51	-4.06	-0.32
12 - 11	74.13	-4.06	-0.44
13 - 12	74.20	-4.06	-0.47
15 - 13	74.49	-4.06	-0.65
16 - 15	74.68	-4.06	-0.38
17 - 16	74.68	-4.06	-0.57
18 - 17	74.57	-4.06	-0.59
19 - 18	57.88	93.33	-0.66
20 - 19	74.69	1.68	-0.47
21 - 20	82.72	68.09	-1.28
22 - 21	76.63	3.64	-0.99
23 - 22	73.14	-142.96	-0.89
24 - 23	78.31	0.36	-0.54
25 - 24	66.51	172.14	-1.54
26 - 25	80.39	-0.50	-0.61
27 - 26	80.62	-0.50	-1.11
28 - 27	68.08	-127.31	-0.80
29 - 28	80.80	-5.84	-0.44
30 - 29	80.68	-5.84	-0.39
31 - 30	80.80	-5.84	-0.66
32 - 31	77.55	-109.12	-0.81
33 - 32	79.58	15.11	-0.83
33R - 33	56.55	-44.23	-3.83
34 - 33R	64.21	-40.21	-2.54

TABLE 3.3B

STAGE POLE ROTATION PARAMETERS -- CENTRAL ATLANTIC

MOTION OF NORTH AMERICA WITH RESPECT TO AFRICA

ANOMALY	LATITUDE	LONGITUDE	ROTATION
2 - 1	79.50	55.55	0.38
2A - 2	80.49	55.55	0.21
3 - 2A	79.37	55.55	0.41
3A - 3	80.60	55.55	0.39
4 - 3A	77.72	55.55	0.38
4A - 4	77.14	55.55	0.19
5 - 4A	80.09	55.55	0.33
5A - 5	79.79	55.55	0.69
5B - 5A	79.08	55.55	0.42
5C - 5B	71.63	-19.45	0.78
5D - 5C	79.77	36.37	0.50
5E - 5D	81.18	36.37	0.27
6 - 5E	81.14	36.37	0.30
6A - 6	80.37	36.37	0.55
6B - 6A	79.29	36.37	0.45
6C - 6B	80.61	36.37	0.35
7 - 6C	80.61	36.37	0.35
8 - 7	80.61	36.37	0.35
9 - 8	31.92	-32.26	1.84
10 - 9	74.53	-4.06	0.46
11 - 10	73.51	-4.06	0.32
12 - 11	74.13	-4.06	0.44
13 - 12	74.20	-4.06	0.47
15 - 13	74.49	-4.06	0.65
16 - 15	74.68	-4.06	0.38
17 - 16	74.68	-4.06	0.57
18 - 17	74.57	-4.06	0.59
19 - 18	61.07	106.59	0.66
20 - 19	74.69	1.68	0.47
21 - 20	85.78	67.20	1.28
22 - 21	76.63	3.64	0.99
23 - 22	70.55	-119.96	0.89
24 - 23	78.31	0.36	0.54
25 - 24	66.26	163.17	1.54
26 - 25	80.40	-0.50	0.61
27 - 26	80.62	-0.50	1.11
28 - 27	65.15	-104.47	0.80
29 - 28	80.80	-5.84	0.44
30 - 29	80.68	-5.84	0.39
31 - 30	80.80	-5.84	0.66
32 - 31	74.28	-86.77	0.81
33 - 32	81.03	19.55	0.83
33R - 33	55.00	-25.31	3.83
34 - 33R	62.89	-24.26	2.54

TABLE 3.4

M-SERIES FINITE POLE ROTATION PARAMETERS FOR THE CENTRAL ATLANTIC SEPARATION OF AFRICA AND NORTH AMERICA

(FROM PINDELL ET AL. (1988))

ANOMALY	LATITUDE	LONGITUDE	ROTATION
101 Ma*	69.95	-20.90	41.91
M-0	66.00	-24.94	54.60
M-4	66.00	-19.76	56.44
M-10	65.93	-19.11	57.51
M-16	65.99	-19.18	59.98
M-21	66.24	-18.86	62.16
M-25	67.01	-16.84	64.81
BSA+	66.60	-14.74	71.95
COB**	66.95	-12.59	74.35
FIT++	67.08	-11.74	75.31

NOTES:

(*)Rotation parameters are interpreted between adjacent pairs of anomalies. Pindell et al. (1988) use 77.03, -20.74, 29.54 for Anomaly 34 reconstructions.

(+)Estimated age of the Blake Spur Anomaly (BSA) is 165 Ma.

(**)Estimated age of the Continent-Ocean Boundary (COB); i.e., the start of sea-floor spreading.

(++)Estimated age for closure of the Central Atlantic with minimal stretching of continental crust.

TABLE 3.5

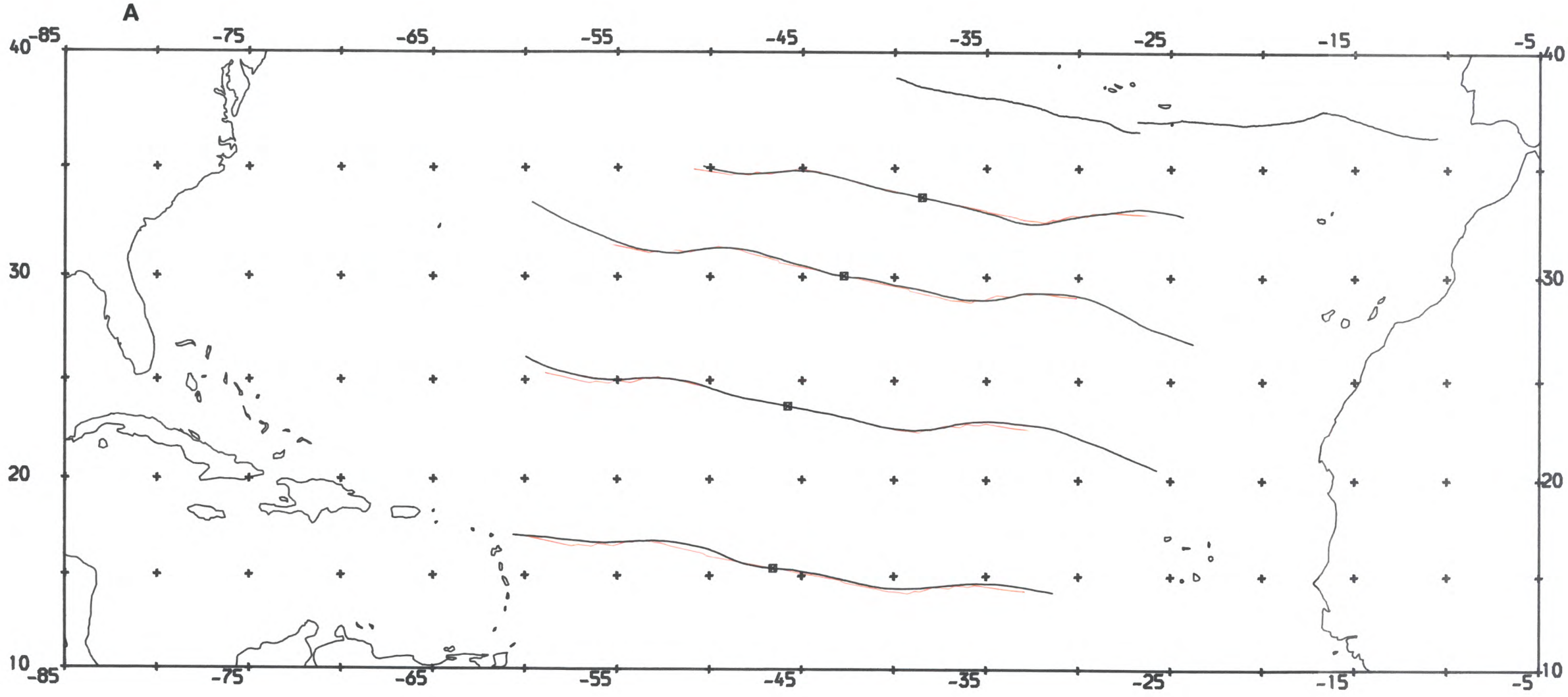
M-SERIES STAGE POLE ROTATION PARAMETERS -- CENTRAL ATLANTIC MOTION OF NORTH AMERICA WITH RESPECT TO AFRICA (FROM PINDELL ET AL. (1988))

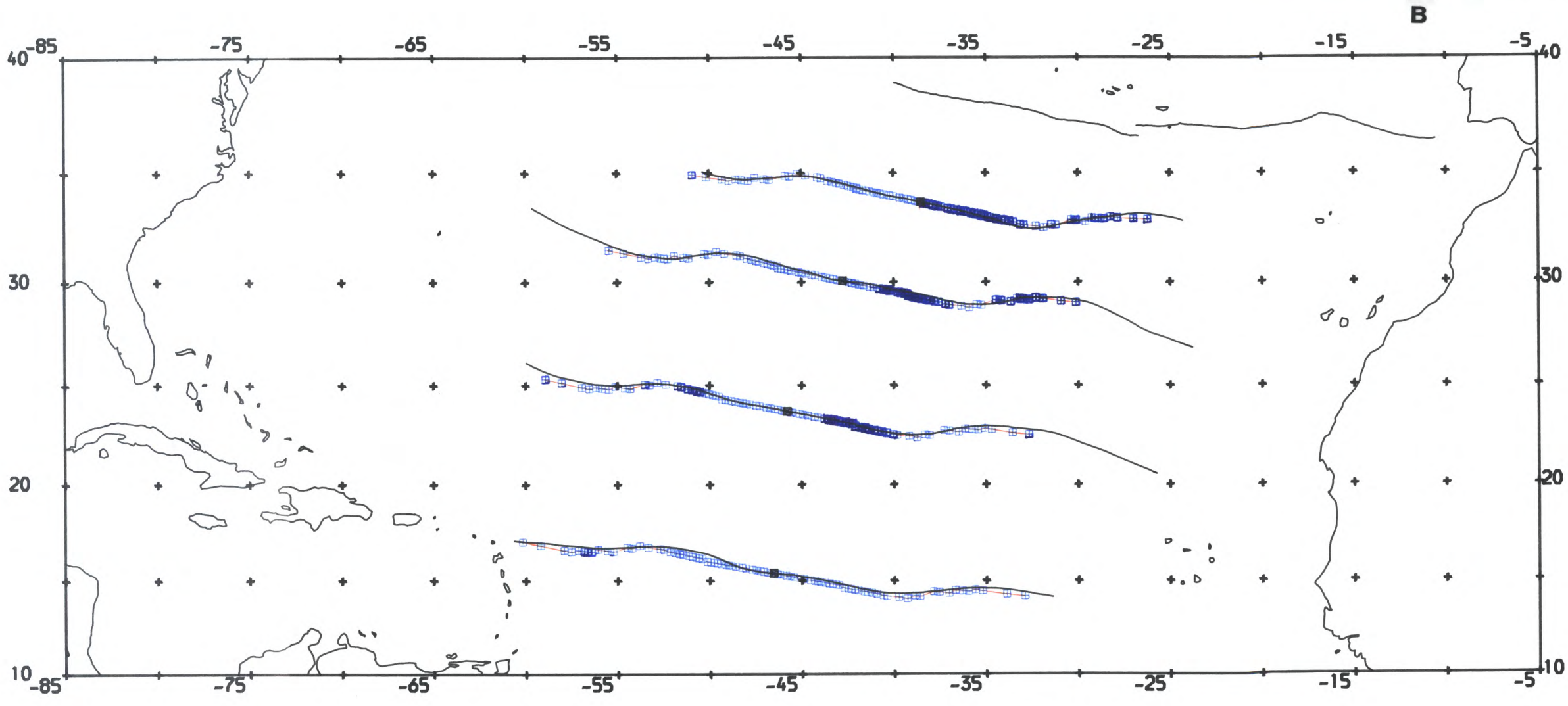
ANOMALY	LATITUDE	LONGITUDE	ROTATION
34 - 101	54.45	-11.21	13.10
101 - M-0	54.45	-11.21	13.10
M-0 - M-10*	67.61	14.68	2.99
M-0 - M-4*	67.64	14.90	1.89
M-4 - M-10*	67.70	14.91	1.10
M-10 - M-16	66.71	-22.15	2.47
M-16 - M-21	73.61	-20.74	2.20
M-21 - M-25	84.29	70.53	2.90
M-25 - BSA	66.52	5.17	7.22
BSA - COB	77.52	67.94	1.06
COB - FIT	77.52	67.94	2.64

NOTES:
(*)Pindell et al. (1988) only give a stage pole for M-0 to M-10. Stage poles for M-0 to M-4 and M-4 to M-10 were independently computed using their finite poles.

Figure 3.3 Kinematic Model: Synthetic Fracture Zone

A: Synthetic fracture zones (red) constructed from rotation parameters determined in this study (Tables 3.2 and 3.3), overlain on the actual traces of the Atlantis, Fifteen-Twenty, Hayes, and Kane Fracture Zones (black) for comparison. Ridge positions are show by squares with x in center (black).
B: Same as A but with addition of anomaly positions shown by squares with + sign in center (blue).


A
-85
-75
-65
-55
-45
-35
-25
-15
-5
40
30
20
10


B
40
30
20
10
-85
-75
-65
-55
-45
-35
-25
-15
-5

models (see 2.5.3) is used again in this chapter. The results are shown in Figures 3.4 to 3.10 and discussed below.

3.3.3a Pitman and Talwani's Model (1972)

The younger anomaly (5, 13, 21) rotation parameters in this model produce a general concordance between the synthetic and the actual fracture zone traces whereas those for the older anomalies produce a marked divergence (Fig. 3.4). In fact, the change in direction of the synthetic fracture zones is the opposite of the that which the fracture zones actually undergo. Hence, this portion of the model must be considered far less successful than the part that deals with the North Atlantic.

It is interesting to note that very little mention of this part of their model is found in the subsequent literature and that the rotation parameters in ensuing studies are quite different. In view of the remarkable amount of agreement between current models for the Central Atlantic (Tables 3.1 and 3.2) and the larger data base that they had for this area (Pitman and Talwani, 1972, Figs. 1 and 2), the lack of success of this part of their model is surprising.

3.3.3b Philips and Forsyth's Model (1972)

As with their results for the North Atlantic the synthetic and actual fracture zones show little relation with each other, although Anomalies 5 and 13 lie close to the fracture zones (Fig. 3.5). The unidirectional trend of the synthetic fracture zone trace is a consequence of using a fixed pole for all rotation parameters. As noted above (2.5.3b) this model is rarely cited in the literature and will not be discussed further.

Figure 3.4 Pitman and Talwani (1972): Synthetic Fracture Zone

Synthetic fracture zone (red) contructed from the published rotation parameters of Pitman and Talwani (1972), overlain on the Atlantis, Fifteen-Twenty, Hayes, and Kane Fracture Zones (black) for comparison. Anomaly positions are shown by squares with + in center (blue) and ridge positions by squares with x in center (black). Anomalies used are 5, 13, 21, 25, 33 (originally identified as 31).

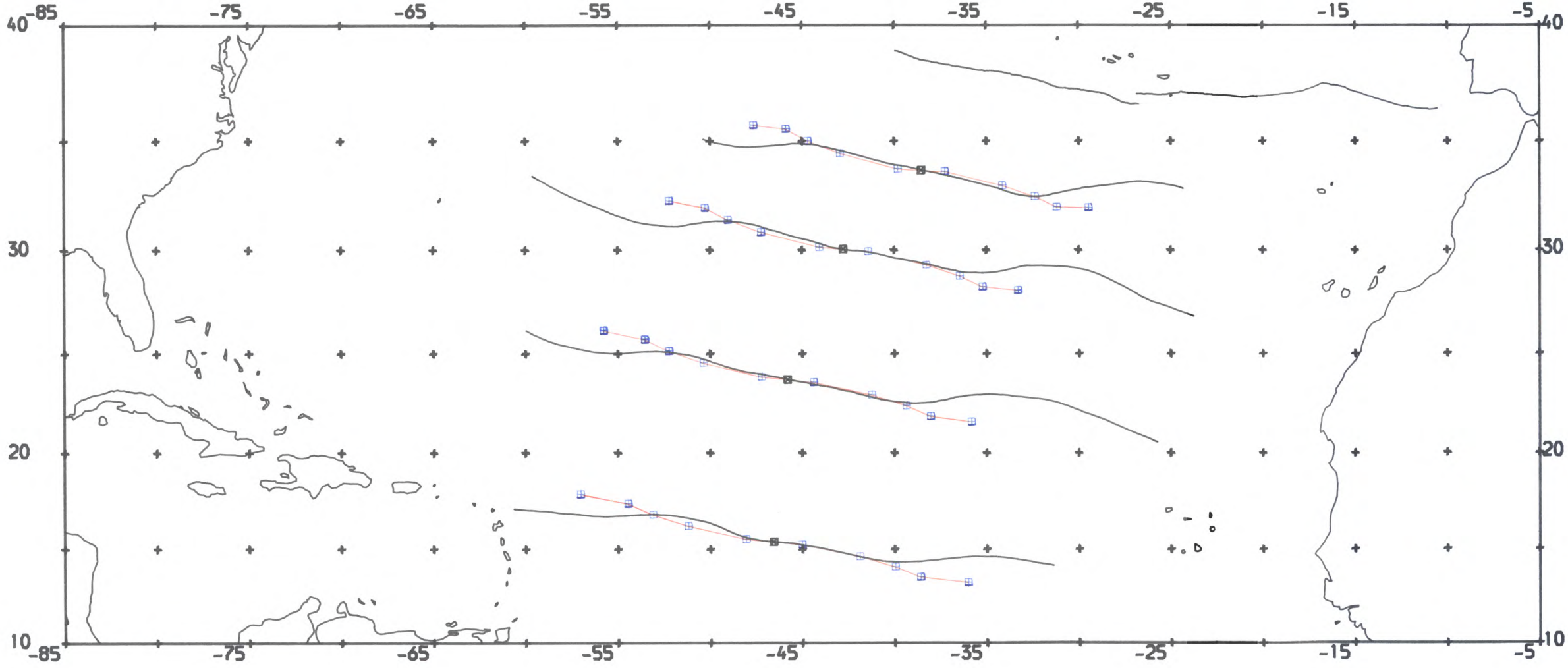
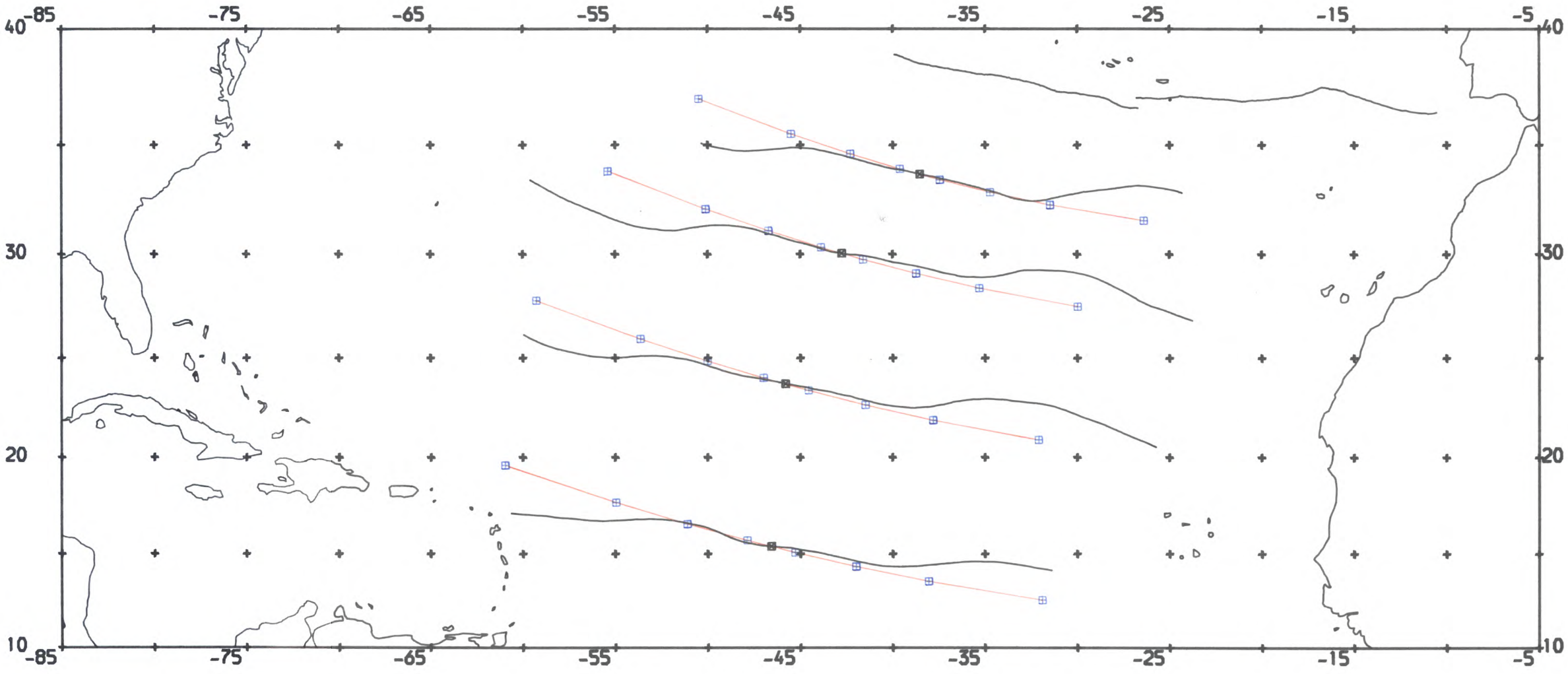

-85
-75
-65
-55
-45
-35
-25
-15
-5
40
30
20
10

Figure 3.5 Philips and Forsyth (1972): Synthetic Fracture Zone

Synthetic fracture zone (red) contructed from the published rotation parameters of Philips and Forsyth (1972), overlain on the Atlantis, Fifteen-Twenty, Hayes, and Kane Fracture Zones (black) for comparison. Anomaly positions are shown by squares with + in center (blue) and ridge positions by squares with x in center (black). Anomalies used are 5, 13, 28R, and 105 Ma.


-85
-75
-65
-55
-45
-35
-25
-15
-5
40
30
20
10

3.3.3c Sclater, Hellinger, and Tapscott's Model (1977)

The results of this comparison have a pattern similar to those to their model for the North Atlantic. There is very reasonable agreement between the synthetic and actual fracture zones for the younger anomalies (5, 6, and 13), but after that they begin to diverge (Fig. 3.6). Although, the positions of Anomalies 22 and 34 are close to the fracture zone the motion path along which they are found is not accurate.

3.3.3d Olivet, Bonnin, Beuzart, and Auzende's Model (1984)

This kinematic model uses fewer anomalies than any other, hence it is to be expected that their results are "rougher" than others. It is apparent from Figure 3.7a that the poles used for Anomalies 13 and 24 are reasonable with respect to how they fit the fracture zone but are less satisfactory with respect to the flow line they generate. The synthetic fracture zone beyond (i.e. older than) Anomaly 24 is unrepresentative of the direction of seafloor spreading, particularly between Anomaly 33 and the pre-Anomaly 34 position, which is displaced by hundreds of kilometers.

The use of so few anomalies makes this model more difficult to evaluate than many others. The large spacing tends to either hide or exaggerate minor discrepancies depending on the scale utilized. In Figures 3.7b-e the interval between the ridge and Anomaly 13 has been enlarged 3 times. In each of these figures, the deviation between the synthetic and actual fracture zones can be seen and compared with that shown in Figure 3.7a. The smaller scale shows clearly that the path of the synthetic fracture zone

Figure 3.6 Sclater et al. (1977): Synthetic Fracture Zone

Synthetic fracture zone (red) contructed from the published rotation parameters of Sclater et al. (1977), overlain on the Atlantis, Fifteen-Twenty, Hayes, and Kane Fracture Zones (black) for comparison. Anomaly positions are shown by squares with + in center (blue) and ridge positions by squares with x in center (black). Anomalies used are 5, 6, 13, 22, 29, and 34.

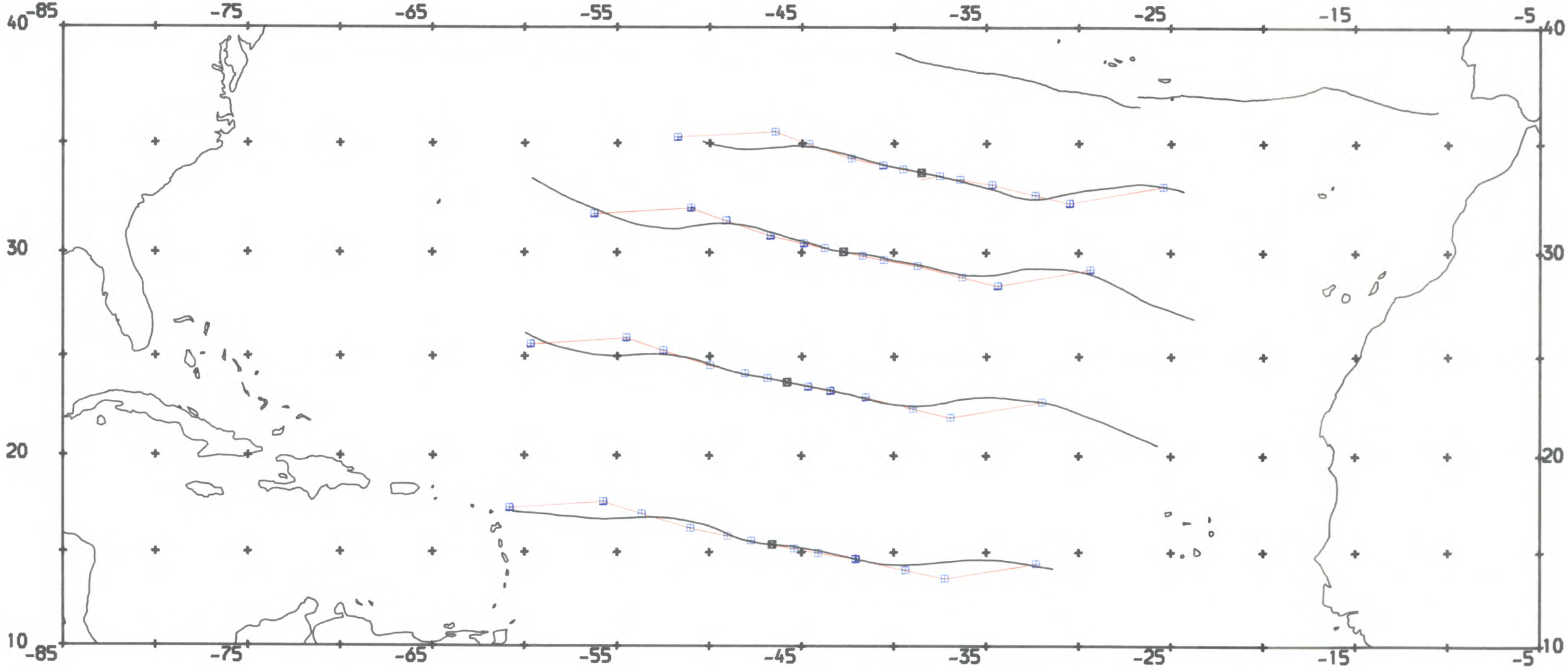
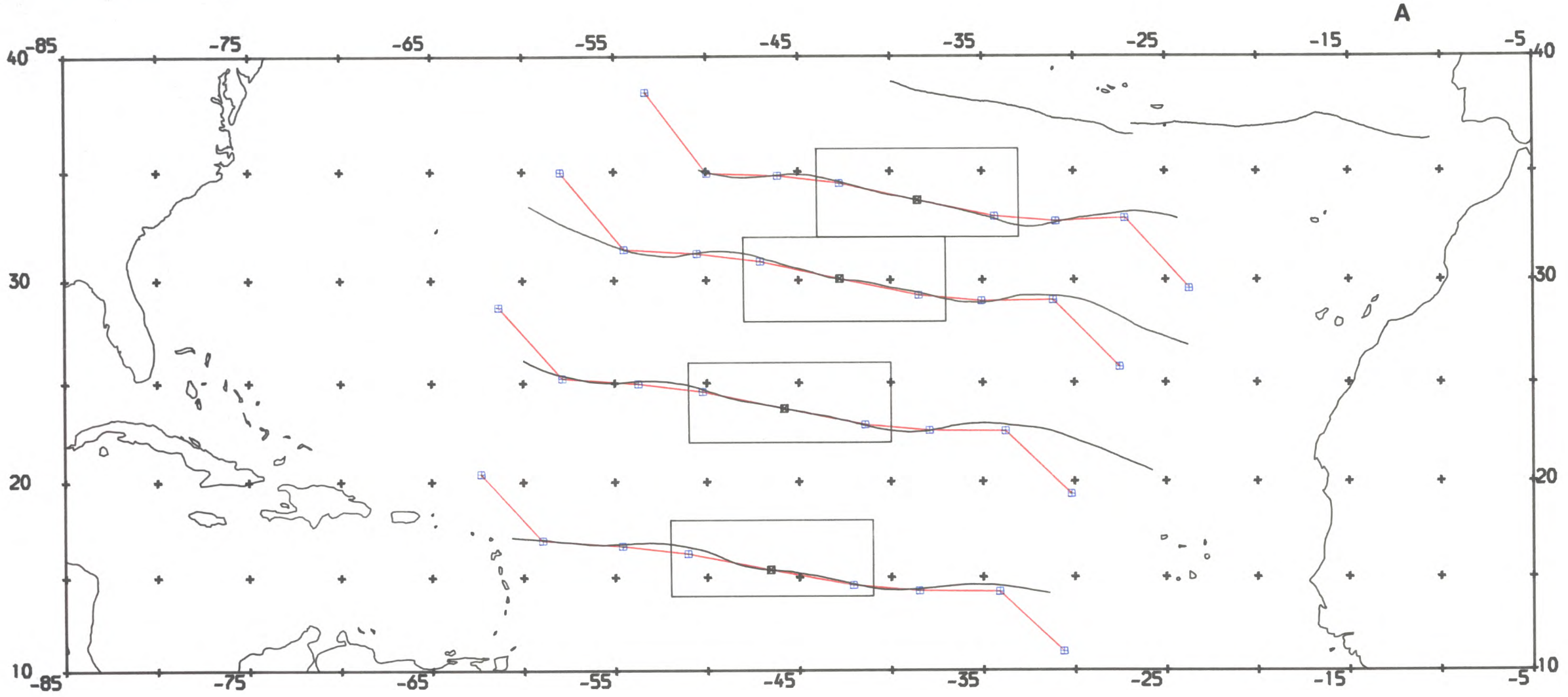
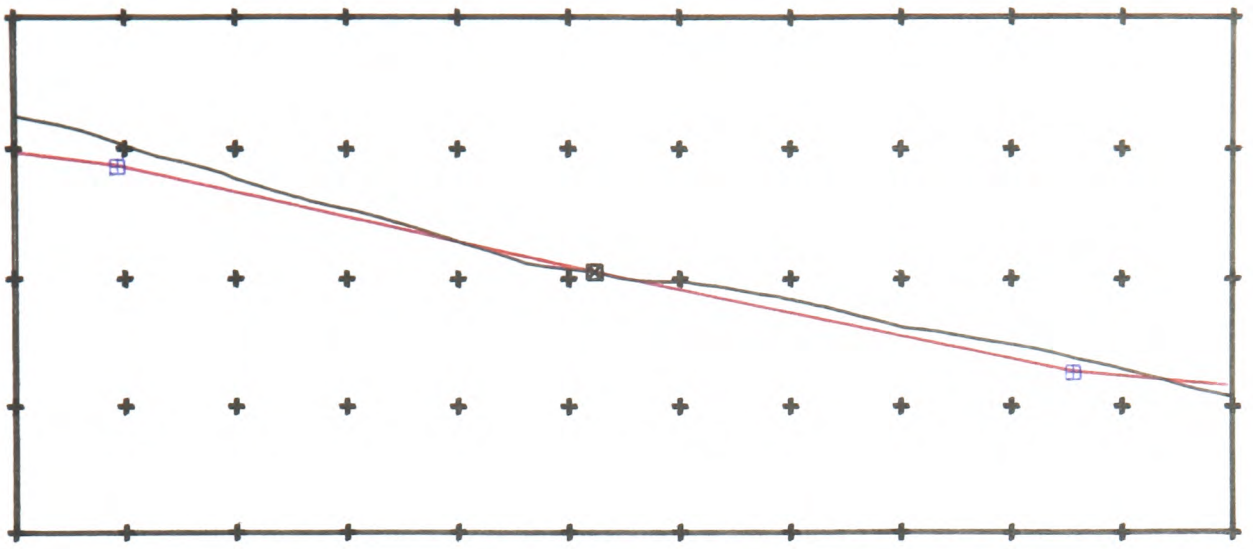

40
30
20
10
-85
-75
-65
-55
-45
-35
-25
-15
-5

Figure 3.7 Olivet et al. (1984): Synthetic Fracture Zone

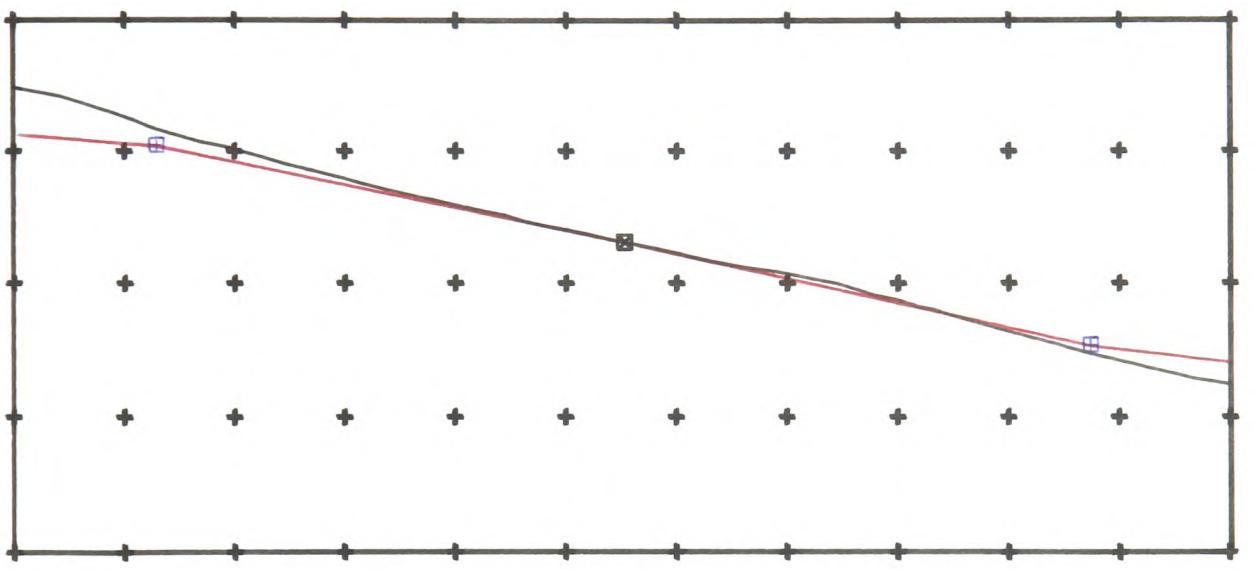
A: Synthetic fracture zone (red) contructed from the published rotation parameters of Olivet et al. (1984), overlain on the Atlantis, Fifteen-Twenty, Hayes and Kane Fracture Zones (black) for comparison. Anomaly positions are shown by squares with + in center (blue) and ridge positions by squares with x in center (black). Anomalies used are 13, 24, 33, and pre-34.
B: Synthetic fracture zone overlain on Hayes Fracture Zone. Scale is three times that of 3.7A. Legend is the same as that of 3.7A.
C: Synthetic fracture zone overlain on Atlantis Fracture Zone. Scale is three times that of 3.7a. Legend is the same as that of 3.7A.
D: Synthetic fracture zone overlain on Kane Fracture Zone. Scale is three times that of 3.7a. Legend is the same as that of 3.7A.
C: Synthetic fracture zone overlain on Fifteen-Twenty Fracture Zone. Scale is three times that of 3.7a. Legend is the same as that of 3.7A.


A
-85
-75
-65
-55
-45
-35
-25
-15
-5
40
30
20
10

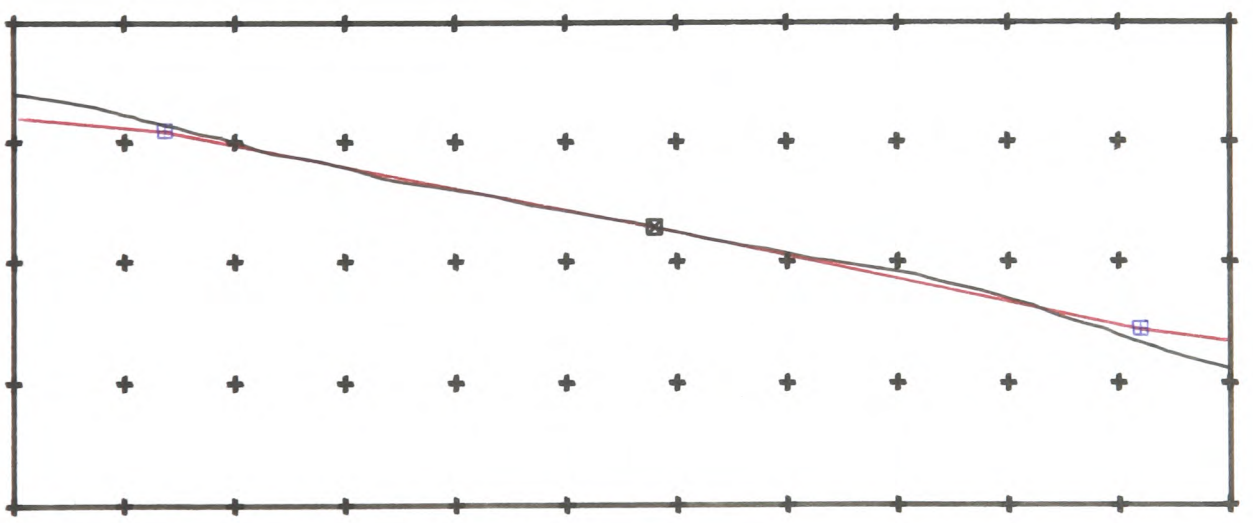
B



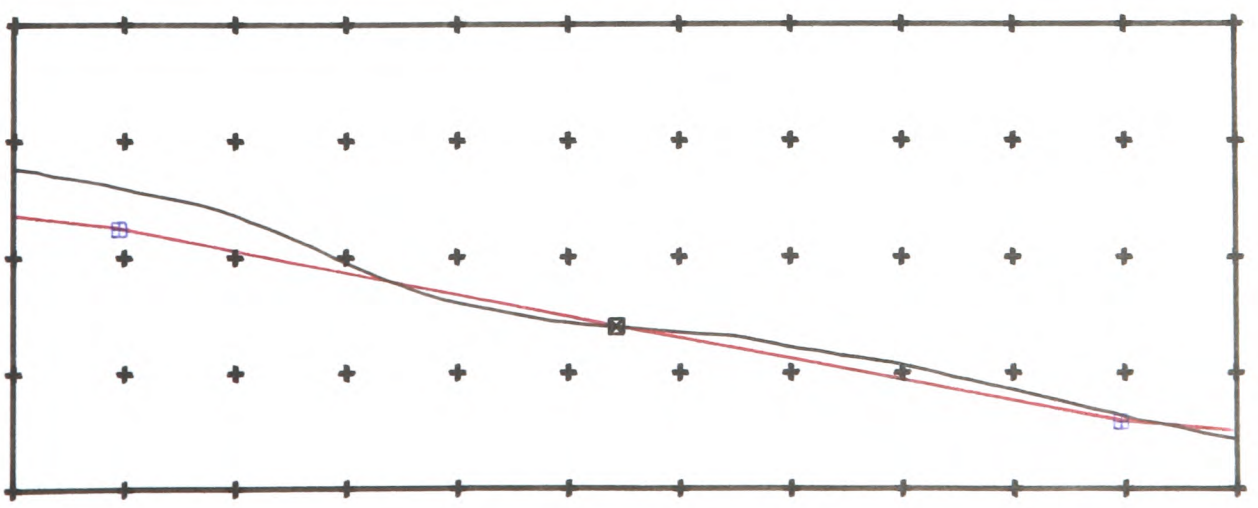
C



D



E



is not in accord with much of the actual fracture zone. Much of the difficulty could be eliminated by using additional anomalies.

3.3.3e Savostin, Sibuet, Zonenshain, Le Pichon, and Roulet's Model (1986)

The rotation parameters are from various sources, although Savostin (1981) and Olivet et al. (1984) are the most prominent contributers. They are given in Table 2 of Savostin et al. (1986). As with their compilation for the North Atlantic, the synthetic fracture zone deviates significantly from the actual one (Fig.3.8). Some of the anomaly positions are very close to the fracture zone, but the motion vector between these positions is inconsistent with that of the transform faults and fracture zones.

3.3.3f Klitgord and Schouten's Model (1986)

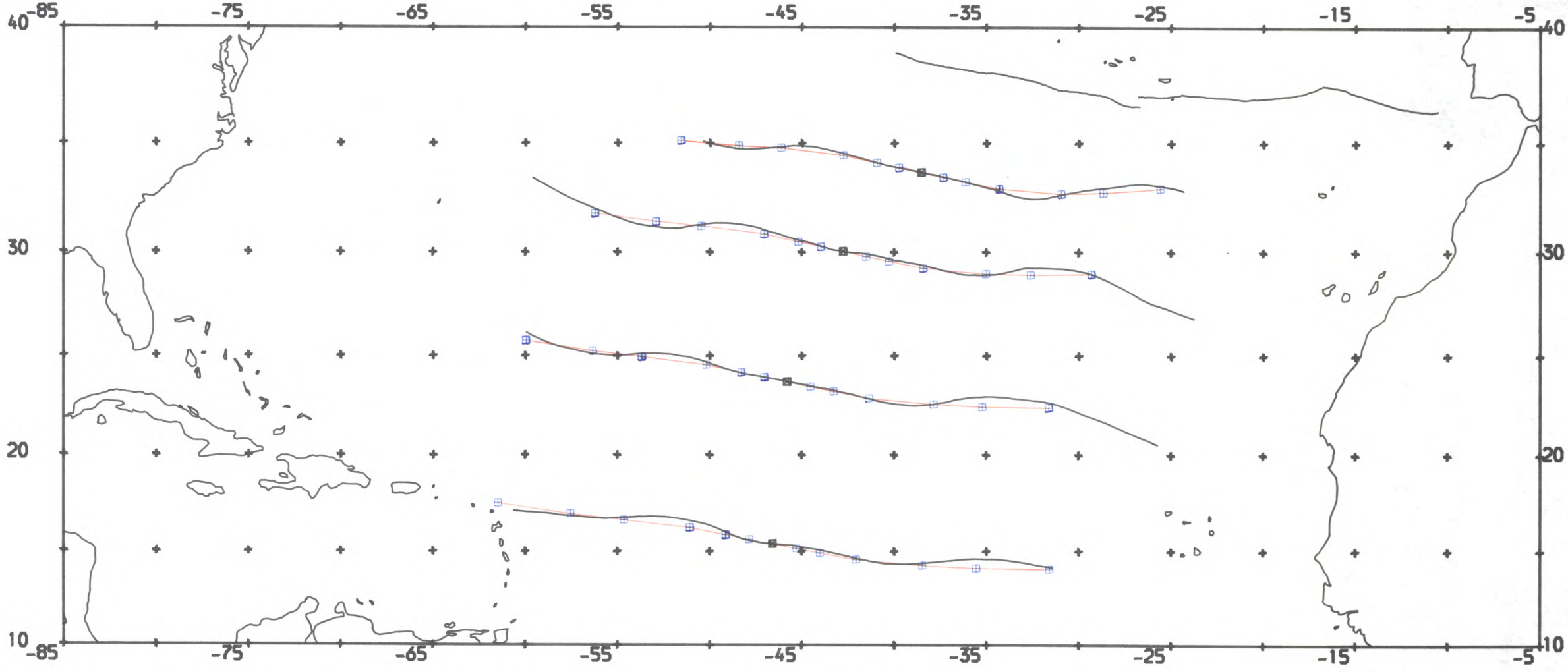
In their analysis of the motion of Africa with respect to Europe, Livermore and Smith (1985) used an earlier version of this model for the separation of Africa and North America. This is the most recent version of those rotation parameters and is examined in place of those used by Livermore and Smith. As can be seen in Figure 3.9, they have set a standard upon which future models must improve. In a sense, this work has moved Central Atlantic reconstructions out of the field of modeling and into the realm of science. The task now is not produce a newer, different model, but to reduce the errors in this work.

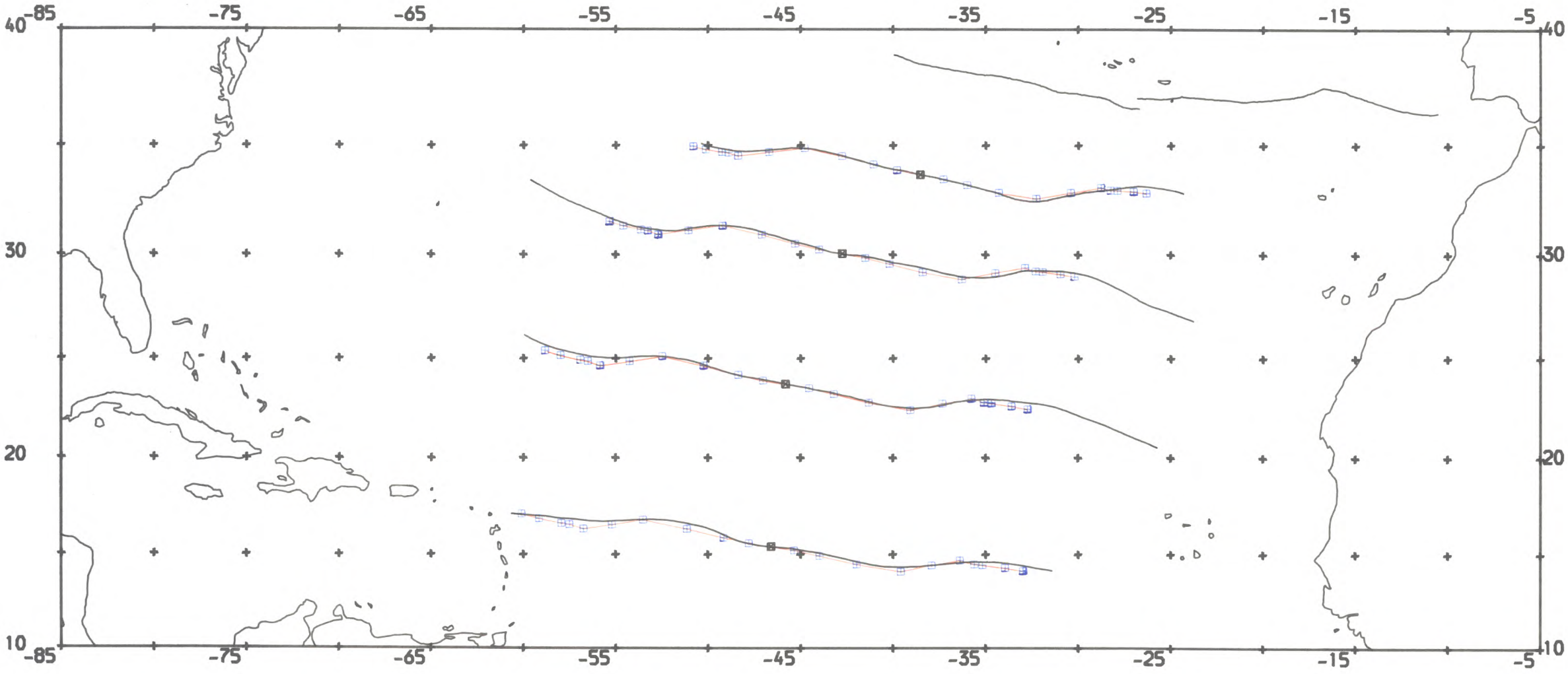
3.3.3g Pindell, Cande, Pitman, Rowley, Dewey, LaBreque and Haxby's Model (1988)

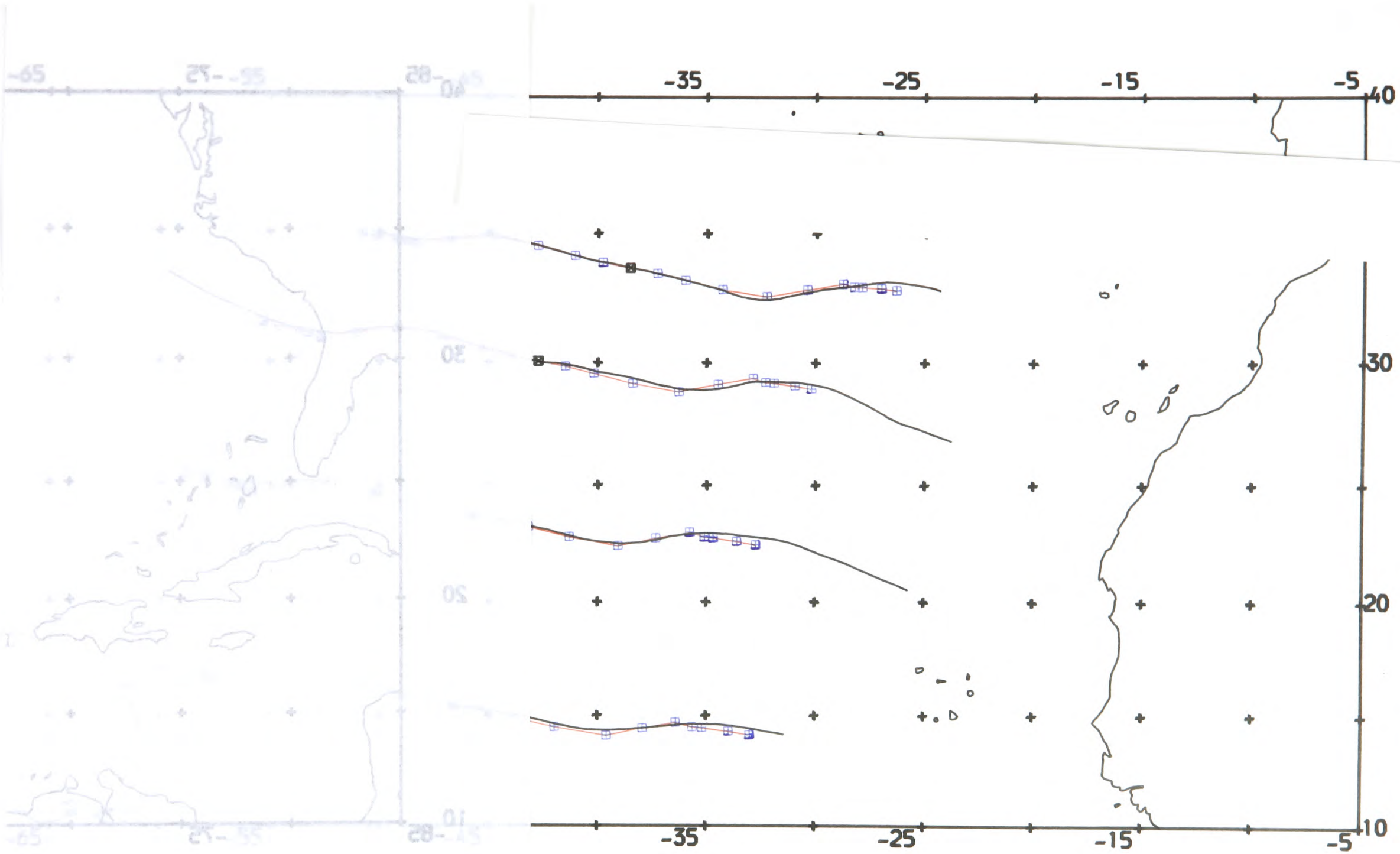
This model varies only slightly from that of Klitgord and Schouten (1986) (Table 3.2) and, to an extent, takes up the task,

Figure 3.8 Savostin et al. (1986): Synthetic Fracture Zone

Synthetic fracture zone (red) contructed from the published rotation parameters of Savostin et al. (1986), overlain on the Atlantis, Fifteen-Twenty, Hayes, and Kane Fracture Zones (black) for comparison. Anomaly positions are shown by squares with + in center (blue) and ridge positions by squares with x in center (black). Anomalies used are 5, 6, 13, 24, 30, and 34.


40
30
20
10
-85
-75
-65
-55
-45
-35
-25
-15
-5


-85
-75
-65
-55
-45
-35
-25
-15
-5
40
30
20
10


-35
-25
-15
-5
40
30
20
10
-35
-25
-15
-5

suggested above, of reducing the errors in Klitgord and Schouten's (1986) parameters. Rotation parameters of previous workers (particularly Klitgord and Schouten (1986)) were examined on an Evans and Sutherland computer using interactive graphics to compare directly anomaly picks and fracture zone traces as well as solutions (J. Pindell, pers. comm.).

Pindell et al. (1988) have improved the fit to the fracture zone for some anomalies, particularly in the region between Anomaly 21 and Anomaly 33 (Fig. 3.10). This was done partly by slightly revising poles and partly by the addition of rotation parameters for Anomaly 24.

3.3.3h Discussion

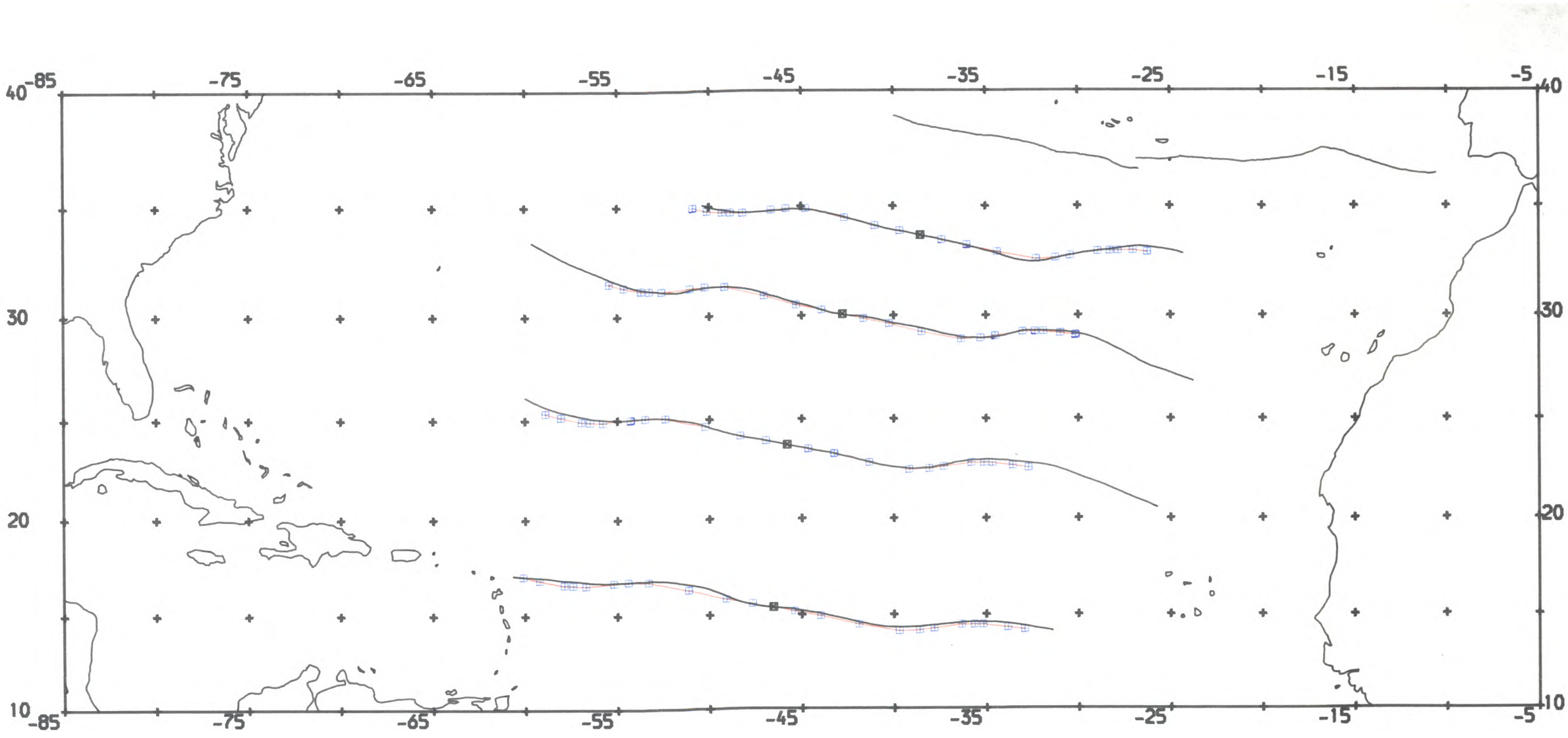
Figures 3.4 - 3.10, show that Central Atlantic evolution has been far less complex to model than North Atlantic evolution. Also, the most recent models have not varied significantly. In a sense, they reflect the attempt to minimize errors in existing models, rather than to develop different ones. Despite the apparently greater simplicity in modeling the ocean, early models were far less successful than similar models for the North Atlantic (compare Figure 3.4 with Figure 2.5). The difference between earlier and present-day models is largely a result of an increase in knowledge of the positions of fracture zones.

3.4 Discussion of the Kinematic Model

The Central Atlantic provides one of the better laboratories for studies of plate kinematics. There is ample data on magnetic anomalies, as well as sufficient numbers of large and small

Figure 3.10 Pindell et al., (1988): Synthetic Fracture Zone

Synthetic fracture zone (red) contructed from the published rotation parameters of Pindell et al., (1988), overlain on the Atlantis, Fifteen-Twenty, Hayes, and Kane Fracture Zones (black) for comparison. Anomaly positions are shown by squares with + in center (blue) and ridge positions by squares with x in center (black). Anomalies used are 5, 6, 13, 21, 24, 25, 30, 32, 33, and 34.


-85
-75
-65
-55
-45
-35
-25
-15
-5
40
30
20
10

offset fracture zones to constrain plate motion direction. It is, therefore, not unreasonable that there seem to be no major differences between the last 3 major Central Atlantic studies (Klitgord and Schouten, 1986; Pindell et al., 1988; this study). Indeed, many of the rotation parameters for "standard anomalies" in this work are based on those proposed in the other studies.

The spreading rate in the Central Atlantic is slow compared with the Pacific but faster than the North Atlantic. It provides, therefore, another opportunity to test the hypothesis, suggested in Chapter 2, that large-offset fracture zones, particularly in slow spreading oceans, are the best guides to past spreading direction. This hypothesis is questioned by Klitgord and Schouten (1986) who note that the structure of large offset transforms "...is usually a composite of structural trends generated at both spreading center intersections...." Their discussion does not take account of spreading rate, the critical variable in determining the width of the principal deformation zone in the transform fault (Fox and Gallo, 1984; 2.5.2).

Examination of Figures 3.3, 3.9, and 3.10 indicates that Klitgord and Schouten (1986) are wrong. In all cases, synthetic fracture zone orientations correlate well with actual fracture zone trends. This suggests that, if there is a "critical spreading velocity" above which the principal deformation zone in large offset fracture zones is not localized, it is greater than the 3 - 4 cm/year Central Atlantic spreading rate.

As in the North Atlantic, spreading rates show variations

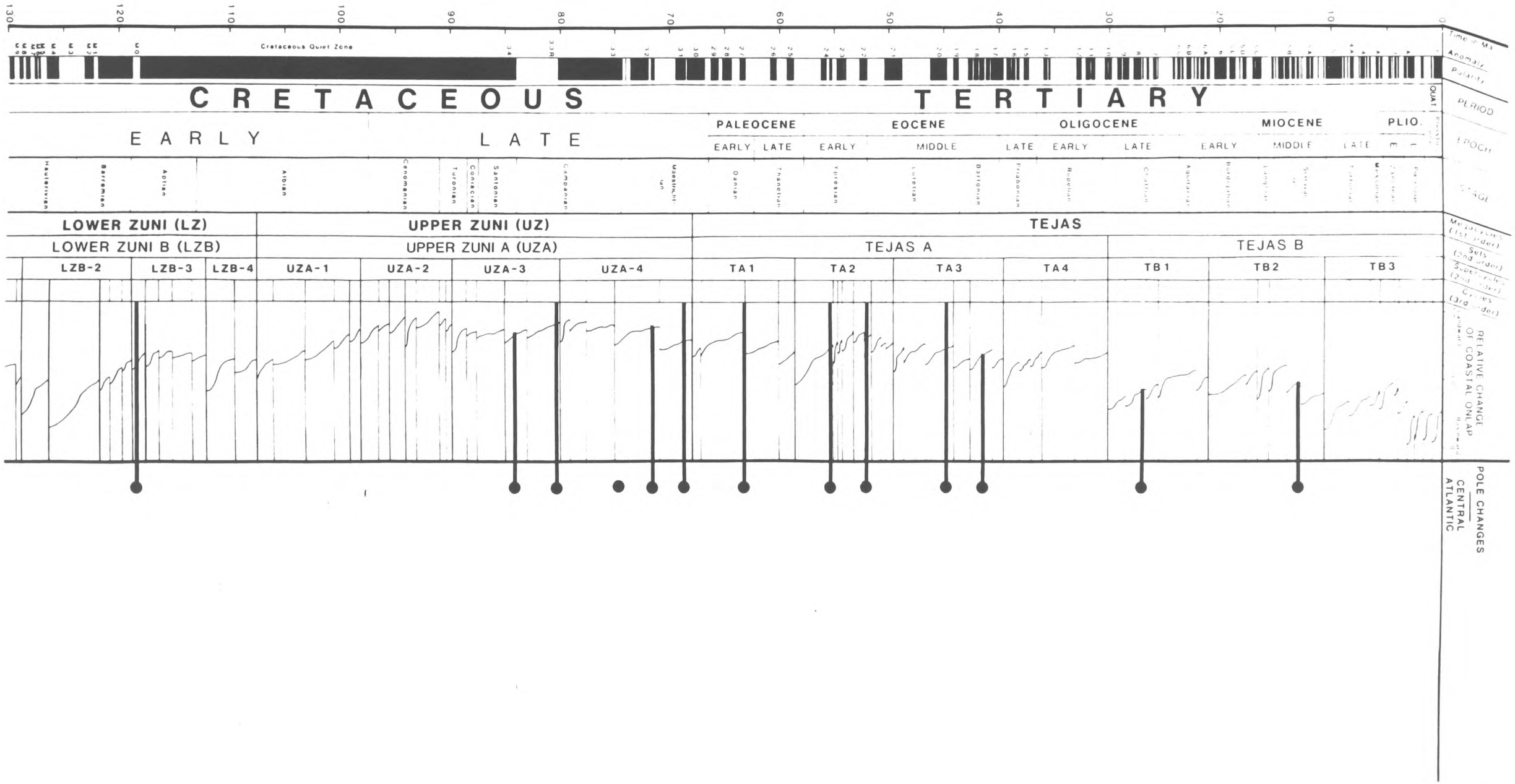
between fracture zones (Klitgord and Schouten, 1986, Fig. 4b) and pole changes are found to occur at anomalies other than those commonly used in other studies (Table 3.2; Figure 3.11). This latter finding should not be considered unusual in light of the different methodology employed in this work, but may have significance in other areas of geological study.

In Figure 3.11, Central Atlantic pole changes are shown on a geologic timescale with the most recently published curve of coastal onlap (Haq et al., 1987). Visual examination suggests a correlation between pole changes and the upper boundaries of seismic stratigraphic sequences found by Haq et al. (1987) on continental margins, with pole changes preceeding sequence terminations by 1 - 3 million years. This correlation suggests a cause and effect mechanism, whereby changes in plate boundary configuration (indicated by changing poles of rotation) cause variation of in-plane stress. The variation of in-plane stress results in apparent changes of sea level (Cloetingh et al., 1985) and has been shown to be a mechanism for changing the subsidence patterns of sedimentary basins, thereby altering the stratigraphy in basins and on their margins (Karner, 1986). The time lag between the pole change and the sequence boundary is approximately the time needed for stresses to build to the level needed for them to propagate rapidly through the plate (S. Cloetingh, personal communication, 1988).

Changing in-plane stress has different effects upon marginal and basinal sedimentary sequences. A compressional in-plane

Figure 3.11 Changes in Pole of Rotation: Central Atlantic Ocean

Pole changes in the Central Atlantic are plotted on the geological time scale. The Berggren et al. (1985) timescale is used for the Cenozoic and the Kent and Gradstein (1985) timescale for the Mesozoic. Also shown is the curve of coastal onlap of Haq et al. (1987) and the correlation between pole changes and sequence boundaries.


Time in MA
Anomaly
Polarity
PERIOD
EPOCH
STAGE
CRETACEOUS
TERTIARY
EARLY
LATE
PALEOCENE
EOCENE
OLIGOCENE
MIOCENE
PLIO.
QUAT.
EARLY
LATE
EARLY
MIDDLE
LATE
EARLY
LATE
EARLY
MIDDLE
LATE
E
L
Cretaceous Quiet Zone
Hauterivian
Barremian
Aptian
Albian
Cenomanian
Turonian
Coniacian
Santonian
Campanian
Maastrichtian
Danian
Thanetian
Ypresian
Lutetian
Bartonian
Priabonian
Rupelian
Chattian
Aquitanian
Burdigalian
Langhian
Serravallian
Tortonian
Messinian
Zanclean
Piacenzian
LOWER ZUNI (LZ)
LOWER ZUNI B (LZB)
LZB-2
LZB-3
LZB-4
UPPER ZUNI (UZ)
UPPER ZUNI A (UZA)
UZA-1
UZA-2
UZA-3
UZA-4
TEJAS
TEJAS A
TEJAS B
TA1
TA2
TA3
TA4
TB1
TB2
TB3
Megasequences (1st order)
Sets (2nd order)
Supersequences (2nd order)
Cycles (3rd order)
RELATIVE CHANGE OF COASTAL ONLAP
POLE CHANGES
CENTRAL ATLANTIC

stress will cause the deepening of basin, with concomitant uplift of the basin margin, whereas an extensional in-plane stress will cause uplift within the basin, while at the same time causing subsidence on the margins. In either case, eustatic sealevel need not have changed at all, nor is it necessary to invoke reactivated faults as a mechanism for producing increased subsidence or causing uplift.

The North Sea provides an excellent example of how sedimentary styles and sequences may change in reponse to changing in-plane stress. The Danian of the North Sea is a fairly thin (<100 m) sequence of pelagic chalk. It is overlain by a very thick Paleocene sequence (>1,100 m) of sandstones and shales. Seismic reflection data show no indication of old faults being reactivated nor of new ones developing and becoming active. Accelerated or rapid cooling cannot be invoked as an explanation as the increased subsidence occurs long after the initiation of the thermal sag phase in the North Sea, at a time when there is relatively little eustatic sea level change.

Pole changes at Anomalies 30 and 27 (North and Central Atlantic, respectively) (Figs. 2.15 and 3.11), shortly before the beginning of accelerated North Sea subsidence and the start of a period of seafloor spreading reorganizations in the North Atlantic, undoubtedly varied the in-plane stress conditions. Moreover, the pole change at Anomaly 30 coincides with the start of the phase of little relative motion between Africa and Europe. Taken together this is a rather striking case for tectonic

control of sedimentary sequences caused by variation of in-plane lithospheric stress.

CHAPTER 4

THE MOTION OF AFRICA RELATIVE TO EUROPE

4.1 Introduction

The paleopositions of plates in convergent zones cannot be directly reconstructed because the evidence largely has been destroyed. Magnetic anomalies and fracture zones, which give the rate and direction of motion, are part of the oceanic lithosphere which begins its return to the mantle at consuming plate boundaries., i.e. subduction zones.

Reconstructions must be made in other ways, one of which is by using evidence from other oceans and is done by completing the finite difference circuit between adjacent sets of plates separated by spreading oceans. This finite difference gives the relative motion between the plates of primary interest. The rationale for using this method and the methodology used to determine the finite difference is briefly reviewed below. For a more complete discussion see Dewey et al. (1973), LePichon et al. (1973), and Ladd (1976).

4.2 Finite Difference Solutions

The use of the finite difference solution to determine the relative motion between two converging plates is based upon a theorem from spherical geometry that holds that two rotations

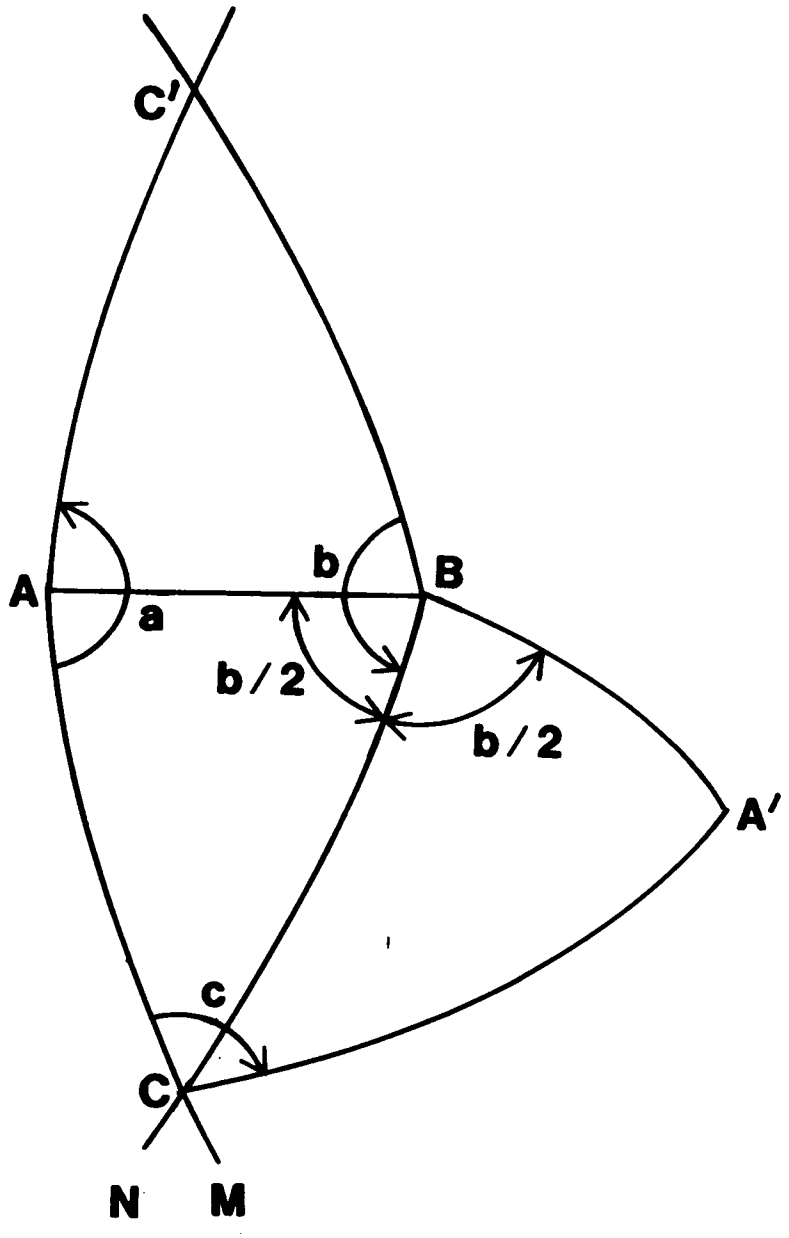
about intersecting axes on a sphere cannot exist alone. If the rotational axes on a sphere pass through its center, they intersect and create a single rotation that is the equivalent of the two independent rotations.

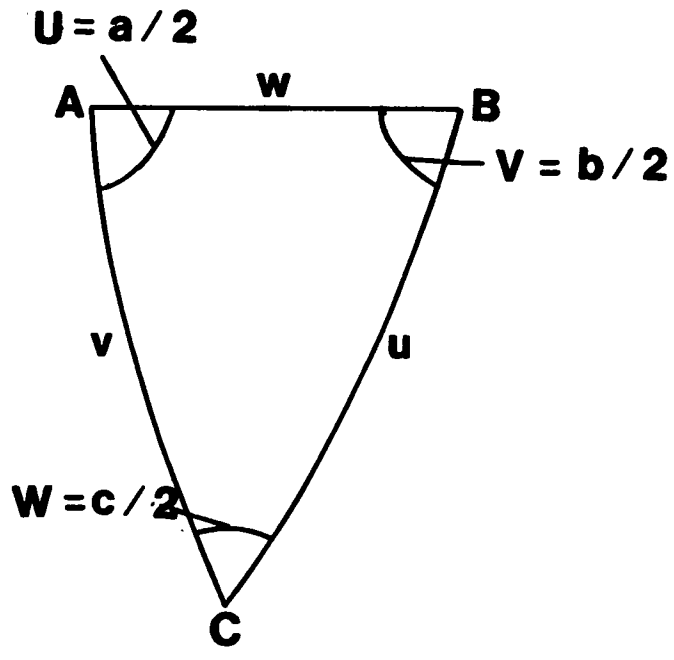
The combination of rotations is elegantly demonstrated by a simple construction shown in Figure 4.1. A and B are points where axes originating at the center of the sphere (O) intersect the surface. If rotation a is performed about OA and followed by rotation b about OB, the problem becomes one of finding the axis of rotation and angle of the rotation equivalent to rotations a and b. To do this, great circles AB, AM, and BN are constructed such that AM and BN make the angles a/2 and b/2, respectively, with AB and intersect at C. The angle a/2 is in the direction opposite to the sense of rotation about A and b/2 is in the same direction as the sense of rotation about B. When rotation a is performed about OA, C is rotated to C' and returned to its original position by rotation b about OB. The spherical triangles ABC and ABC' are equal and the rotations a and b have left C unchanged. Therefore, if there are motions on the sphere due to rotations a and b, then it must be a rotation about OC.

The angle of the rotation about OC is found by considering the spherical triangle ABC whose angles are U = a/2, V = b/2, and W = c/2 and whose sides are the arcs u, v, and w. By application of the law of cosines (cos w = cosu cosv + sinu sinv cosW) to the spherical triangle, the important angles in the construction can be computed. The solution is defined uniquely by the four real

Figure 4.1: Euler Construction

Euler construction for the combination of separate rotations on a sphere. Euler's theorem and construction provide the geometrical basis for the finite-difference solution used in determining the relative motion of Africa with respect to Europe. See text for discussion.





(modified from Buerger, 1956)

Cayley-Klein parameters or can be written in linear vector space notation, where "...the rotation is defined as an orthogonal transformation of a three-dimensional euclidian vector space onto itself." (LePichon et al., 1973).

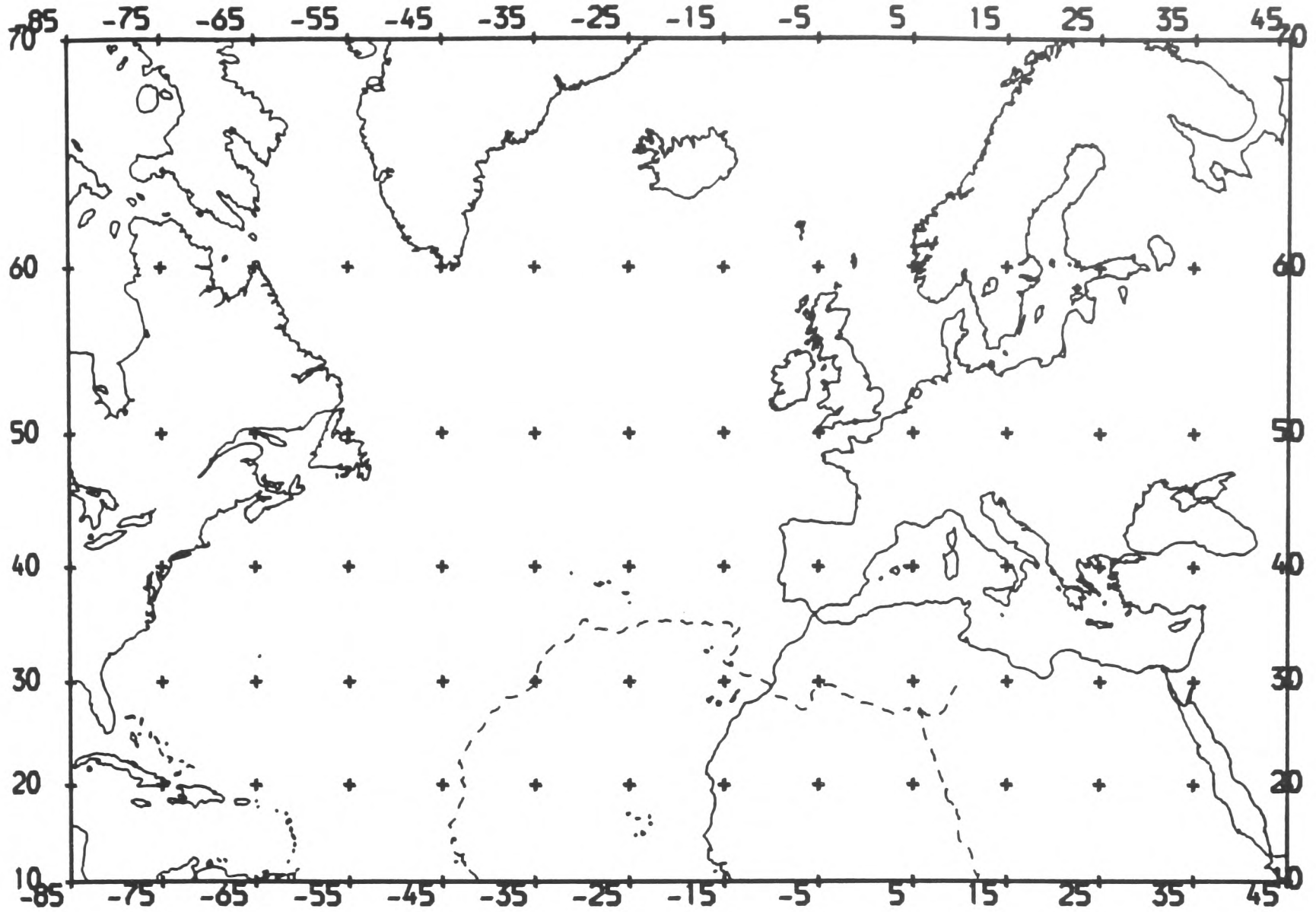
The manner in which the finite difference between the motion of Africa with respect to Europe is determined is illustrated in Figure 4.2. Because the aim is to find the position of Africa with respect to Europe the latter is held fixed. Africa is first rotated to its position with respect to North America at the time in question. This has the effect of closing the Central Atlantic by the required amount. The second required rotation restores North America to its position with respect to Europe at that time, thus closing the North Atlantic Ocean by the required amount. The finite difference between these rotations gives the rotation required to restore Africa to its position with respect to Europe at that particular time.

The procedure utilized by Dewey et al. (1973) is different from that described above. Dewey et al. (1973) determined the finite difference between the positions of Africa and North America during a particular time interval and, after doing the same for North America and Europe, utilized these rotations to determine the rotation needed to alter the position of Africa with respect to Europe for the time interval. This was done for all successive intervals. Although this procedure is different from that given above, the reconstructed positions of Africa will be the same. The difference between the two methods is merely

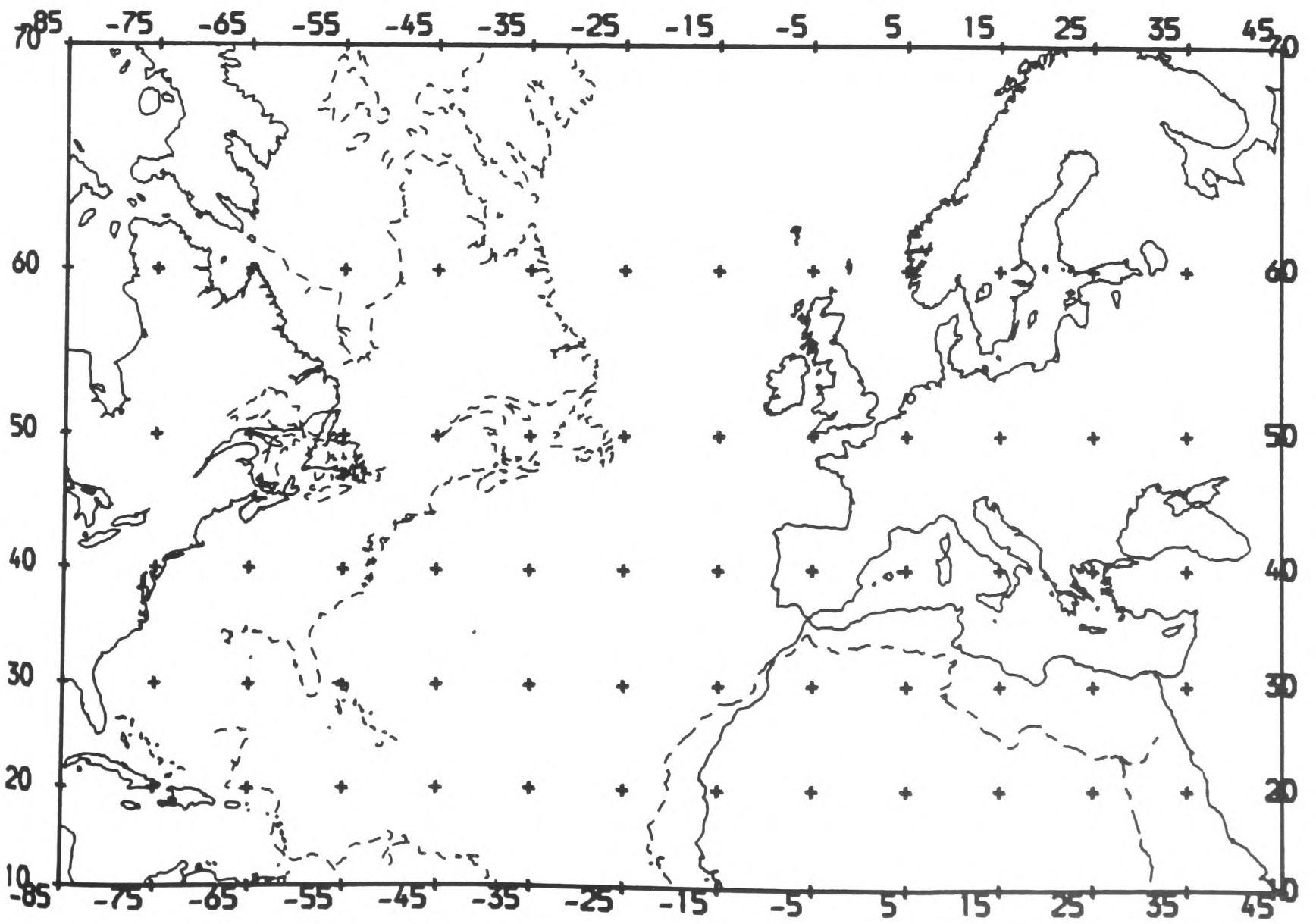
Figure 4.2: Finite-Difference Solution: Africa/Europe

The finite difference between the motion of Africa with respect to North America and of North America with respect to Europe yields the reconstructed position of Africa with respect to Europe. (Europe is shown in present day coordinates and with present day geography.)
A) Present day situation in solid lines and Africa (dashed) also shown rotated to its position with respect to North America at Anomaly 33 (74.9 Ma).
B) North America (dashed) rotated to its Anomaly 33 position with respect to Europe. Africa (dashed) is rotated from its Anomaly 33 position using the same rotation parameters as are used for North America. This gives the position of Africa with respect to Europe at this anomaly. (Greenland has been omitted from this reconstruction for clarity.)

A


-85 -75 -65 -55 -45 -35 -25 -15 -5 5 15 25 35 45
70
60
50
40
30
20
10

B


-85 -75 -65 -55 -45 -35 -25 -15 -5 5 15 25 35 45
70
60
50
40
30
20
10

that one utilizes finite-difference (stage) poles and the other finite (reconstruction) poles (see 1.2 for discussion of poles).

4.3 Kinematic Model

4.3.1 Rotation Parameters

The rotation parameters for the opening of the North and Central Atlantic Oceans (Tables 2.3, 3.2, and 3.4) were used to compute rotation parameters for the motion of Africa with respect to Europe by the method outlined above. The results of these computations are given in Table 4.1. Previously published rotation parameters for this motion are given in Table 4.2.

4.3.2 Presentation of Africa's Motion

The motion of Africa with respect to Europe can be presented diagramatically in two ways. The first of these is by showing the present day coastline being rotated to progressively older positions. The second is by choosing several points, also on the present day coastline, rotating them to progressively older positions, and connecting them. The former is best for showing the style or type of motion with respect to Europe, whereas the latter best illustrates the path of relative motion.

In Plate VII, the position of Africa is shown relative to the present day positions of Africa and Europe for all anomalies from 34 to the present and for selected Keathley or M-Series anomalies. In Plate VIII, the positions of 5 points on the present day African margin are traced back to ~175 Ma to show the

TABLE 4.1

FINITE POLE ROTATION PARAMETERS

FOR THE

MOTION OF AFRICA WITH RESPECT TO EUROPE

ANOMALY	LATITUDE	LONGITUDE	ROTATION
2	2.39	162.74	0.16
2A	1.20	-16.52	-0.24
3	11.04	-14.56	-0.39
3A	7.49	-15.01	-0.55
4	10.14	-14.33	-0.69
4A	1.55	163.68	0.81
5	0.55	-15.78	-0.94
5A	6.72	-14.34	-1.18
5B	18.06	-14.70	-1.36
5C	12.03	-19.83	-1.87
5D	15.97	-18.96	-2.08
6	24.04	-17.32	-2.33
6A	23.38	-17.17	-2.58
6B	25.66	-16.55	-2.79
7	27.06	-15.96	-3.11
8	30.21	-15.12	-3.29
9	29.82	-21.29	-5.55
10	30.08	-21.07	-5.86
11	29.66	-20.99	-6.06
12	30.53	-20.70	-6.36
13	29.26	-20.67	-6.65
15	31.00	-20.18	-7.10
16	33.03	-19.90	-7.36
17	33.77	-19.44	-7.76
18	32.40	-17.73	-8.18
19	32.19	-15.71	-8.28
20	32.34	-15.48	-8.58
21	35.08	-15.54	-10.39
22	34.07	-14.21	-11.11
23	33.06	-15.87	-11.51
24	33.04	-14.59	-10.77
25	33.12	-12.61	-9.87
26	32.98	-12.35	-10.20
27	30.36	-9.29	-10.57
28	31.56	-11.09	-10.85
29	31.65	-10.90	-11.09
30	31.52	-10.73	-11.29
31	32.57	-9.51	-11.30
32	33.60	-10.39	-11.65
33	33.51	-10.42	-11.61
33R	34.01	-11.77	-14.09
34	34.82	-11.66	-14.64

TABLE 4.2

PUBLISHED FINITE ROTATION PARAMETERS

MOTION OF AFRICA WITH RESPECT TO EUROPE

ANOMALY	LATITUDE	LONGITUDE	ROTATION	REFERENCE
5!	9.60	136.60	1.80	(1)
5*	31.30	-33.40	2.90	(2)
5	27.10	-27.90	-2.40	(3)
5	22.70	-31.90	-1.74	(4)
5	30.90	-20.40	-1.70	(5)
6	37.80	-19.00	-3.10	(5)
13!!	9.50	140.80	6.30	(1)
13	29.30	-26.60	-7.80	(3)
13	22.40	-28.80	-6.67	(4)
13	20.80	-16.40	-4.10	(5)
13	24.90	-16.40	-4.90	(6)
21**	34.40	-2.50	6.80	(2)
21	33.70	-18.80	-12.90	(3)
21	34.80	-23.20	-10.91	(4)
23	33.70	-21.00	-11.57	(4)
24	31.90	-16.60	-14.80	(3)
24	32.60	-20.30	-11.73	(4)
24	33.50	-18.00	-9.90	(5)
24	34.40	-16.00	-10.40	(6)
25+	28.40	-150.30	-3.30	(2)
28++	50.80	163.90	13.00	(1)
30	36.40	-15.30	-12.74	(4)
30	33.50	-16.60	-12.50	(5)
31-33	20.10	-11.30	-16.00	(3)
32	34.70	-15.30	-13.14	(4)
33	35.30	-15.20	-15.29	(4)
33R=	25.40	163.80	-5.00	(2)
34==	33.80	-14.10	-16.00	(5),(6)
34	34.50	-14.00	-16.10	(4)

REFERENCES CITED:
(1)Phillips and Forsyth, 1972; (2)Dewey *et al.*, 1973; (3)Biju-Duval *et al.*, 1977; (4)Livermore and Smith, 1986; (5)Savostin *et al.*, 1986; (6)Olivet *et al.*, 1984.

NOTES:
(!)Rotation parameters are given for 10 Ma which is slightly older (1 million years) than Anomaly 5.

(*)Rotation parameters are stagepole rotation parameters for Anomaly 5 to the present.

(!!)Rotation parameters are given for 35 Ma which is the approximate age of Anomaly 13.

(**)Rotation parameters are stagepole rotation parameters for Anomaly 21 to Anomaly 5.

(+)Rotation parmeters are stagepole rotation parameters for Anomaly 25 to Anomaly 21.

(++)Rotation parameters are given for 65 Ma which is the approximate age of Anomaly 28.

(=)Rotation parameters are stagepole rotation parameters for 80Ma (the approximate age of Anomaly 33R) to Anomaly 25.

(==)Rotation parameters are given for Anomaly 34 but the age cited by Savostin *et al.* (1986) is 80Ma which is approximately the age of Anomaly 33R.

All anomaly ages are referred to the Berggren *et al.* (1985) and Kent and Gradstein (1985) time scales.

path of Africa's motion. Simplified versions of Plates VII and VIII are given as Figures 4.3 and 4.4 by the use of selected anomalies.

4.3.3 Africa's Motion

From Figures 4.3 and 4.4 it is obvious that Africa's motion may be subdivided into several parts. The first of these began prior to the Blake Spur Anomaly and continued until at least Anomaly M-0. The motion is one of sinistral strike-slip and marks the initial separation of Africa and North America as the Central Atlantic began to form by lithosperic stretching and seafloor spreading.

A second phase of motion began in the interval between Anomaly M-0 and Anomaly 34. This period of 34 million years is the Cretaceous Quiet Zone and marks a period in which no reversals of the earth's magnetic field are recognized. During this time interval Africa's motion changed from that of east-southeasterly directed sinistral strike-slip to northeasterly directed compression.

The timing of this change is difficult to determine. The absence of magnetic reversals might have been overcome if Central Atlantic fracture zones were better defined for seafloor of this age. However, oceanic crust of this age has undergone the greatest part of its thermal subsidence with the concomitant loss of topographic contrast across the fracture zone. Also, the thickness of sediment cover on oceanic crust of this age in the

Figure 4.3: Kinematic Model: Reconstructed Positions

Africa's position with respect to Europe at selected anomalies is reconstructed by finite-difference solution using Atlantic seafloor spreading data. Present day coastlines of Europe and Africa are shown in black. Reconstructed positions of Africa are shown for Anomaly 5: red; Anomaly 6: green; Anomaly 13: blue; Anomaly 21: black; Anomaly 24: red; Anomaly 30: green; Anomaly 33: blue; Anomaly 34: black; Anomaly M-0: red; Anomaly M-4: green; Anomaly 10: blue; Anomaly M-16: black; Anomaly M-21: red; Anomaly M-25: green; Blake Spur Anomaly: blue; Continent-Ocean Boundary: black; Fit: red.

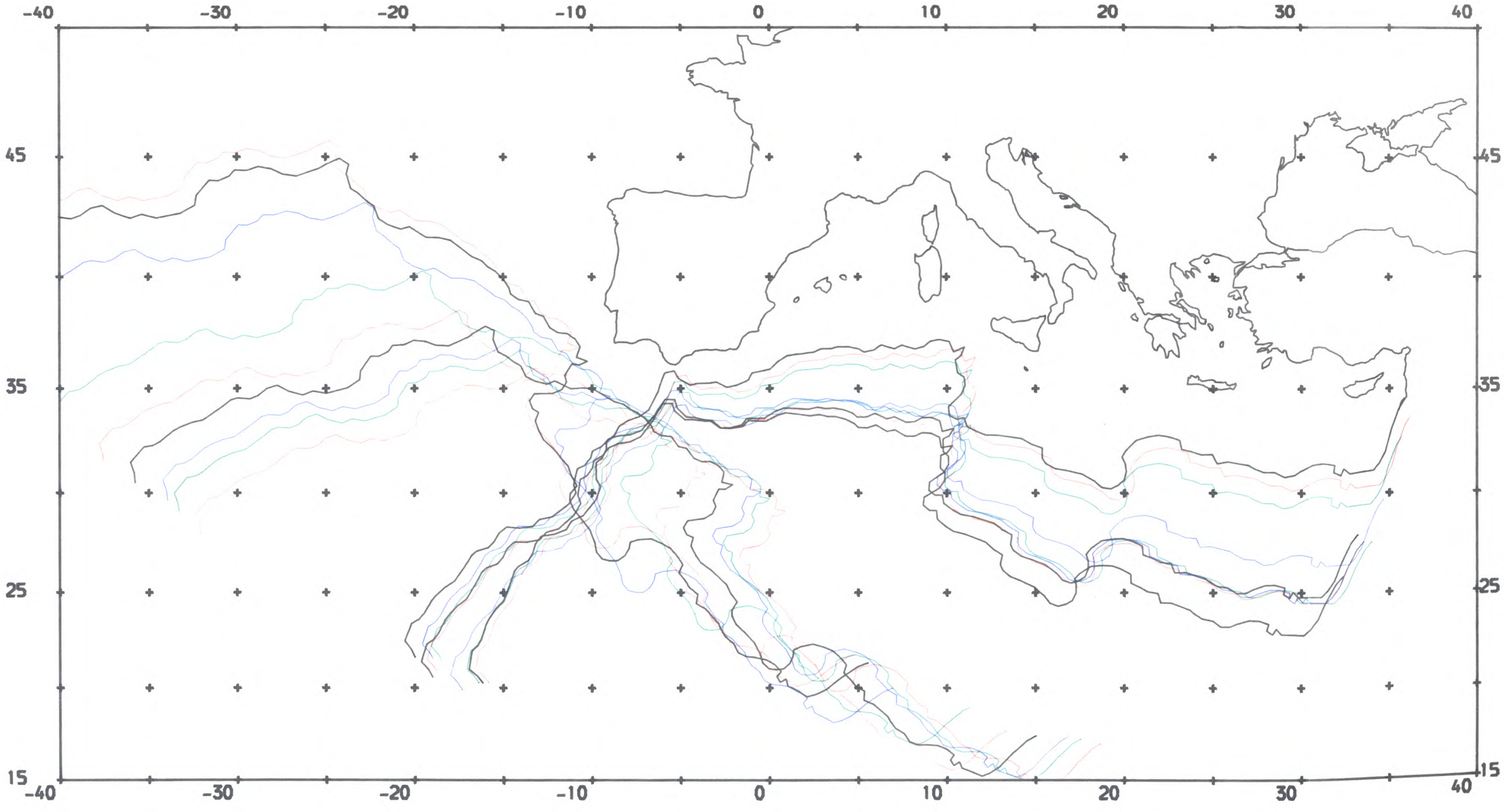
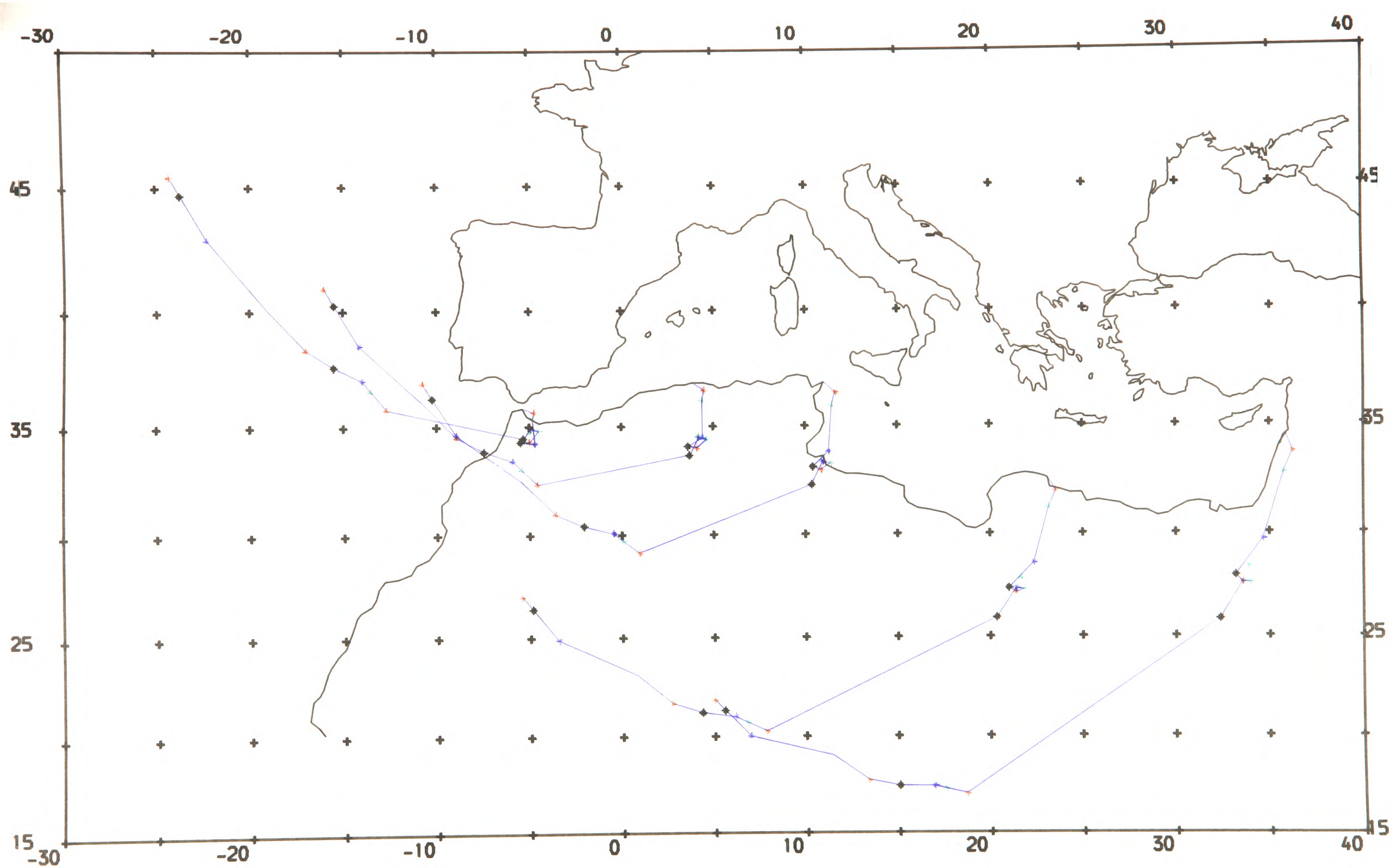

-40
-30
-20
-10
0
10
20
30
40
45
35
25
15

Figure 4.4: Kinematic Model: Path of Relative Motion

The path of Africa's motion relative to Europe is shown for 5 points on the present day African coast. The position of these points at selected anomalies is shown by stars using the same color sequence as in Figure 4.3.


-30
-20
-10
0
10
20
30
40
45
35
25
15

Central Atlantic ranges from over 500 meters to more than 2,000 meters (Emery and Uchupi, 1984), further obscuring fracture zone traces. The result is that, even if a constant rate of seafloor spreading is assumed, calculated rotation parameters have a greater uncertainty because of the lessened control on the direction of seafloor spreading.

In the North Atlantic, the record of seafloor spreading in this time interval is even more poorly known (see Chapter 2). Rotation parameters other than those for Anomaly 34 or closure of the North Atlantic are highly speculative. Nevertheless, it is instructive to use intermediate poles to see whether the timing of this motion change can be constrained in some manner.

Pindell et al. (1988) give an intermediate pole for 101 Ma which was determined by interpolation between their Anomaly 34 and M-0 poles (Table 3.4). Similarly, Klitgord and Schouten (1986) give a Central Atlantic pole for the Cenomanian-Turonian boundary (91 Ma). These have been combined with Kristoffersen's (1978) and Srivastava and Tapscott's (1986) North Atlantic closure poles. The tabulated results are given in Table 4.3 and shown graphically in Figure 4.5. Figure 4.5 also shows Africa's position using rotation parameters suggested by Dewey et al. (1989) and a position calculated with the 100 Ma Atlantic rotation parameters of Olivet et al. (1984) (Table 4.3).

The rotation parameters calculated using Olivet et al.'s (1984) data yield a solution which appears to be totally wrong because it would require northeast or northnortheast motion from

TABLE 4.3

INTERPOLATED ROTATION PARAMETERS FOR MOTION OF AFRICA DURING THE CRETACEOUS QUIET ZONE

ANOMALY	LATITUDE	LONGITUDE	ROTATION	REFERENCE
North Atlantic Poles:				
Closure	77.98	150.25	23.71	(1)
Closure	71.20	147.19	23.38	(2)
100 Ma	87.20	161.20	23.08	(3a)
Central Atlantic Poles:				
101 Ma	69.95	-20.90	-41.91	(4)
91 Ma	73.82	-19.48	-34.28	(5)
100 Ma	69.60	-10.90	-46.20	(3b)
Africa with respect to Europe Poles:				
100Ma	43.60	2.70	-23.60	(3b),(3a)
101 Ma	40.39	-9.47	-25.02	(4),(1)
101 Ma	38.99	-10.60	-27.74	(4),(2)
91 Ma	34.11	-9.72	-17.31	(5),(1)
91 Ma	33.12	-11.42	-20.07	(5),(2)

REFERENCES CITED:

(1)Srivastava and Tapscott, 1986; (2)Kristoffersen, 1978; (3)Olivet et al., 1984; (4)Pindell et al., 1988; (5)Klitgord and Schouten, 1986.

Figure 4.5: Cretaceous Quiet Zone Reconstructions

A: Reconstructions for 91 Ma (red) and 101 Ma (green) using the North Atlantic closure pole of Kristoffersen (1978) and Central Atlantic poles of Klitgord and Schouten (1986) (91 Ma) and Pindell et al. (1988) (101 Ma). Present day coasts of Europe and Africa as well as reconstruction of Africa at Anomalies 34 (84 Ma) and M-0 (118 Ma), the Cretaceous Quiet Zone boundaries, are in black.
B: As in A, except that the reconstructions are made using the North Atlantic closure pole of Srivastava and Tapscott (1986).
C: Reconstruction for 100 Ma (red) using finite-difference solution determined from Atlantic rotation parameters of Olivet et al. (1984). Present day coasts of Europe and Africa as well as reconstruction of Africa at Anomalies 34 (84 Ma) and M-0 (118 Ma), the Cretaceous Quiet Zone boundaries, are in black.
D: Reconstruction for 92 Ma (red) using rotation parameters of Dewey et al. (1989). Present day coasts of Europe and Africa as well as reconstruction of Africa at Anomalies 34 (84 Ma) and M-0 (118 Ma), the Cretaceous Quiet Zone boundaries, are in black.

A

-30 -20 -10 0 10 20 30 40

45

35

25

15

B

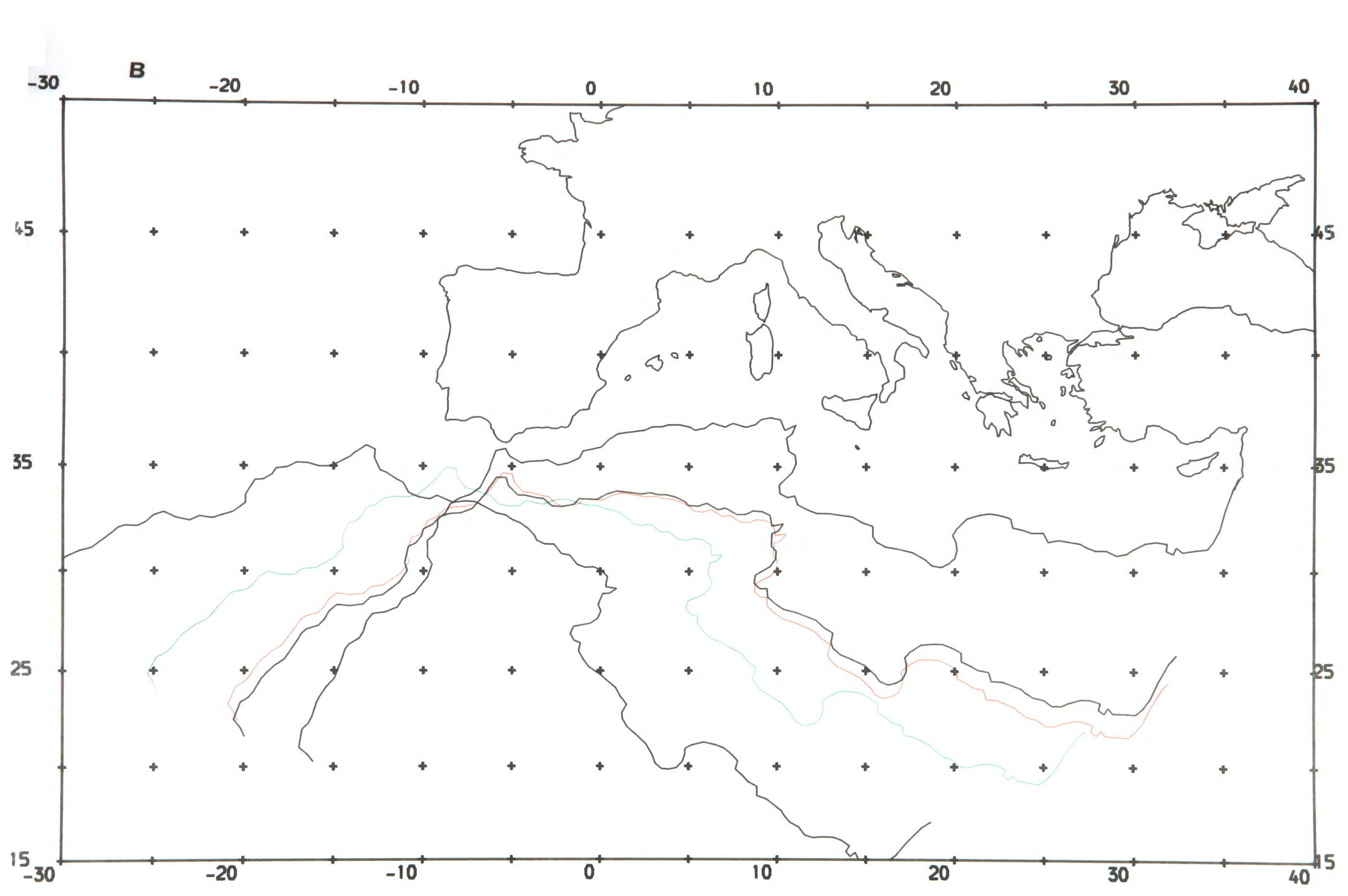
-30 -20 -10 0 10 20 30 40

45

35

25

15



-30 -20 -10 0 10 20 30 40

C

-30 -20 -10 0 10 20 30 40

45

35

25

15

D

-30 -20 -10 0 10 20 30 40

45

35

25

15

118 Ma until 100 Ma followed by west to east, dextral strike-slip motion until 84 Ma. There is no evidence in support of such motions. The most likely explanation is an error in their paper, which results in a spurious solution.

The positions that result from the other solutions are much more reasonable. Both imply that Africa's motion changed at, or shortly after, Anomaly M-0. The computed position of Africa at 101 Ma shows that a change is necessary prior to this time, assuming the interpolated position to be valid.

In any case, the change from eastsoutheast strike-slip to northeasterly directed compression must have occurred prior to the Cenomanian-Turonian boundary. Dewey et al. (1989) suggested, based on cited ages for high-pressure Alpine metamorphism, that the change coincided with this boundary. However, a very long period of time, spanning about 40 million years (120 to 80 Ma), is given as the possible dates during which this metamorphism could occur (Hunziker, 1974). The computed intermediate poles suggest an earlier change of motion is more likely (Figure 4.5).

There are additional reasons to support the earlier change. An earlier change of motion smooths the motion path and makes the change of direction less sudden. As will be shown below (4.3.4), sudden changes of direction, which characterized earlier models, are an artifact of the misinterpretation, or the lack, of data. Continuing Africa's eastsoutheast motion until Cenomanian time not only produces a rather sudden change in direction, but also requires very rapid motion for 9 million years to reach the

Anomaly 34 position (Figs. 4.3 and 4.5).

An earlier date takes into account not only the Sesia-Lazo metamorphic data, but also the early motion of Iberia. As noted previously (2.5.1), although Anomaly 34 is the first anomaly clearly seen on both sides of the Atlantic, Anomaly M-0 has been mapped near the coast of Iberia by Group Galice (1979). The presence of Anomaly M-0 indicates that relative motion of Iberia with respect to Europe, Africa, and North America began relatively early and further suggests that Europe may have begun to move with respect to North America earlier than indicated by magnetic anomaly data. If this is so, a Cenomanian age for the change in Africa's motion relative to Europe is clearly too late.

The northeasterly directed motion that commenced in the Cretaceous Quiet Zone continued until Anomaly 30, at which time the third stage of motion begins. This anomaly marks the beginning of a period of very slow convergence during which Africa's motion is not well defined. The apparent slowdown in convergence, with indications of strike-slip motion, is the result of two factors. The first is geological; the beginning of continental collision between parts of the northern and southern Tethyan margins occurred at about this time (see 6.4, 6.5) and, at a slightly later time, reorganizations of seafloor spreading occurred in the North Atlantic (2.5.1). The second factor is an artifact of the finite difference method. When two vectors are added, their errors are multiplied. Combining rotation poles from two oceans results in a combined pole whose potential error

is greater than that for either of the original poles.

The end of this interval of uncertain motion and start of the next phase is at Anomaly 23 time, shortly after seafloor spreading commenced in the Norwegian-Greenland Sea and the end of major changes in spreading direction in the North Atlantic. At this time, Africa's motion "resumed" on a northeasterly course, which gradually changed to the north-northeast and north.

The final phase of motion begins at Anomaly 5, although smaller pole changes at Anomalies 5A, 5B, and 5C (Table 4.1) portend this final phase. At this time, Africa's motion became northwesterly directed dextral transpression. This is the first model to note this variation in motion. Previous work has suggested that Africa's motion had a northerly vector from Anomaly 5 to the present.

4.3.4 Comparison With Other Models

There are no independent criteria for evaluating models of Africa's motion with respect to Europe. Synthetic fracture zones, which constrain models for spreading oceans and which were used to compare models for the North and Central Atlantic (2.5.3, 3.3.3), have no direct relevance in this context. They indicate only a minimum error that will exist in reconstructed continental positions, but say little about the relative motion path itself. In this section, various models of Africa-Europe relative motion are examined in the light of what is known from the Atlantic data upon which they are based.

In all models, the early (Jurassic-Early Cretaceous) motion path is reasonably well represented, although the positioning of Africa may be incorrect. This is a consequence of lack of adherence to fracture zone constraints (2.5.3, 3.3.3) as well as differences (methodological and geological) in the initial continental reconstruction. It reflects the fact that only the Central Atlantic was opening at this time. In the ensuing discussion, attention will be paid mainly to the Late Cretaceous-Tertiary relative motion path, with discussion of the pre M-0 phase kept to a minimum for the above mentioned reasons.

There are seven published kinematic models for the relative motion of Africa with respect to Europe. Five of them are discussed, in varying degrees of detail, below. Philips and Forsyth's (1972) model is omitted because of major discrepancies between its synthetic fracture zone traces and the Atlantic fracture zones (Figs. 2.6 and 3.5). Smith's (1971) model, which also utilized a fixed pole of rotation opening model, is also omitted from discussion. Two additional solutions have been constructed. The first uses the Atlantic parameters of Sclater et al. (1977). The second, the "DNAG model", was computed using Atlantic parameters published in the Decade of North American Geology volume on the Atlantic (Vogt and Tucholke, 1986). These are discussed after the published models.

Before commencing discussion of the models, an additional warning must be given. Each model is discussed in general terms, but the specifics of relative motion vary greatly along a plate

margin depending upon its configuration and the location of any particular point with respect to the pole of rotation. Hence, although the overall direction of relative motion between the two major, converging lithospheric plates is discussed, detailed motion along parts of the boundary may vary by more than 90° and, locally, be accompanied by changes in the type of motion.

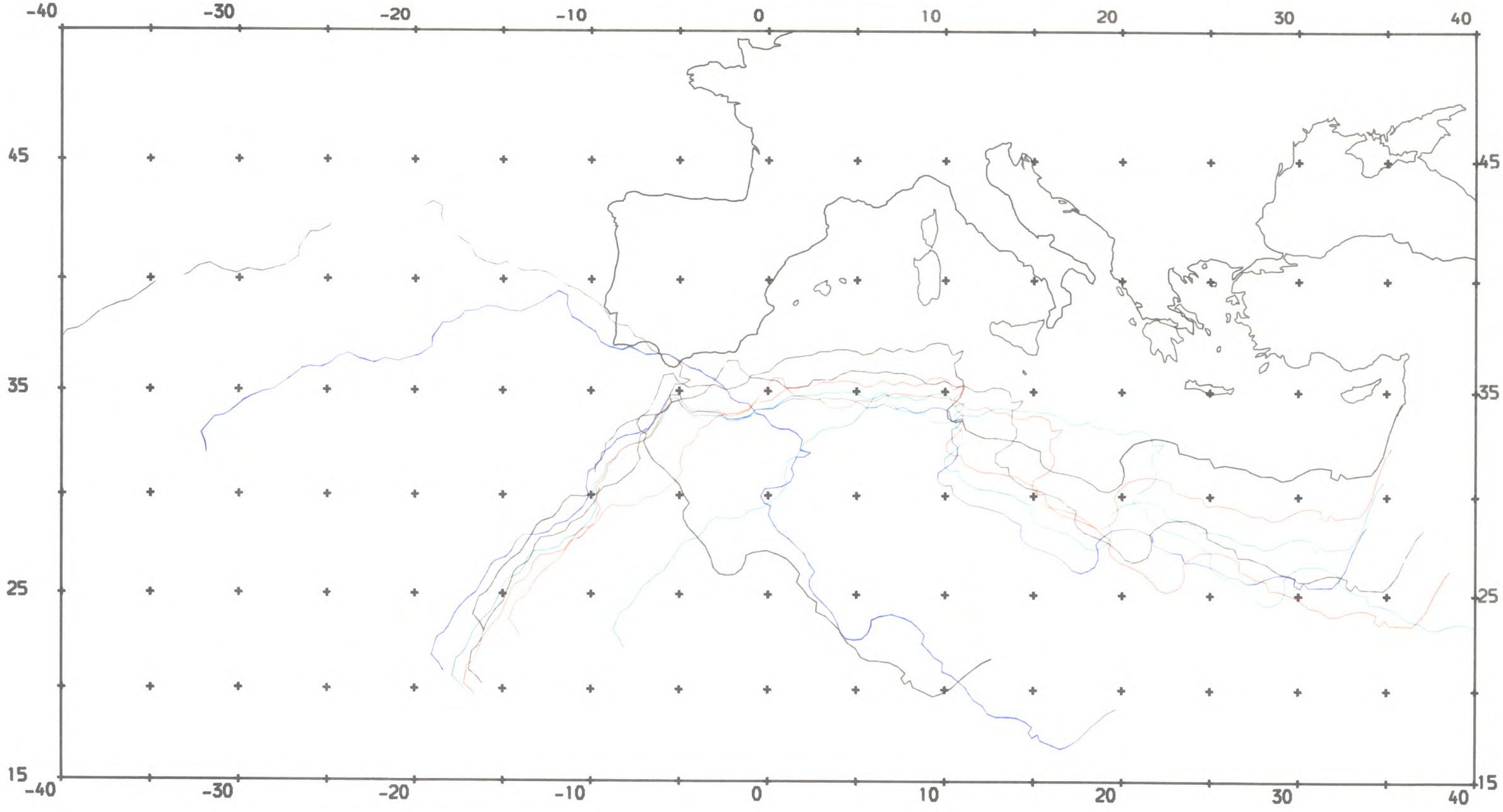
4.3.4a Dewey, Pitman, Ryan, and Bonnin's Model (1973)

Of all kinematic models which deal with the relative motion of Africa with respect to Europe this is the most well known, having been cited several hundreds of times in other works (J.F. Dewey, pers. comm., 1988). It was developed using Pitman and Talwani's (1972) Atlantic seafloor spreading parameters. Although now dated, and its flaws evident, the broad outlines of the model are consistent with the minimal data base upon which it was based.

As Figure 4.6 shows, the most enigmatic feature of the model is the sudden change from northeasterly to northwesterly directed motion at approximately 80 Ma, the time when seafloor spreading was thought to have initiated in the North Atlantic. Subsequent work has shown this sudden change to be an artifact of the extrapolation used to determine motion between North America and Europe prior to Anomaly 31 (later reidentified as Anomaly 33) and the unconstrained Central Atlantic rotation parameters for this anomaly (Fig. 3.4). Similarly, the east-west strike-slip motion between Anomalies 25 and 21 is a consequence of untenable Central Atlantic rotation parameters for Anomaly 25 (Fig.3.4).

Figure 4.6: Dewey et al. (1973): Africa-Europe Reconstructions

Reconstructions of Africa's position with respect to Europe using rotation parameters recalculated from Dewey et al. (1973) and Pitman and Talwani (1972). Present day coasts of Europe and Africa are in black. Reconstructed positions of Africa are shown for Anomaly 5: red; Anomaly 13: green; Anomaly 21: blue; Anomaly 25: black; Anomaly 33: red; 80 Ma: green; 148 Ma: blue; 180 Ma: black.


-40
-30
-20
-10
0
10
20
30
40
45
35
25
15

4.3.4b Biju-Duval, Dercourt, and LePichon's Model (1977)

This kinematic model has generally been overlooked despite the fact that it took account of the increased Atlantic data that became available after the publication of Pitman and Talwani's (1972) model. The most probable reason for this is that despite the additional data the pattern of relative motion is very similar to that of Dewey et al. (1973) (Fig. 4.7). The problem of sudden, somewhat arbitrary changes in plate motion were still unresolved. It was, however, the first model to recognize the problem of locating Africa during the Cretaceous Quiet Zone, with an interpolation between the Anomaly M-2 and Anomaly 31-33 poles being used to provide a Cenomanian (90 Ma) reconstruction pole.

4.3.4c Olivet, Bonnin, Beuzart, and Auzende's Model (1984)

This model utilized only some of their Atlantic poles to describe the Africa-Europe relative motion path. To make the model as complete as possible, solutions have been computed for Atlantic rotation parameters which were not used in the Africa-Europe model. The computed solution for 100 Ma is undoubtedly erroneous (4.3.3) and is not included in the discussion. It is, however, shown in Figure 4.8.

The use of so few anomalies, including computed additions, makes comparisons difficult. There is no indication of the early Tertiary minor motion phase noted in this work, nor of the post-Anomaly 5 change to northwesterly directed compression. However, such differences may be hidden by the relatively gross time intervals. Of more import is that the apparent motion path between Anomalies M-0 and 34 also does not suggest the change

Figure 4.7: Biju-Duval et al. (1977): Africa-Europe Reconstructions

Reconstructions of Africa's position with respect to Europe using rotation parameters of Biju-Duval et al. (1977). Present day coasts of Europe and Africa are in black. Reconstructed positions of Africa are shown for Anomaly 5: red; Anomaly 13: green; Anomaly 21: blue; Anomaly 24: black; Anomaly 33: red; 90 Ma: green; Anomaly M-2: blue; Anomaly M-25: black; Fit: red.

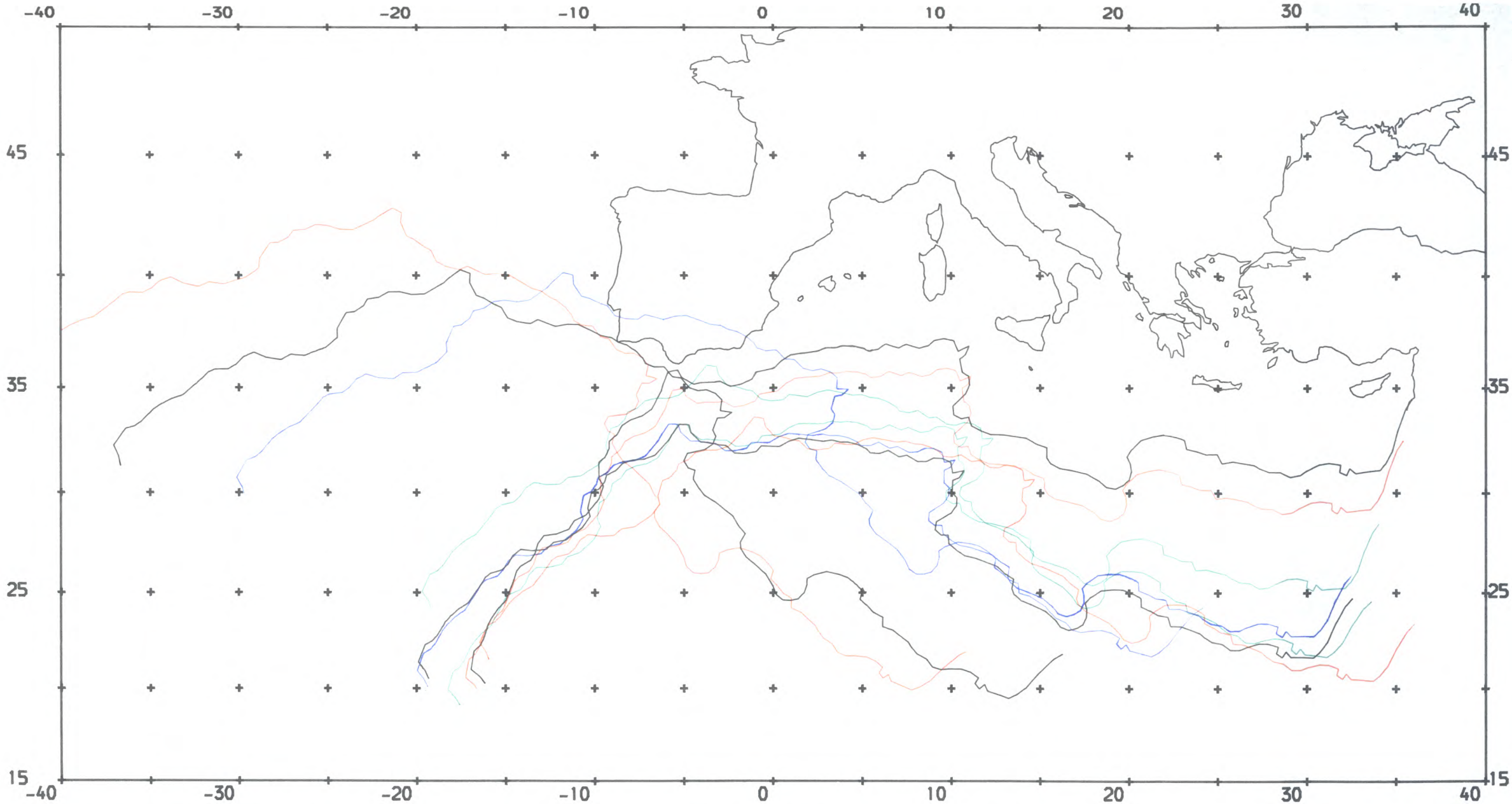
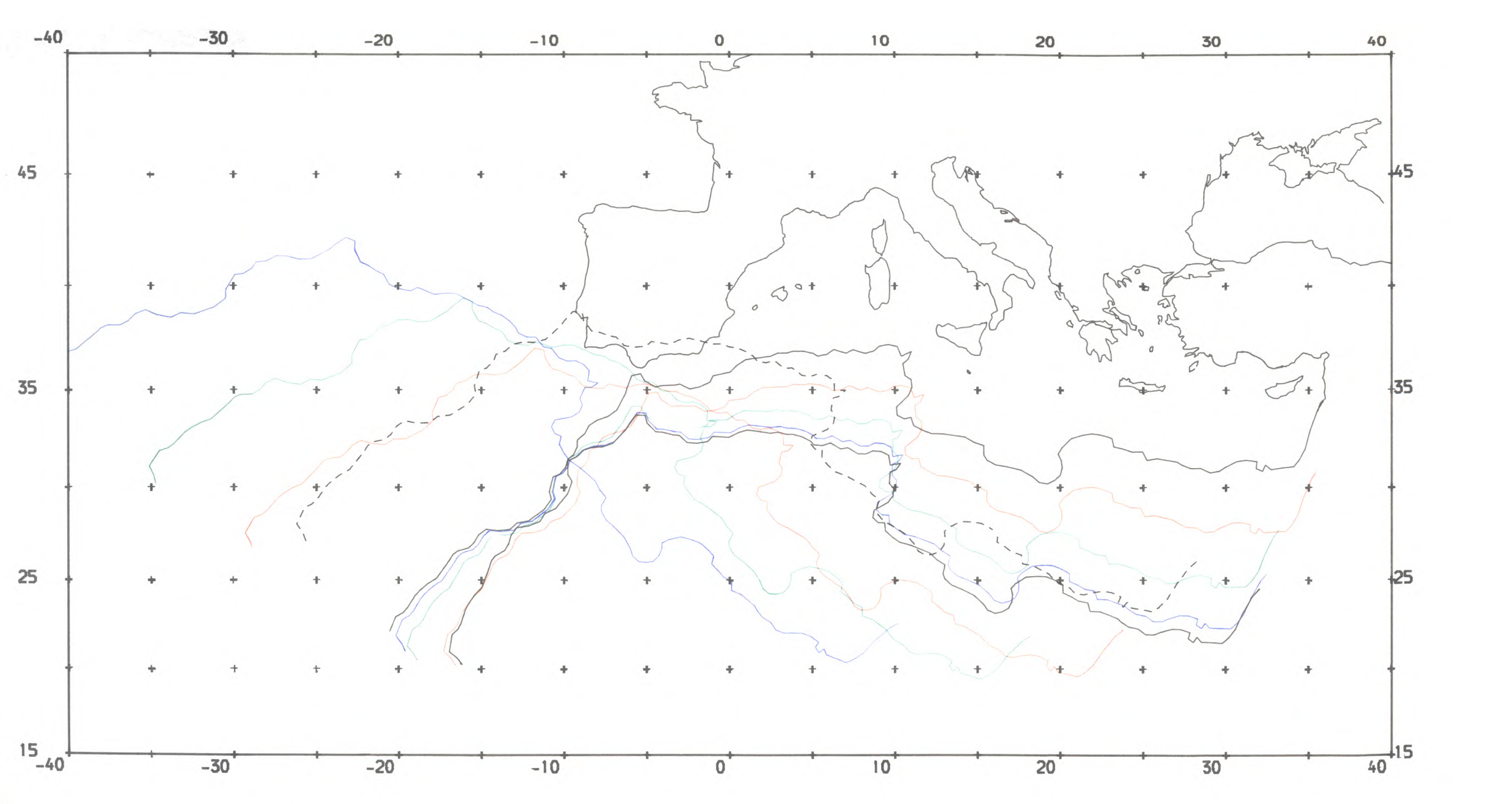

-40
-30
-20
-10
0
10
20
30
40
45
35
25
15

Figure 4.8: Olivet et al. (1984): Africa-Europe Reconstructions

Reconstructions of Africa's position with respect to Europe using rotation parameters of Olivet et al. (1984). Present day coasts of Europe and Africa are in black. Reconstructed positions of Africa are shown for Anomaly 13: red; Anomaly 24: green; Anomaly 33: blue; Anomaly 34: black; Anomaly M-0: red; Anomaly M-22: green; Fit: blue. Reconstruction for 100 Ma, computed from Olivet et al.'s Atlantic parameters is shown in dashed black line. See text for discussion of the 100 Ma reconstruction.


-40
-30
-20
-10
0
10
20
30
40
45
35
25
15

from strike-slip to compression evident in other studies and dictated by the geology of the region. This change is only observed after Anomaly 34. Given the data available when the study was made the large spacing between anomalies that were used is hard to comprehend. Therefore, the model has little to offer and adds little to our understanding of Africa-Europe kinematics.

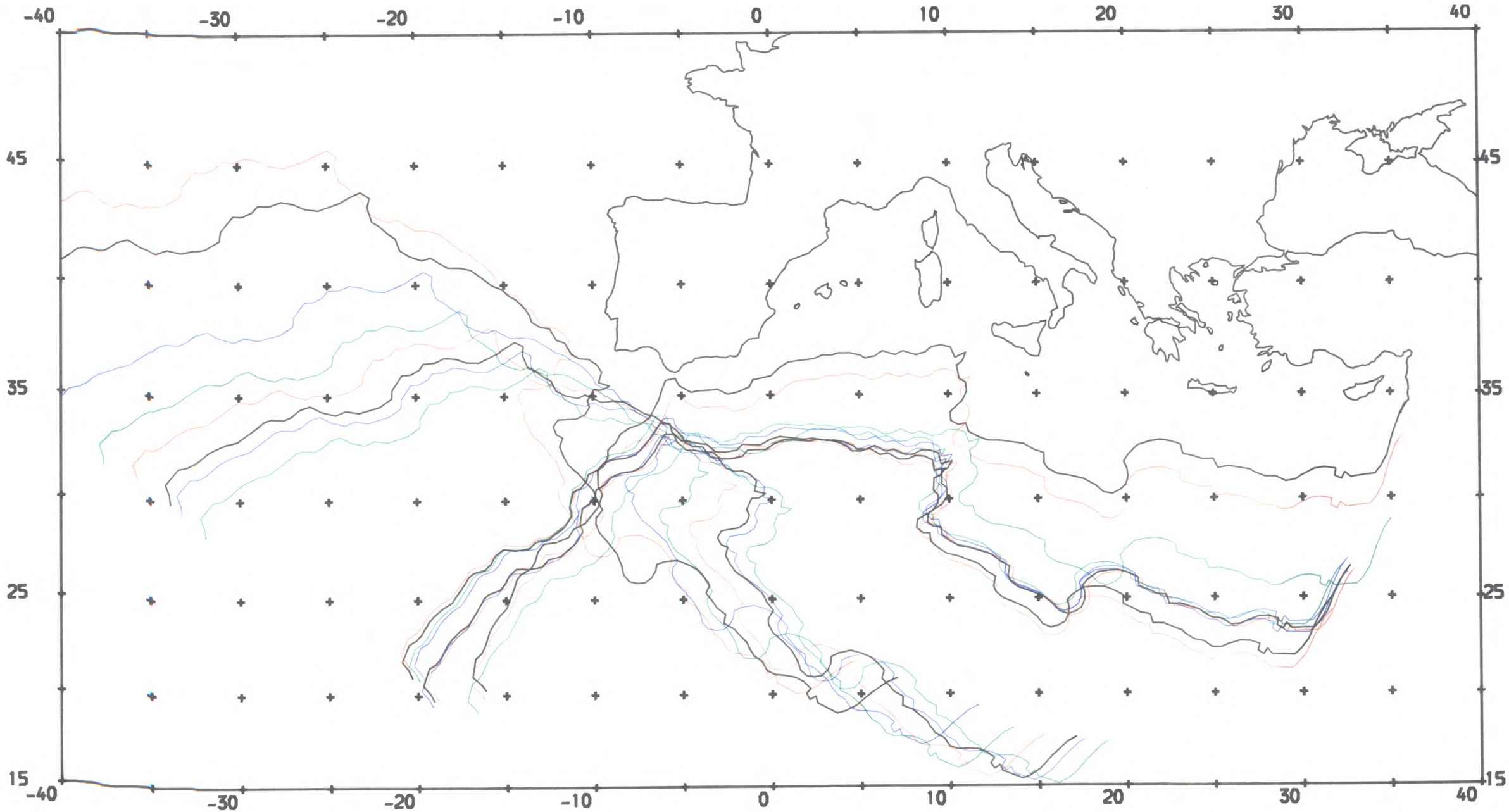
4.3.4d Livermore and Smith's Model (1985)

As mentioned previously (1.1), this model was the first to incorporate Klitgord and Schouten's (1982) data for the Central Atlantic and was first presented at a conference several years prior to publication. The model showed clearly that sudden and unusual changes in direction of relative motion were a consequence of the lack of, or the misinterpretation of, data and of errors in computing the Atlantic solutions. Africa's path was demonstrated to be smoother and simpler than previously thought.

A major feature of Africa's motion, the period of uncertain motion between Anomaly 30 and Anomaly 21, was suggested in their reconstructions (Livermore and Smith, 1985, Figs. 5.12, 5.13; Fig. 4.9) but not commented upon with respect to events in the circum-Mediterranean region. Rather, they noted 1) that in a hotspot frame of reference both plates would have had northward motions for this time interval and 2) that not all tectonic or kinematic events would necessarily coincide with the anomaly data available to them. Despite this the model represents a major breakthrough because it eliminated many of the sudden, unusual changes in plate motion that characterized earlier models.

Figure 4.9: Livermore and Smith (1985): Africa-Europe Reconstructions.

Reconstructions of Africa's position with respect to Europe using rotation parameters of Livermore and Smith (1985). Present day coasts of Europe and Africa are in black. Reconstructed positions of Africa are shown for Anomaly 5: red; Anomaly 13: green; Anomaly 21: blue; Anomaly 23: black; Anomaly 24: red; Anomaly 30: green; Anomaly 32: blue; Anomaly 33: black; Anomaly 34: red; Anomaly M-0: green; Anomaly M-4: blue; Anomaly M-11: black; Anomaly M-16: red; Anomaly M-21: green; Anomaly M-25: blue; Blake Spur Anomaly: black; Fit: red.


-40
-30
-20
-10
0
10
20
30
40
45
35
25
15

4.3.4e Savostin, Sibuet, Zonenshain, Le Pichon, and Roulet's Model (1986)

As discussed previously this model is an amalgam of rotation parameters from various sources. Two features characterize the model. The first is a sudden change from N-S convergence to E-W dextral strike-slip between Anomaly 13 and Anomaly 6, after which N-S convergence again predominates (Fig. 4.10). Savostin et al. (1986) explain this by a major slowdown in the rate of seafloor spreading in the Central Atlantic, without a similar slowing of North Atlantic spreading (Fig. 4.11).

When other Central Atlantic spreading data is examined slowdowns of similar magnitude are found to have occurred (Fig. 4.11). However, none of the other models show the strike-slip motion present in this model. Moreover, analysis of Savostin et al.'s (1986) North Atlantic spreading rate data indicates a major slowdown in the Miocene (Anomaly 6 to Anomaly 5) (Fig. 4.11). This slowdown, which is not found in other models, is required to reestablish Africa's northward motion (Fig. 4.11).

The foregoing clearly suggests that a slowdown in the rate of seafloor spreading in the Central Atlantic is unlikely to have caused the change of motion between Anomalies 6 and 13. A more likely explanation for this drastic change in motion during the Oligocene is the very large rotation angle (8.3°) of Savostin (1981) for Anomaly 13 in the North Atlantic (Table 2.2). This rotation (used in the Savostin et al. (1986) model) is greater by 1^{0} - 1.5° than that given in other models and can easily account for the displacement. It also accounts for the slowdown in North

Figure 4.10: Savostin et al. (1986): Africa-Europe Reconstructions

Reconstructions of Africa's position with respect to Europe using rotation parameters of Savostin et al. (1986). Present day coasts of Europe and Africa are in black. Reconstructed positions of Africa are shown for Anomaly 5: red; Anomaly 6: green; Anomaly 13: blue; Anomaly 24: black; Anomaly 30: red; Anomaly 34: green; Anomaly M-0: blue; Anomaly M-17: black; Anomaly M-22: red; Blake Spur Anomaly: green; Fit: blue.

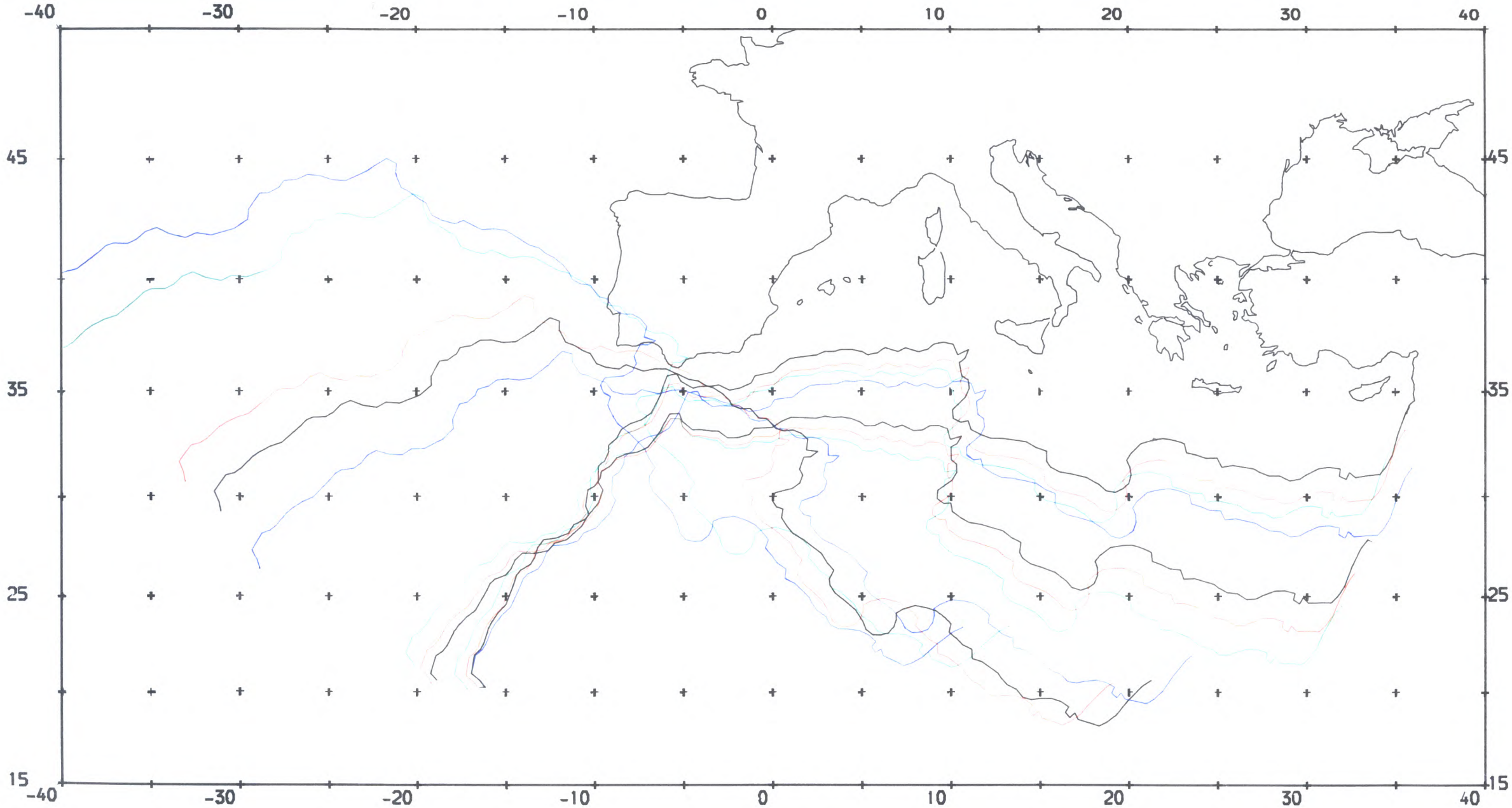
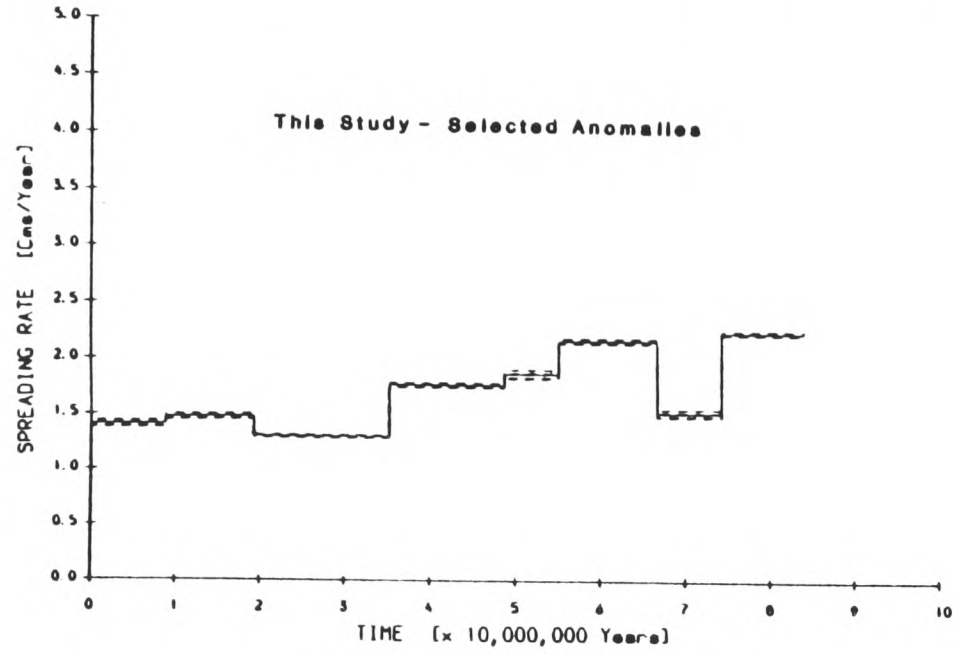

-40
-30
-20
-10
0
10
20
30
40
45
35
25
15

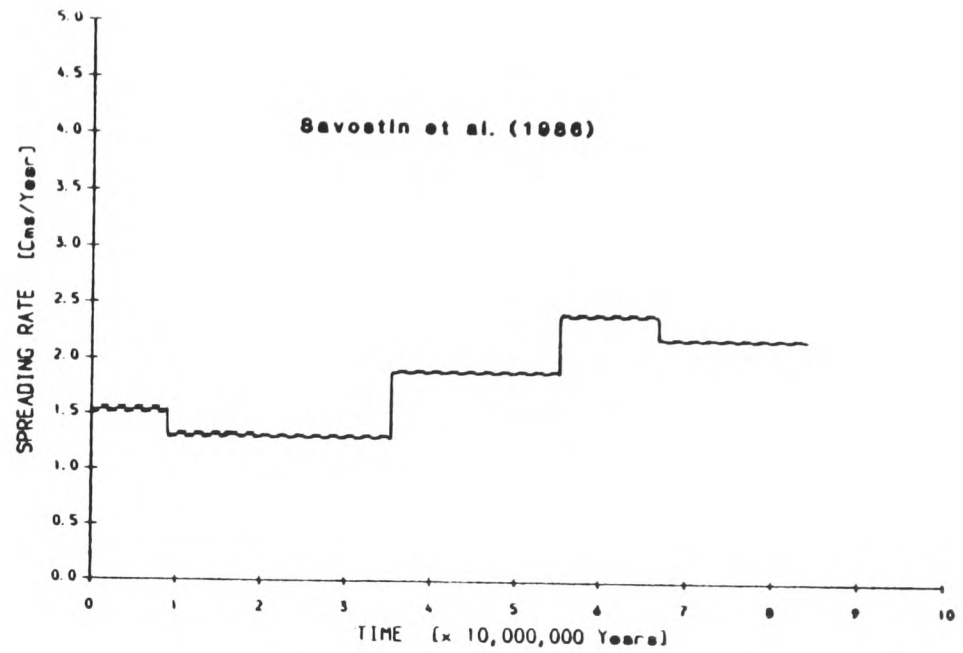
Figure 4.11: Atlantic Spreading Rates: Recent Models

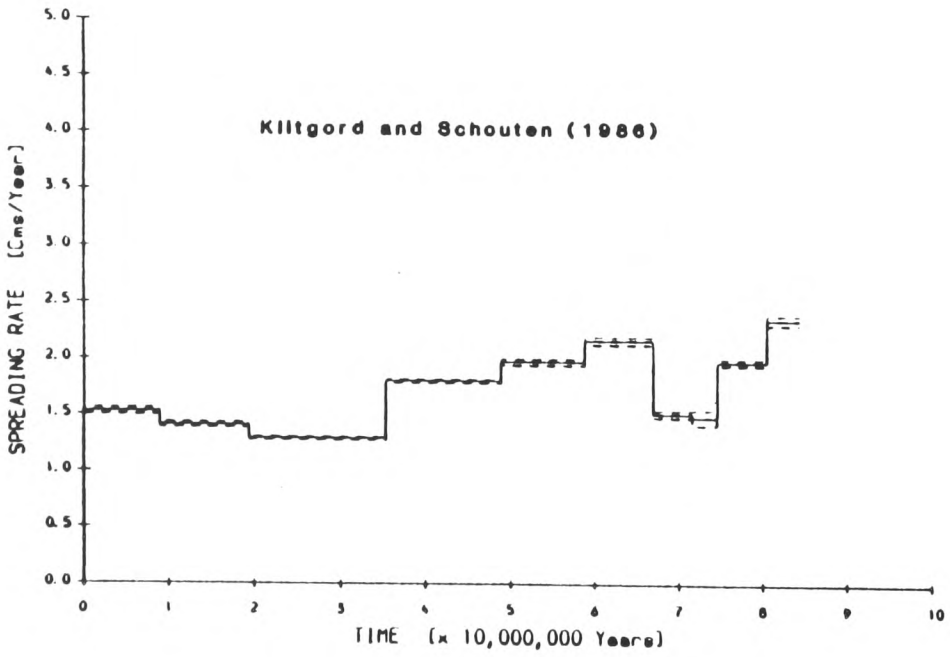
A: Seafloor spreading rates for the most recent models of Central Atlantic evolution. In all models a decrease in spreading rate between Anomalies 13 (35 Ma) and 6 (19 Ma) is seen. Savostin et al. (1986) suggest that this slowdown is the reason for the change from northward compression to dextral strike-slip in their model at this time.
B: Seafloor spreading rates for the most recent models of North Atlantic evolution. Savostin et al. (1986) propose that a decrease in spreading rate between Anomalies 6 (19 Ma) and 5 (9 Ma) reestablishes northward compression as the mode of Africa's motion. However, this slowdown is seen only in their model and not in any other. See text (4.3.4e) for discussion.

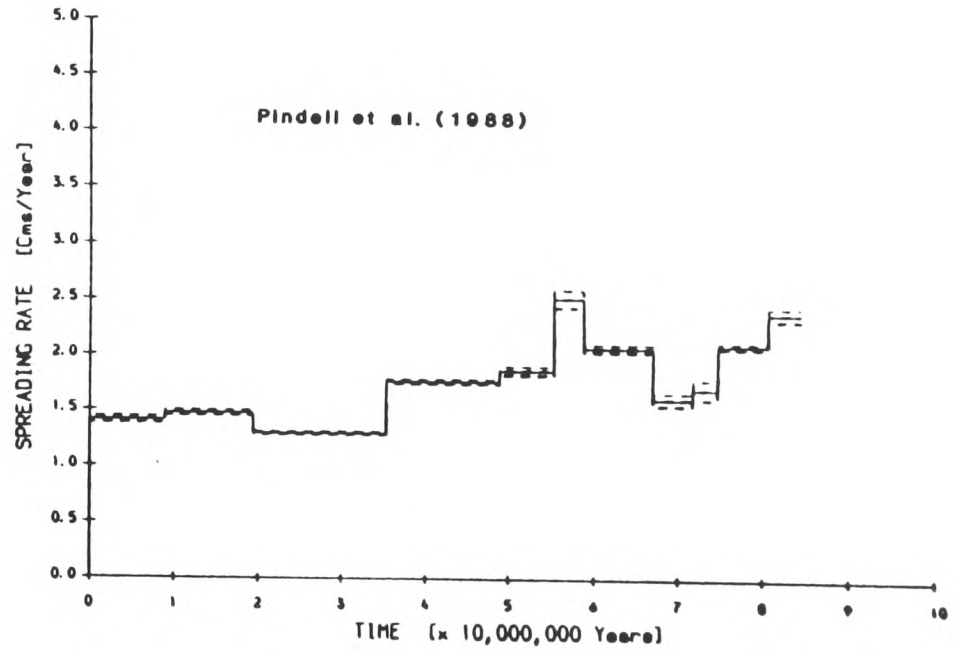
B

CENTRAL ATLANTIC SPREADING RATES



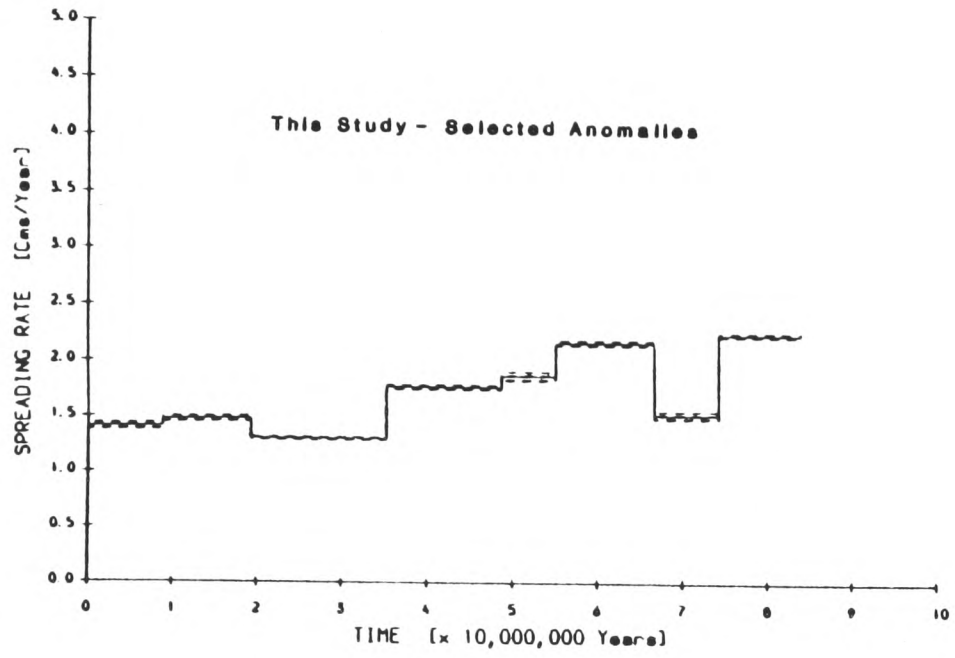


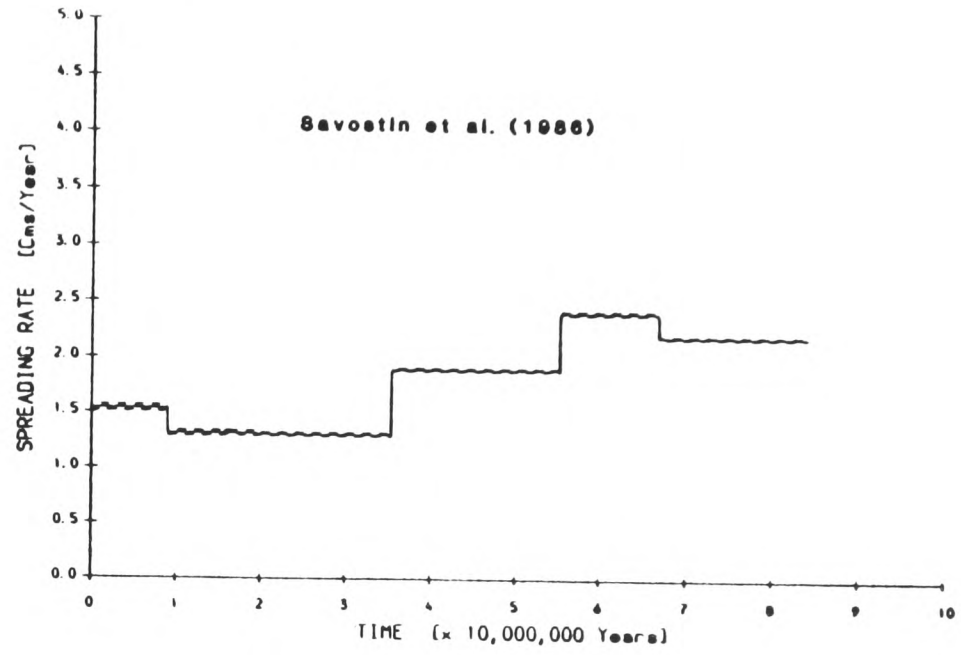


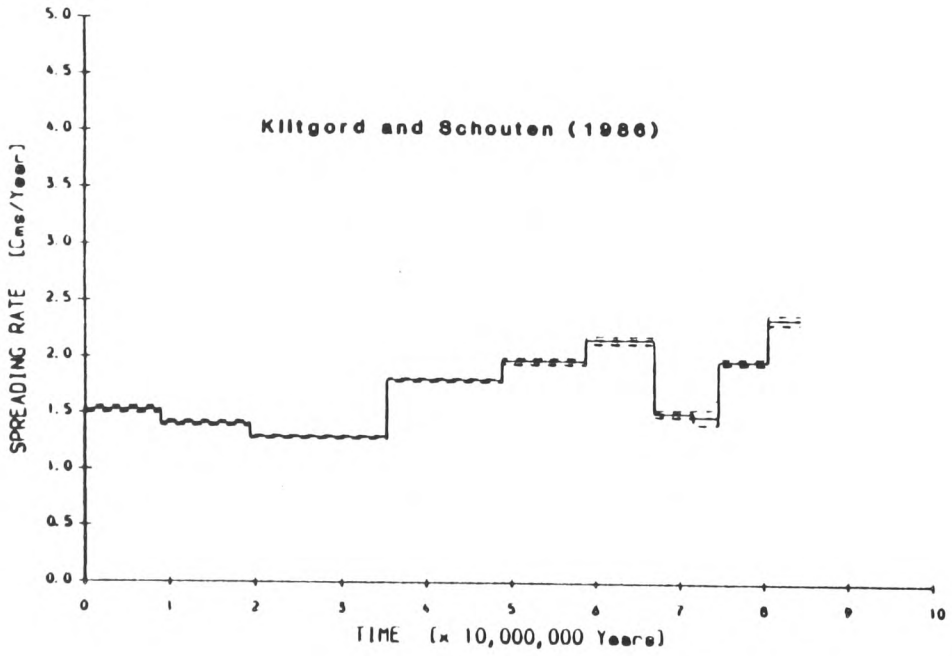


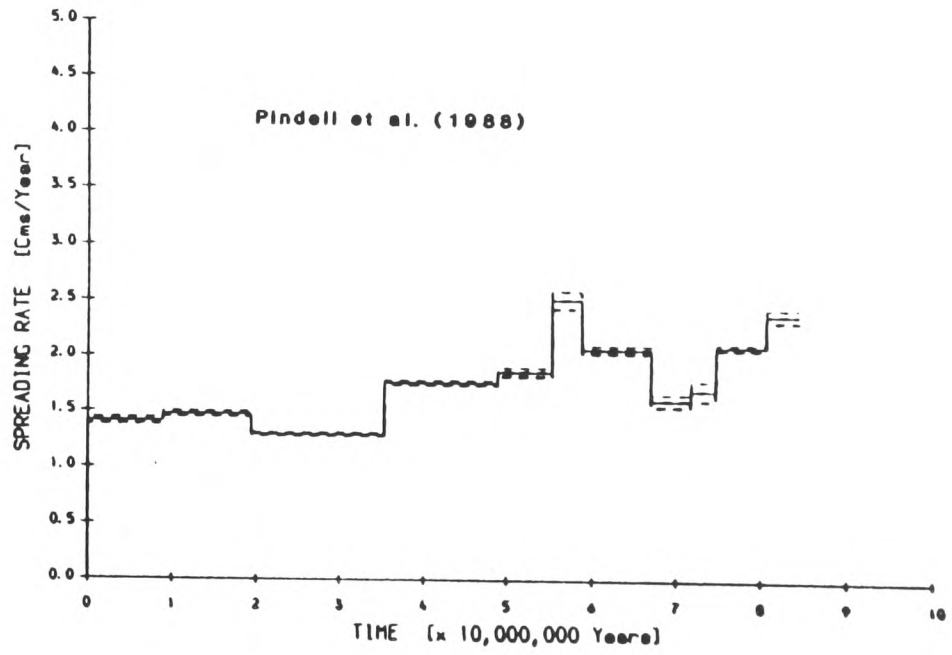
B

CENTRAL ATLANTIC SPREADING RATES









Atlantic spreading between Anomalies 6 and 5 because Savostin's (1981) rotation angle (3.8°) is significantly less than other rotations for Anomaly 6 (Tables 2.2 and 2.3).

The second feature of the model is that it has northeastward motion of Africa commencing prior to Anomaly M-0 (Fig. 4.10). As M-0 is the oldest anomaly mapped in the North Atlantic (and only in the eastern Atlantic, see 2.5.1), it is highly unlikely that oceanic lithosphere significantly older than 118 Ma exists, unrecognized, in the North Atlantic.

4.3.4f Sclater, Hellinger, and Tapscott's Model (1977)

This model presented rotation parameters for North and Central Atlantic seafloor spreading without computing the finite difference between them. The finite difference solution was computed independently as part of this study. The results are given in Table 4.4 and shown in Figure 4.12. The hints of a model similar to many of the more recent ones are present. Between 65 Ma and 53 Ma, there is little north-south convergence, although the model suggests a large amount of dextral strike-slip for this interval. This interval is preceded by one in which the motion is rather uncertain. The differences between this and earlier models result from increased knowledge of magnetic anomaly ages and locations, incorporation of bathymetric and age-depth data in determining rotation parameters, and a revised fit of the continents.

4.3.4g DNAG Model (1986)

This "model" was constructed using Klitgord and Schouten's (1986) Central Atlantic rotation parameters and Srivastava and

TABLE 4.4

FINITE POLE ROTATION PARAMETERS

FOR THE

MOTION OF AFRICA WITH RESPECT TO EUROPE

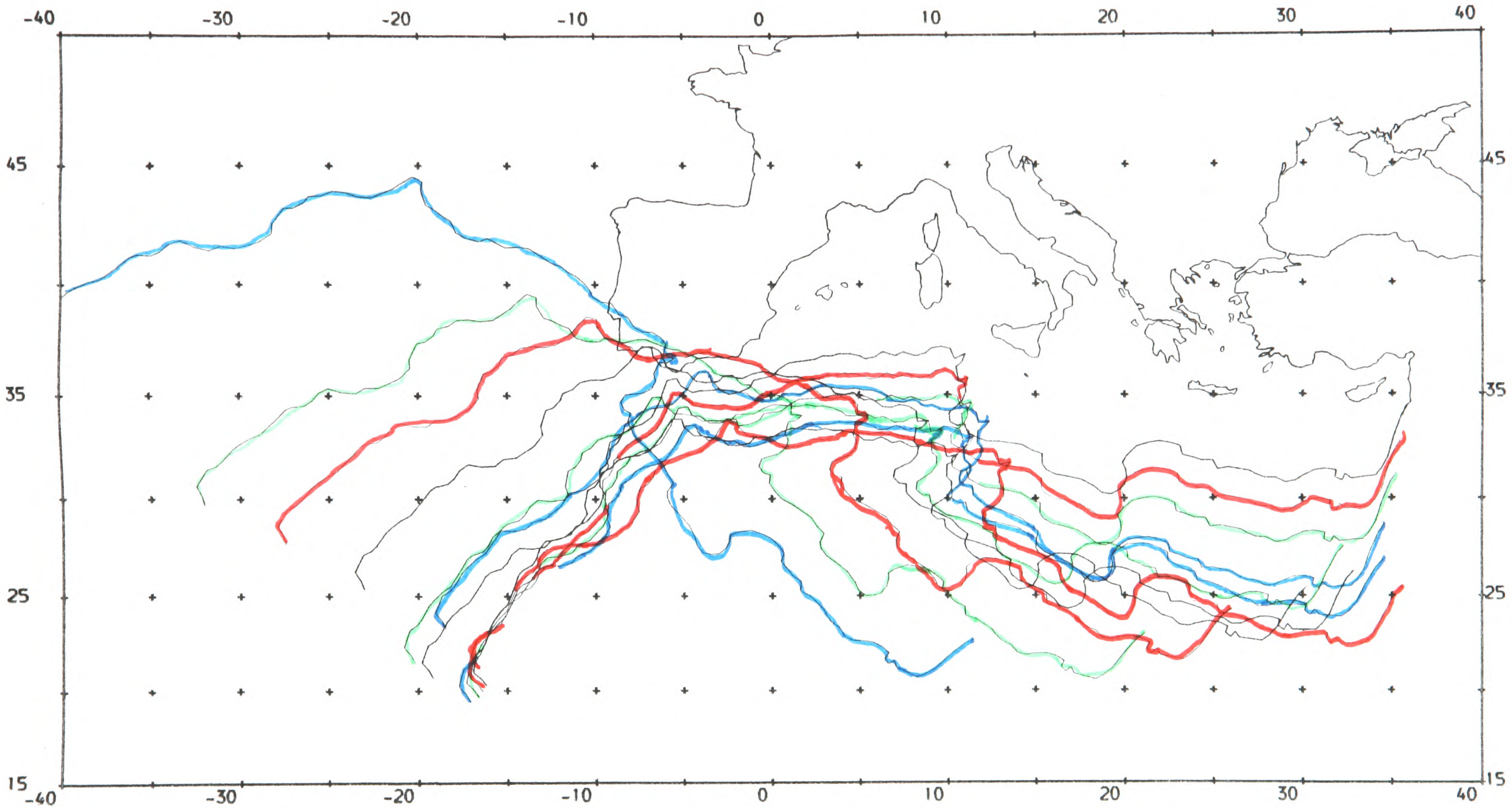
Sclater, Hellinger, and Tapscott (1977)

ANOMALY*	LATITUDE	LONGITUDE	ROTATION
5	25.74	-27.04	-1.93
6	26.11	-25.84	-4.08
13	26.45	-23.98	-7.44
22	33.27	-15.49	-12.76
29	21.93	-12.89	-12.83
34	38.39	-10.82	-12.36
95 Ma	29.79	-3.09	-14.03
110 Ma	39.53	-1.12	-20.69
125 Ma	44.35	0.12	-27.60
140 Ma	47.63	-0.42	-34.61
165 Ma	51.09	2.45	-51.08

NOTES: Anomalies 5, 6, 13, 22, 29, and 34 are given by Sclater et al. (1977) as equivalent to 10 Ma, 21 Ma, 38 Ma, 53 Ma, 65 Ma, and 80 Ma respectively.

Figure 4.12: Sclater et al. (1977): Africa-Europe Reconstructions

Reconstructions of Africa's position with respect to Europe using rotation parameters calculated from Sclater et al. (1977). Present day coasts of Europe and Africa are in black. Reconstructed positions of Africa are shown for Anomaly 5: red; Anomaly 5: green; Anomaly 13: blue; Anomaly 22: black; Anomaly 29: red; Anomaly 34: green; 95 Ma: blue; 110 Ma: black; 125 Ma: red; 140 Ma: green; 165 Ma: blue.


-40
-30
-20
-10
0
10
20
30
40
45
35
25
15

Tapscott's (1986) North Atlantic parameters, which were published in the DNAG volume on the Western North Atlantic (Vogt and Tucholke, 1986). Two versions of this model, using European Plate and Porcupine Plate rotation parameters for North Atlantic spreading, are presented (Fig. 4.13). Tabulated results are given in Table 4.5.

As can be seen in Figure 4.13, there is little difference between these solutions. The major difference is that Africa's position, prior to Anomaly 13, is slightly more easterly using the European Plate rotation parameters than it is using those for the Porcupine Plate. This is not surprising in the light of the nature of the Porcupine Plate solution, which is merely a small rotation of the European plate about a fixed pole (see 2.5.3i).

In many respects, the "DNAG Model" is similar to the one developed in this study. However, the "DNAG Model" does not have the capability of having its resolution improved immediately. Indeed, given the resolution used in this comparison, the phases of motion seen in this studv are mirrored in the "DNAG Model".

One particular difference is that during the period of relatively little motion (latest Cretaceous to early Tertiary, Anomalies 30 to post-24), this model shows a greater uncertainty with regard to Africa's position, because of Africa's easterly position at Anomaly 33. It is clear from Figure 2.13 that Srivastava and Tapscott's (1986) Anomaly 33 rotation parameters do not lie along the trace of the Charlie-Gibbs Fracture Zone, more so for the European Plate than for the Porcupine Plate.

TABLE 4.5A

FINITE POLE ROTATION PARAMETERS

FOR THE

MOTION OF AFRICA WITH RESPECT TO EUROPE

Srivastava and Tapscott (1986)

and

Klitgord and Schouten (1986)

ANOMALY	LATITUDE	LONGITUDE	ROTATION
5	3.21	-12.66	-0.81
6	19.84	-13.54	-2.31
13	26.22	-20.87	-5.14
21	31.13	-18.45	-9.01
25	29.55	-16.91	-10.31
30	30.48	-15.06	-9.09
33	23.57	-12.84	-9.92
34	32.22	-13.00	-14.15
M-0	43.63	-6.54	-35.84
M-4	44.71	-5.65	-37.86
M-10N	45.04	-5.17	-38.85
M-16	46.51	-4.92	-41.02
M-21	48.06	-4.50	-42.88
M-25	50.08	-2.52	-45.27
BSA	52.48	0.34	-52.35
FIT-MIN	53.14	1.20	-54.74
FIT-MAX	53.38	1.53	-55.69

TABLE 4.5B

FINITE POLE ROTATION PARAMETERS

FOR THE

MOTION OF AFRICA WITH RESPECT TO THE PORCUPINE PLATE

Srivastava and Tapscott (1986)

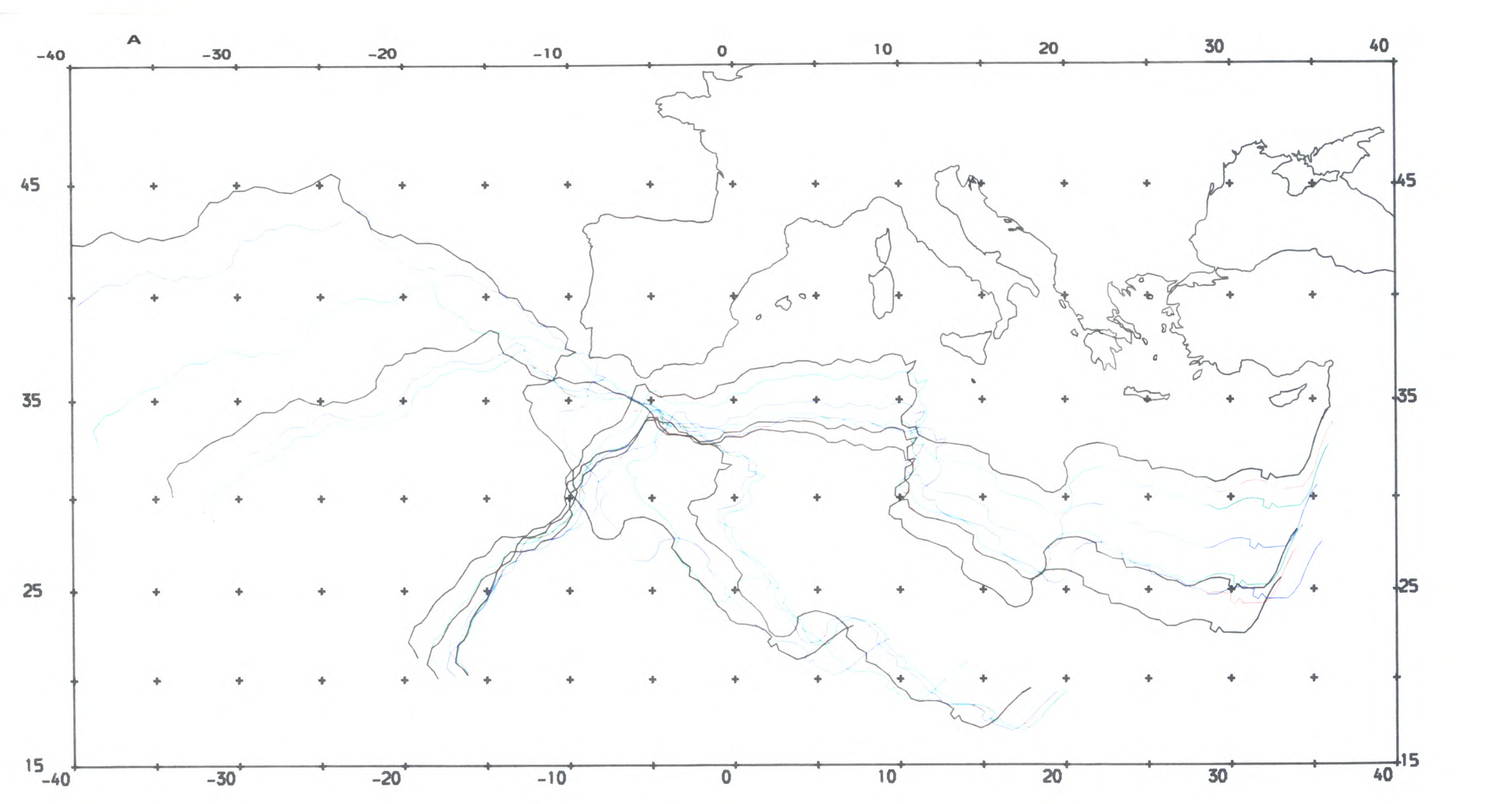
and

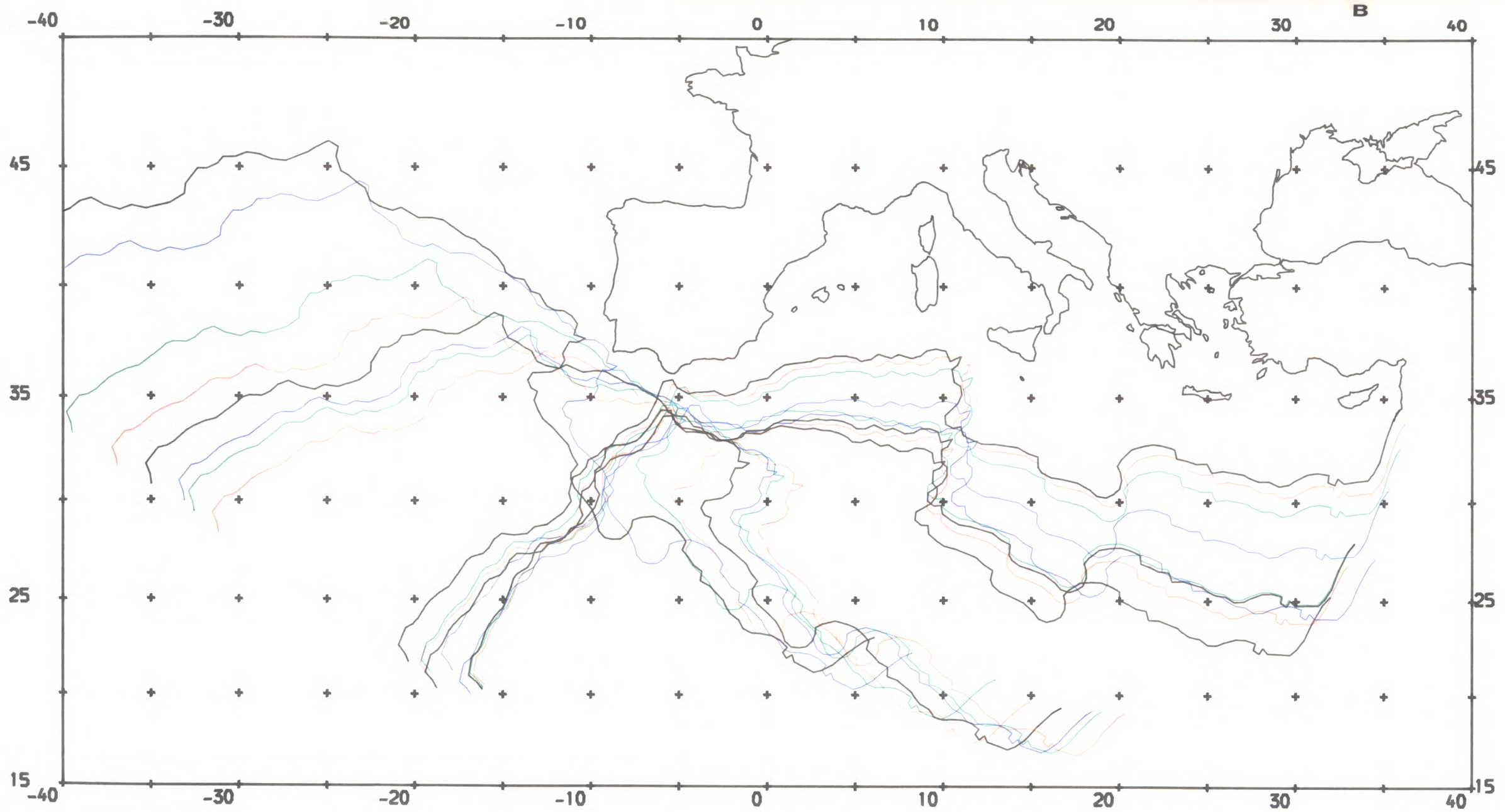
Klitgord and Schouten (1986)

ANOMALY	LATITUDE	LONGITUDE	ROTATION
5	3.21	-12.66	-0.81
6	19.84	-13.54	-2.31
13	26.22	-20.87	-5.14
21	34.27	-17.01	-10.02
25	33.84	-14.86	-11.87
30	35.04	-12.87	-10.67
33	28.70	-11.25	-11.42
34	35.16	-11.80	-15.75
M-0	44.36	-6.28	-35.57
M-4	45.35	-5.42	-39.60
M-10N	45.65	-4.96	-40.60
M-16	47.03	-4.71	-42.78
M-21	48.50	-4.28	-44.64
M-25	50.41	-2.33	-47.04
BSA	52.67	0.47	-54.14
FIT-MIN	53.29	1.32	-56.53
FIT-MAX	53.53	1.64	-57.48

Figure 4.13: DNAG (1986): Africa-Europe Reconstructions

Reconstructions of Africa's position with respect to Europe using rotation parameters calculated from Klitgord and Schouten (1986) for the Central Atlantic and Srivastava and Tapscott (1986) for the North Atlantic. Both European Plate (A) and Porcupine Plate (B) models for the North Atlantic were used. Present day coasts of Europe and Africa are in black. Reconstructed positions of Africa are shown for Anomaly 5: red; Anomaly 6: green; Anomaly 13: blue; Anomaly 21: black; Anomaly 25: red; Anomaly 30: green; Anomaly 33: blue; Anomaly 34: black; Anomaly M-0: red; Anomaly M-4: green; Anomaly M-10N: blue; Anomaly M-16: black; Anomaly M-21: red; Anomaly M-25: green; Blake Spur Anomaly: blue; Fit: black.


A
-40
-30
-20
-10
0
10
20
30
40
45
35
25
15


B
-40
-30
-20
-10
0
10
20
30
40
45
35
25
15

This deviation results in the easterly position and the greater uncertainty concerning the motion path.

4.3.4h Discussion

Models for the relative motion of the African Plate with respect to the European Plate can be divided into three groups. The first group consists of models published (or developed) prior to 1978. The second and third groups were published in 1984 and after. The difference between these two is that the Group 3 models were the product of working directly with magnetic anomaly data and fracture zone data, whereas the Group 2 relied upon the published (and unpublished) rotation parameters of others.

Group 1 models are characterized by sudden, unusual changes in Africa's motion. This has been shown to be a consequence of the lack of data or the misinterpretation of data. Examples of the first are the state of knowledge concerning Central Atlantic fracture zones and the existence of the M-Series anomalies. The sudden changes in the Dewey et al. (1973) model are caused by the lack of such relevant data. The misidentification of Anomaly 33 as Anomaly 31, and its use by Dewey et al. (1973) also contributed to these changes.

Group 2 and 3 models were developed with the advantage of a vastly improved data base. The data for group 2, however, varied in both age and quality. The classic examples are Livermore and Smith (1985), who used Francheteau's (1973) data for Anomaly 13 in the Central Atlantic along with Klitgord and Schouten's (1982) superior data, and Savostin et al. (1986), who used an amalgam of

data which led to some unusual results (4.3.4e).

The use of roughly the same magnetic anomalies in most models leads to a situation wherein the reconstructed position of Africa can be directly compared at various times. This approach has not been taken in this study because non-unique solutions for North, and to a lesser extent Central, Atlantic kinematics render such comparisons inconsequential. Rather, the path of relative motion was deemed to be the feature more deserving of comparison. This was evaluated for each model with regard to the Atlantic data used in determining the finite-difference solution. In particular, the fit of synthetic fracture zones in the Atlantic was considered of prime importance. In addition, the relative motion path was compared with those of the most recent models, particularly the model derived in this study.

The general trend of kinematic modeling has been towards a smoother relative motion path without the sudden, unusual changes in direction that characterized the earliest models. Smoothness is regarded as a criterion for evaluating relative the Africa-Europe relative motion path because of the lack of sharp, unusual azimuth changes in Atlantic fracture zones. Even disagreement with respect to the identification and positioning of anomalies seems to be less important than the fit to fracture zones. This is shown by the "DNAG Model", wherein Africa's easterly position at Anomaly 33 is dictated by the poor fit to the Charlie-Gibbs

Fracture Zone in the North Atlantic.

4.4 Discussion of the Kinematic Model

The importance of accurately determining the relative motion of Africa with respect to Europe has been recognized since this motion was recognized as the causal mechanism for the Alpine Orogeny (Argand, 1916; Heim, 1922; Staub, 1924; Termier, 1903). It was, however, fifty to seventy years before the plate tectonic paradigm showed how the kinematics and timing of the relative motion between the continents could be determined with any accuracy (Dewey et al., 1973; Smith, 1971). This insight was a consequence of the geometric constraints imposed by moving torsionally rigid plates on a spherical surface (Le Pichon et al., 1973; Morgan, 1968).

To date, all studies of the relative motion of Africa with respect to Europe have had two common characteristics. The first is that the motion has been analyzed in the European frame of reference, although Livermore and Smith (1985) also presented the motion in the African and hotspot frames of reference. This commonality is inconsequential except that it provides a basis for comparison (4.3.4). The second characteristic is that the results have been shown as a series of "time-lapse" frames at 10 - 15 million year intervals.

Althought the model presented herein has been discussed in terms of different phases of motion, and only selected anomalies are shown in Figures 4.3 and 4.4, the time frame available is on the order of 2 - 3 million years (Plates VII and VIII). The use

of all available anomalies in the Atlantic, tied closely to orientation of fracture zones, provides the greatest possible control on Africa's position through time. This is because it eliminates as much interpolation as possible.

From Plates VII and VIII, it appears that there is still a great deal of error in the Atlantic data, as the detailed motion is not as smooth as the averaged motion in the models discussed above. In addition, the averaged motion in the Atlantic may, itself, be an artifact. As discussed in 2.6 and 3.4, there is evidence from changing offsets in fracture zones that rates of seafloor spreading may vary between adjacent fracture zone segments. Hence, the spreading rate of an ocean is merely the average of the particular segments which contain the greatest amount of magnetic anomaly data used in the reconstruction.

In slow spreading oceans like the North Atlantic, the problem becomes even more complicated because overlapping lava flows and dike injection of different polarity make mapping of the edge of an anomaly tenuous, particularly in those areas with little data. This inherent error is but one factor increasing the uncertainty. However, knowing the possible errors serves to constrain the uncertainty. The lack of smoothness in the detailed Africa motion path indirectly sets the limits on possible errors in the reconstructed path and positions.

CHAPTER 5

REGIONAL GEOLOGY

5.1 Introduction

The Western Mediterranean Sea is composed of small, young basins that have formed from latest Oligocene or earliest Miocene time until the present. Some of these basins have formed on stretched or thin continental crust whereas others are floored by oceanic or oceanic-like crust.

Surrounding the Western Mediterranean is a nearly continuous system of orogenic belts. Many of these orogenic belts are only slightly older than the basins they surround. The structural polarity of these mountain belts is outward, away from the Mediterranean. The only exceptions are structures on islands within the Mediterranean and the double sided orogen of the Pyrenees. The major tectonic units are shown in Figure 5.1.

5.2 Mountain Ranges and Associated Basins

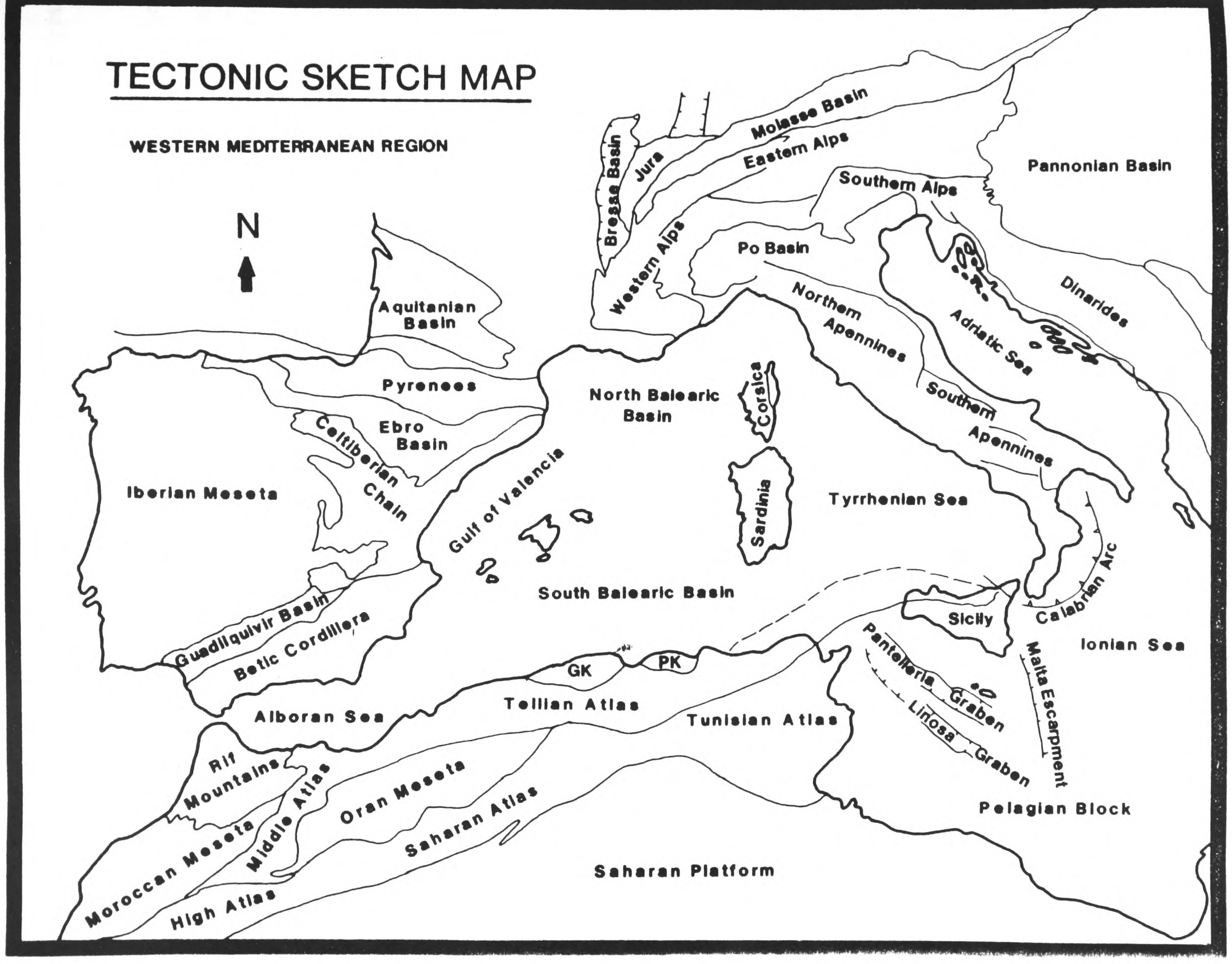
The orogenic belts that surround the Western Mediterranean region can be divided into 2 groups. The dominant group consists of ranges that 1) are Alpine (*sensu lato*) in age, 2) involve the closing of former oceans, and 3) have thick- and thin-skinned, fold and thrust belt structures. Ranges of this type, in addition to the Alps, include the Betic Cordillera (Spain), the

Figure 5.1: Tectonic Sketch Map: Western Mediterranean Region

Sketch map of the major tectonic units in the Western Mediterranean region that are discussed in the text. GK = Grande Kabylie; PK = Petite Kabylie.

TECTONIC SKETCH MAP

WESTERN MEDITERRANEAN REGION



pyrenees (Spain and France), the Rif (Morocco), the Tell or Tellian Atlas (Algeria and Tunisia), and the Apennines (Italy).

The second group, limited in number and found mostly in North Africa, includes the High, Middle, Saharan and Tunisian Atlas ranges. This group is distinguished by a style of uplift and deformation that is best characterized as basin inversion, with existing faults being reactivated with a different sense of motion and commonly with a dip slip component. Nappe-like or thrust structures are seen only at the margins of such the mountain ranges, whereas the central tectonic framework remains rather undeformed (Stets and Wurster, 1982). These observations, as well as those by others (e.g. Mattauer et al., 1977), indicate that significant crustal shortening, via lateral motions, did not occur. However, significant crustal thickness is found under such ranges, e.g., 40 km under the High Atlas of Morocco (Tadili et al., 1986). Hence some amount of shortening must have occurred. The Pyrenees are in some respects similar to this type, but are considered by most as Alpine (sensu lato) mountains.

5.2.1 Betic Cordillera and Guadilquivir Basin

The Betic Cordillera is commonly divided into three zones: Betic, Subbetic, and Prebetic. The Betic Zone, the internal part of the orogen, consists primarily of variably metamorphosed Triassic and older rocks. The Sub- and Prebetic Zones, the external part of the orogen, consist of unmetamorphosed rocks of Mesozoic and Cenozoic age (Rondeel and Simon, 1974; Kampschuur

and Rondeel, 1975). The zonation is thought to reflect the Mezozoic paleogeography (Cruz-Sanjulian, 1976; Garcia-Hernandez et al., 1980) of a passive continental margin.

The Betic Zone is divided in ascending structural sequence, and decreasing metamorphic grade, into the Nevado-Filabride, Alpujarride, and Malaguide complexes. The Ballabona-Cucharon complex, between the Nevado-Filabrides and the Alpujarrides, is distinguished by some authors (Egeler and Simon, 1969).

The Prebetic is largely autochthonous, strongly deformed locally, and characterized by shallow marine sedimentation with a strong terrigenous influence. Differentiation of the Prebetic into Internal and External Zones is based on the Internal Prebetic having greater thickness and fewer hiatuses, as well as a somewhat more pelagic character.

The Subbetic subdivision into Internal, Median, and External Zones, with a locally recognized Ultra-Internal Zone, is made on similar grounds. The greatest subsidence and thickness and fewest hiatuses are in the Median Zone. The Subbetic rocks are thicker, more continuous, and more pelagic than their Prebetic counterparts. They are also allochthonous and more deformed.

Between the Pre- and Subbetic some authors have recognized an intermediate facies sequence, the Intermediate Units, of very thick pelagic sequences as well as carbonate turbidites and breccias, which are characteristic of an unstable environment (shelf break?).

In the westernmost part of the Betics is a unit known as the

Campo de Gibraltar. This unit is variably referred to the Betic or Subbetic Zone or considered as an Ultra-Betic Zone because of its allochthonous nature. It is composed dominantly of Upper Cretaceous and Paleocene foraminiferal sands alternating with marl and argillite and is commonly described as a flysch or flysch-like formation (Perconig, 1960-62).

The structural setting of the Betic Cordilleras is generally thought to be a series of nappe-like (Internal Zone) and fold and thrust belt (External Zone) structures thrust on a decollement of Triassic evaporites to the north, northwest, and west. Tectonic models for the Betics generally suggest the presence of an Alboran Plate which was emplaced in its current position from the eastnortheast to the westsouthwest in the Miocene (Andrieux et al., 1971; Leblanc and Olivier, 1984; Makel et al., 1984; Dercourt et al., 1986). Geophysical data, mostly from seismic refraction experiments, have shown that there are differences in crustal thickness between the eastern and central Betics (Banda and Ansorge, 1980; Medialdea et al., 1986). These differences are probably the effect of late stage extension and strike-slip.

The Guadilquivir Basin, the foreland basin of the Betic Cordillera, is a typical foreland basin. The basement on which it sits dips toward the core of the orogenic belt in response to the load imposed by thrust sheets. The basement dip is clearly seen in reflection seismic profiles which cross the basin and adjacent parts of the Subbetic, as well as from depth to basement maps constructed using data from wells that reached basement

(Perconig and Martinez Diaz, 1977; Julivert et al., 1980).

In addition to flexing downward the basement is also bowed up along the northern edge of the basin. This flexural bulge, a typical feature of foreland basins (Turcotte, 1979; Beaumont, 1981; Karner and Watts, 1983), has an average elevation of 300 - 400 m and trends ENE-WSW for more than 400 km. In reflection seismic sections the basinal sediments can be seen to onlap and pinch out against the bulge that migrated progessively northward in response to the advancing thrust loads (J. Suarez, ENIEPSA, pers. comm., 1985). To the east the basin narrows and terminates against the Prebetic (Fig. 5.1).

The Betic Cordillera contains large tracts of Miocene, Pliocene, and Quaternary sediments that are both marine and continental in nature. These basins formed a connection between the Atlantic and Mediterranean Seas (Benson, 1976; Montenat et al., 1976; Muller and Hsu, 1987) that was maintained until the Messinian when they were deformed and connection to the Atlantic severed. The formation of these basins is responsible for imparting a Basin and Range-like physiography to southern Spain.

The manner in which the basins formed is controversial. Some workers suggest transtensional motion along strike-slip or transcurrent faults (Martin-Algarra et al., 1988; Sanz de Galdeano et al., 1985), whereas others suggest an origin related to body forces generated during the process of orogenic collapse (Dewey, 1988; Platt and Vissers, 1989).

5.2.2 Rif, Tell, and Associated Basins

The Rif of Morocco is considered by many as a continuation, across the Straits of Gibraltar, of the Betic Cordillera. The Tell or Tellian Atlas of Algeria and Tunisia has similarly been equated, in terms of structure and stratigraphy, with the Rif (Caire, 1978; Wildi, 1983), hence they are discussed together. The subdivision of the Rif and Tell is quite complex (compare Choubert and Faure-Muret, 1974; Caire, 1974, 1978; Wildi, 1983). In addition to the Internal and External Zones, flysch nappes are generally recognized and assigned variably to either larger zone.

The Rif is commonly divided into 4 zones: the Rifides, the Zone Ultrafiaine, the Rif, and the Prerif. The first two make up the Internal Zone and the last two the External Zone. The Tell is divided differently by different workers. Caire (1974, 1978) distinguishes 5 zones, whereas Wildi (1983) only recognizes 3 major zones but discusses many subunits in each. For both authors the zones have paleogeographic significance.

Internal Zones: The most internal zone of the Rif, the Rifides, is subdivided into 3 units. The Sebtides consist of minor amounts of Precambrian (?) and Paleozoic rocks, which have been somewhat metamorphosed, whereas the Ghomarides are relatively unmetamorphosed Paleozoic strata ranging in age from Silurian to Permian (Choubert and Faure-Muret, 1974). The Sebtides and Ghomarides are thought to correspond, respectively, to the Alpujarride and Malaguide units of the Betic Cordillera (Durand Delga and Kornprobst, 1963).

The bulk of the Rifides consists of the "Chaines Calcaires", a sequence of limestones and dolomites, predominantly of Triassic and Jurassic age, but which includes rocks as old as Permian and as young as Oligocene (Durand-Delga et al., 1960-62). The Cretacous section of the "Chaines Calcaires" is approximately 1 km thick and locally has siliciclastic detritus as well as limestones and cherty limestones (Durand-Delga et al., 1960-62).

The Internal (northernmost) Zone of the Tell is made up of the Kabylie Massifs, Grande and Petite, which are located on the coast of Algeria (Fig. 5.1). These massifs have a crystalline basement, thought to be of Precambrian and Paleozoic age, but which yield radiometric dates of 85 - 95 Ma as well as Hercynian ages. The significance of these Cretaceous ages and of younger ages is a matter of debate (compare Monie et al., 1988 with Bossiere and Peucat, 1985, 1986). The Mesozoic and Paleocene section above the basement is generally complete and is composed mostly of carbonates until the Albian, after which a more mixed mode of sedimentation becomes the norm. The latest Paleogene and Neogene sediments are syn- and post-orogenic clastics.

Flysch Nappes: The Zone Ultrarifaine (Rif Internal Zone) consists of three flysch nappes, Nappe de Beni Ider, Nappe de Tizirene, and Nappe Numidienne that rest partly in the Internal Zone and partly in the External Zone. The Nappe Numidienne is of Oligo-Miocene, and possibly upper Eocene age. The other two are older. The Nappe de Beni Ider ranges from Cenomanian to Oligocene and the Nappe de Tizirene from Upper Jurassic to Lower Cretaceous.

The older nappes consist of calcareous marls that give way to calcareous sands. The youngest nappe (Nappe Numidienne) is argillaceous and marly near its base but becomes sandier and in many locales is a nearly pure quartz sandstone. This Numidian facies is found along the entire margin of North Africa, in Sicily, and southern Italy (Wezel, 1970). The Zone Ultrarifaine has been compared to the Betic Campo de Gibraltar in terms of facies and tectonic pattern (Faure-Muret and Choubert, 1971).

The Nappe Massylienne, the Nappe Mauretanienne, and the Nappe Nummidienne are flysch nappes occupying positions between the Kabyles and the External Zone of the Tell. The first nappe was defined in the Petite Kabylie (Bouillin et al., 1970) and the second in the Grande Kabylie (Gelard, 1969). The flysch sections for which these two nappes were named are Lower Cretaceous in age, although both contain older and younger rocks. The third flysch nappe, the Nappe Nummidienne, is the youngest of the three. It is Oligo-Miocene in age.

The Tellian flysch nappes are correlated with nappes in the Zone Ultrarifaine. In particular, the Nappe Mauretanienne is correlated with the Nappe de Tizirene and with the Nappe de Beni Ider, where the Upper Cretaceous and younger rocks are separated from the Lower Cretaceous by a decollement. Wildi (1983) also subdivides the Nappe de Tizirene even further by distinguishing a Nappe de Melloussa-Choumat and correlating it with the Nappe Massylienne. Structurally the Nappe Massylienne (and its Rifian equivalent) is considered to occupy a more external position than

the Nappe Mauretanienne with the Nappe Nummidienne having the highest structural position (Durand Delga and Fontbote, 1980).

External Zones: In the external zone, the Rif Zone (sensu stricto) consists of units that are considered autochonous or parautochthonous (Les Fenetres, Unites de Ketama and Nkor-Temsamane), units considered allochthonous (Nappes de Senhadja, Aknoul, Habt, and Ouezzane), and others whose interpretation is disputed (Unites de Tanger and Loukkoe) (Choubert and Faure-Muret, 1974; Durand Delga, 1960-62). Marls, marly limestones, limestones, flysch, and sandstone are the main lithologies.

Shortening in both the allochton and autochthon is estimated at up to 50% or greater by Choubert and Faure-Muret (1974), who give a maximum cross-strike outcrop dimension of 50 km for any of these units. The allochthonous units are thought to have been thrust over the autochthon. Bucci (1984) notes that palinspastic restorations, based on proprietary data from AMOCO Oil Company, suggest southward movement of up to 500 km for allochthonous units containing Cretaceous rocks.

The most external part of the Rif is the Prerif Zone, which is bounded on the southwest by the Rharb Basin and on the east and southeast by the Middle Atlas. The Prerif consists of a Prerif Nappe, and, possibly, the Nappe d'Ouezzane. The latter is also considered part of the Rif Zone (sensu stricto). The Prerif Nappe is thought to have been emplaced by thrusting and gravity sliding but its place of origin is uncertain. The stratigraphic succession of this unit extends from Triassic onward, with a gap

between the lower Tertiary and the Tortonian, and consists mainly of marls, marly limestones, and limestones. The lowest Tortonian contains many reworked remnants of the missing interval. This interval is also seen in windows of the Nappe d'Ouezzane.

The Tellian External Zone is subdivided into 3 units from north to south, the Ultra-Tellian Zone, the Tellian Zone (sensu stricto), and the Peni-Tellian Zone. The Tellian Zone (s.s.) is the most important, having the most complete Mesozoic and Cenozoic section, and is itself subdivided into the Upper (or High), Middle, and Lower Tellian Units. The subdivision reflects the paleogeographic (north to south) and structural positions (top to base) of the units (Wildi, 1983).

The sedimentary character of the external zone changes from sandstones, shales and limestones in the Peni-Tellian Zone and Lower Tellian (s.s.) Unit, to marls and marly limestones in the Middle Tellian (s.s.) Zone, and, finally, to marls and pelites mixed with conglomerates and breccias in the Upper Tellian (s.s.) Unit and the Ultra-Tellian Zone. This zonal structure represents a facies progression from nearshore to shelf break.

Structure: The structure of the Rif is largely a series of nappes thrust variably to the south, southwest, and west. As noted previously, the amount of shortening and displacement of the various tectonic units is uncertain. Most models for the tectonic evolution of the Rif emphasize the nappe complex, but there is also evidence for strike-slip motion (LeBlanc, 1980; Olivier, 1981-82;, Morley, 1987), which may be enhanced by the

presence of older structures (Rod, 1962; Kanes et al., 1973). However, the crustal structure of Morocco does not suggest a composite of crustal blocks (Hatzfeld and Bensari, 1977; Tadili et al., 1986) as may be true for the Betic Cordillera.

The general structure of the Tell is a series of nappes and thrust sheets that have been emplaced from the north toward the south with the Internal Zone(s) generally being uppermost and the External Zone(s) being lowermost (Caire, 1974; Keiken, 1960-62; Wildi, 1983). Tectonic scenarios for this region most commonly suggest that the Kabylies were originally part of an Alboran microplate, which was dismembered as it moved westward during Alpine orogenic events (see for example Andrieux et al., 1971; Durand Delga and Fontbote, 1980; Wildi, 1983; Dercourt, Zonenshain et al., 1986). More recently it has been suggested that the Kabylies were a part of the European continent until Late Oligocene-Early Miocene time (Dewey et al., 1989).

Basins: The Rif is bordered to the south and southwest by the Rharb Basin. This basin has a twofold history. Its Mesozoic and early Tertiary evolution is linked to the breakup of Pangea and the development of the Moroccan Atlantic passive continental margin. The late Tertiary history is a consequence of the emplacement of thrust complexes in the Rif and is clearly seen in the isopach pattern for Miocene and younger rocks and the depth to basement determined from over 300 wells (Bucci, 1984). Both the thickness of Miocene sediments and the depth to basement increase toward the Rif. This suggests that the load imposed by

thrust masses has been the dominant subsidence mechanism from Miocene to the present, although the basin has maintained connection with the Atlantic (Moreau et al., 1985/86).

Within the Rif there are several intermontane basins with late Miocene and younger sediments. These basins are generally found in the internal segment of the orogen near the Alboran Sea and along the Nekor Fault in the eastern Rif near Melilla (Groupe de Recherche Neotectonique, 1977). The areal extent of these basins is not nearly as great as those in southern Spain although similar sedimentary sequences occur (Vidal, 1977).

The South Tellian Foredeep is located between the Tell and the Saharan Atlas. It can be followed irregularly from Tunisia to Morocco. The nature and age of the sedimentary succession in this basin complex varies with location. However, continental sediments, synchronous with or closely related to orogenic movements, were deposited from the end of the Early Miocene or beginning of the Middle Miocene (Courme-Rault, 1984). These deposits were later deformed by southward propagating thrusts.

Large areas of Algeria are basins with Upper Miocene to Quaternary sedimentary sequences. The largest intermontane basins are the Chelif, the Mitidja, and the Constantine Basins (Courme-Rault, 1984; Keiken, 1960-62a; Wildi, 1983a). These basins display a wide variety of facies with histories that may commence as early as the lower Miocene, prior to orogenic movements, and continue to the present (Neurdin-Trescartes, 1985).

5.2.3 Apennines, Po Basin, and Apenninic Foredeep

The Apennines, which form the "backbone" of Italy and extend nearly the entire length of the peninsula are a continuation of the Rif and Tell of Africa (Boccaletti et al., 1985). Most of the Italian Peninsula and Sicily are considered as either part of the African continental margin, the "African Promontory" also referred to as "Adria" (Channel et al., 1979), or as part of the "Apulian" microcontinent (Pieri and Mattavelli, 1986).

As with other mountain belts the Apennines are divided into various tectono-stratigraphic units and grouped into Internal and External Zones. The names of these units change along strike because of the length of the chain. A simplified correlation is given in Table 5.1. In general, the Internal Zone units are sequences that formed in oceanic areas that originated during Mesozoic seafloor spreading and External Zone units originated on stretched continental crust (platforms and basins) of the African margin. Thus the units have paleogeographic significance.

In the Northern Apennines the Sicilide Complex is the lowest Internal Zone unit. It consists of Cretaceous to Paleocene shales (> 1,000 m) with calcareous and sandstone intercalations, overlain by a Paleocene-Eocene calcareous-marly flysch (800 m), and capped by calc-alkaline tuffs (Petrignacola Tuffites) that erupted near the Eocene-Oligocene boundary (Dallan-Nardi and Nardi, 1974). The Liguride Complex, characterized by ophiolites and associated sediments, overlies the Sicilide unit. The age of the sedimentary cover of the ophiolites ranges from Lower

TABLE 5.1

TECTONIC UNITS OF THE APENNINES

Zone	Northern Apennines	Central Apennines	Southern Apennines	Sicily
Internal Zone				
	Liguride Complex (Internal and External)	Liguride Complex not in evidence	Liguride Complex	
	Sicilide Complex	Sicilide Complex seen as a few tectonic melanges	Sicilide Complex tectonic melanges are common	
External Zone				
	Toscannide Nappe Sequence	Latium-Abruzzi segment of the Panormide Complex (platform facies)	Abruzzi-Campanian and Campanian-Lucanian segments of Panormide Complex (platform facies)	Panormide Complex
	Medino-Cervarola Complex	Lagonegro Complex (basinal facies)	Lagonegro Complex (basinal facies)	Trapanese Seamounts
	Umbria-Marche Sequence		Umbria-Marche Sequence	Immerese Basin
Foreland				
	Istria-Friulia (?)	Maiella (?)	Apulia / Gargano (?)	Ragusa Plateau (Iblei)

Cretaceous to Paleocene in the western "Internal Ligurides" and to reaches to the Messinian in the eastern "External Ligurides". A part of this latter succession, the Oligo-Miocene of the Langhe, is an overlap sequence that crosses the Sestri-Voltaggio Line, which is thought to be the Alps-Apennines juncture.

In the Central Apennines melanges of tectonically transported Sicilide material have been reported, but the Liguride Complex is not seen. In the Southern Apennines and Sicily the Sicilide Complex is a Tithonian to Turonian arenaceous-shaly flysch that becomes increasingly shaly from the Late Cretaceous to the Eocene when it becomes a calcareous marl. The Eocene-Oligocene boundary is marked by volcanics (Tusa Tuffites that correlate with the Petrignacola Tuffites). In the Central and Southern Apennines flysch sedimentation occurred in the Oligocene and continued into the Miocene.

The Northern Apennine External Zone sedimentary sequences differ from those of the Southern Apennines. In both regions the Triassic starts with continental to shallow marine clastics. In the north, mixed carbonate and clastic facies followed. These are capped by evaporites and carbonate platforms. In the south, shallow water dolomites and evaporites formed thick deposits that onlapped the early clastic source areas. This cut off the clastic supply and allowed cherty limestones to form in basinal settings. No such basinal deposits were formed in the Northern Apennines (Fischer, 1964).

From the Jurassic onward the Northern Apennine sedimentary

pattern became differentiated with development of basinal type sedimentation (Ammonitico Rosso facies) (Bernoulli and Jenkyns, 1974). The Umbria-Marche Sequence, Medino-Cervarola Complex, and the Tuscan Nappe (Table 5.1) all display this sequence and are capped by flysch sequences of Oligocene and/or Miocene age.

The Central and Southern Apennine External Zones are more complex and consist of carbonate platform sequences juxtaposed to basinal sequences. Debris aprons surround most of the former platform areas. The platforms grew persistently from Jurassic until Oligocene or Miocene (?) time, with the exception of a period of emergence from Late Albian to Middle Cenomanian when karsts and bauxite deposits formed (D'Argenio et al., 1975). After this hiatus carbonate production resumed on the platforms and continued until capped by flysch-like clastics in the late Paleogene and early Neogene. These clastics, including the Numidian Flysch also found in North Africa (see 5.2.2), overlie the basinal sequences as well (Lancelot et al., 1977).

The structure of the Apennine chain is that of a thin-skinned, fold and thrust belt similar to those seen in many other orogenic belts, such as the Canadian Rocky Mountains (Mostardini and Merlini, 1986; Hill and Hayward, 1988, Ghelardoni and Riva, 1988). This interpretation is based on deep wells that show repetitions of section at depth, the nature of the stratigraphic succession, geological map patterns, seismic reflection data, and magnetic residual maps, which show a smooth, gently dipping basement. The thin-skinned interpretation contrasts with others

that interpret the deformation as the result of stacking thick nappes that have been transported long distances (Carmignani et al., 1978; Cadet et al., 1980).

The amount of shortening in the Apennines varies along strike. Hill and Hayward (1988) suggest a maximum of 200 km in a Northern Apennine transect between 42o N and 44o N and a minimum of 40 km in a Southern Apennine transect between 40o and 41.5o N. In Western Sicily their suggested 140 km of shortening is similar to the 60 - 70% estimate of Catalano and D'Argenio (1978).

Tectonic models for the evolution of the Northern Apennines depict the orogen as a result of closing of the Ligurian Ocean via subduction and collision of the Corsican and Italian continental margins as Corsica and Sardinia rotated away from the Southern France (Kligfield, 1979; Cohen, 1980). In the Southern Apennines the Apulian margin, formerly part of the Adriatic Promontory of Africa collided with, and was overthrust by, the basement nappes of Calabria (Knott, 1987).

The Po Basin is the Northern Apennine foreland basin. It contains nearly 7,000 m of Pliocene and younger sediment with depocenters close to the mountain front and nearly coincident with a gravity low, suggesting that the thrust front has partly overridden the basin (ANL, 1959; Ogniben et al., 1975). This is confirmed by seismic profiles that cross the basin (Pieri, 1987).

The foreland basin continues to the east and south in the Adriatic Sea until south of Ancona. From this point the basin continues onshore, as the Bradanic Foredeep, until the Gulf of

Taranto is reached (Carissimo et al., 1963; Schwander, 1987). From here, to the southwest and west, the Ionian Sea may be considered part of the foreland basin system. It is seen again in Sicily, as the Catania-Gela Trough (Ogniben, 1985). Within the Apennines, there are a series of Middle (?) Miocene and younger basins that young across the strike of the orogen from west to east and along strike from north to south.

5.2.4 Southern Alps and Po Basin

The Southern Alps are the northernmost extent of the former African or Apulian plate margin, i.e., the Southern Tethyan margin. The Insubric Line, also called the Periadriatic Line, is the boundary between the Southern Alps and the Central Alps. It is also considered, by some workers (e.g. Ogniben, 1985), to be the boundary between the Apulian and European plates. The Austroalpine Nappes, which lie north of the Insubric Line, were also part of the southern plate but have been detached and separated by post-thrusting movements along the Insubric Line.

The limited metamorphism seen in the Southern Alps makes them difficult to discuss in terms of Internal and External Zones. The more metamorphosed Austroalpine Nappes may correspond to an Internal Zone and the Southern Alps as a whole be thought of as an External Zone.

The Southern Alps are considered a prototypical continental margin of alternating highs (platforms) and lows (basins) formed on attenuated continental crust. From east to west (originally

southeast to northwest) these zones are the Friuli Shelf, the Belluno Trough, the Trento Plateau, the Lombardian Basin, and the Canavese Zone. The zonation represents an onshore to offshore transect that has been compared with the Bahama Banks and the Bay of Biscay (Bernoulli, 1981).

As in the Apennines, Early Triassic sedimentation was shallow marine and continental clastics with interbedded carbonates, which gave way by Late Triassic to an evolved carbonate platform. In the Early Jurassic the platform was broken by faulting into the sequence of highs and lows given above. The pattern is very similar to that seen in the Southern Apennines. Above these carbonate successions are terriginous flysch deposits of Turonian-Campanian age (Castellarin, 1976) and Late Paleocene-Middle Eocene age (Cousin, 1981).

Structurally the Southern Alps are an E-W trending, south-vergent, fold and thrust belt (Doglioni and Castellarin, 1985; Laubscher, 1985) whose easternmost section intersects the NW-SE trending Dinarides (Fig. 5.1). It was interaction with the Dinaric Chain that produced a Late Cretaceous-Early Paleogene, west-vergent deformation sequence found in the Southern Alps. The deformation structures produced by this event, in conjunction with the platform and basin geometry, combined to produce a series of positive flower structures during Neogene deformation (Doglioni, 1987; Doglioni and Bosellini, 1987).

Shortening in the Southern Alps is considerably less than suggested for other mountain belts in the Western Mediterranean

region. Doglioni (1987) suggests 10 - 15 km based on line and area balancing, although noting the presence of a 50 - 60 km thick crust (Geise et al., 1982. Laubscher's (1985) estimate of 40 - 60 km shortening is based on similar balancing techniques. Doglioni and Bosellini (1987) indicate that in the east, where the Dinarides are intersected, shortening may be of this order of magnitude also.

Tectonic scenarios for the Southern Alps have centered on gravity tectonics as the principal mechanism for deformation (Auboin, 1964; Van Bemmelen, 1966). More recently, Laubscher (1985) suggested that subduction of continental crust to the north was the cause of deformation, although Geise et al. (1982) suggest subduction of European crust beneath the Southern Alps.

The Po Basin is the foreland basin of the Southern Alps as well as for the Northern Apennines. Isopach maps and seismic reflection profiles show that the bulk of the later Neogene (Late Miocene-Recent) sediment in the basin was derived from a southern source (i.e., the Northern Apennines) but with deep localized depocenters in the northern parts of the basin (Pieri, 1987). Deep seismic studies show that earlier Neogene (Early and Middle Miocene) and Paleogene deposits are locally thicker to the north or more evenly distributed (Cassinis, 1986).

5.2.5 Alps and Molasse Basin

The Alps are undoubtedly the most studied geological feature in the world. The literature concerning them is voluminous and,

unfortunately, confusing. As the Alps are only tangentially involved in the evolution of the Western Mediterranean Sea they are only briefly discussed. The bulk of this section is from five sources: Lemoine et al. (1986), Ogniben (1985), Funk et al. (1987), J.P. Platt lectures (1987), and R. Butler (pers. comms., 1984-1988).

The Alps are the deformed European (northern) continental margin and oceanic sediments of the Tethyan Ocean. The Alps are divided into zones that have paleogeographic significance. The External Zone generally consists of shelf, slope, and rise (?) deposits and the Internal Zone of basinal and oceanic deposits.

The External Zone (Dauphinois in the Western Alps, Helvetics in the Central and Eastern Zone) is considered a classical "miogeosynclinal" terrain with Triassic epicontinental deposits followed by Jurassic to Eocene platform units. Moving toward the internal zone these shelf deposits give way to shaley slope facies of the Ultrahelvetic Zone.

Between the External and Internal Zones lies the Valais Trough (Central and Eastern Alps) and its onstrike continuation the Subbrianconnais (Western Alps). The Valais Trough, denoted by Bundnerschiefer sedimentation (deep-water turbidites and marly clays), is widest in the east and narrows to the west. The Subbrianconnais Zone, transitional between the External and Internal Zones, contains Triassic evaporites and carbonates, Jurassic carbonates and shales, and Cretaceous shales.

The most external unit of the Internal Zone, the Brianconnais,

is considered a fragment of continental crust on which Triassic carbonates and evaporites were deposited prior to Jurassic and Cretaceous pelagic sediments. The most internal unit is the Piemont Zone, divided by some workers into an External Piemont Zone and an Internal Piemont Zone. The latter is synonymous with the Ligurian Tethys. Ophiolitic detritus and "ophiolitoids" (Trumpy, 1982), as well as radiolarian chert, pelagic limestone, and schistes lustres are the typical rock types found. They are interpreted as oceanic crust and sediments.

The gross structure of the Alps is of an External Zone that is dominated by thrust geometries and an Internal Zone of large nappe complexes disrupted by fore- and backthrusts. Metamorphic grade in the External Zone is, at most, lower greenschist facies, whereas high pressure/low temperature assemblages overprinted by higher temperature greenschist facies assemblages are common in the Internal Zone. Tectonic scenarios for the Alps are too numerous to discuss. However, one of the major problems has been to relate structures observed in the field to the relative plate motions of Africa and Europe.

The Molasse Basin is the foreland basin of the Alps, although within the mountain belt flysch ranging from Cretaceous to Eocene age is found. The age of the flysch deposits youngs on across strike traverses from north to south (or east to west). The Molasse Basin contains Miocene and younger rocks. The exact relationship between the flysch deposits and the Molasse Basin has not yet been ascertained.

The European foreland contains an additional basin system of note. The West European Rift System (Rouchy, in prep.) is a N-S oriented intraplate scissure that formed in the Alpine foreland during the Tertiary, and which extends more than 1600 km from the North Sea to the Mediterranean Sea. In detail, the system is composed of a series of individual graben systems that are linked, and shifted laterally, by a series of E-W and ENE-WNW transfer zones. From south to north, the system is subdivided into 1) the Mediterranean segment, 2) the Languedoc-Roussillon-Provence segment, 3) the Bresse-Valence segment, and 4) the Rhine Graben segment. Much of what is known about the rifts comes from extensive geophysical and well data which was accumulated during exploration for hydrocarbons (Rhine Graben, Gulf of Lyon), for potash and salt (Rhine Graben), and for nuclear waste and natural gas repositories (Bresse, Valence, and Manosque Grabens).

Extension began, and was locally greatest, in the Eocene with paroxysmal activity in the Oligocene and episodic activity in the Miocene and Pliocene. The later activity was overprinted by development of the Alpine foreland basin in the Miocene.

5.2.6 Pyrenees, Ebro Basin, and Aquitaine Basin

The Pyrenees differ from the other mountain ranges in the Western Mediterranean region in that they are a double sided orogenic belt but, as with the other orogens, are divided into external and internal zones. The external North and South Pyrenean Zones are separated by an Internal Metamorphic Zone,

sometimes referred to as the Axial Zone (or Paleozoic Axial Zone) and are bordered in their respective forelands by the Aquitaine and Ebro Basins (Mattauer and Henry, 1974). Although double-sided the orogen has an asymmetry that is shown by the dominance of south-directed structures, with north-directed structures increasingly regarded as a series of backthrusts (Fischer, 1984).

The boundary between the North Pyrenean Zone and the Axial Zone is the North Pyrenean Fault. This fault is a major tectonic lineament separating crust 50 km thick to the south from 30 km thick crust to the north (Hirn et al., 1980; Daignieres et al., 1982). Between the South Pyrenean Zone and the Axial Zone the Gavarnie Thrust, a major low angle thrust fault which dips to the north, forms the boundary. The North and South Pyrenean Frontal Thrusts mark the boundaries between the Pyrenean Zones and the foreland regions of the Aquitaine and Ebro Basins.

Subdivisions within the external zones are recognized. In the north the Sub-Pyrenean Zone is recognized between the North Pyrenean Frontal Thrust and the Petites Pyrenees Thrust (Peybernes and Souquet, 1984). In the innermost part of South Pyrenean Zone, the High Primary Range lies just south of the North Pyrenean Fault (the boundary with the Axial Zone) in the southern part of this zone the Marginal Sierras Zone is recognized (Soquet et al., 1977). In addition to these latitudinal zones, a series of northeast trending "en echelon" faults segmented the Pyrenees longitudinally and greatly influenced sedimentation and deformation patterns (Puigdefabregas

and Souquet, 1986).

The Axial Zone consists of Paleozoic rocks metamorphosed during the Hercynian Orogeny to greenschist and amphibolite facies (Mattauer and Henry, 1974). Unconformably above this is a Permo-Triassic series of redbeds and evaporites interpreted by Souquet et al. (1977), as molasse from the former orogenic highlands. This was followed by the establishment of a carbonate platform in the Jurassic, which continued until the Aptian when basinal marls, followed by flysch lying above an intra-Aptian unconformity, marked a deepening of the basin. No rocks younger than Albian are found in the Axial Zone. Rocks similar to those of the Axial Zone are found also in the northeastern part of the North Pyrenean Zone.

The North Pyrenean Zone stratigraphy for the Permo-Triassic, Jurassic, and Lower Cretaceous is very similar to that of the Axial Zone, although in the Sub-Pyrenean Zone the Jurassic to mid-Albian interval is missing. Basinal conditions existed in the North Pyrenean Zone throughout the Late Cretaceous and Early Tertiary, whereas the Sub-Pyrenean Zone rocks are mostly of shallow water facies. The southern external zone shows a similar stratigraphy but with two differences. In the Marginal Sierra Zone, the sequence is continuous from the Late Triassic and throughout the external zones the Permo-Triassic sequence consists mostly of Late Triassic evaporites.

Various structural and tectonic models have been presented for the evolution of the Pyrenees and its offshore continuation into

the north Spanish margin. Boillot and Capdevila (1977) suggested that the deformation was due to southerly directed subduction of oceanic crust whereas Williams (1984) and Williams and Fischer (1984) prefer northerly subduction to generate a low angle, north dipping decollement. A third model proposes early gravity gliding of nappes from the Axial Zone followed by later compression (Choukroune and Seguret, 1973). A model emphasizing long lived strike-slip motion on the North Pyrenean Fault produces a cross-section like the gravity gliding model (Souqet et al., 1977). Deep seismic reflection experiments by the ECORS Pyrenees Team (1988) has produced data upon which a new model, showing strong deformation of the North Pyrenean Fault, has been based.

The Pyrenean foreland basins are the Ebro Basin to the south and the Aquitaine Basin to the north. The latter has had a more complex evolutionary history (Brunet, 1984; Boillot, 1986).

The Ebro Basin, triangular in shape, is bounded on the north by the Pyrenees, on the southwest by the Celtiberian Range, and on the southeast by the Catalonian Coast Range. Of all these, the Pyrenees have exerted the greatest influence on the evolution of the basin. An isobath map of the base Tertiary shows thicknesses up to 7,000 m near the mountain front. Thickness decreases sharply to the south and is accompanied by an equally sharp variation from marine to continental facies (Busquets et al., 1985). Most of the Tertiary, which commonly rests directly on the Cretaceous, consists of late Eocene-Oligocene and thinly

developed Miocene (Ager, 1980). The pattern of thicker, earlier developed sedimentary packages adjacent to the mountain front is typical of foreland basin deposition, as is the variation from marine to continental facies away from the mountain front (P. Allen, pers. comm., 1988).

The history of the Aquitaine Basin is more complex than that of the Ebro Basin in that it reflects an early phase of rift and passive margin basin development and a later history as a Pyrenean foreland basin. The timing of conversion from an extensional regime to a compressional one is shown elegantly in subsidence plots from wells in the basin (Brunet, 1984).

Three phases of fault related subsidence are seen throughout the basin. The first two are synchronous (Late Triassic, Early Cretaceous) whereas the third is diachronous. The third phase is Paleocene-Eocene in age and is oldest in the south and east and is progressively younger to the north and west. This is exactly the pattern that would be predicted for a foreland basin adjacent to a mountain range in which the deformation becomes increasingly younger to the west as thrust sheets impinge from the south.

Within the Pyrenees, mostly in the eastern part of the orogen, there are a series of syn- and post-orogenic intermontane basins that are Neogene in age. Their location and mode of formation is generally related to reactivation of older structures, with most of them originating as pull-apart basins between NE to NNE trending strike-slip faults.

5.2.7 Atlas Chain (North Africa)

The origin and development of the Atlas Chain is rather different from that of the Alpine system (sensu lato) as noted at the start of this section. The High and Middle Atlas are narrow "mobile" belts bounded by the stable platform regions of the Moroccan and Oran Mesetas and the African craton (Fig. 5.1). These platform regions are made up of Paleozoic rocks deformed and metamorphosed in the Variscan Orogeny and, in the case of the craton south of the South Atlas Fault, of Precambrian rocks. The Atlas consists mostly of Mesozoic strata, with some Tertiary rocks on the flanks of the belt. The western end of the High Atlas strikes at a high angle into the Atlantic margin of Morocco. The Saharan Atlas is a continuation of the High Atlas of Morocco.

Faults bordering and within the Atlas strike E-W, ENE-WSW, and NE-SW (UNESCO, 1968). Within the High Atlas the fault pattern exhibits lozenge and rhomboidal-shaped units (Laville and Petit, 1984; Stets and Wurster, 1982). Sediment thickness changes drastically across border faults, as well as across faults within the range. Lithology and facies show that continental to shallow-marine environments prevailed from Triassic to Cretaceous time (Seufert, 1988; Stets and Wunster, 1982). Little or no subsidence is observed in the bordering platform regions. The pattern and type of sedimentation, in conjunction with the pattern of faults, suggests that the Atlas originated as a rift and/or pull-apart basin system. The Triassic onset of

sedimentation in the Atlas suggests a strong connection with the rifting that led to the formation of the Central Atlantic.

In Turonian time subsidence ceased in the High and Middle Atlas. The style of deformation and uplift that followed was described above. In contrast to the High and Middle Atlas, subsidence in the Saharan Atlas did not cease in the Turonian. Rather, it continued through the Cretaceous, although changing somewhat in character from west to east. In the western Saharan Atlas shallower, more restricted facies were predominant in the Jurassic with more open marine carbonates deposited to the east. In the Cretaceous the western region received mostly siliciclastic (sandstones and shales) sedimentation while the eastern region continued to have carbonates deposited. The easternmost part of the Saharan Atlas continued having open marine conditions until Eocene time (Sander, 1970).

At its easternmost extent, in Tunisia, the Saharan Atlas changes strike from NE-SW to N-S and becomes known as the North-South Axis. This axis is the boundary between the onshore continuation of the Pelagian Shelf (the Sahel) and the Atlas Chain. At its northernmost extent the North-South Axis encounters a zone of intense deformation known as the "Zone of Diapirs" (Perthuisot, 1981). Within the entire region of the eastern Saharan Atlas, the North-South Axis, and the on- and offshore Pelagian Shelf there are a series of young basins whose axes strike NW-SE or WNE-ESE.

5.3 Western Mediterranean Sea

The Mediterranean Sea is commonly subdivided into two main sectors: the Eastern Mediterranean, which consists largely of old oceanic crust considered a remnant of the Mesozoic Tethys, and the Western Mediterranean, which is made up of a series of young (Miocene-Recent) basins. The dividing point is between 15o and 20o East longitude in the Ionian Sea.

Much of what is known of the Mediterranean Sea is from data obtained by various types of geophysical survey. Drilling in various parts of the Mediterranean Sea has also provided a great deal of data, although it is unevenly distributed. For example, in the Tyrrhennian Sea the Deep Sea Drilling Project and the Ocean Drilling Project have drilled 9 boreholes in 3 cruises (Fig. 5.2), whereas the entire Eastern Mediterranean has only been drilled at 10 sites. Commercial boreholes have yielded a great deal of data about the Gulf of Valencia and the Gulf of Lyon but very little drilling has been done in most other regions.

5.3.1 Alboran Sea

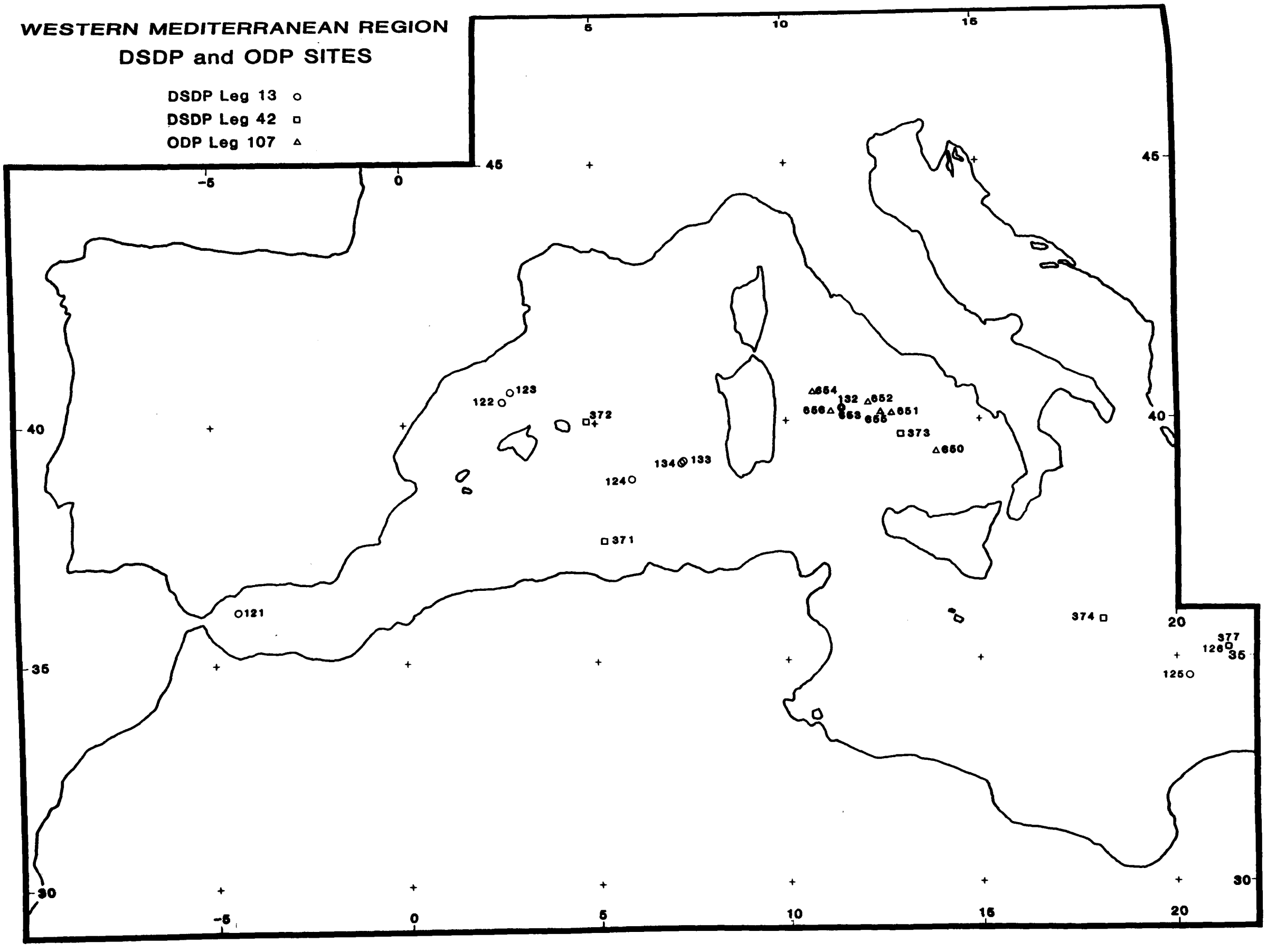
The westernmost part of the Mediterranean Sea, the Alboran Sea, lies between the African and European plates. It is a small basin (180 x 320 km) bounded north and south by the Betic and Rif orogenic belts, respectively. On the west only a narrow, shallow connection to the Atlantic Ocean through the Straits of Gibraltar breaks the apparent continuity of this orogenic system. On the east the Alboran Sea opens into the South Balearic Basin.

Figure 5.2: DSDP and ODP Drilling Sites: Locations and Stratigraphy

A: Location map showing placement of DSDP and ODP drilling sites. Symbols: DSDP Leg 13 = circle; DSDP Leg 42 = square; ODP Leg 107 = triangle. Note: Site 132 in the Tyrrhenian Sea was drilled on Leg 13 and reoccupied on Leg 107 as site 653.
B: Stratigraphic sections for DSDP Leg 13 sites in the Western Mediterranean. Note that site 120 is not shown on map. This is an Atlantic Drill site at Gorringe Bank that was drilled on this leg. Legend is given after D.
C: Stratigraphic sections for DSDP Leg 42 sites in the Western Mediterranean.
D: Stratigraphic sections for ODP Leg 107 sites in the Western Mediterranean. Note that all sites are in the Tyrrhenian Sea.

WESTERN MEDITERRANEAN REGION
DSDP and ODP SITES

DSDP Leg 13 ○
DSDP Leg 42 □
ODP Leg 107 △



DSDP Site 120

DSDP Site 121

DSDP Site 122

DSDP Site 123

DSDP Site 124

DSDP Site 125

DSDP Site 126

DSDP Site 132

DSDP Site 133

DSDP Site 134

Q

TERTIARY

PLEIST-OCENE

PLIO-CENE

MIO-CENE

OLIGO-CENE

EO-CENE

PALEO-CENE

16 Ma +/- 1 K-Ar

21 Ma +/- 2 K-Ar and Fission Track

JURASSIC

CRETACEOUS

Late

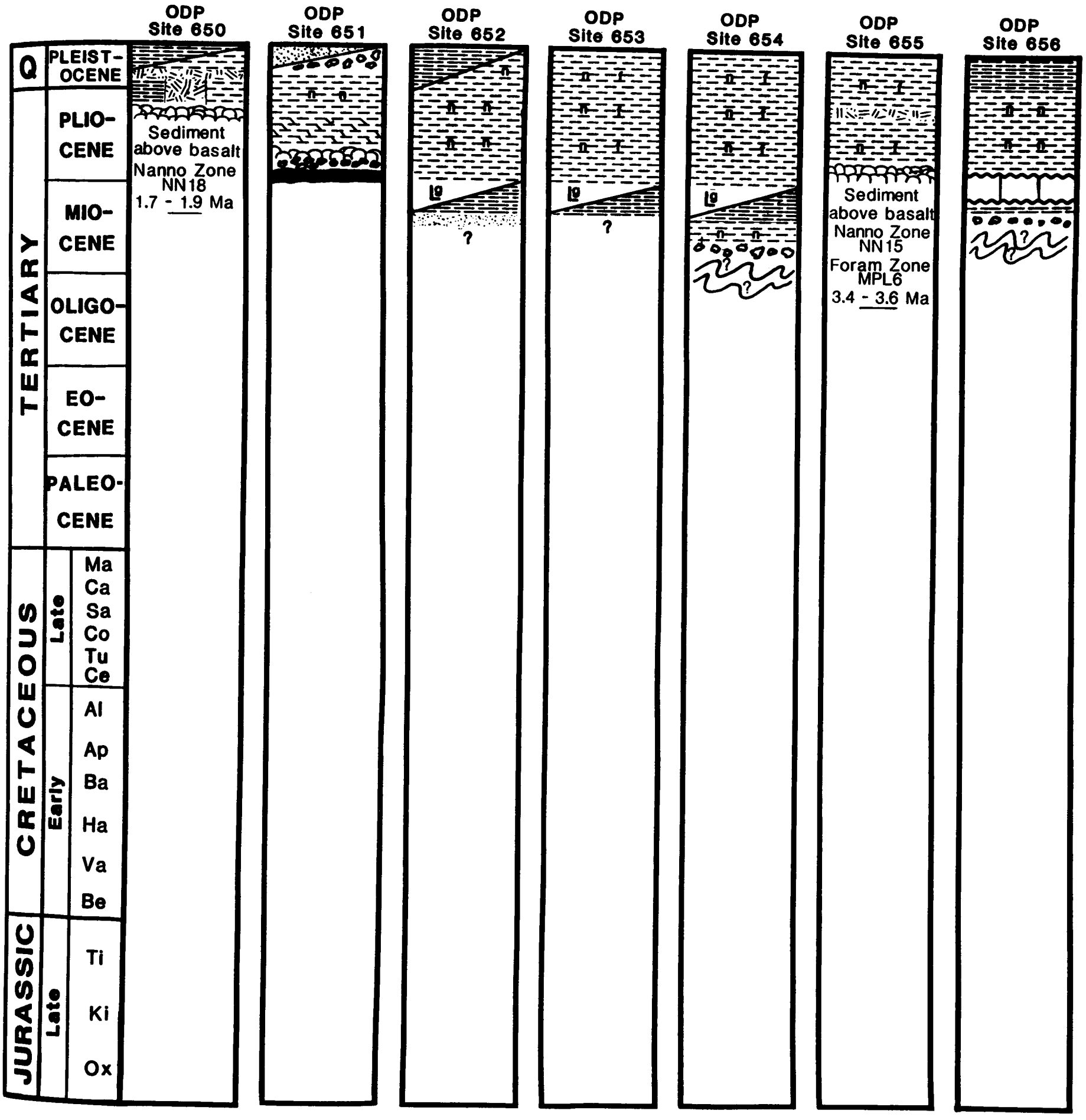
Early

Late

Ma
Ca
Sa
Co
Tu
Ce

Al
Ap
Ba
Ha
Va
Be

Ti
Ki
Ox

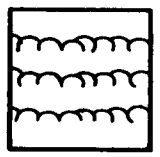

ODP Site 650
ODP Site 651
ODP Site 652
ODP Site 653
ODP Site 654
ODP Site 655
ODP Site 656
Q
PLEIST-OCENE
TERTIARY
PLIO-CENE
MIO-CENE
OLIGO-CENE
EO-CENE
PALEO-CENE
CRETACEOUS
Late
Early
JURASSIC
Late
Ma
Ca
Sa
Co
Tu
Ce
Al
Ap
Ba
Ha
Va
Be
Ti
Ki
Ox
Sediment above basalt
Nanno Zone NN18
1.7 - 1.9 Ma
Sediment above basalt
Nanno Zone NN15
Foram Zone MPL6
3.4 - 3.6 Ma



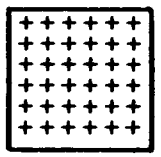
Deformed and metamorphosed basement



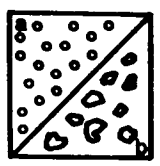
Pelagic and Neritic
a)Limestones
b)Dolomites



Pillow Lavas

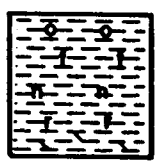


Granites and Granitic Rocks

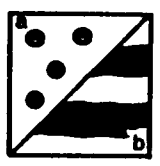


a)Conglomerates

b)Breccias



Marls and Oozes
c coccolith
f foraminiferal
n nannofossil
r radiolarian
\ dolomitic

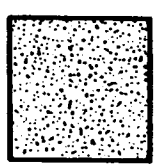


a)Ophiolites

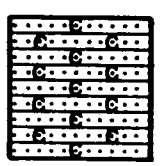
b)Ultramafics



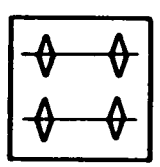
Coal



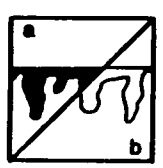
Sandstones



Carbonate Turbidites



Volcanics
-collisional

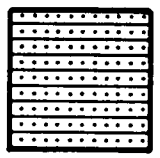


a)Bauxites

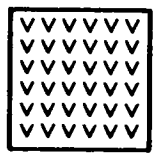
b)Karsts



Silt-, Mud-, and Claystones



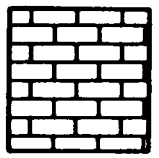
Turbidites



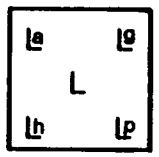
Volcanics
-subduction



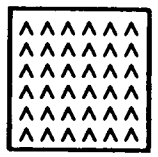
Olistostromes and Slumps



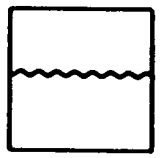
Platform Limestones



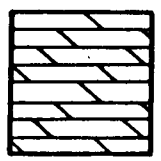
Evaporites
g gypsum
a anhydrite
h halite
p potassic salts



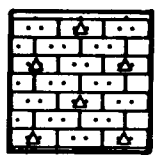
Volcanics
-extension



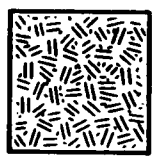
Unconformity



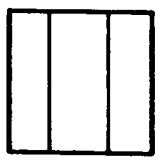
Platform Dolomites



Radiolarites and Chert



Volcanic Ash



Missing Record

The Alboran Sea is divided into two basins (eastern and western) by the Alboran Ridge, which trends between NE and ENE. Although the western basin is shallower, neither reachs depths much greater than 1500 meters (Fig. 5.3) (Auzende et al., 1979; Finetti and Morelli, 1973; IBCM, 1981; Laughton, 1975). It is only where the Alboran Sea merges with the Algero-Balearic Basin that oceanic-like depths (> 2,500 m) are reached.

The structure of the Alboran Sea is known almost entirely from geophysical data. Direct sampling by dredging in shallower regions and drilling during DSDP Leg 13 provided additional information. Seismic refraction experiments indicate that the mean Moho depth beneath the Alboran Sea is 16 km with a mean crustal velocity of 6.0 - 6.3 km/sec (Working Group, 1978). A low velocity (Vp = 7.5 km/sec) below the Moho, near the center of the sea, is interpreted as thinned continental crust that overlies anomalous upper mantle material and is consistent with the high heat flow (2.22 +/- 0.4 Heat Flow Units [HFU]) measured in the central part of the Alboran Sea (Erikson et al., 1977).

Free air gravity anomaly maps show a strong positive anomaly (> 70 gammas) that correlates well with the Alboran Ridge (Finetti and Morelli, 1973, Plates I and IV). A strong residual magnetic anomaly (> 200 gammas) with the same trend as the Alboran Ridge is offset to the northeast (Finetti and Morelli, 1973, Plates I and X; Olivet et al., 1973, Fig. 10). This and other strong anomalies are associated with the distribution of volcanic material. Volcanic material of trachy-andesitic nature

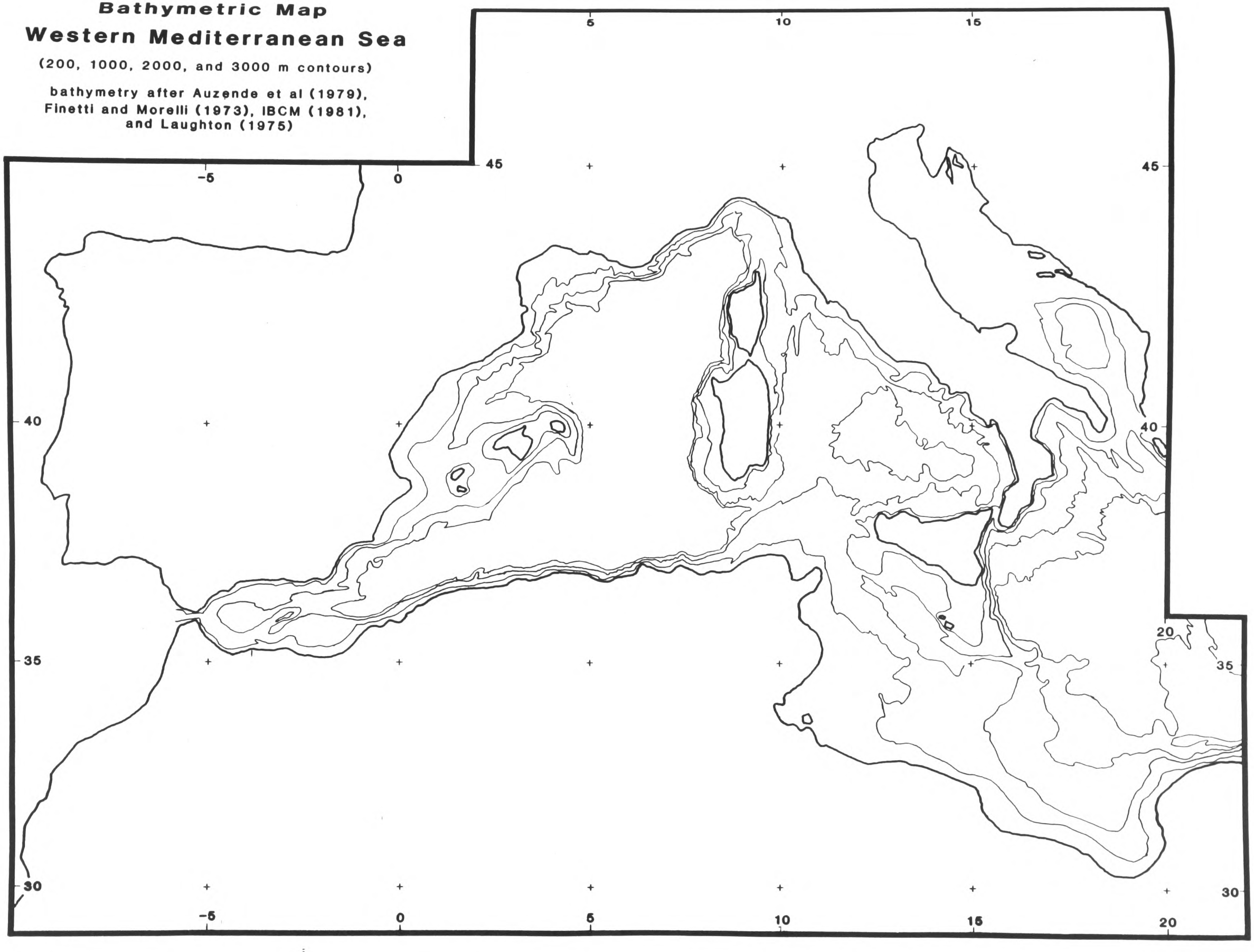
Figure 5.3: Simplified Bathymetry of the Western Mediterranean

Simplified bathymetric map of the Western Mediterranean Sea. Features of note are the division of the Alboran Sea into two sub-basins by the Alboran Ridge, the narrowness of the continental shelves in most regions (especially along the North African margin), and the abyssal depths in the Balearic Seas and the Tyrrhenian Sea. Data complied from Auzende et al. (1979), Finetti and Morelli, 1973, IBCM, 1981, and Laughton, 1975).

Bathymetric Map
Western Mediterranean Sea

(200, 1000, 2000, and 3000 m contours)

bathymetry after Auzende et al (1979),
Finetti and Morelli (1973), IBCM (1981),
and Laughton (1975)



is known from dredging and sampling on Alboran Island (Giermann et al., 1968).

The sedimentary sequence of the Alboran Sea is known from drilling at DSDP Site 121 (Fig. 5.2) and seismic reflection data. Much of this sequence has been correlated with data from other parts of the Western Mediterranean Sea. At Site 121 a sequence of Upper Pleistocene marl ooze (290 m thick) conformably overlies a Lower Pleistocene-Lower Pliocene section of graded sands (turbiditic) and marl ooze (396 m thick). Below an Upper Miocene (Messinian) unconformity are 190 m of pelagic marl with minor turbiditic sand intercalations. These marls and sands were originally dated as Tortonian (Nesteroff, 1973) but subsequent work has reassigned them to the Messinian (Montenat et al., 1975). The entire sequence overlies a basement of metamorphic rocks, similar to those found in the Rif and Betic Mountains (Kornprobst, 1973). Steiger and Frick (1973) have determined a K-Ar age of 16 +/- 1 Ma from a sample of this basement rock.

Various models have been proposed to explain the tectonic evolution of the Alboran Sea region. Those that view the Alboran Sea as an extensional feature may be grouped into 3 main classes: mantle diapir, back-arc basin, and Alboran Plate. The last two are closely related. In addition, Megias (1982) has a model for the Alboran Sea that has it as a compressional feature.

Models invoking mantle diapirism as a mechanism for basin formation have been suggested for many Mediterranean basins, particularly the Tyrrhenian Sea (van Bemmelen, 1973; Wezel,

1985). A similar model has been suggested for the Alboran Sea by Weijermars (1985). The suggest cause of the diapiric uprise is the passage of the Alboran Sea over a site of "... small-scale convective upwelling which occurs nowadays under the Atlas Mountains 450 km to the south-east..." (Weijermars, 1985).

According to this model the lithospheric doming caused by the upwelling resulted in nappes being shed by gravity spreading to the north and south. As the upwelling site was passed the heat source was removed, resulting in the initiation of cooling and subsidence. The initiation of orogeny in the Betic and Rif and of subsidence in the Alboran Sea constrains the timing of passage over the site of upwelling.

Dewey (1989) and Platt and Vissers (1989) have also suggested that gravity spreading is the driving mechanism for much of the Betic and Rif deformation. However, they attribute the cause to orogenic collapse of overthickened lithosphere in the collision zone. This overthickened crust also initiated the extension which formed the Alboran Sea.

The origin of the Alboran Sea as a back-arc basin, suggested by LePichon et al. (1972) and Auzende et al. (1973), is based on the continuity of the Rif and Betic around the Arc of Gibraltar and on an ENE-WSW tectonic grain in the Alboran Sea. The model suggests that the Rif and Betic internal zones moved southwest via strike-slip faults after Iberia collided with the African margin above a north-dipping subduction zone. Motion along these faults resulted in the opening of the Alboran Sea, analogous to

the mechanism suggested for formation of the Sunda Arc (Fitch, 1972; Karig et al., 1979).

The Alboran Sea has also been modeled as part of a microplate, formed of the Rif and Betic internal zones, that moved westward or southwestward above a major extension of the Pico-East Azores Fracture Zone, between the European and African plates. The model, proposed by Andrieux et al. (1971), is based on contrasting ages and styles of deformation and lithological differences between the internal and external zones in both the Rif and Betic orogens. Similar models have been suggested to account for deformation in the Betic and Rif adjacent to major strike-slip faults (De Smet, 1984; LeBlanc and Olivier, 1984).

Megias (1982) has modeled the origin of the Alboran Sea and the bounding Betic and Rif orogens as the products of subduction. There are two reasons that this model is of interest. It is based upon deep seismic data (processed to 8 seconds TWT) which shows the deep structure of the basin. In an area where lithospheric plates are colliding compressional features are expected and this is the only model that suggests a distinctly compressional mode of origin for the Alboran Sea.

Megias' (1982) suggests that 3 "subduction zones" were active in the Betic-Rif-Alboran Sea area during the Miocene. The presence of subduction zones is inferred from identification on seismic sections of "accretionary prisms". These "accretionary prisms" and "subduction zones" might better regarded as fold and thrust belts, as Megias recognizes the limited amount of oceanic

crust available for subduction at the time.

The "accretionary prism" beneath the Alboran Sea is regarded as a mechanical accomodation to the collision and cessation of thrusting between the internal and external zones of the Betics, as well as the thrusting in North Africa. It marks the suture between the internal zone of the Betics and the Alboran plate. Thus the Alboran Sea may be regarded as a form of forearc or foreland basin.

5.3.2 The Gulf of Valencia

The Gulf of Valencia (Valencia Trough) lies off the east coast of Iberia, is bounded to the south by the Balearic Islands, and opens to the Gulf of Lyon and the Balearic Basin to the north. As with the Alboran Sea the structure is known mostly from geophysical studies but a large number of commercial boreholes have provided information about the stratigraphy.

The maximum bathymetry of 2,000 meters is reached only near the northernmost extent of the Gulf of Valencia where it opens into the Balearic Sea. Over most of its area the depth is between 1,000 and 1,800 meters, with a broad shelf adjacent to the Iberian coast in the south (Auzende et al., 1979; Finetti and Morelli, 1973; IBCM, 1981; Laughton, 1975).

The Gulf of Valencia is bisected by a central trough (Valencia Trough) that collects sediment from deep canyons that strongly incise the Iberian margin. A negligible free-air gravity anomaly indicates that despite the thick sediment the basin seems to be in isostatic equilibrium, although the Bouger gravity anomaly is positive and increases to the north (Finetti and Morelli, 1973). A NE-SW trending line of magnetic anomalies that bisects the Valencia Gulf (Vogt et al., 1971) can be seen to correspond to volcanic intrusions and outcrops (Morelli and Nicholich, 1980). The age of these volcanics is 19 - 21 Ma (Ferrara et al., 1973).

Seismic refraction results in the northern Gulf of Valencia are suggestive of thinned continental crust with Vp = 6.7 - 7.5 km/sec occurring below 13 km (Hinz, 1972). In the southern part

of the Gulf of Valencia slightly lower velocities (Vp = 6.6 - 6.8 km/sec), recorded from shallower crustal depths (5 km) (Fahlquist and Hersey, 1969) can also be interpreted in the same way. High heat flow values of 1.79 - 2.15 HFU (calculated from Cermak and Hurtig, 1979) are consistent with this interpretation.

The sedimentary sequence in the Gulf of Valencia is known from DSDP drill sites 122 and 123 (Fig. 5.2), various commercial boreholes, and reflection seismic data. It has been correlated with onland sections in boreholes and outcrop. The Quaternary and Pliocene sequence consists largely of graded sands and silts, interpreted as turbidites and contourites, interbedded with nannofossil ooze and marl. Under a Messinian (Upper Miocene) unconformity, salt, gypsum, and dolomite deposited during the Messinian Salinity Crisis are present locally. A thick Miocene section of sandstones, claystones, and limestones generally overlies either Oligocene redbeds or karstified Cretaceous limestones. Toward the center of the Gulf of Valencia rocks of Jurassic, Triassic, and Paleozoic age are locally exposed beneath the unconformity.

The Gulf of Valencia is thought to have formed when the Balearic Islands rifted away from the eastern margin of Iberia. The similarity of Balearic Mesozoic rocks with those of the Betic Cordillera, the steep northwestern margin of the Balearic Islands, which can be interpreted as a normal fault, the faulted eastern margin of Iberia, the thin crust which underlying the Gulf, concomitant with high heat flow, all point to this mode of

origin. Abundant Early Miocene volcanic ash and sedimentary sections of Oligocene or Early Miocene age above an unconformity cutting Mesozoic rocks constrain the age of this event.

5.3.3 Western Mediterranean Sea

The physiographic province that is generally referred to as the Western Mediterranean Sea encompasses the region west of Corsica and Sardinia, east of the Balearic Islands, south of France, and north of Algeria and Tunisia. This area is also known as the Balearic Sea (Ryan et al., 1970), the Algero-Provencal Basin (Carter et al., 1972), and the Algerian-Balearic Basin (Auzende and Olivet, 1974). This work follows the usage of Ryan et al. (1970) but divides the region into a North Balearic Basin and a South Balearic Basin (Fig. 5.1). The former basin also includes the Gulf of Lyon and the Ligurian Sea. The basis of the division is the slightly different ages of the basins, with the South Balearic Basin being slightly younger, and the difference in the width of the continental margins.

The greatest depth reached in either basin is slightly more than 2,800 m (Fig. 5.3) (Auzende et al., 1979; Finetti and Morelli, 1973; IBCM, 1981; Laughton, 1975). Both basins are characterized by flat abyssal plains that occupy the greater part of the province. There is no obvious physical break between the basins. The northern basin plain is, however, marked by small hills that are thought to be salt domes related to the movement of Messinian evaporites (Vanney and Gennesseaux, 1985).

The shelves that surround the Balearic Basins are, for the most part, very steep and narrow. Only in the Gulf of Lyon, on the Balearic Rise (south of Mallorca and Menorca), and on the Western Sardinian and Northern Tunisian margins do the shelves attain any appreciable width (Ryan et al., 1970). The shelf on the Algerian margin, east of the Alboran Sea, is only 10 km wide.

The crustal structure of the Balearic Sea, as determined by seismic refraction survey, is quite similar in both the northern and southern basins. In the North Balearic Basin oceanic layer 2 velocities (5.0 - 5.8 km/sec) were found in most stations and oceanic layer 3 velocities (6.6 - 6.8 km/sec) occurred throughout the deep basin. Mantle velocities were more variable with 8.0 km/sec values at a depth of 11 km at most stations but softer 7.7 km/sec values at others (Hirn et al., 1977). This is interpreted as oceanic crust, that may contain remnants of highly attenuated continental crust within it.

Hinz (1973) reported that the crustal structure of the South Balearic Basin contained a 5 km thick oceanic layer 3 with Vp = 6.0 - 7.4 km/sec that passed into rocks with Vp = 8.0 km/sec at a depth of 12 km. This velocity is typical of mantle rocks and the Moho depth is typical of oceanic crust.

Both seismic reflection studies and drilling by Deep Sea Drilling Project Legs 13 and 42 have shown that the stratigraphy of the basins is rather straight forward (Fig. 5.2). Above the acoustic basement, which is interpreted as oceanic crust, is a Lower Miocene (?) - Tortonian section that is locally reaches

3,000 m in thickness (Rehault et al., 1984). The overlying Messinian section consists of gypsum (anhydrite at depth), dolomite, and halite, deposited in shallow water and subaerial environments during the Messinian Salinity Crisis. The evaporite sequence is 2 km thick. The Plio-Quaternary sequence consists of pelagic and hemipelagic marls and oozes and basinal turbidites. Thicknesses range from 500 - 2,500 m (Finetti and Morelli, 1973).

Heat flow data from the Balearic Basin shows a mean value of 92 +/- 10 mW/m2 but with much variation. When cooling models for oceanic crust are applied to this basin the same age-depth relationship is found (Hutchison et al., 1985). Studies in the Gulf of Lyon, which forms the northwest margin of the North Balearic Basin, also indicate that subsidence follows an exponential curve after correction for sediment compaction, paleobathymetry, and sea level fluctuations (Bessis, 1986). It can be concluded that subsidence on both the margin and deeper basin is thermally driven and that the cause was attenuation of the lithosphere. An additional point of interest concerning the heat flow in the Balearic Basin noted by Hutchison et al. (1980) is that the values increase from west to east and that a similar pattern is found in the Tyrrhenian Sea.

From a variety of data, some cited above, it is generally agreed that the North Balearic Basin formed as Corsica and Sardinia rotated away from Provence in Latest Oligocene-Earliest Miocene time. The manner in which the South Balearic Basin formed is less clear, although it seems to have opened as the

Kabylies rifted from the Balearic Islands and moved southeast above a northwest-dipping subduction zone (Rehault et al., 1984).

5.3.4 Tyrrhenian Sea

The Tyrrhenian Sea is the youngest basalt-floored basin in the Mediterranean Sea and probably in the world (Kastens, Mascle, et al., 1988). The Tyrrhenian is triangular in shape and bounded on the northeast and south by peninsular Italy and Sicily and on the west by Corsica and Sardinia (Figs. 5.1, 5.3). Connection to the rest of the Mediterranean is mostly through the Sardinian-Tunisian Strait on the southwest with minor connections through the Straits of Messina on the southeast, through the Straits of Bonifacio on the west, and into the Ligurian Sea to the north.

The Tyrrhenian Sea has been extensively studied, most recently by ODP Leg 107 (Fig. 5.2) (Kastens, Mascle, et al., 1987). The deepest parts of the Western Mediterranean Sea, with depths exceeding 3,600 m (Fig. 5.3) (Auzende et al., 1979; Finetti and Morelli, 1973; IBCM, 1981; Laughton, 1975), occur in the Vavilov and Marsili Basins, which are Tyrrhenian Sea subbasins.

Numerous seismic studies in the Tyrrhenian have elucidated its crustal structure (Duchesnes et al., 1986 and references cited therein). Beneath most of the Tyrrhenian the depth to the Moho is less than 15 km and in the central and southeast regions (Vavilov and Marsili Basins) it is 8 km. Seismic velocities of 6.5 -6.5 km/sec are found in the lower crust above the Moho and velocities of 7.75 - 7.9 below. These mantle velocities are

typical of those found in rifted environments but the structure is interpreted as oceanic. The Moho deepens between the Vavilov and Marsili Basins because a rifted fragment of continental crust separates these basins (K. Kastens, pers. comm., 1988).

Seismicity in the Tyrrhenian Sea defines the presence of a NW dipping Benioff Zone with earthquakes recorded at depths as great as 500 km (Anderson and Jackson, 1987 and references cited therein). Most present day seismic activity is concentrated in the 230 - 300 km depth range but the level of seismic activity is low at all depths. Anderson and Jackson (1987) interpret the low-level of seismic activity and the absence of large, shallow thrust events at the surface projection of the zone to infer that subduction has ceased.

Drilling by ODP Leg 107 has shown that the Vavilov Basin formed in the Early Pliocene (< 4 Ma) and the Marsili Basin in the Late Pliocene (< 2 Ma) (Fig. 5.2). The transect drilled on Leg 107 showed that the Tyrrhenian Sea has older sedimentary deposits in the northwest and that the deepest sediment becomes younger to the southeast (Kastens, Mascle, et al., 1987).

Heat flow values in the Tyrrhenian Sea are very high. Della Vedova et al. (1984) and Hutchison et al. (1985) recorded values in excess of 200 mW/m2 with an average value on the order of 150 mW/m2 for the central part of the sea. Values near the Sardinian margin are much lower. This trend of higher values from west to east is in accord with a younger basin to the southeast. As in the Balearic Basin, Hutchison et al. (1985) found a concordance

between heat flow vs. age curves for the Tyrrhenian with those predicted by cooling curves for major oceanic plates.

Various models have been put forth for the tectonic evolution of the Tyrrhenian. At one time the Tyrrhenian was considered a piece of foundered continental crust, in part because of dredge hauls from the deep basins that brought up continental type rocks (Heezen et al., 1971). It has also been thought that the process of "krikogenesis", i.e., large scale, diapiric upwelling from the mantle to produce doming and followed by sudden collapse was the main tectonic process (Wezel, 1985). Most current models take cognizance of the subduction zone beneath the sea and suggest some type of back-arc spreading, possibly accompanied by trench roll-back, as the mechanism of formation (e.g., Malinverno and Ryan, 1986).

CHAPTER 6

GEOLOGICAL MODEL OF WESTERN MEDITERRANEAN EVOLUTION

6.1 Introduction

The Western Mediterranean Sea evolved from Late Oligocene or Earliest Miocene time to the present. The "Alpine Cycle" events in the Tethyan or Mediterranean realm and the Atlantic region prior to formation of the Western Mediterranean Sea began in the Permian when the Pangean assembly of the continents ended. The completion of continental assembly caused a change from a global state of deviatoric compression to one of deviatoric tension, induced and enhanced by trench suction forces and body forces in an overthickened lithosphere (Dewey, 1988a). The Mesozoic and Cenozoic history that preceded the formation of the Western Mediterranean is summarized and discussed in sections 6.2 -6.6. This history is presented in the kinematic and geological context established in Chapters 2, 3, 4, and 5.

6.2 Pre-Seafloor Spreading (Late Permian-Early Jurassic)

The rifting processes that led to the establishment of the North Atlantic, Central Atlantic, and Neo-Tethyan (in the sense of Sengor, 1984) Oceans began in the Triassic or earlier. Ziegler (1988) dates the start of rifting in the Greenland-Norwegian Sea at 330 Ma (Middle Carboniferous) and in other parts

of the North Atlantic region (Bay of Biscay, Rockall Trough, Grand Banks of Newfoundland) at 240 - 260 Ma (Late Permian). These dates seem a bit early in light of the absence of Lower and (commonly) Middle Triassic sediment over much of Iberia, Maritime Canada, Morocco, and Eastern North America (Manspeizer et al., 1978 and references cited therein). Further east, in the Western Tethyan region, rifts formed from the Late Permian to the Middle Triassic, although the large-scale rifting that preceeded the formation of oceanic crust began in the Latest Triassic or Early Jurassic. For much of the Triassic this region was blanketed by carbonate platform systems.

By Early Jurassic time block faulting and rifting had a firm hold in the Tethyan and Central Atlantic regions. In the Newark Series of eastern North America Early Jurassic volcanics, dike swarms, and sills are intercalated with rift clastics. The dike trends are independent of the axes of the older Triassic basins (May, 1971). A similar situation obtains throughout the Tethyan region where Bernoulli (1981) has shown that the locus of early Jurassic rifting and subsequent seafloor spreading did not follow the sites of Middle Triassic subsidence and rifting.

6.3 Start of Seafloor Spreading (Early and Middle Jurassic)

Seafloor spreading started in the Central Atlantic about 170 - 175 Ma in the Bathonian or Bajocian, whereas in the Ligurian Tethys it began earlier. The earliest identifiable magnetic anomaly in the Central Atlantic is the Blake Spur Magnetic

Anomaly (165 Ma, Table 3.4, Appendix C). Based on the change from carbonate platform to pelagic facies deep-sea conditions were fully established in the Tethyan realm by the Toarcian, with some areas receiving pelagic sediments as early as Hettangian or Pliensbachian (Bernoulli and Jenkyns, 1974).

The extensional tectonic regime (rifting and seafloor spreading) in both areas became connected by a sinistral shear zone or transform fault. The exact nature and location of this boundary is impossible to ascertain but it must lie in Southern Europe, Northern Africa, or between them. Rod (1962) discussed the fault patterns of northwestern Africa and defined a major structure, the Agadir Fault, generally known as the South Atlas Fault or Lineament, a dextral strike-slip fault. Manspeizer et al. (1978) suggested the existence of a "Tethyan Fracture Zone" with sinistral displacement that runs near the present day North African coast and through the Rif. This fracture zone would connect with the Cobequid-Chedabucto Fault in Nova Scotia, a right lateral fault (Schenk, 1971). Manspeizer et al. (1978) also suggested that a correlation might be made between the westernmost segment of the South Atlas Fault, the Tizi n'Test Fault, and the southern end of the Boston-Ottawa Seismic Zone (Fletcher et al., 1978; 3.2.3a).

The most likely location for a major shear zone is the area of the present day Straits of Gibraltar. Although these straits only formed in the Late Neogene (K. Kastens, LDGO, pers. comm., 1986), there are several reasons to suggest this locality. A

prominent difference in gravity characteristics between the Betics and the Rif can be interpreted as a major boundary (Uchupi et al., 1976). There is an absence of igneous rocks in the Upper Triassic-Lower Jurassic of Newfoundland, the British Isles, and Western Europe and an abundance of them in the Newark Series of North America and the Moroccan High and Middle Atlas (Manspeizer et al., 1978; Ziegler, 1988). The Straits of Gibraltar region coincides with the boundary between these provinces on a pre- or early seafloor spreading reconstruction (Fig. 6.1).

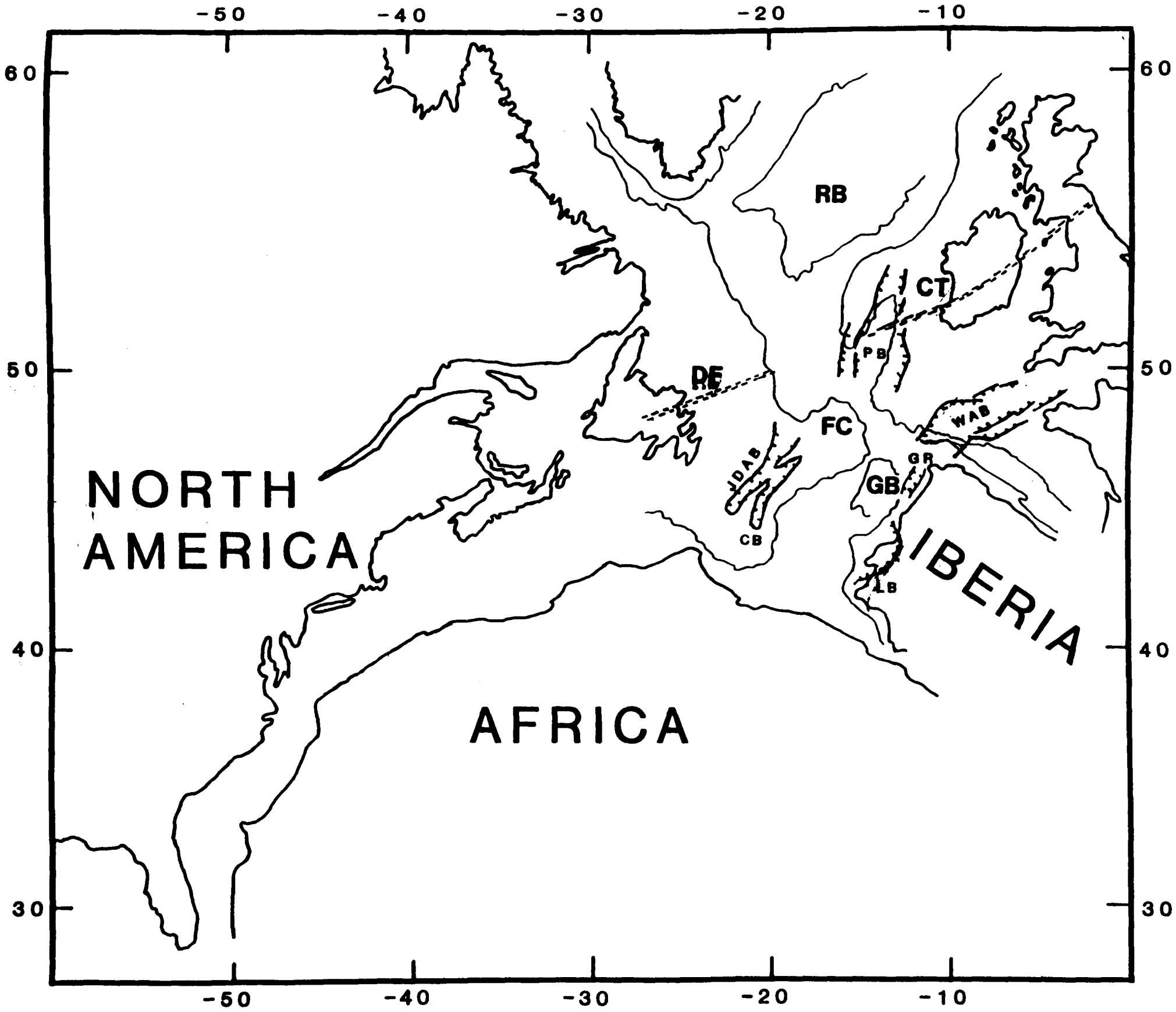
In addition, the Betic Cordillera of Spain has metabasites whose geochemical affinities are those of oceanic fracture zones (Bodiner et al., 1987). Moreover, the Betic Cordillera has only minor amounts of Jurassic volcanism (Julivert et al., 1980). A fracture zone margin in southern Spain would correlate nicely with the southern margin of the Grand Banks and the Southeast Newfoundland Ridge (Fig. 3.1, 6.1). The southern Grand Banks margin is known to be a transform margin that has the same strike as the Southeast Newfoundland Ridge (Todd et al., 1988). A consequence of locating the shear zone in the Straits is to keep the Kabylies attached to the European plate. An alternate view, with the Kabylies attached to Africa, is given by Ziegler (1988).

6.3.1 Early Jurassic Reconstruction

The reconstruction shown in Figure 6.1 was made using rotation parameters from Pindell et al. (1988) and Pindell (1985) for the Central Atlantic region. The North Atlantic closure pole, from

Figure 6.1: Early Jurassic Atlantic Reconstruction

Reconstruction of the North and Central Atlantic Oceans and restoration of Iberia to its pre-seafloor spreading position using rotation parameters given in Table 6.1. Rotation parameters for closure of the North Atlantic are from Kristoffersen (1978), for the Central Atlantic from Pindell et al. (1988), and for the Labrador Sea from Srivastava (1978). Legend: (large letters) CT = Clare Trend, DF = Dover Fault, FC = Flemish Cap, GB = Galicia Bank, RB = Rockall Bank; (small letters) CB = Carson Basin, GR = Galicia Rift, JDAB = Jeanne d'Arc Basin, LB = Lusitanian Basin, PB = Porcupine Basin, WAB = Western Approaches Basin


-50
-40
-30
-20
-10
60
50
40
30
NORTH
AMERICA
AFRICA
IBERIA
RB
CT
PB
PE
FC
WAB
GR
GB
JDAB
CB
LB

Kristoffersen (1978) is used because it incorporates closure of the Rockall Trough but allows independent closure of the Labrador Sea as discussed below.

6.3.1a Rockall Trough

The Rockall Trough is considered an extinct spreading center associated with limited formation of oceanic crust (Cande et al., 1988). Magnetic lineations in the southern part of the trough were interpreted as contemporaneous with pre-Anomaly 34 (84 Ma) crust further to the south (Roberts et al., 1981). These magnetic lineations were reexamined recently in conjunction with seismic reflection and refraction data. Magnetic highs were seen to coincide with highly reflective basement and reinterpreted as part of a system of volcanic ridges (Barra Volcanic Ridge System) in light of the extensive igneous activity in the region (Megson, 1987). The volcanic ridges were not correlatable with the pattern of magnetic anomalies resulting from seafloor spreading.

It is clear from gravity modeling and seismic data, however, that the crust of the Rockall Trough, especially the southern part, has been severely attenuated. Lower crustal seismic velocities of 6.6 - 6.8 km/s were recorded for the lower crust in the trough. Estimates of the amount of extension involved range from 230 km (Hanisch, 1984) to 300 km, with a Beta value (as defined by McKenzie, 1978) of approximately 4 (Megson, 1987). Beta values of 4 or more are typically associated with the onset seafloor spreading (J.F. Dewey, pers. comm., 1986). In light of this the Rockall Trough may best be regarded as oceanic-like

crust of indeterminate age, which is probably correlatable with the latest part of the Cretaceous Quiet Zone. Magmatism related to the British Tertiary Igneous Province and/or Thulean volcanism associated with the onset of seafloor spreading between Greenland and Eurasia may have overprinted the original magnetic signature.

6.3.1b Laborador Sea

The southern part of the Laborador Sea underwent seafloor spreading from Anomaly 33 (74.3 Ma) until sometime after Anomaly 20 (44.7 Ma). However, further north, in the area of the Nares Strait, compression and strike-slip (?) motion occurred for part of this interval (Early Tertiary). Seafloor spreading commenced in the Greenland Sea at Anomaly 24 (55.1 Ma), hence the Nares Strait may have been a plate boundary between Greenland and North America from Early to Middle Eocene. This is disputed by Dawes and Kerr (1982) who have shown that geological boundaries can be traced from Greenland to Ellesmere Island.

Srivastava (1978) has computed poles for rotations which close the Labrador Sea (North America with respect to Greenland) and the Rockall Trough (Greenland with respect to Europe) based on his study of magnetic anomalies. The combination of these poles is very similar to the pole used to close the North Atlantic in this study. Srivastava's (1978) rotation was used to close the Labrador Sea.

6.3.1c Bay of Biscay and Rotation of Iberia

The early Cenozoic (mostly Early Eocene) compression along the north coast of Iberia, contemporaneous with the Pyrenean Orogeny, deformed and possibly destroyed part of the crust of the Bay of

Biscay. This part of the North Atlantic had been formed by seafloor spreading in Late Cretaceous time.

Returning Iberia to its original position with respect to the Amorican margin of France is done by matching geological features from that region with those in northern Spain (Ries, 1978). These features form the Iberian-Amorican Arc and are generally thought to be Hercynian in age. Lefort (1979) has suggested that the arc is actually an older structure but without disputing that correlations can be made.

Determination of the reconstructed position of Iberia with respect to Europe was made using the geology and by computing a finite difference solution. The rotation parameters used and the computed result are given in Table 6.1.

6.3.1d Other Aspects of the Reconstruction

Some Paleozoic sutures fit well on the reconstruction. In particular, the Clare Trend (west of Porcupine Bank) and offshore portions of the Dover Fault (west of Orphan Knoll) are near the site of the future Charlie-Gibbs Fracture Zone in the North Atlantic. When extended onshore these major lineaments seem to correlate with suggested locations of the Iapetus Suture in Ireland (C.A. Price, pers. comm., 1988) and Newfoundland (Williams, 1978).

The rotation chosen for Iberia puts Galicia Bank slightly south of Flemish Cap and places the NNE trending rift system (Galicia Rift) that lies east of Galicia Bank on line with the southwestern end of the Western Approaches Basin, which lies

TABLE 6.1

ROTATION PARAMETERS FOR IBERIA WITH RESPECT TO EUROPE

Rotation of Iberia with respect to North America:

Latitude	Longitude	Rotation	Reference
70.33°	-11.08°	-51.09°	Srivastava and Tapscott (1986)

Rotation of North America with respect to Europe:

Latitude	Longitude	Rotation	Reference
71.20°	148.40°	23.08°	Kristoffersen (1978)

Rotation of Iberia with respect to Europe:

Latitude	Longitude	Rotation	Reference
47.04°	-2.35°	-35.60°	Finite Difference of (1) and (2)

southwest of the British Isles. This rift system continues further south as the Lusitanian Basin in Portugal.

The Porcupine Basin, east of Ireland, correlates with the Jeanne d'Arc and Carson Basins of the Grand Banks. The earliest sediments in these rifts are all of similar ages (Triassic-Early Jurassic), as well as having similar sequence stratigraphies, and episodes of clastic influx (Hiscott et al., 1988). Reflection seismic data southwest of Orphan Knoll and northwest of Flemish Cap show the presence of Jurassic basins whose axes trend NE-SW (Tankard and Welsink, 1987; Welsink et al., 1988).

6.4 Seafloor Spreading and Adria's Detachment (Oxfordian-Albian)

In the Western Tethyan (or Western Mediterranean) region the Late Jurassic-Early Cretaceous interval was marked by the sinistral motion of Africa with respect to Europe (see 4.3.3). Continued subsidence and basin differentiation occurred in most of the region (Durand-Delga and Fonbote, 1980; Lemoine et al., 1986; Wildi, 1983; Winterer and Bosellini, 1981). Similarly, in the Central Atlantic, continued seafloor spreading increased the width of the ocean with concomitant deepening of the basin driven by thermal and loading subsidence (Tucholke and McCoy, 1986).

The ocean that formed in the region of the present-day Western Mediterranean (variously termed Piemont-Ligurian Ocean (van Wamel, 1987), Neotethys (Sengor, 1984), Ligurian Tethys (Lemoine et al., 1986)) probably never exceeded a few 100 kms in width and

was characterized by long transform segments that offset short spreading centers (Treves, 1984). The Gulf of California would be a present day analogue. In the next paragraph three lines of evidence are put forward in support of this hypothesis.

The presence of various elongate strips of continental crust that lie parallel to former continental margins in the Apennines and Alps, (e.g., the Brianconnais Zone; "ribbon continents" of Trumpy (1982)) clearly point in this direction. Ophiolites in the Northern Apennines have abundant serpentine, apparently exposed at the seafloor without an extrusive carapace, abundant breccias, and highly fractionated basalts (Abbate et al., 1980). Such features are typical of a transform fault environment. Finally, the sinistral strike-slip motion between Africa and Europe is consistent with a NE-SW trending ocean dominated by transform faults.

In the region of the present-day Eastern Mediterranean Sea collision of northernmost Adria (African Promontory of Channel et al.,1979; Italo-Dinarid Promontory of Ziegler, 1988) with Europe began prior to the Barremian (Burchfiel, 1980; Debelmas et al., 1980; Mountrakis, 1986). It was this collision that most likely triggered the detachment of the promontory from Africa.

Detachment of Adria is suggested by several lines of evidence, including paleomagnetism, seismic data, and a combination of geological and plate kinematic data. Paleomagnetic data shows differences between the areas north (Southern Alps) and south (Northern Appenines) of the Po Valley. Van den Berg (1979)

suggested the presence of a large fault beneath this valley and inferred that motion along the fault decoupled the Southern Alps from the rest of Italy by Late Turonian time.

Platt et al. (1989) reviewed kinematic data from the Alpine Arc and compared it with Africa's motion from Mid-Cretaceous to the present. They showed that the patterns were not compatible. One conclusion they drew was that Adria had detached from Africa by the Tertiary and probably by Mid-Cretaceous.

Expanding spread profiles (ESP) from a two ship experiment in the Eastern Mediterranean were recently presented by Huchon et al. (1989). These ESPs showed crustal velocity structures that could only be interpreted as oceanic. Sediment loads from the ESP locations were decompacted and removed using backstripping techniques. The depths to basement determined by this process indicated that the crust underlying the Ionian Sea was 100 Ma or older. The ages suggested for locations to the east were older. This would be in accord with separation of Adria prior to 124 Ma (Barremian). Earlier seafloor spreading in the east would impart a counterclockwise rotation and a NW to WNW trajectory to Adria.

In the area north of the present day Azores-Gibraltar Fracture Zone extension was occurring with seafloor spreading starting between Iberia and the Grand Banks after the Barremian, as well as in the Bay of Biscay. The most likely time for these separations is the Albian, which is marked by a regression in these areas (Emery and Uchupi, 1984). Extension and limited seafloor spreading probably occurred in the southern Rockall

Trough at this time (see 6.3.1).

6.5 Early Alpine Orogenesis (Late Cretaceous)

The Late Cretaceous is marked by seafloor spreading in the North Atlantic that had the effect of making Africa move NE with respect to Europe. This initiated closure of the Tethyan Ocean in the Western Mediterranean region. The timing of the change in Africa's motion was discussed in section 4.3.3.

Cretaceous deformation is known from all sectors of the Alps but ages given for Eo-Alpine events in various locations differ widely. Desmons (1980) cites ages of 90 - 70 Ma (Turonian-Maastrichtian) for the Western Alps, whereas Trumpy and Niggli (1980) and Faupl et al. (1980) give Albian (113 - 97.5 Ma) ages for events in the Central and Eastern Alps, respectively. Older isotopic dates of 110 - 120 Ma, for eclogite metamorphism in the Sesia-Lazo Zone, have also been reported (Compagnoni et al., 1975; Hunziker, 1974).

Deformational and metamorphic events of this age are also noted in other areas. Diaz de Federico et al. (1980), Durand-Delga and Fontbote (1980), and Vegas and Banda (1982) note the start of compressional deformation in the Internal Zone of the Betic Cordillera. In the North African Rif and Tell there is compression suggested by stratigraphic evidence (Wildi, 1983) and in the Kabylies by radiometric age dates (Bossiere and Peucat, 1985, 1986; Monie et al., 1988). If the Kabylies are attached to

the European plate, as suggested below, then the ages of these radiometric dates accord well with those suggested for the metamorphism in the Betics by Torres-Roldan (1979).

Shortly after the Campanian (Anomaly 34) spreading stopped in the Bay of Biscay, although it was well established as far north as the Charlie-Gibbs Fracture Zone. In regions further north (Rockall Trough) spreading may have begun by this time and had definitely begun in the Laborador Sea by Anomaly 33 (see 6.3.1).

6.6 Meso-Alpine Tectonics (Paleocene-Eocene)

The early and middle Paleogene was a period of remarkable tectonic and kinematic activity in most of the world's oceans and on the continents (see Rona and Richardson, 1978 and Williams, 1986 for worldwide reviews). Changes in North Atlantic seafloor spreading had a major influence on Africa/Europe kinematics and ensuing tectonics.

In the North Atlantic, the Charlie-Gibbs Fracture Zone records a change of spreading direction at about the time of Anomaly 27 (63.5 Ma) (see 2.5.1). There are few tracklines near Charlie-Gibbs at this location and the interval between reversals is very short near the Cretaceous-Tertiary border. Therefore the change may have initiated slightly earlier. This change in North Atlantic kinematics correlates nicely with the initiation of an episode of little relative motion between Africa and Europe (see 4.3.3).

The orientation of Charlie-Gibbs changed again at Anomaly 25 - Anomaly 24 time. The change marked the beginning of seafloor spreading in the Norwegian-Greenland Sea. The interval between Anomaly 29 (65.5 Ma) and Anomaly 24 (55 Ma) is marked in the North Atlantic by a vast outpouring of basaltic lava known as the Thulean volcanism. The region effected was 1,500 - 2,000 km long and 200 km (at that time) wide and is much larger than the Deccan Traps (D. Roberts, BP, pers. comm., 1987). The Thulean Province is centered on Iceland and extends from Charlie-Gibbs, where the Thulean Rises formed (see 2.4.2a), to 65o N. Related volcanic activity is known from West Greenland near Baffin Bay.

The volcanism marks the northermost part of the North Atlantic as being different from the region between Charlie-Gibbs and the Azores-Gibraltar Fracture Zone, as well as from the Central Atlantic. Volcanism in these regions is related more to rift events, associated with leaky transform faults, or with passage over a hotspot and was minor compared with the Thulean volcanism. Volcanic production in the Norwegian-Greenland Sea was voluminous to the extent that the spreading center had to have either started subaerially or been above sealevel early in its history (J. Mutter, LDGO, pers. comm., 1987). Similarly, much of the volcanism in the Rockall region has been shown to be subaerial (Roberts et al., 1984),

The cause of Thulean volcanism is uncertain. A relationship to a hot spot is suspect because the province is centered on Iceland (White and McKenzie, 1989). However, compression in the

Nares and Davis Straits may have locked seafloor spreading in the Labrador Sea and caused the ridge to jump to the eastern side of Greenland. The timing of the Eurekan Orogeny is given by the Eureka Sound Formation (4,000 m of Early Tertiary continental clastics) (Miall, 1986). Termination of this sedimentation is coeval with cessation of spreading in the Labrador Sea.

The reorganization of spreading related to Thulean volcanism had ramifications in the Western Mediterranean-Tethyan region. Dewey et al. (1989) noted the correlation between period of minor Africa-Europe relative motion and the "Paleocene Restoration" (Trumpy, 1973). Subsequent to Anomaly 24, concurrently with the start of spreading between Greenland and Europe, Africa again moved northwards relative to Europe.

This "resumption" of motion is coincident with Meso-Alpine deformational and metamorphic events, generally thought to be due to the collision of Adria and Europe. It is marked by thrusting in the Penninic and Austro-Alpine domains and by Barrovian metamorphism, which peaked in Latest Eocene or Earliest Oligocene time. Adria during this interval continued to move northwesterly with respect to Europe (Platt et al., 1989).

In the Alpine foreland extension began in the Lower Rhine Graben in the Paleocene(?) and progressed southward. The Bresse and Valence Basins formed in the Late Eocene. Extension in the West European Rift System (Rouchy, in prep.) became progressively younger to south and southwest. The amount of extension in much of this basin system was small, with Beta factors of 1.1 - 1.15

typical of the Bresse and Valence Basins (Helman, unpub. data). Only in the Western Mediterranean segment (including the Valencia Trough) was the amount of extension very large.

At the same time that Adria was moving to the northwest with respect to Europe, Iberia was moving to the northeast. Although deformation in the Pyrennes began in the late Cretaceous, it reached a culmination in the Eocene (Puidefabregas and Souquet, 1986). By the end of the Eocene Iberia was sutured to Europe. Subsidence plots for the eastern Aquitaine Basin show sudden increases in subsidence rate in the Late Cretaceous or Early Paleocene. Similar increases began progressively later to the west (Brunet, 1984, Figs. 3,4,5,6).

Northeasterly motion of Iberia is also suggested by the pattern of deformation along the North Spanish Margin. Boillot et al. (1979) showed, using seismic reflection profiles, that the amount of shortening there decreased, and occurred progressively later, to the west. This pattern is compatible with northeasterly motion of Iberia.

Grimaud et al. (1982) suggested that Iberia moved northwest to form the Pyrenees and cause deformation along the North Spanish Margin. An additional consequence of this would be that strike-slip motion in the Atlantic would have formed the King's Trough and compression the Azores-Biscay Rise. Compressional features are not seen on seismic sections of the Azores-Biscay rise and there are no offset magnetic anomalies in the King's Trough region. In addition, the stratigraphic hiatus associated with

formation of King's Trough is Oligocene-Miocene in age, i.e. post Pyrenean (Shipboard Scientific Party, 1987). This data, together with the evidence from the Pyrennes and the Aquitaine Basin show that the model of Grimaud et al. (1982) is incorrect.

In southern Iberia deformation in the Betic Zone of the Betic Cordillera began by the Eocene (Diaz de Federico, 1980). A major question that arises with respect to these and other deformations in the Western Mediterranean region is the polarity of the subduction zone that consumed the Tethys. This is discussed below.

6.6.1 Polarity of Subduction

The polarity of subduction in the Tethys is uncertain. The proponents of southward subduction note that it explains the (presently) west-verging ophiolite nappes of Corsica and would be continuous with the polarity of Alpine subduction (Rehault et al., 1984; Harris, 1985; van Wamel, 1987). East-verging structures in the Southern Apennines, ranging in age from Cretaceous to Pliocene, are described by Knott (1987) and Dietrich (1988). This vergence is compatible with a north or northwest dipping subduction zone. Abbate et al. (1980), Hill and Hayward (1980), and Trevers (1984), also proponents of northward subduction, explain the Corsican nappes as backthrusts on the landward edge of an accretionary prism. The model suggested here favors an older south-dipping subduction zone from Corsica northward and a north-dipping zone from Corsica south.

An additional line of evidence for north-dipping subduction comes from the realm of geophysics. Spakman (1986) used seismic tomography to image the structure of the mantle and showed images that appear to show a continuous north-dipping slab that extended from the eastern Mediterranean to Iberia. Details of the data and the techniques used were not published in Spakman's (1986) summary report. However, if additional work shows this structure to be real then many models of Alpine and Mediterranean tectonics will be in need of revision.

The polarity of subduction has a major ramification with regard to subsequent extensional tectonics. Kastens, Mascle et al. (1988) noted a similarity between their observations in the Tyrrhenian Sea and simple shear extensional models proposed by Wernicke (1985) and Lister et al. (1986). If older structures are reactivated with an opposite sense of motion then the polarity of subduction could be a major factor in controlling post- or late-orogenic extension.

In the Tyrrhenian, south-dipping subduction would provide structures compatible withthe low-angle detachment faults suggested by the Leg 107 scientists. In addition to providing structures that may be reactivated, subduction polarity may bear upon the architecture of rift zones that may develop there in the manner discussed by Rosendahl (1987) and Reynolds (1984).

6.7 Evolution of the Western Mediterranean (Oligocene-Present)

The model presented for the Late Tertiary evolution of the Western Mediterranean region is presented as a series of reconstructions, at selected time intervals, from 38 Ma to the present. In each reconstruction, the direction of Africa's motion, as determined by finite difference solution, is shown. Similarly, vector triangles show the direction and proportional amount of motion of different continental blocks and microplates; absolute magnitudes of motion are not shown. The reconstructions are fixed to Europe and other microplates and continental blocks move in this frame of reference. In addition, events in the Atlantic realm may also be commented upon.

6.7.1 Latest Eocene-Priabonian 38 Ma (Fig. 6.2)

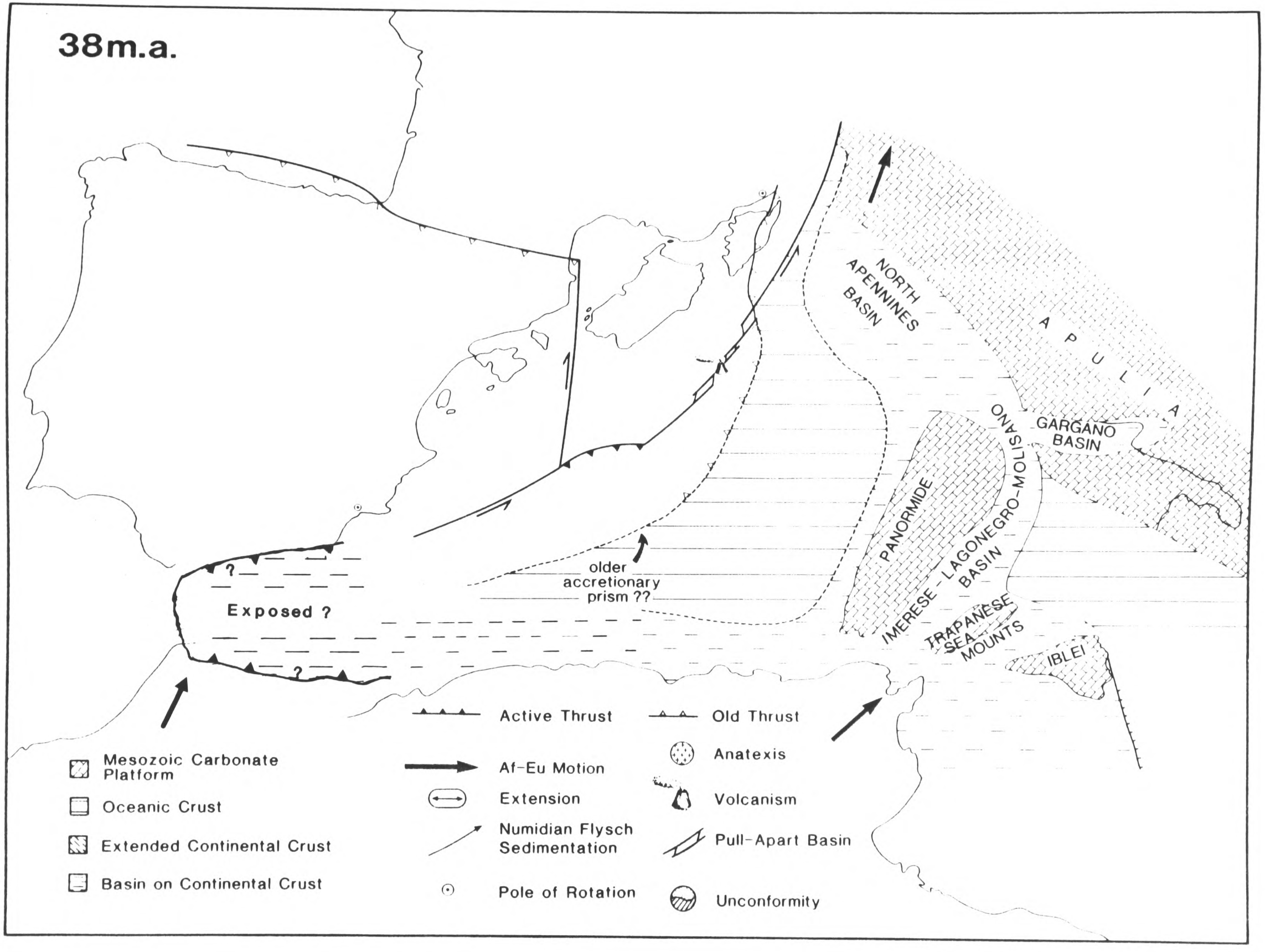
The origin of the present day Western Mediterranean Sea postdates the cessation of several important orogenic events, Penninic thrusting in the Alps (Trumpy, 1980), the Pyrenean Orogeny (Fischer, 1984), and collision in Corsica (Harris, 1985). These events ended in latest Eocene or earliest Oligocene time. The relationships of various units at this time form the starting point for the reconstructions.

Corsica, Sardinia, and the Balearic Islands are restored to their appropriate positions against the coasts of France and Spain. The Kabylies and Calabria probably sit outboard or slightly west of these blocks. These units are not shown because, with presently available data, their locations cannot be

Figure 6.2: Kinematic Reconstruction of the Western Mediterranean Latest Eocene - Priabonian 38 Ma

This frame of the reconstruction shows the events occurring and the relations of tectonic elements in Latest Eocene - Priabonian time (38 Ma).

Legend (also shown on figure and on Fig. 6.3): Diagonal bricks = Mesozoic carbonate platform. Solid horizontal lines = oceanic crust. Dashed diagonal lines = newly extended continental crust. Dashed horizontal lines = basin on continental crust. Line with filled barbs = active thrust (barbs on overthrust side). Line with un filled barbs = old thrust. Heavy arrows = direction of Africa's motion relative to Europe. Plus marks = anatexis. Double arrows within circles = extension. Volcanoes = volcanism. Long thin arrows = direction of Numidian Flysch sedimentation. Parallelogram = pull-apart basin. Circle with dot in center = pole of rotation (unlabeled if site of future pole). Dots above diagonal lines (within circles) = unconformity. Short straight arrow = stretching lineation. Triangles = vector triangles showing relative motion of various blocks with respect to Europe and Africa. Explanation of reconstruction is given in text.


38m.a.
NORTH APENNINES BASIN
APULIA
GARGANO BASIN
ONSHORE
PANORMIDE
IMERESE - LAGONEGRO-MOLISANO BASIN
TRAPANESE SEA MOUNTS
IBLEI
older accretionary prism ??
Exposed ?
Mesozoic Carbonate Platform
Oceanic Crust
Extended Continental Crust
Basin on Continental Crust
Active Thrust
Af-Eu Motion
Extension
Numidian Flysch Sedimentation
Pole of Rotation
Old Thrust
Anatexis
Volcanism
Pull-Apart Basin
Unconformity

well-constrained. South and east of these blocks, on the northwest margin of a tract of Neotethyan (Jurassic?) oceanic crust, was an accretionary wedge that was active prior to this time but with opposite vergence to the Alps (Dietrich, 1988; Knott, 1987). This oceanic fragment, roughly 300 km wide, separated the southeastern margin of the European plate from Adria and the North African rifted margin.

The Adria and African margins at this time consisted of a series of carbonate platforms and basins. The paleogeographic reconstruction is considerably simpler than many previously published for the Southern Apennines. D'Argenio et al. (1973) and Scandone et al. (1974) depicted three carbonate platforms (Panormide, Apulia, and an intermediate platform) separated by two basins (Lagonegro and Molise). The clear continuity of the Lagonegro into the Molise Basin to the north indicates that the tectonic windows (Campagna, Monte Alpi), cited as evidence of the intermediate platform, are blocks of Apulia pushed up along late Cenozoic strike-slip faults.

Moreover, a clear continuity exists between these basins, the Tellian (North Africa) and Imerese (Sicily) Basins to the south, and the North Apennines Basin. Therefore, the first reconstruction shows two main carbonate platforms (Panormide and Apulia) separated by this basin system. It is, nevertheless, recognized that the connection between the Panormide Platform in the Southern Apennine domain and the Panormide Platform in Sicily is not clear because these carbonates do not outcrop in the

southern part of Calabria (Scandone et al., 1974).

Eastward of the Imerese Basin were the Trapanese Seamounts and, further to the east, the Iblei Block. The Iblean Block underwent platformal-type sedimentation during the Triassic and Miocene but received basinal sediments in the intervening time. To the north and east, the Lagonegro-Molise Basin passed into the Apulia Platform. The latter extended northwards to the Northern Apennines interrupted only by the Gargano Basin which received sediment until at least Eocene time, after which it was inverted (Martinis and Pavani, 1967). The inversion of the Gargano Basin, which accompanied fragmentation of the Apulian Platform, has been attributed to continental collision in the Alps (Trumpy, 1980).

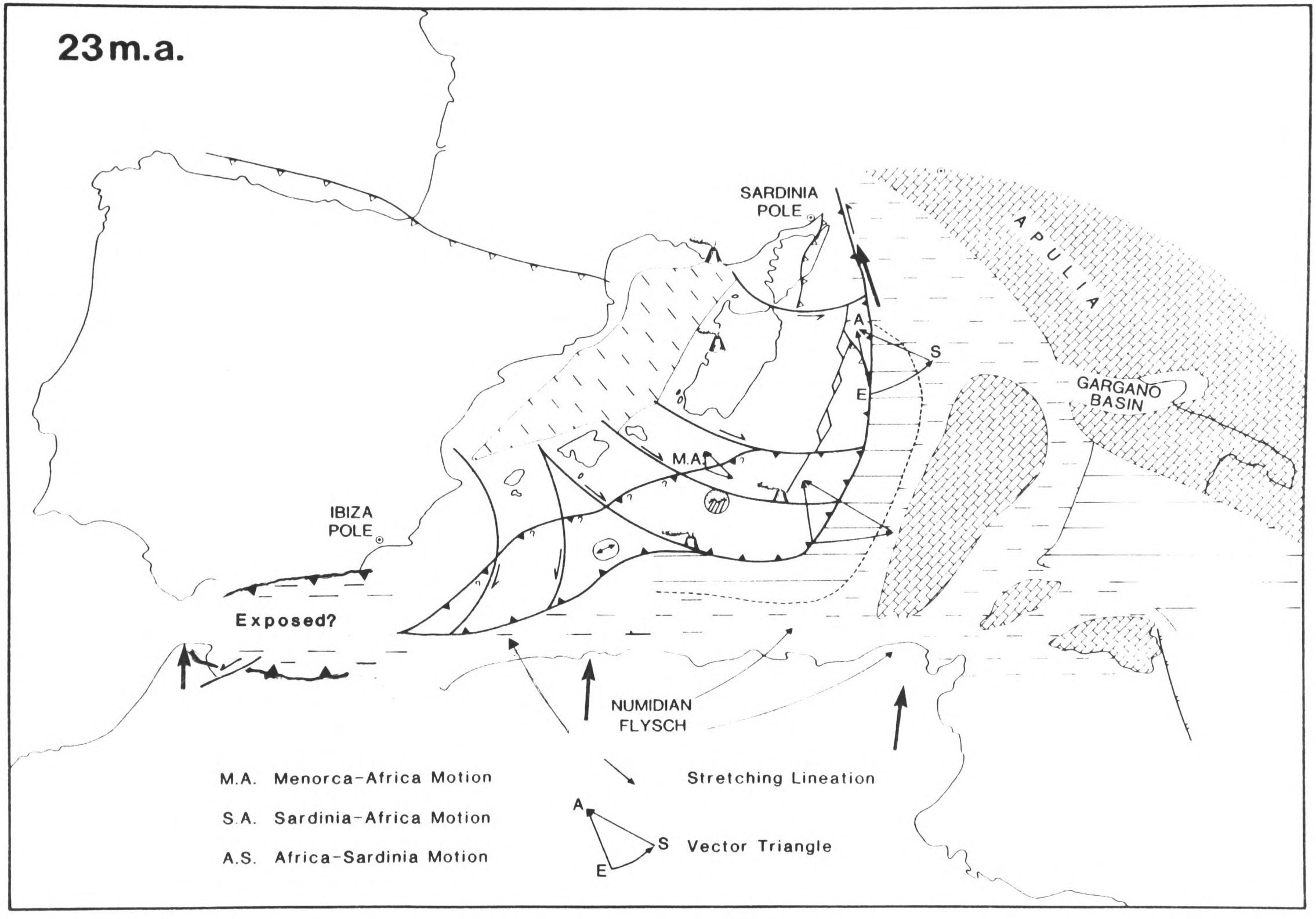
The disposition of units further to the west in the North African-Southern Spain region is more uncertain. The paleogeographic situation of the Betic Internal Zone units is unclear. Most tectonic models for the Betic region show an Alboran block or subplate, consisting largely of the Betic (s.s.) units, moving W or WSW. However, there are no major strike-slip faults of this age in the Betic region.

In the Rif, only the Jebha Fault, near the Straits of Gibraltar, may have been active at that time. However, most movement on this left-lateral fault is of Middle Burdigalian age and displacement is only 50 km, with only the Internal Zone of the Rif offset by its motion (Olivier, 1981-82; Leblanc and Olivier, 1984). The Nekor Fault, further to the east, is even younger, with most motion in the Tortonian. Displacement is

Figure 6.3: Kinematic Reconstruction of the Western Mediterranean Earliest Miocene - Aquitanian 23 Ma

This frame of the reconstruction shows the events occurring and the relations of tectonic elements in Earliest Miocene - Aquitanian time (23 Ma).

Legend (also shown on figure and on Fig. 6.2): Diagonal bricks = Mesozoic carbonate platform. Solid horizontal lines = oceanic crust. Dashed diagonal lines = newly extended continental crust. Dashed horizontal lines = basin on continental crust. Line with filled barbs = active thrust (barbs on overthrust side). Line with un filled barbs = old thrust. Heavy arrows = direction of Africa's motion relative to Europe. Plus marks = anatexis. Double arrows within circles = extension. Volcanoes = volcanism. Long thin arrows = direction of Numidian Flysch sedimentation. Parallelogram = pull-apart basin. Circle with dot in center = pole of rotation (unlabeled if site of future pole). Dots above diagonal lines (within circles) = unconformity. Short straight arrow = stretching lineation. Triangles = vector triangles showing relative motion of various blocks with respect to Europe and Africa. Explanation of reconstruction is given in text.


23 m.a.
SARDINIA
POLE
APULIA
A
S
E
GARGANO
BASIN
M.A.
IBIZA
POLE
Exposed?
NUMIDIAN
FLYSCH
M.A. Menorca-Africa Motion
S.A. Sardinia-Africa Motion
A.S. Africa-Sardinia Motion
Stretching Lineation
A
S
E
Vector Triangle

similar to the Jebha fault and it also is a left-lateral fault (Leblanc, 1980).

The location of the Betic Internal Zones was probably slightly east of their present locations. Transcurrent motion on the Jebha and Nekor Faults carried them toward their present location, but large-scale thrusting to the N and NW concomitant with extension driven by gravity forces emplaced them in their present location.

Compression in the Betic region had begun prior to this time. Erosional and non-depositional hiatuses of Eocene age are found throughout and the deposition of conglomerates in flysch sequences of Middle Eocene age is known (Ager, 1980; Garcia-Hernandez et al., 1980).

From this time onwards, in the eastern area the model shows the progressive closure of older basins and deformation of the carbonate platforms, concomitant with rifting fragments of continent from the European mainland and the opening of new basins as these continental fragments undergo translation to the southeast. The western area is dominated by compression at first, causing the build-up of a thick orogenic welt, and later by extension, driven by body forces produced by overthickening of the lithosphere.

6.7.2 Earliest Miocene-Aquitanian 23 Ma (Fig. 6.3)

By this time, extensional tectonics were evident throughout the eastern region. In the Algero-Provencal or North Balearic

Basin Sardinia had begun to to drift from the French mainland, although Corsica had not. The pole about which Sardinia rotated was close to the northern tip of Corsica.

Various lines of evidence (field work, paleomagnetics, magnetic anomalies, bathymetry, reflection seismic) have been put forth by different authors to support the concept of differential rotation between Corsica and Sardinia. Some of this data is open to different interpretion (compare Bayer et al., 1973 with Burrus, 1984) and none leads to unambiguous conclusions. The preponderance of evidence clearly suggests that, at some time in their history, Corsica and Sardinia moved independently.

In the Gulf of Valencia, Mallorca and Menorca had begun to rotate away from Iberia about the Sardinia pole of rotation. It is necessary, however, to use an independent rotation pole to restore Ibiza and Frontera to what seems to be their original position. Parallel with the length of the Kabylie-Calabria thrust belt, extension was also occurring. Further to the southwest, in the Betic region, extension may also have been occurring at this time (Platt and Vissers, 1989).

However, extension in the two regions may have been driven by different forces. The extension in the area of the Rif and Betic Cordillera is the result of overthickening of the lithosphere leading to delamination of lithospheric mantle and formation of the Alboran Sea by orogenic collapse. Extension in the Western Mediterranean is related to back-arc spreading and/or formation of the West European Rift System (see 5.2.5).

Two major characteristics of this system are the ages of the basins and the amount of erosion prior to basin formation. This rift system originates in the Paleocene or Eocene in Northern Europe in the Rhine Graben. The basins to the south become succeedingly younger with the Bresse and Valence Basins forming in Late Eocene-Early Oligocene time and basins in southern France (e.g. Manosque Basin) forming in Mid-Oligocene. The second characteristic of this system is that the underlying basement has been extensively eroded. In southern France, heavily weathered basement as old as Albian is exposed beneath these basins.

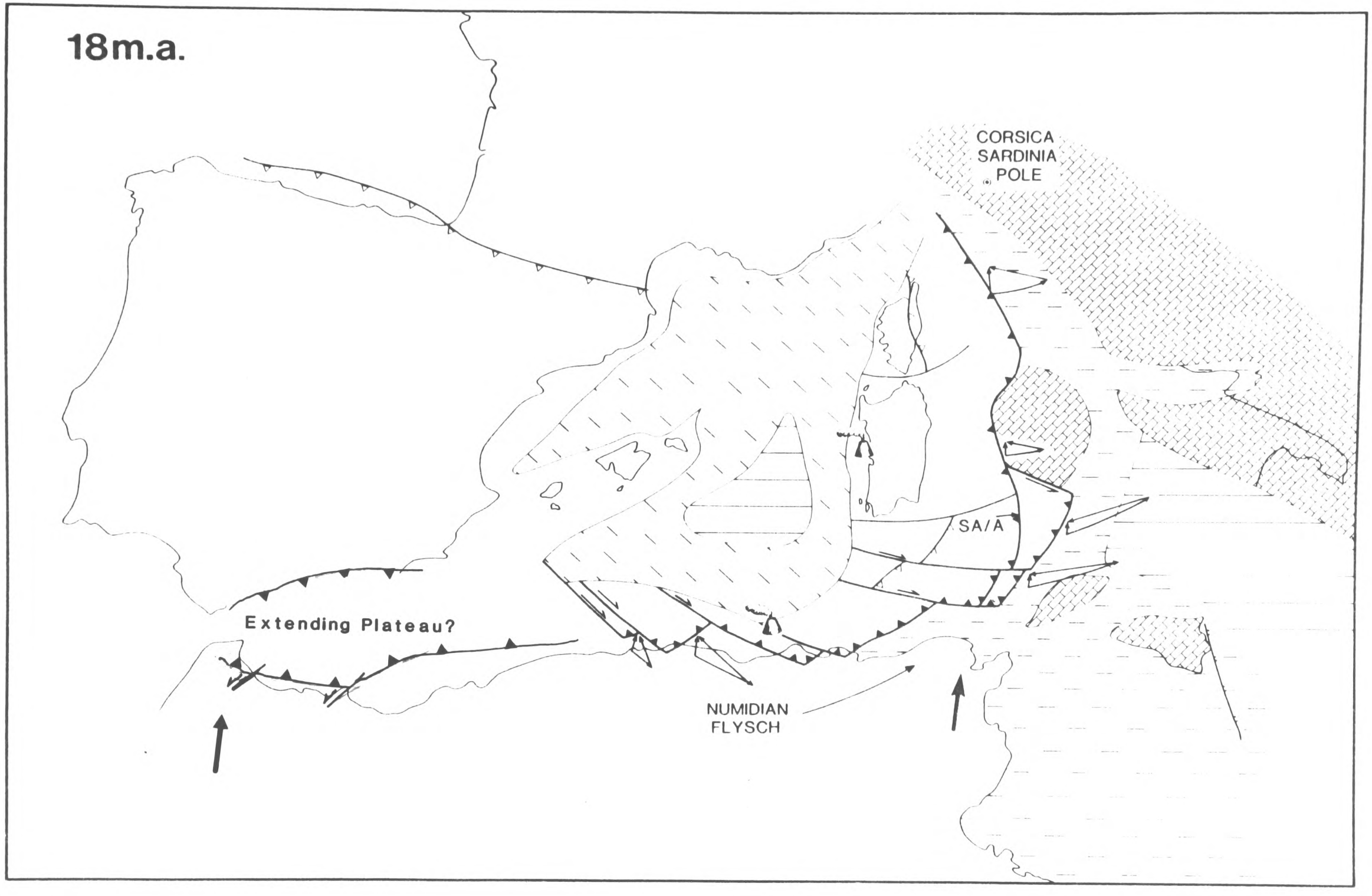
The two characteristics suggest that the West European Rift underwent progressive heating and uplift with extensive erosion prior to basin formation. The age progression suggests that this may be related to motion across a hotspot. The basement beneath the Valencia Trough is known to be heavily karstified Cretaceous limestone suggesting largescale uplift and erosion. Moreover, the pattern of heatflow found there is different from what might be expected. Heat flow in the Valencia Trough does not increase to the north where the greatest extension occurs but to the south, the region of least extension (M. Steckler, LDGO, 1989). The pattern is what might be expected from migration across a hotspot.

Compressional tectonics went hand in hand with extension. In the Northern Apennines, the start of deformation has been dated at 27 Ma (Carmignani et al., 1978; Kligfield et al., 1986). Much of the older oceanic crust has been subducted or obducted.

Figure 6.4: Kinematic Reconstruction of the Western Mediterranean
Early Miocene - Burdigalian 18 Ma

This frame of the reconstruction shows the events occurring and the relations of tectonic elements in Early Miocene - Burdigalian time (18 Ma).

Legend (also shown on Figs. 6.2 and 6.3): Diagonal bricks = Mesozoic carbonate platform. Solid horizontal lines = oceanic crust. Dashed diagonal lines = newly extended continental crust. Dashed horizontal lines = basin on continental crust. Line with filled barbs = active thrust (barbs on overthrust side). Line with un filled barbs = old thrust. Heavy arrows = direction of Africa's motion relative to Europe. Plus marks = anatexis. Double arrows within circles = extension. Volcanoes = volcanism. Long thin arrows = direction of Numidian Flysch sedimentation. Parallelogram = pull-apart basin. Circle with dot in center = pole of rotation (unlabeled if site of future pole). Dots above diagonal lines (within circles) = unconformity. Short straight arrow = stretching lineation. Triangles = vector triangles showing relative motion of various blocks with respect to Europe and Africa. Explanation of reconstruction is given in text.


18m.a.
CORSICA
SARDINIA
POLE
SA/A
Extending Plateau?
NUMIDIAN
FLYSCH

Subduction of oceanic lithosphere lead to the development of an accretionary wedge with transport direction to the present day northeast (Knott, 1987). At the same time, extension occurred in the internal part of the Kabylie-Calabria belt (Knott, 1988) and sinistral stike-slip motion occurred between Corsica and the Northern Apennines (Waters, 1986). Unconformities of this age have been recognized in South Calabria (Capo d'Orlando Formation), the Kabylies, and Sicily covering faults thought to be related to Alpine thrusting with European vergence (Bonardi et al., 1981).

Subduction was accompanied by major calc-alkaline volcanism in Western Sardinia and Southeastern France (Savelli et al., 1979), which shed volcaniclastic detritus into the Sicilian and Apennine sectors of the trench (Tufiti di Tusa of Ogniben, 1964, 1969 correlative with the Petrignacola Tuffites, see 5.2.3). Similar detritus deposited in the Kabylie trench (Durand-Delga, 1981) was probably derived from transform-related volcanism (Knott and Turco, in prep.). Deposition of quartzo-arenitic Numidian Flysch in the Immerese-Lagonegro-Molise Basin system and on the subsiding Panormide Platform (Bifurto Formation of Selli, 1962) and its margins (Giunta, 1985; Ogniben, 1969) seems to have been related to the formation of a peripheral bulge on the North African margin.

Numidian Flysch was also deposited further to the west near the juncture of the Tell and the Rif. In the Betic-Rif region the Ronda and Beni-Bouchera peridotites were emplaced as

indicated by isotopic ages of the surrounding contact aureoles (Torres-Roldan, 1979; Diaz de Federico, 1980).

6.7.3 Early Miocene-Burdigalian 18 Ma (Fig. 6.4)

By this time Corsica and Sardinia had completed their rotation about a combined pole. The completion of this rotation is dated by Montigny et al. (1981) at 19 Ma +/- 1 Ma using paleomagnetic data. Similar dates have been obtained by Ferrara et al. (1973) on volcanic ash from DSDP Site 123 in the Gulf of Valencia dated at 22 - 19 Ma using the K-Ar method. This ash, derived from a 129.5+ m thick sequence is considered to be the slope accumulation of a volcano that was located in the Gulf of Valencia (Nesteroff et al., 1973). Only the southernmost part of the Algero-Provencal Basin (also known as the South Balearic Basin) remained to be formed as the Kabylies and Calabria migrated southeastward.

Deformation had now begun throughout most of the region. The final consumption of Neotethys led rapidly to a collision between the Liguride accretionary wedge and the Panormide Platform. What had been the southeast margin of Neotethys was deformed in a greenschist facies ductile shear zone. The Southern Apennines thrust front propagated rapidly into the Lagonegro Basin whereas collision was less advanced in the northern part of the Panormide Platform (Perrone, 1982). The northern and southern portions of this platform became separated by a oblique ramp while at the same time the Anzio-Ancona line

developed as a frontal ramp.

Along the North African margin, emplacement of the Kabylies and deformation in Tunisia had just begun (Boullin, 1984). Calc-alkaline volcanism continued in Sardinia but also occurred along the African margin from Dellys to Tunis (Bellon, 1980). At the same time, deposition of Numidian Flysch continued in the Imerese-Lagonegro-Molise Basin system (Catalano and D'Argenio, 1978).

Extension was also underway in the Alboran Sea region. Platt and Vissers (1989) have suggested that delamination of mantle lithosphere occurred and the Alboran Sea region was an extending plateau. The Internal Zones of the Betics were juxtaposed to the External Zones as shown by the presence of detritus derived from the former in the latter (Vegas and Banda, 1982). Extension in the Alboran Sea was enhanced by motion along strike-slip faults that extend onshore in North Africa. The Jebha Fault can be traced offshore into the ridge separating the East and West Alboran Basins.

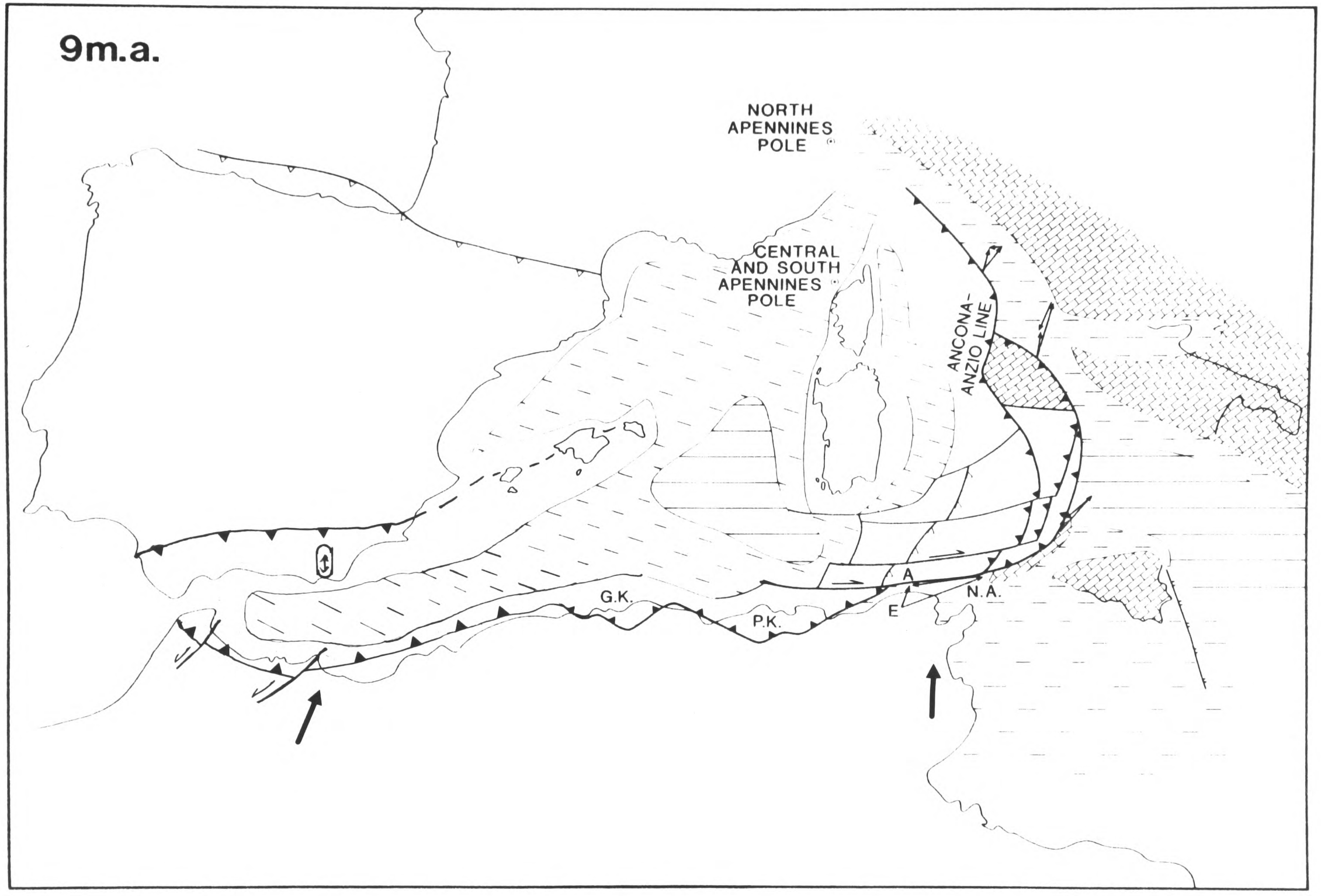
6.7.4 Late Miocene-Tortonian 9 Ma (Fig. 6.5)

Throughout the Middle Miocene, compression continued in all parts of the Apennines. The motion of the North Apennines is described by a pole of rotation that is independent of that for the Central and Southern Apennines. This is indicated by the change of the Anzio-Ancona Line from a frontal to an oblique ramp (La Vecchia, 1985).

Figure 6.5: Kinematic Reconstruction of the Western Mediterranean Late Miocene-Tortonian 9 Ma

This frame of the reconstruction shows the events occurring and the relations of tectonic elements in Late Miocene - Tortonian time (9 Ma).

Legend (also shown on Figs. 6.2 and 6.3): Diagonal bricks = Mesozoic carbonate platform. Solid horizontal lines = oceanic crust. Dashed diagonal lines = newly extended continental crust. Dashed horizontal lines = basin on continental crust. Line with filled barbs = active thrust (barbs on overthrust side). Line with un filled barbs = old thrust. Heavy arrows = direction of Africa's motion relative to Europe. Plus marks = anatexis. Double arrows within circles = extension. Volcanoes = volcanism. Long thin arrows = direction of Numidian Flysch sedimentation. Parallelogram = pull-apart basin. Circle with dot in center = pole of rotation (unlabeled if site of future pole). Dots above diagonal lines (within circles) = unconformity. Short straight arrow = stretching lineation. Triangles = vector triangles showing relative motion of various blocks with respect to Europe and Africa. Explanation of reconstruction is given in text.


9m.a.
NORTH
APENNINES
POLE
CENTRAL
AND SOUTH
APENNINES
POLE
ANCONA-
ANZIO LINE
G.K.
P.K.
A
E
N.A.

Apenninic thrusting was accompanied by formation of a continuous foredeep in front of the chain. This foredeep and its piggy-back basins migrated toward the Apulian Platform as the thrust belt advanced (Pescatore, 1978). Numidian Flysch was resedimented from the piggy-back basins into the foredeep (Arenarie di Stigliano of Selli, 1962).

Subduction of Ionian Sea oceanic crust resulted in formation of a passive roof duplex at the mountain front. Varicoloured clays were backthrust over the Lagonegro Basin, Panormide Platform, and the Liguride and Calbride Complexes, and Numidian Flysch was carried on the varicoloured clay backthrust nappe (E. Turco and S. Knott, pers. comm., 1987).

In Western Sicily, right lateral strike-slip faulting was a dominant mode of deformation as an accretionary prism was emplaced above the Trapanese Sea Mounts. In North Africa, major deformation occurred as the Kabylies collided with and were emplaced upon the continental margin.

East of Corsica and Sardinia, stretching had begun in the region that would become part of the Tyrrhenian Sea (Hsu, 1977; Scandone, 1979). This extension was initiated by the start of a major change in the Africa-Europe pole of rotation that began at Anomaly 5C or 5B time (see 6.7.4a below).

Extension was also evident in the westernmost part of the region. Southern and southeastern Spain have many basins with known Tortonian sediments (Julivert et al., 1972). These basins are herein considered part of the collapsing orogen that formed

the Alboran Sea. Deformation in the fold and thrust belts of the Betic and Rif Cordilleras was also well underway at this time as attested to by the sediments found in the Guadilquivir and Rharb Basins.

6.7.4a Extension in the Tyrrhenian

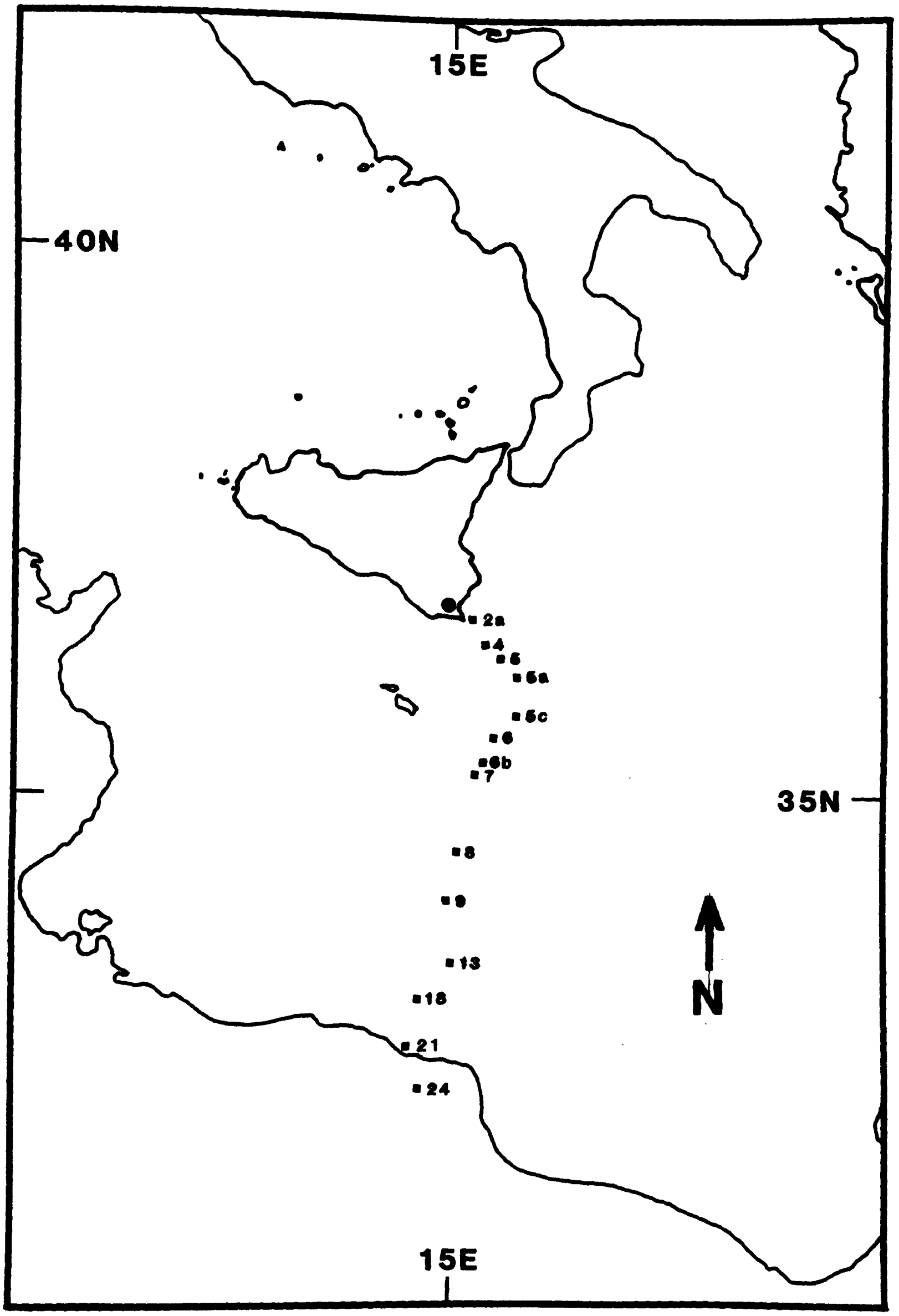
One of the major questions of Western Mediterranean geology has been to determine what triggered the opening of the Tyrrhenian Sea. Seismic stratigraphy and drilling results from Leg 107 all indicated that rifting began in the Tortonian (Leg 107 Shipboard Party, 1986; K. Kastens, LDGO, pers. comms., 1988,1989) as did the ages of onshore related basins in the Northern Apennines (Lavecchia, 1988, Fig. 3). Prior to the start of back-arc spreading subduction had been active for at least 20 million years, as indicated by the Oligocene age of calc-alkaline volcanics on Sardinia.

Prior to Anomaly 6 motion of Africa with respect to Europe was approximately northwards (Fig. 6.6; see also Fig. 4.3, Fig. 4.4, and Table 4.1). Shortly after, beginning with Anomaly 5D, the pole of rotation began to migrate southward. As it did so the motion changed and became directed toward the northwest. Under this new regime the direction of motion and the dip of the downgoing slab became nearly parallel, whereas previously the motion had been oblique.

Similar changes in motion, i.e., from oblique to orthogonal convergence, have been proposed as an enabling condition for the onset of extension in Pacific back-arc basins (Jurdy, 1979; Fein

Figure 6.6: Africa's Motion Path South of the Tyrrhenian Sea (Late Cenozoic)

The path of Africa's motion relative to Europe is shown for a point in Iblei (Southeastern Sicily), which is considered part of the African foreland. The path was generally N or NNE until 5C or 5B when it began to change to a NW trajectory. This change occurs just prior to the earliest extension in the Tyrrhenian Sea. Drilling on ODP Leg 107 reached Tortonian sediments on the Sardinian continental margin where extension began. The locus of extension seems to have shifted to the southeast with time parallel with the motion vector of Africa.


15E
40N
2a
4
5
5a
5c
6
6b
7
35N
8
9
13
16
21
24
N
15E

and Jurdy, 1986). These authors have also noted extension in back-arc basins seems to be limited temporally to a 10 - 15 million year period. A similar change is probably the enabling condition to start extension in the Tyrrhenian Sea and as mentioned previously seismic evidence suggests that subduction, and back-arc extension, have ceased (Anderson and Jackson, 1987).

6.7.5 Late Miocene-Tortonian 7 Ma (Fig. 6.7)

The major change in boundary conditions discussed above as the cause of extension in the Tyrrhenian was essentially completed by Anomaly 5 (8.9 Ma). In addition to intiating extension in the Tyrrhenian this change enhanced extension in the south of Sicily (Pantellaria, Linosa). At this time, the motion of Calabria and Northeast Sicily became southeasterly directed as these blocks began to rotate about an independent pole of rotation (Calabria Pole). The change in pole of rotation also aided in driving the deformation in the Betic Cordillera to the west.

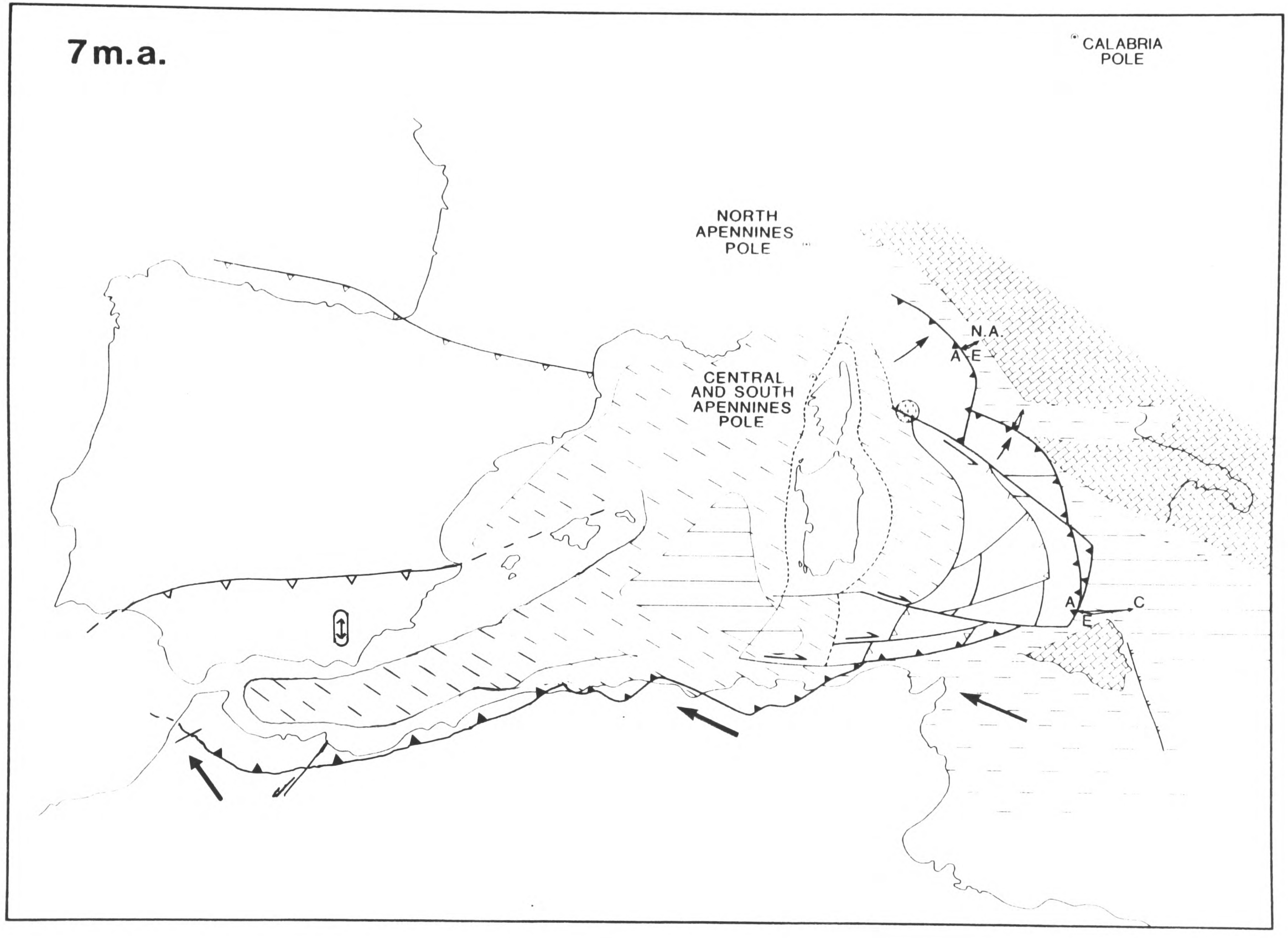
In the Northern Apennines, deformation had largely ceased with remaining deformation due essentially to bending (Eldredge et al., 1985). Crustal thickening led to anatexis and emplacement of the Elba Granite. In the Southern Apennines, Sunda-style tectonics (Beck, 1986) resulted in strike-slip faults throughout Calabria and into Sicily. The Calabrian Arc began to deform by heterogeneous simple shear (Turco and Knott, in prep.) Along the North African margin, and in Tunisia, older thrusts were reactivated along the new transform direction defined by the new

Figure 6.7: Kinematic Reconstruction of the Western Mediterranean Late Miocene - Tortonian 9 Ma

This frame of the reconstruction shows the events occurring and the relations of tectonic elements in Late Miocene - Tortonian time (9 Ma).

Legend (also shown on Figs. 6.2 and 6.3): Diagonal bricks = Mesozoic carbonate platform. Solid horizontal lines = oceanic crust. Dashed diagonal lines = newly extended continental crust. Dashed horizontal lines = basin on continental crust. Line with filled barbs = active thrust (barbs on overthrust side). Line with un filled barbs = old thrust. Heavy arrows = direction of Africa's motion relative to Europe. Plus marks = anatexis. Double arrows within circles = extension. Volcanoes = volcanism. Long thin arrows = direction of Numidian Flysch sedimentation. Parallelogram = pull-apart basin. Circle with dot in center = pole of rotation (unlabeled if site of future pole). Dots above diagonal lines (within circles) = unconformity. Short straight arrow = stretching lineation. Triangles = vector triangles showing relative motion of various blocks with respect to Europe and Africa. Explanation of reconstruction is given in text.

7 m.a.


CALABRIA
POLE
NORTH
APENNINES
POLE
CENTRAL
AND SOUTH
APENNINES
POLE
N.A
A
E
A
E
C

Africa-Europe pole of rotation.

In Southern Spain extension continued with the formation of new basins accompanied by compression that led to the deformation and inversion of others. Recent work in the Lorca Basin of Spain suggests that this basin may have formed only in Latest Tortonian or possibly early Messinian time (J.M. Rouchy, unpublished diatom stratigraphy, 1989). As the Lorca Basin has little or no Pliocene sediment it appears that it formed and was uplifted in a very short time span.

6.7.6 Earliest Pliocene-Zanclean 5 Ma (Fig. 6.8)

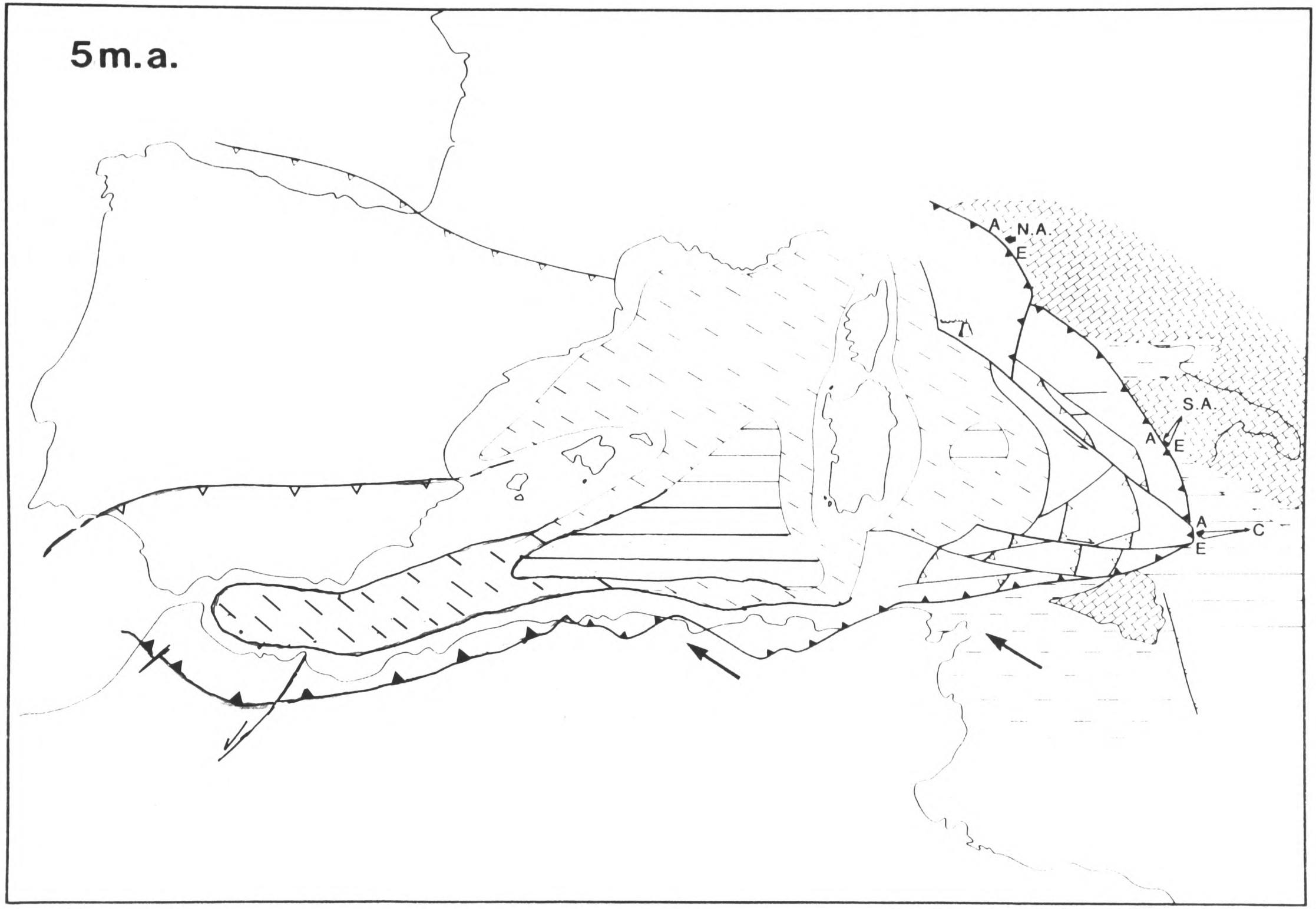
This frame of the reconstruction depicts the situation immediately after the conclusion of the most dramatic event in Mediterranean evolution, the Messinian Salinity Crisis. During this event, the Mediterranean desiccated completely resulting in deposition of evaporites throughout, as well as in the Apennine foredeep (Hsu et al., 1973). Blanketing the evaporites, after the refilling of the basin from the Atlantic, is a Globigerina ooze (Trubi Formation).

Extension in the Tyrrhenian continued throughout this event with the formation of oceanic crust. The locus of extension migrated to the southeast, possibly a result of Calabria advancing through a break in the Apulian Platform into the Ionian Sea (Malinverno and Ryan, 1986). In the Southern Apennines and Calabria, compression continued accompanied by motion on strike-slip faults. In the Northern Apennines, volcanism began in the

Figure 6.8: Kinematic Reconstruction of the Western Mediterranean Earliest Pliocene - Zanclean 5 Ma

This frame of the reconstruction shows the events occurring and the relations of tectonic elements in Earliest Pliocene - Zanclean time (5 Ma).

Legend (also shown on Figs. 6.2 and 6.3): Diagonal bricks = Mesozoic carbonate platform. Solid horizontal lines = oceanic crust. Dashed diagonal lines = newly extended continental crust. Dashed horizontal lines = basin on continental crust. Line with filled barbs = active thrust (barbs on overthrust side). Line with unfilled barbs = old thrust. Heavy arrows = direction of Africa's motion relative to Europe. Plus marks = anatexis. Double arrows within circles = extension. Volcanoes = volcanism. Long thin arrows = direction of Numidian Flysch sedimentation. Parallelogram = pull-apart basin. Circle with dot in center = pole of rotation (unlabeled if site of future pole). Dots above diagonal lines (within circles) = unconformity. Short straight arrow = stretching lineation. Triangles = vector triangles showing relative motion of various blocks with respect to Europe and Africa. Explanation of reconstruction is given in text.


5m.a.
A
N.A.
E
S.A.
A
E
A
C
E

Tuscany region as a result of anatexis (Barberi et al., 1974).

The Alboran Sea had formed and was well below sea level by this time as show by 190 m of Messinian sediment below an erosional surface associated with the salinity crisis. In the Betic Cordillera thrust deformation had largely ceased but motion along strike-slip faults, particularly in southeast Spain continued as an accommodation.

6.7.7 Late Pliocene-Piacenzian 3 Ma (Fig. 6.9)

Through the Early Pliocene, the Tyrrhenian Basin continued to form as the locus of extension moved steadily to the southeast as shown by 3.5 m.y. old basalts in the Vavilov Basin (Leg 107 Shipboard Party, 1986). Intramontane grabens developed in the Calabrian Arc and Southern Apennines by back-arc extension, gravity collapse of overthickened crust, and strike-slip (pull-apart and compatibility basin) mechanisms.

In northeastern Sicily, right-lateral motion began on an older lineament, the Taormina Line, while compression continued in the Southern Apennines and the Sicilian foredeep. Volcanism in the Northern Apennines is well developed by this time.

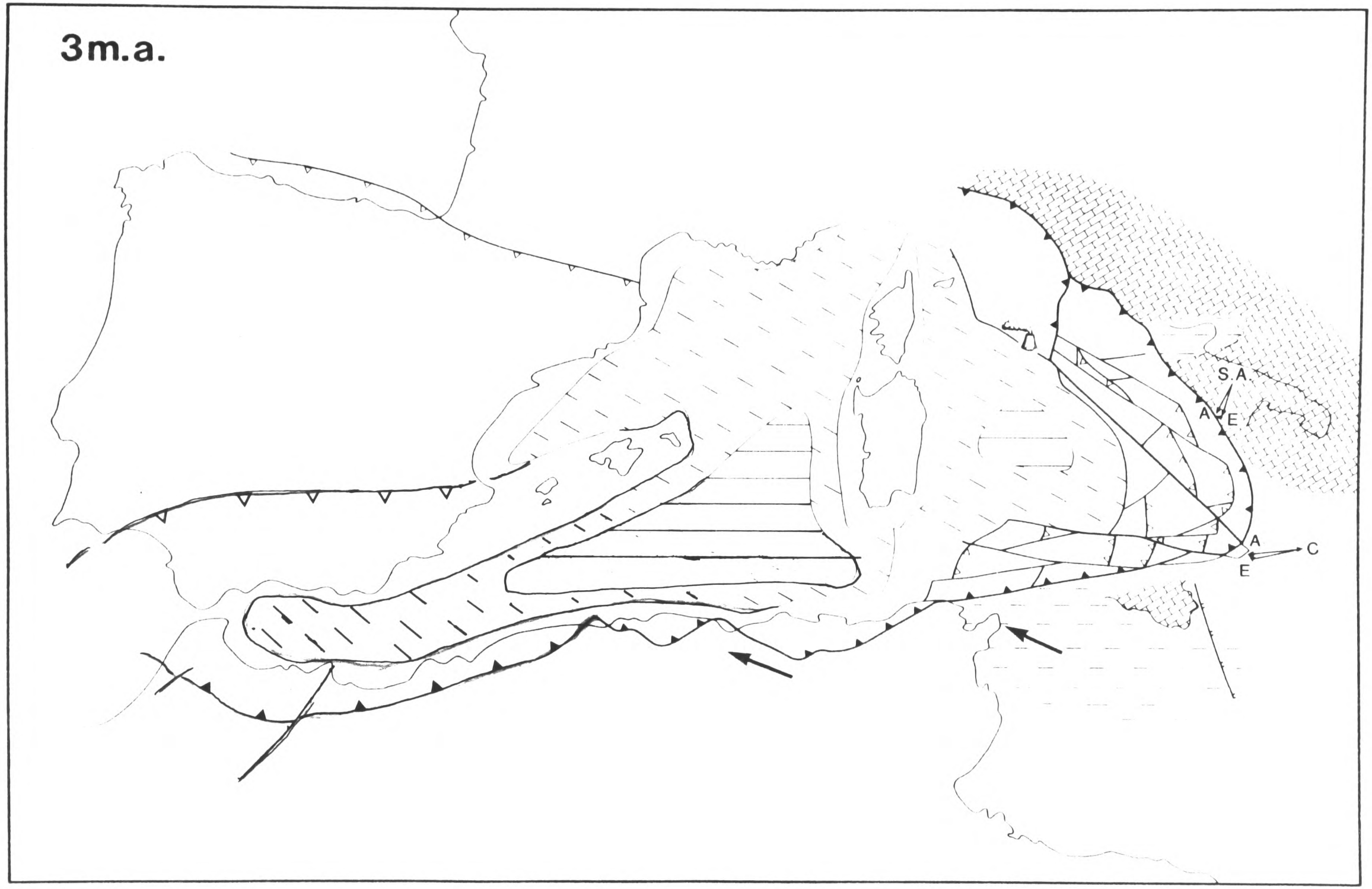
The Alboran Sea was by this time a fully evolved basin receiving turbiditic sands and marl oozes in a thick sedimentary sequence. Calc-alkaline volcanism occurred in the Cabo de Gata Complex in the southeastern most regions of southern Spain as well as in parts of North Africa where deformation in the Rif and Tell was essentially complete (Bellon, 1980).

Figure 6.9: Kinematic Reconstruction of the Western Mediterranean Late Pliocene - Piacenzian 3 Ma

This frame of the reconstruction shows the events occurring and the relations of tectonic elements in Late Pliocene - Piacenzian time (3 Ma).

Legend (also shown on Figs. 6.2 and 6.3): Diagonal bricks = Mesozoic carbonate platform. Solid horizontal lines = oceanic crust. Dashed diagonal lines = newly extended continental crust. Dashed horizontal lines = basin on continental crust. Line with filled barbs = active thrust (barbs on overthrust side). Line with un filled barbs = old thrust. Heavy arrows = direction of Africa's motion relative to Europe. Plus marks = anatexis. Double arrows within circles = extension. Volcanoes = volcanism. Long thin arrows = direction of Numidian Flysch sedimentation. Parallelogram = pull-apart basin. Circle with dot in center = pole of rotation (unlabeled if site of future pole). Dots above diagonal lines (within circles) = unconformity. Short straight arrow = stretching lineation. Triangles = vector triangles showing relative motion of various blocks with respect to Europe and Africa. Explanation of reconstruction is given in text.

3m.a.



6.7.8 Piacenzian to Holocene 3 Ma - Present (Fig. 6.10)

The locus of Tyrrhenian extension continued to shift to the southeast as shown by oceanic basalts less than 2 m.y. old in the Marsili Basin (Leg 107 Shipboard Party, 1986). The segmentation and southeastward motion of the Calabrian Arc was aided by a series of strike-slip faults that display both left-lateral (Southern Apennines, northern Calabria) and right-lateral (southern Calabria, Sicily) offsets. Block rotations, counterclockwise and clockwise respectively, occurred along these faults and pull-apart basins were formed (Turco and Knott, in prep.). In front of the Calabrian Arc a large accretionary wedge formed (Kastens, 1981; Rossi and Sartori, 1981). Behind the arc, in the Aeolian Islands, calc-alkaline and acidic volcanism occurred.

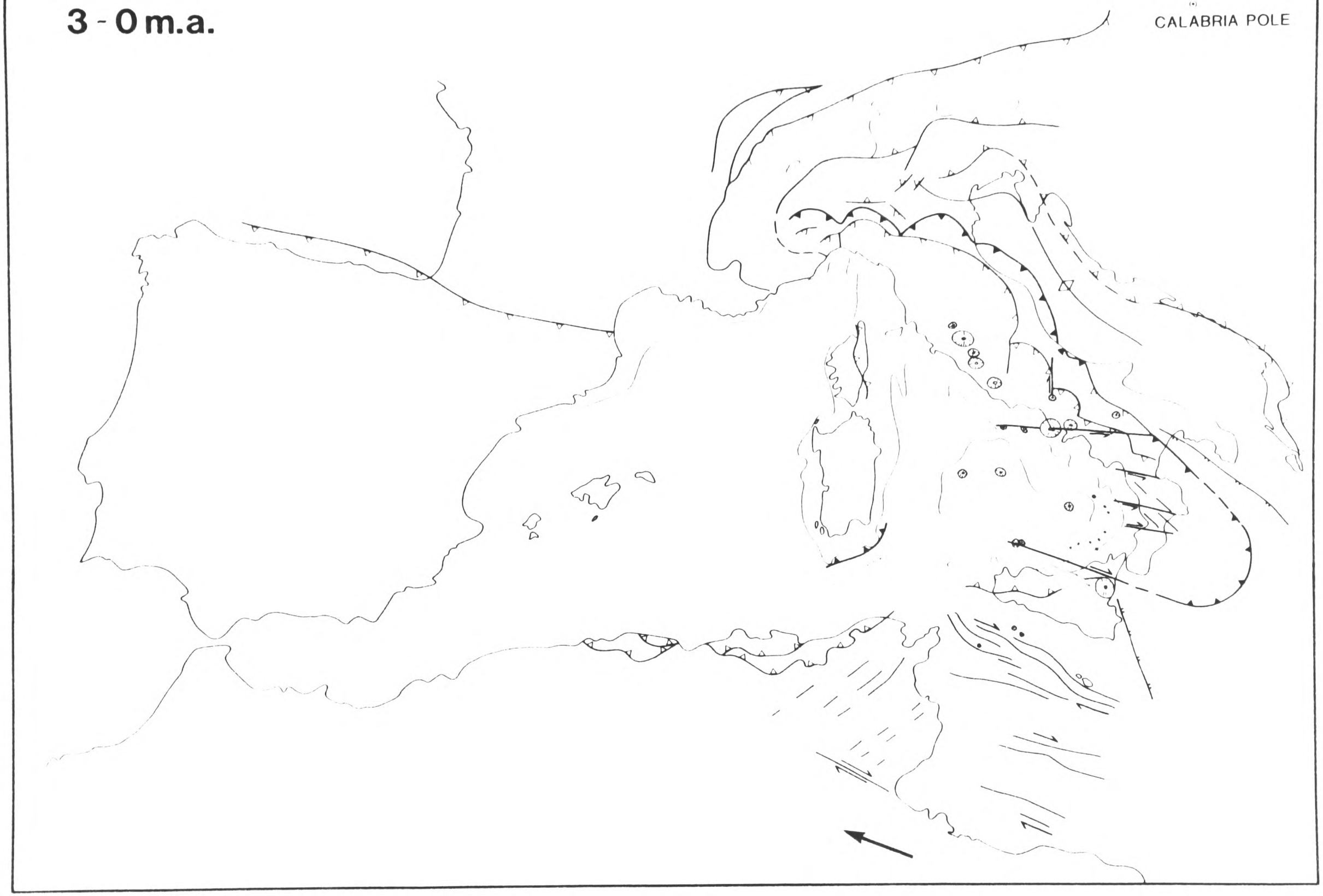
In the Southern Apennines, as in the Calabrian Arc, most deformation was controlled by strike-slip tectonics. In the southern part of the Southern Apennines, these faults are oriented roughly ENE-WSW and to the north N-S. No compressional structures are found in Pliocene deposits around Mount Vulture (Mostardini and Merlini, 1986). Thus the Southern Apennines appears to be a transition region between the Calabrian Arc and the slightly older Northern Apennines arcuate belt. Alkaline volcanism occurred in the Southern Apennines (Roman Province, Mount Vesuvius, Mount Vulture) and in Sicily (Mount Etna).

Figure 6.10: Kinematic Reconstruction of the Western Mediterranean Late Pliocene - Piacenzian to Holocene 3 Ma to Present

This frame of the reconstruction shows the events occurring and the relations of tectonic elements from Late Pliocene - Piacenzian time to the Holocene (3 Ma to Present).

Legend (also shown on Figs. 6.2 and 6.3): Diagonal bricks = Mesozoic carbonate platform. Solid horizontal lines = oceanic crust. Dashed diagonal lines = newly extended continental crust. Dashed horizontal lines = basin on continental crust. Line with filled barbs = active thrust (barbs on overthrust side). Line with un filled barbs = old thrust. Heavy arrows = direction of Africa's motion relative to Europe. Plus marks = anatexis. Double arrows within circles = extension. Volcanoes = volcanism. Long thin arrows = direction of Numidian Flysch sedimentation. Parallelogram = pull-apart basin. Circle with dot in center = pole of rotation (unlabeled if site of future pole). Dots above diagonal lines (within circles) = unconformity. Short straight arrow = stretching lineation. Triangles = vector triangles showing relative motion of various blocks with respect to Europe and Africa. Explanation of reconstruction is given in text.

3 - 0 m.a.



CHAPTER 7

DISCUSSION AND CONCLUSIONS

The Western Mediterraean basins evolved between the converging European and African plates. Previous kinematic models have attempted to relate these large plate motions directly to the tectonics of the region. The underpinning of these types of analyses lies in regarding plate boundaries as crustal scale shear zones whose geometry involves extension parallel with the shear direction determined by stretching lineations (Ramsay and Graham, 1970). A consistent orientation of stretching lineations throughout a region is an indicator of transport direction that is equated with the direction of plate motion (Shackleton and Reis, 1984).

In Western Europe, recent studies have related stretching lineations in the Alps (Baird and Dewey, 1986; Choukroune et al., 1986) and various macro- and micro-stress indicators (tectonic stylolites, tensional joints, slickensides on fault planes or bed-to-bed surfaces, orientation of fold axes) in the Alpine foreland (Bergerat, 1987; Letouzey, 1986) to plate motions. However, the conclusions of such studies are strongly dependent on the model of Africa-Europe relative plate motion to which they are tied.

However, Africa's motion with respect to Europe is not always the factor that determines the geological evolution of this

region. Rather, as shown by vector triangles in Figs. 6.2 - 6.5 and 6.7 - 6.9, the motion of individual blocks with respect to each other often outweighs the importance of the Africa-Europe motion in creating the geology we observe today.

During the interval 23 Ma - 18 Ma, the direction of Africa-Europe motion is between N and NNE. However, the Africa-Europe side of all vector triangles (Fig. 6.3) indicates the least amount of motion. In the east, along the Apennines trend, ESE to ENE directions dominate whereas in the south, along the African margin, the direction of greatest motion is SE to SSE. These directions are in accord with orientations mapped in Calabria (Dewey et al., 1989; Hutton and Turco, in prep.), in the Northern Appenines (Carmignani et al., 1978), Tunisia (Carr and Miller, 1979), and Algeria (Raymond, 1977). Moreover, this time interval is highlighted by the formation of the Gulf of Valencia and the largest part of the Algero-Provencal or North Balearic Basin. The axes of these basins is generally perpendicular to the vectors Menorca/Africa and Sardinia/Africa respectively (Figs. 6.3, 6.4).

During other time intervals, the antithesis of this situation obtains. From Anomaly 5 (8.9 Ma) to the present the motion of Africa with respect to Europe seems to directly control the deformation observed in the Western Mediterranean. Compressive features in the front of the Calabrian Arc are perpendicular to the direction of Africa's motion. The axes of the Tyrrhenian Sea and the Linosa and Pantellaria Grabens are all parallel with this

motion. Indeed, as discussed in 6.7.4a the change in Africa's motion seems to have induced extension in the Tyrrhenian.

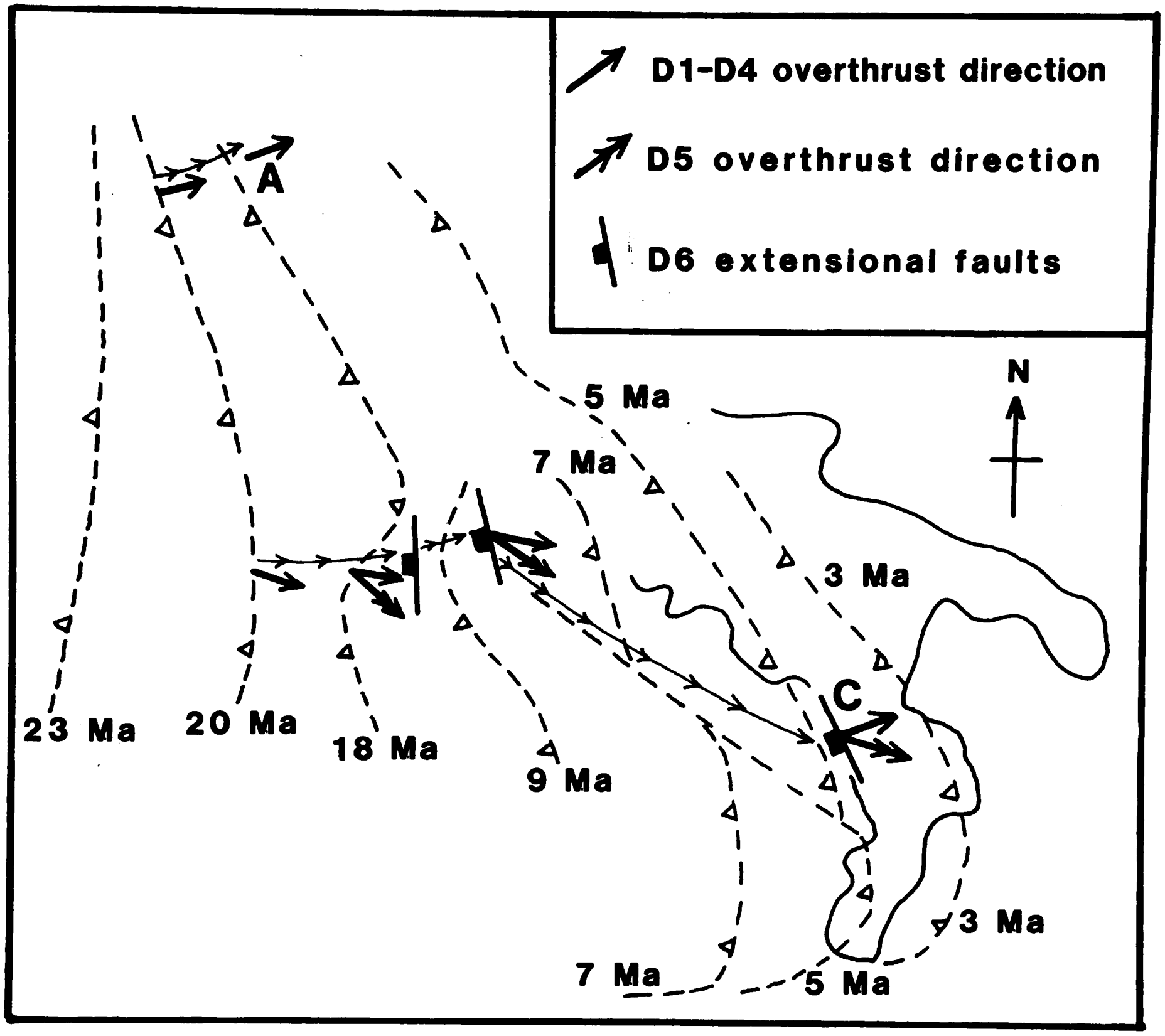
The lack of a direct relationship between the motion of Africa and deformation in the Western Mediterranean region points out one of the dangers inherent in plate tectonic analyses, namely that knowing the plate kinematics of a region is not a simple panacea that obviously or directly explains all observed geology. However, the kinematics provide a starting point for prediction and for testing and refining the model. The case of Tyrrhenian extension is one of the better illustrations of this point.

The motion of Africa with respect to Europe (Figs. 4.3, 4.4) is much simpler and smoother than previously depicted. Despite this, the geological sequences encountered in the region are complicated. The complexity results from the interaction of various blocks within the collisional realm. The kinematics of the major plates merely provide the framework within which these more complex interactions take place. Nevertheless, coherent, testable models can, such as this, can be constructed to explain the features and relationships observed.

In the Cetraro region of Calabria part of this model has been tested. Hutton and Turco (in prep.) recorded a polyphase sequence of deformational events that can be correlated with this model. The correlation is shown if Figure 7.1. A more complete discussion of the relationship is found in Dewey et al. (1989).

Figure 7.1: Relationship between Kinematics and Structure

Evolutionary diagram demonstrating how the structures observed at C (Cetraro area, Calabria) can be related to the sequential development of the Apennine thrust system (rotating southern extension of the Alpine system [sensu lato]) (D1 - D4, D5) and extension in the Tyrrhenian Sea (D6). Once formed the structures are passively carried by the gross rotation of the thrust system and later strike-slip displacement. A = Apuane Alps (data from Carmignani et al., 1978). Dashed barbed lines = sequential position of the major thrust system. Thin, solid, arrowed lines = locii of movement for Cetraro and Apuane structural packages. Figure is from Dewey et al. (1989)


D1-D4 overthrust direction
D5 overthrust direction
D6 extensional faults
A
C
N
23 Ma
20 Ma
18 Ma
9 Ma
7 Ma
5 Ma
3 Ma
7 Ma
5 Ma
3 Ma

CHAPTER 8

REFERENCES

Abbate, E., Bortolotti, V., and Principi, G., 1980, Apennine ophiolites: a peculiar ocean crust: Ofioliti, Vol. 1, p.59-96.

Accademia Nazionale Lince (ANL), 1959, I giacimento gassiferi dell'Europa Occidentale: Atti Convenzione Milano, 1957, Vol. 2, 729pp.

Addy, S.K. and Kagami, H., 1979, Sedimentation in a closed trough north of the Iberia Abyssal Plain in the north-east Atlantic: Sedimentology, Vol. 26, p.561-576.

Ager, D.V., 1980, The Geology of Europe: McGraw-Hill Book Co. Ltd., London, 535pp.

Alvarez, W., 1976, A former continuation of the Alps: Bulletin of the Geological Society of America, Vol. 87, p.891-896.

_____, Corozza, T., and Wezel, F.C., 1974, Fragmentation of the Alpine orogenic belt by microplate dispersal: Nature, Vol. 248, p.309-314.

Anderson, H. and Jackson, J., 1987, The deep seismicity of the Tyrrhenian Sea: Geophysical Journal of the Royal Astronomical Society, Vol. 91, p.613-637.

Andrieux, J., Fontbote, J.M., and Mattauer, M., 1971, Sur un modele explicatif de l'Arc de Gibraltar: Earth and Planetary Science Letters, Vol. 12, p.191-198.

Argand, E., 1916, Sur l'arc des Alpes occidentales: Eglogae Geologicae Helvetiae, Vol. 14, p.145-191.

Auboin, J., 1964, Esquisse paleogeographique et structurales des chaines alpines: Geologische Rundschau, Vol. 53. p.480-534.

Austin, J.A., Jr., Schlager, W., Palmer, A.A., et al., 1986, Proceedings of the Ocean Drilling Program, Initial Reports, Vol. 101, Pt. A: National Science Foundation, 569pp.

Auzende, J.M., Bonnin, J., and Olivet, J.L., 1973, The origin of the western Mediterranean basin: Journal of the Geological Society of London, Vol. 129, p.607-620.

_____ and Olivet, J.L., 1974, Structure of the Western Mediterranean Basin: in Burk, C.A. and Drake, C.L., (eds.),

The Geology of Continental Margins, Springer-Verlag, New York, p.723-731.

_____, Monti, S., and Olivet, J.L., 1979, Carte Bathymetrique de la Mediterranee Occidentale, 1:1,500,000: Centre National Pour L'explotation des Oceans, Brest, France.

Baird, A.W. and Dewey, J.F., 1986, Structural evolution in thrust belts and relative plate motion: the Upper Penine Piemont Zone of the Internal Alps, southwest Swizerland and northwest Italy: Tectonics, Vol. 5, p.375-387.

Banda, E. and Ansorge, J., 1980, Crustal structure under the central and eastern part of the Betic Cordillera: Geophysical Journal of the Royal Astronomical Society, Vol. 63, p.515-532.

_____, Ansorge, J., Boloix, M., and Cordoba, D., 1980, Structure of the crust and upper mantle beneath the Balearic Islands (Western Mediterranean): Earth and Planetary Science Letters, Vol. 49, p.219-230.

_____, Surinach, E., Aparacio, A., Sierra, J., and Ruiz de la Parte, 1981, Crust and upper mantle structure of the central Iberian Meseta (Spain): Geophysical Journal of the Royal Astronomical Society, Vol. 67, p.779-789.

_____, Udias, A., Mueller, S., Mezcua, J., Boloix, M., Gallart, J., and Aparicio, A., 1983, Crustal structure beneath Spain from deep seismic sounding experiments: Physics of the Earth and Planetary Interiors, Vol. 31, p.277-280.

Barberi, F., Innocenti, F., Marinelli, G., and Mazzuoli, R., 1974, Vulcanismo e tettonica a placche: esempi nell' area mediterranea: Memorie della Societa Geologica Italian, Vol. 13, p.327-358.

Bayer, R., LeMouel, J.L., and LePichon, X., 1973, Magnetic anomaly pattern in the western Mediterranean: Earth and Planetary Science Letters, Vol. 19, p.168-176.

Beaumont, C., 1981, Foreland basins: Geophysical Journal of the Royal Astronomical Society, Vol. 65, p.291-329.

Beck, M.E., 1986, Model for Late Mesozoic-Early Tertiary tectonics of coastal California and western Mexico and speculations on the origin of the San Andreas Fault: Tectonics, Vol. 5, p.49-64.

Bellon, H., 1980, Chronologie radiometrique (K-Ar) des manifestations magmatique autour de la Mediterranee occidentale entre 33 et 1 Ma: in Wezel, F.C., (ed.), Sedimentary Basins of Mediterranean Margins, C.N.R. Italian

Project of Oceanography, Tecnoprint, Bologna, p.341-360.

Benson, R.H., 1976, Miocene deep-sea ostracodes of the Iberian Portal and the Balearic Basin: Marine Micropaleontology, Vol. 1, p.249-262.

Bergerat, F., 1987, Stress fields in the European platform at the time of Africa-Eurasisa collision: Tectonics, Vol. 6, p.99-132.

Berggren, W.A., Kent, D.V., Flynn, J.J., and Van Couvering, J.A., 1985, Cenozoic geochronology: Bulletin of the Geological Society of America, Vol. 96, p. 1,407-1,418.

Bernoulli, D., 1972, North Atlantic and Mediterranean Mesozoic facies: a comparison: in Hollister, C.D. and Ewing, J.I., et al., Initial Reports of the Deep Sea Drilling Project, Vol. 11: U.S. Government Printing Office, Washington, D.C., p.801-871.

_____, 1981, Ancient continental margins fo the Tethyan Ocean: in Bally, A.W., (ed.), Geology of Passive Continental Margins: History, Structure, and Sedimentological Record: American Association of Petroleum Geologists Education Course Notes #19, Tulsa, Okla., p.5.1-5.36.

_____ and Jenkyns, H.C., 1974, Alpine, Mediterranean, and Central Atlantic Mesozoic facies in relation to the early evolution of Tethys: in Dott, R. H., Jr. and Shaver, R.H., (eds.), Modern and Ancient Geosynclinal Sedimentation: Society of Economic Paleontologists and Mineralogists Special Publication #24, Tulsa, Okla., p.129-160.

Bessis, F., 1986, Some remarks on the study of subsidence of sedimentary basins. Application to the Gulf of Lions margin (Western Mediterranean): Marine and Petroleum Geology, Vol. 3, p.37-63.

Biju-Duval, B., Letouzey, J., Montadert, L., Courrier, P., Mugniot, J.F., and Sancho, J., 1974, Geology of the Mediterranean Sea basins: in Burk, C.A. and Drake, C.L., (eds.), The Geology of Continental Margins, Springer-Verlag, New York, p.695-721.

_____, Dercourt, J., and Le Pichon, X., 1977, From the Tethys Ocean to the Mediterranean Sea: a plate tectonic model: in Biju-Duval, B. and Montadert, L., (eds.), Structural History of the Mediterranean Basins: Editions Technip, Paris, p.143-164.

Bird, J., (ed.), 1980, Plate Tectonics: American Geophysical Union, Washington, D.C., 1,021pp.

Blanpied, C. and Bellaiche, G., 1983, The Jarrafa Trough (Pelagian Sea): structural evolution and tectonic significance: Marine Geology, Vol. 52, p.M1-M10.

Boccaletti, M., Conedera, C., Dainelli, P., and Gocev, P., 1985, Tectonic Map of the Western Mediterranean Area: C.N.R. Publication #158, Florence, Italy, 1:2,500,000.

Bodinier, J.-L., Morten, L., Puga, E., and Diaz de Federico, A., 1987, Geochemistry of metabasites from the Nevado-Filabride Complex, Betic Cordilleras: relics of a dismembered ophiolitic sequence: Lithos, Vol. 20, p.235-245.

Boillot, G., 1986, Comparison between the Galicia and Aquitaine margins: Tectonophysics, Vol. 129, p.243-245.

_____ and Capdevila, R., 1977, The Pyrenees: subduction or collision: Earth and Planetary Science Letters, Vol. 35, p.151-160.

_____, Auxietre, J.L., Dunand, J.P., Dupeuble, P.A., and Mauffret, A., 1979, The northwestern Iberian margin: a Cretaceous passive margin deformed during Eocene: in Talwani, M., Hay, W., and Ryan, W.B.F., (eds.), Deep Drilling Results in the Atlantic Ocean: Continental Margins and Paleoenvironments: Maurice Ewing Series, Vol. 3, American Geophysical Union, Washington, D.C., p.138-153.

Bonardi, G., Giunta, G., Perrone, V., Russo, M., Zuppetta, A., and Ciampo, G., 1981, Osservazioni sull'evoluzione dell'arco calabro-peloritano nel Miocene inferiore: la formazione di Stilo-Capo d'Orlando: Bollettino della Societa Geologica Italiana, Vol. 99, p.365-393.

Bosshard, E. and MacFarlane, D.J., 1970, Crustal structure of the western Canary Islands from seismic refraction and gravity data: Journal of Geophysical Research, Vol. 75, p.4,901-4,918.

Bossiere, G. and Peucat, J.-J., 1985, New geochronological information by Rb-Sr and U-Pb investigations from the pre-Alpine basement of Greande Kabylie (Algeria): Canadian Journal of Earth Sciences, Vol. 22, p.675-685.

_____, 1986, Structural evidence and Rb-Sr, 39-40 Ar mica ages relationships for the existence of an Hercynian deep crustal shear zone in Grande Kabylie (Algeria) and its Alpine reworking: Tectonophysics, Vol. 121, p.277-294.

Bott, M.P.H., 1985, Plate tectonic evolution of the Icelandic Transverse Ridge and adjacent regions: Journal of Geophysical Research, Vol. 90, p.9,953-9,960.

_____ and Watts, A.B., 1971, Deep structure of the continental margin adjacent to the British Isles: in Delaney, F.M., (ed.), The Geology of the East Atlantic Continental Margin: Institite of Geological Sciences Report 70-14, London, p.89-109.

Bouillin, J.P., 1984, Nouvelle interpretation de la liason Apennin-Maghrebides en Calabre: consequences sur la paleogeographie tethysienne entre Gibraltar et les Alpes: Revue de Geologie Dynamique et de Geographie Physique, Vol. 25, p.321-338.

_____, Durand Delga, M., Gelard, J.P., and Leikine, M., 1970, Definition d'un flysch massylien et d'un flysch mauretanien au sein des flyschs allochtones de l'Algerie: Comptes Rendu de la Academie Science, Paris, Series D, Vol. 270, p.2,249-2,252.

Bourbon, M., 1978, Mesozoic evolution of Western North Atlantic and Northern Tethyan margins: a comparison: in Benson, W.E., Sheridan, W.E., et al., Initial Reports of the Deep Sea Drilling Project, Vol. 44: U.S. Government Printing Office, Washington, D.C., p.949-969.

Brunet, M.F., 1984, Subsidence history of the Aquitaine Basin determined from subsidence curves: Geological Magazine, Vol. 121, p.421-428.

Bucci, J., 1984, Basin Analysis, Thermal History, and Hydrocarbon Generation of the Rharb Basin, Morocco: M.S. Thesis, University of South Carolina, Columbia, S.C., 91pp.

Buerger, M.J., 1956, Elementary crystallography: an introduction to the fundamental geometrical features of crystals: John Wiley and Sons, New York, 528pp.

Bullard, E.C., Everett, J.E., and Smith, A.G., 1965, The fit of the continents around the Atlantic: Philosophical Transactions of the Royal Society of London, Series A, Vol. 258, p.41-56.

Burchfiel, B.C., 1980, East European Alpine system and the Carpathian orocline as an example of collision tectonics: Tectonophysics, Vol. 63, p.31-61.

Burollet, P.F., Mugniot, J.M., and Sweeney, P., 1978, The geology of the Pelagian Block: the margins and basins off southern Tunisia and Tripolitania: in Nairn, A.E.M., Kanes, W.H., and Stehli, F.G., (eds.), The Ocean Basins and Margins, Vol. 4B, The Western Mediterranean: Plenum Press, New York, p.331-359.

Burrus, J., 1984, Contribution to a geodynamic synthesis of the

Provencal Basin (northwestern Mediterranean): Marine Geology, Vol. 55, p.247-269.

Busquets, P., Orti, F., Pueyo, J.J., Riba, O., Rosell-Ortiz, L., Saez, A., Salas, R., and Taberner, C., 1985, Evaporite depositon and diagenesis in the saline (potash) Catalan Basin, Upper Eocene: in Mila, M.D. and Rosell, J., (eds.), 6th European Regional Meeting Excursion Guidebook: International Association of Sedimentologists, Llerida, Spain, p.11-59.

Cadet, J.-P., Bonneau, M., Charvet, J., Durr, S., Elter, P., Ferriere, J., Scandone, P., and Thiebault, F., 1980, Les chaines de la Mediterranee moyen et orientale: Les Apennins: in Aubuoin, J., Debelmas, J., and Latreille, M. (eds.), Geologie des Chaines Alpines Issues de la Tethys: Memorire du Bureau de Recherches Geologiques et Minieres #115, Orleans, p.98-118.

Caire, A., 1974, Eastern Atlas: in Spencer, A.M., (ed.), Mesozoic-Cenozoic Orogenic Belts: Data for Orogenic Studies: Geological Society of London Special Publication #4, Scottish Academic Press, Edinburgh, p.47-59.

_____, 1978, The Central Mediterranean mountain chains in the Alpine orogenic environment: in Nairn, A.E.M., Kanes, W.H., and Stehli, F.G., (eds.), The Ocean Basins and Margins, Vol. 4B, The Western Mediterranean: Plenum Press, New York, p.201-256.

Cande, S.C., 1978, Anomalous behavior of the paleomagnetic field inferred from the skewness of anomalies 33 and 34: Earth and Planetary Science Letters, Vol. 40, p.275-286.

_____, and Kent, D.V., 1976, Constraints imposed by the shape of marine magnetic anomalies on the magnetic source: Journal of Geophysical Research, Vol. 81, p.4,157-4,162.

_____, and Kristoffersen, Y., 1977, Late Cretaceous magnetic anomalies in the North Atlantic: Earth and Planetary Science Letters, Vol. 35, p.215-224.

_____, Labreque, J.L., Larson, R.L., Pitman, W.C., III, Golovchenko, X., and Haxby, W.F., 1988, Magnetic Lineations of the World's Ocean Basins, 1:26,950,000: American Association of Petroleum Geologists, Tulsa, Okla., 1 sheet.

Cann, J.R., 1971, Petrology of the basement rocks from Palmer Ridge, N.E. Atlantic: Philosophical Transactions of the Royal Society of London, Series A, Vol. 268, p.605-644.

Carissimo, L., D'Agostino, O. Loddo, C., and Pieri, M., 1963, Petroleum exploration by AGIP Minereria and new geological

information in Central and Southern Italy from the Abruzzi to the Taranto Gulf: Sixth Petroleum International Congress, Section 1, p.267-292.

Carmignani, L., Giglia, G., and Kligfield, R., 1978, Structural evolution of the Apuane Alps: an example of continental margin deformation in the Northern Apennines, Italy: Journal of Geology, Vol. 86, p.487-504.

Carr, M.D. and Miller, E.L., 1979, Overthrust emplacement of the Numidian Flysch Complex in the westernmost Modgod Mountains, Tunisia: Geological Society of America Bulletin, Part 2, Vol. 90, p.886-923.

Carter, T.G., Flanagan, J.P., Jones, C.R., Marchant, F.L., Murchison, R.R., Rebman, J.H., Sylvester, J.C., and Whitney, J.C., 1972, The new bathymetric chart and physiography of the Mediterranean Sea: in Stanley, D.J., (ed.), The Mediterranean Sea: A Natural Sedimentological Laboratory: Dowden, Hutchinson, and Ross, Stroudsburg, Pa., p.1-23.

Cassinis, R., 1986, The geophysical exploration of the upper crust from the Ligurian Coast to the northern margin of the Po Valley: problems and results: Tectonophysics, Vol. 128, p.381-394.

Castellarin, A., 1976, Ipotesi palaeogeografica sul bacino del flysch Sudalpino Cretacico: Bollettino della Societa Geologica Italiana, Vol. 95, p.501-511.

Catalano, R. and D'Argenio, B., 1978, An essay of palinspastic restoration across Western Sicily: Geologia Romana, Vol. 17, p.145-159.

Cermak, V. and Hurtig, E., 1979, Heat Flow Map of Europe: in Cermak, V. and Rybach, L., (eds.), Terrestrial Heat Flow in Europe: Springer-Verlag, Berlin, 1 sheet.

Channell, J.E.T. and Horvath, F., 1976, The African-Adriatic Promontory as a paleogeographic premise for alpine orogenic movements in the Carpatho-Balkan region: Tectonophysics, Vol. 35, p.71-101.

_____, D'Argenio, B., and Horvath, F., 1979, Adria, the African promontory in Mesozoic Mediterranean paleogeography: Earth-Science Reviews, Vol. 15, p.213-292.

Choubert, G. and Faure-Muret, A., 1974, Moroccan Rif: in Spencer, A.M., (ed.), Mesozoic-Cenozoic Orogenic Belts: Data for Orogenic Studies: Geological Society of London Special Publication #4, Scottish Academic Press, Edinburgh, p.37-46.

Choukroune, P. and Seguret, M., 1973, Tectonics of the Pyrenees: role of gravity and compression: in de Jong, K.H. and Schoulten, R., (eds.), in Gravity and Tectonics: John Wiley and Sons, New York, p.141-156.

_____, Ballevre, M., Cobbold, P., Gautier, V., Merle, O., and Vuicher, J.P., Deformation and motion in the Western Alpine Arc: Tectonics, Vol. 5, p.215-226.

Cloetingh, S., McQueen, H., and Lambeck, K., 1985, On a tectonic mechanism for regional sea level variations: Earth and Planetary Science Letters, Vol. 75, p.157-166.

Cohen, C.R., 1980, Plate tectonic model for the Oligo-Miocene evolution of the Western Mediterranean: Tectonophysics, Vol. 68, p.283-311.

Compagnoni, R., Dal Piaz, G.V., Hunziker, J.C., Gosso, G., Lompardo, B.T., and Williams, P.F., 1975, The Sesia-Lazo Zone, a slice of continental crust with Alpine high- pressure, low-temperature assemblages in the Western Italian Alps: Rendiconti della Societa Italiana di Mineralogia e Petrologia, Vol. 33, p.281-334.

Cordoba, D., Banda, E., and Ansorge, J., 1987, The Hercynian crust in northwestern Spain: a seismic survey: Tectonophysics, Vol. 132, p.321-333.

Courme-Rault, M.-D., 1984, Sur le Miocene de l'Algerie centrale et orientale; l'age de la mise en place des nappes telliennes: Revue de Geologie Dynamique et de Geographie Physique, Vol. 25, p.127-144.

Cousin, M., 1981, Les rapports Alpes-Dinarides: les confins de l'Italie et de la Yougoslavie: Societe Geologique du Nord, Vol. 5, p.1-52.

Cox, A., (ed.), 1973, Plate Tectonics and Geomagnetic Reversals: W.H. Freeman, San Francisco, 702pp.

_____ and Hart, R.B., Plate Tectonics - How It Works: Blackwell Scientific Publishing, Oxford, 392pp.

Crough, S.T., 1981, Mesozoic hotspot epeirogeny in eastern North America: Geology, Vol. 9, p.2-6.

Cruz-Sanjulian, J., 1976, Essay on the paleogeography of the western part of the Betic Cordillera: Neues Jahrbuch fur Geologie und Palaontologie, Monatshefte, Vol. 7, p.385-394.

Dabrio, C.J., Gonzalez-Donoso, J.M., Rivas, P., and Vera, J.A., 1971, Geology of the Sub-Betic Zone: in Freeman, T. and

Simancas, R., (eds.), Guidebook for Tenth International Field Institute, Spain: American Geophysical Union, Washington, D.C., p.171-196.

Daignieres, M., Gallart, J., Banda, E., and Hirn, A., 1982, Implications of the seismic structure for the orogenic evolution of the Pyrenean Range: Earth and Planetary Science Letters, Vol. 57, p.88-100.

Dallan Nardi, L. and Nardi, R., 1974, Schema stratigrafico e strutturalle dell' Appennino Settentrionale: Memorie Accademia Luniguiana, Vol. 62, p.1-212.

D'Argenio, B., Pescatore, T., and Scandone, P., 1973, Schema geologico dell'Appennino meridionale (Campania e Lucania): Convegno "Moderne vedute sulla geologia dell'Apennino": Atti Accademia Lincei, Quaderno 183, p.49-72.

_____, Castro, D., Emiliani, C., and Simone, L., 1975, Bahamian and Apenninic limestones of identical lithology and age: American Association of Petroleum Geologists Bulletin, Vol. 59, p.524-533.

Dawes, P.R. and Kern, J.W., 1982, Nares Strait and the drift of Greenland: a conflict in plate tectonics: Meddeleser om Gronland: Vol. 8, 392pp.

Debelmas, J., Oberhauser, R., Sandulescu, M., and Trumpy, R., 1980, L'arc alpino-carpathique: in Aubouin, J., Debelmas, J., and Latreille, M., (eds.), Geologie des Chaines Alpines Issues de la Tethys: Memoire du Bureau de Recherches Geologiques et Minieres #115, Orleans, p.86-96.

Della Vedova, B., Pelli, G., Foucher, J.P., and Rehault, J.P., 1984, Geothermal structure of the Tyrrhenian Sea: Marine Geolgy, Vol. 55, p.271-289.

Dercourt, J., Zonenshain, L.P., et al., 1986, Geological evolution of the Tethys belt from the Atlantic to the Pamirs since the Lias: Tectonophysics, Vol. 123, p.241-315.

DeSmet, M.E.M., 1984, Wrenching in the External Zone of the Betic Cordilleras, southern Spain: Tectonophysics, Vol. 107, p.57-79.

Desmons, J., 1980, The Western Alps: correlation of the phases of deformation, metamorphism, and magmatism: in Aubouin, J., Debelmas, J., and Latreille, M., (eds.), Geologie des Chaines Alpines Issues de la Tethys: Memoire du Bureau de Recherches Geologiques et Minieres #115, Orleans, p.294.

Dewey, J.F., 1975, Finite plate evolution: some implications for

the evolution of rock masses at plate margins: American Journal of Science, Vol. 275-A, p.260-284.

_____, 1988, Extensional collapse of orogens: Tectonics, Vol. 7, p.1,123-1,139.

_____, 1988a, Lithospheric stress, deformation, and tectonic cycles: the disruption of Pangaea and the closure of Tethys: in Audley-Charles, M.G. and Hallam, A., (eds.), Gondwana and Tethys: Geological Society of London Special Publication #37, Oxford University Press, Oxford, p.23-40.

_____, Pitman, W.C., III, Ryan, W.B.F., and Bonnin, J., 1973, Plate tectonics and the evolution of the Alpine System: Bulletin of the Geological Society of America, Vol. 84, p.3,137-3,180.

_____, Helman, M.L., Turco, E., Hutton, D.H.W., and Knott, S.D., 1989, Kinematics of the Western Mediterranean: in Coward, M.P., Dietrich, D., and Park, R.G., (eds.), Alpine Tectonics: Geological Society of London Special Publication #45, Blackwell Scientific, Inc., Oxford, p.265-283.

Diaz de Federico, A., Puga, E., Torres-Roldan, R., and Vera, J.A., Correlation of the phases of deformation, metamorphism, and magmatism in the Betic ranges: in Aubouin, J., Debelmas, J., and Latreille, M., (eds.), Geologie des Chaines Alpines Issues de la Tethys: Memoire du Bureau de Recherches Geologiques et Minieres #115, Orleans, p.291-293.

Dietrich, D., 1988, Sense of overthrust shear in the Alpine nappes of Calabria (Southern Italy): Journal of Structural Geology, Vol. 10, p.373-381.

Dillon, W.P. and Sougy, J.M.A., 1974, Geology of West Africa and Canary and Cape Verde Islands: in Nairn, A.E.M. and Stehli, F.G., (eds.), The Ocean Basins and Margins, Vol. 2, The North Atlantic: Plenum Press, New York, p.315-390.

_____, Paull, C.K., Buffler, R.T., and Fail, J.P., 1979, Structure and development of the southeast Georgia Embayment and northern Blake Plateau: preliminary analysis: in Watkins, J.S., Montadert, L., and Dickerson, P.W., (eds.), Geological and Geophysical Investigations of Continental Margins: American Association of Petroleum Geologists Memoir #29, Tulsa, Okla., p.27-41.

Doglioni, C., 1987, Tectonics of the Dolomites (Southern Alps, Northern Italy): Journal of Structural Geology, Vol. 9, p.181-193.

_____ and Castellarin, A., 1985, A geologica schematic

cross section of the eastern Southern Alps: Rendiconti della Societa Geologica Italiana, Vol. 8, p.35-36.

_____ and Bosellini, A., 1987, Eoalpine and Mesoalpine tectonics in the Southern Alps: Geologische Rundschau, Vol. 76, p.735-754.

Durand-Delga, M., 1981, Overtures oceanique de Mediterranee occidentale et dislocation des chaines alpines: in Wezel, F.C., (ed.), Sedimentary Basins of Mediterranean Margins, C.N.R. Italian Project of Oceanography, Tecnoprint, Bologna, p.417-431.

_____, Hottinger, L., Marcais, J., Mattauer, M., Milliard, Y., and Suter, G., 1960-62, Donnees actuelles sur la structure du Rif: in Durand Delga, M., Bordet, P., et al., Livre a la Memoire du Professeur Paul Fallot, Vol. 1: Memoire Hors-Serie de la Societe Geologique de France, Paris, p.399-422.

_____ and Kornprobst, J., 1963, Esquisse geologique de la region de Ceuta (Maroc): Bulletin de la Societe Geologique de France, Vol. 5, p.1,049-1,057.

_____ and Fontbote, J.M., 1980, Le cadre structurale de la Mediterranee occidentale: in Aubouin, J., Debelmas, J., and Latreille, M., (eds.), Geologie des Chaines Alpines Issues de la Tethys: Memoire du Bureau de Recherches Geologiques et Minieres #115, Orleans, p.67-85.

ECORS Pyrenees Team, 1988, The ECORS deep reflection seismic survey across the Pyrenees: Nature, Vol. 331, p.508-511.

Einarsson, P., 1979, Seismicity and earthquake focal mechanisms along the Mid-Atlantic plate boundary between Iceland and the Azores: Tectonophysics, Vol. 55, p.127-153.

_____, 1986, Seismicity along the eastern margin of the North Atlantic plate: in Vogt, P.R. and Tucholke, B.E., (eds.), The Geology of North America, Vol. M, The Western North Atlantic Region: Geological Society of America-Decade of North American Geology Series, p.99-116.

Eldredge, S., Bachtadse, V., and Van der Voo, R., 1985, Paleomagnetism and the orocline hypothesis: Tectonophysics, Vol. 119, p.153-179.

Elter, P., 1975, L'ensemble ligure: Bulletin de la Societe Geologique de France: Vol. 17, p.984-997.

Emery, K.O. and Uchupi, E., 1984, The Geology of the Atlantic Ocean: Springer-Verlag, New York, 1,050pp.

Erickson, A.J., Simmons, G., Ryan, W.B.F., 1977, Review of heat flow data from the Mediterranean and Aegean Seas: in Biju-Duval, B. and Montadert, L., (eds.), Structural History of the Mediterranean Basins: Editions Technip, Paris, p.263-280.

Ewing, M., Ewing, J., and Talwani, M., 1964, Sediment distribution in the oceans: the Mid-Atlantic Ridge: Bulletin of the Geological Society of America, Vol. 75, p.17-36.

Faupl, P., Frank, W., and Frisch, W., 1980, Phases of the evolution of the Eastern Alps: in Aubouin, J., Debelmas, J., and Latreille, M., (eds.), Geologie des Chaines Alpines Issues de la Tethys: Memoire du Bureau de Recherches Geologiques et Minieres #115, Orleans, p.295-296.

Faure-Muret, A. and Choubert, G., 1971, Les cordilleres Betiques (Espagne): in Tectonique de l'Africque, Science de la Terre 6, UNESCO, Paris, p.47-60.

Fein, J.B. and Jurdy, D.M., 1986, Plate motion controls on back-arc spreading: Geophysical Research Letters, Vol. 13, p.456-459.

Ferrara, G., Bigazzi, G., Bonadonna, F.P., and Giuliani, O., 1973, Radiometric dating of the Valencia volcanic rocks: in Ryan, W.B.F., Hsu, K.J., et al., Initial Reports of the Deep Sea Drilling Project, Vol. 13: U.S. Government Printing Office, Washington, D.C., p.773.

Finetti, I. and Morelli, C., 1973, Geophysical exploration of the Mediterranean Sea: Bolletino di Geofisica Teorica ed Applicata, Vol. 15, p.263-341.

Fischer, A.G., 1964, The Lofer cycles of the Alpine Triassic: Kansas Geological Survey Bulletin, Vol. 169, p.107-149.

Fischer, M.W., 1984, Thrust tectonics of the North Pyrenees: Journal of Structural Geology, Vol. 6, p.721-726.

Fitch, T.J., 1972, Plate convergence, transcurrent faults, and internal deformation adjacent to Southeast Asia and the Western Pacific: Journal of Geophysical Research, Vol. 77, p.4,432-4,460.

Fleming H.S., Cherkis, N.Z. and Heirtzler, J.R., 1970, The Gibbs Fracture Zone: a double fracture zone at 52o 30'N in the Atlantic Ocean: Marine Geophysical Research, Vol. 1, p.37-45.

Fletcher, J.B., Sbar, M.L., and Sykes, L.R., 1978, Seismic trends and travel-time residuals in eastern North America and their tectonic implications: Bulletin of the Geological Society of

America, Vol. 89, p.1,656-1,676.

Foland, K.A. and Faul, H., 1977, Ages of the White Mountain intrusives - New Hampshire, Vermont, Maine, U.S.A.: American Journal of Science, Vol. 277, p.888-904.

Fox, P.J. and Gallo, D.G., 1984, A tectonic model for ridge-transform-ridge plate boundaries: implications for the structure of oceanic lithospere: Tectonophysics, Vol. 104, p.205-242.

Francheteau, J., 1973, Plate tectonic model of the opening of the Atlantic Ocean south of the Azores: in Tarling, D.H. and Runcorn, S.K., (eds.), Implications of Continental Drift to the Earth Sciences: Academic Press, New York, p.197-202.

Frei, L.S. and Cox, A., 1987, Relative displacement between Eurasia and North America prior to the formation of oceanic crust in the North Atlantic: Tectonophysics, Vol. 142, p.111-136.

Funk, H., Oberhausli, R., Pfiffner, A., Schmid, S., and Wildi, W., 1987, The evolution of the northern margin of Tethys in Eastern Switzerland: Episodes, Vol. 10, p.102-106.

Garcia-Hernandez, M., Lopez-Garrido, A.C., Rivas, P., Sanz de Galdeano, C., and Vera, J.A., 1980, Mesozoic palaeogeographic evolution of the external zones of the Betic Cordillera: Geologie en Mijnbouw, Vol. 59, p.155-168.

Gavasci, A.T., Fox, P.J., and Ryan, W.B.F., 1973, Petrography of rocks from the crestal area of Gorringe Bank: in Ryan, W.B.F., Hsu, K.J., et al., Initial Reports of the Deep Sea Drilling Project, Vol. 13: U.S. Government Printing Office, Washington, D.C., p.749-752.

Geise, P., Reutter, K.J., Jacobshagen, V., and Nicolich, R., 1982, Explosion seismic crustal studies in the Alpine Mediterranean region and their implications to tectonic processes: in Berckhemer, H. and Hsu, K., (eds.), Alpine-Mediterranean Geodynamics: American Geophysical Union Geodynamics Series #7, Wash., D.C., p.39-73.

Gelard, J.P., 1969, Le flysch a base schisto-greseuse de la bordure meridionale et oriental du massif de Chellata: le flysch mauretanien (Grand Kabylie): Bulletin de la Societe Geologique de France, Vol. 11, p.676-686.

Ghelardoni, R. and Riva, E., 1988, Mesozoic Sedimentation and Tertiary Decollement Tectonics in the Umbria-Marche Thrust Belt: Field Trip Guidebook #4, American Asssociation of Petroleum Geologists Mediterranean Basins Conference, Nice,

France, 68pp.

Giermann, G., Pfennenstiel, M., and Wimmenaurer, W., 1968, Relations entre morphologie, tectonique et volcanisme en mer d'Alboran (Mediterranee occidental): Comptes Rendu Sommaire de la Societe Geologique de France, Vol. 10, p.116-118.

Giunta, G., 1985, Problematiche e ipotesi sul Bacino Numidico nelle Maghrebidi siciliane: Bollettino della Societa Geologica Italiana, Vol. 104, p.239-256.

Gradstein, F.M., Grant, A.C., and Jansa, L.F., 1977, Grand Banks and the J-Anomaly Ridge: a geological comparison: Science, Vol. 197, p.1,074-1,076.

Grimaud, S., Boillot, G., Collette, B., Mauffret, A., Miles, P.R. and Roberts, D.G., 1982, Western extension of the Iberian-European plate-boundary during the early Cenozoic (Pyrenean) convergence: a new model: Marine Geology, Vol. 45, p.63-77.

Grimison, N.L. and Chen, W.-P., 1986, The Azores-Gibraltar plate boundary: focal mechanisms, depths of earthquakes, and their tectonic implications: Journal of Geophysical Research, Vol. 91, p.2,029-2,047.

Group Galice, 1979, The continental margins of Galicia and Portugal: acoustical stratigraphy and structural evolution: in Ryan, W.B.F., Sibuet, J.-C., et al., Initial Reports of the Deep Sea Drilling Project, Vol. 47, Pt. 2: U.S. Government Printing Office, Washington, D.C., p.633-662.

Groupe de Recherche Neotectonique de l'Arc de Gibraltar, 1977, L'histoire tectonique recente (Tortonian a Quaternaire) de l'Arc de Gibraltar et des bordures de la mer d'Alboran: Bulletin de la Societe Geologique de France, Vol. 19, p.575-614.

Hanisch, J., 1984, The Cretaceous opening of the northeast Atlantic: Tectonophysics, Vol. 101, p.1-23.

Haq, B.U., Hardenbol, J., and Vail, P.R., 1987, Chronology of fluctuating sea levels since the Triassic: Science, Vol. 235, p.1,156-1,167.

Harland, W.B., Cox, A.V., Llewellyn, P.G., Pickton, C.A.G., Smith, A.G., and Walters, R., 1982, A Geologic Time Scale: Cambridge University Press, Cambridge, 128pp.

Harris, L.B., 1985, Direction changes in thrusting of the Schistes Lustres in Alpine Corsica: Tectonophysics, Vol. 120, p.37-56.

Harrison, C.G.A., 1972, Poles of rotation: Earth and Planetary Science Letters, Vol. 14, p.31-38.

Hatzfeld, D. and Bensari, D., 1977, Grand profils sismiques dans la region de l'arc de Gibraltar: Bulletin de la Societe Geologique de France, Vol. 19, p.749-756.

Haxby, W., 1985, The Gravity Field of the World's Oceans: U.S. Office of Naval Research.

Heezen, B.C., Gray, C., Segre, A.C., and Zarduski, E.F.K., 1971, Evidence of foundered continental crust beneath the Central Tyrrhenian Sea: Nature, Vol. 229, p.327-329.

Heim, A., 1922, Geologie de Schweiz II(2): Die Schweizen Alpen II: Leipzig, Tauchnitz, p.477-1,118.

Heirtzler, J.R., Dickson, G.O., Herron, E.M., Pitman, W.C., III, and LePichon, X., 1968, Marine magnetic anomalies, geomagnetic field reversals, and motions of the ocean floor and continents: Journal of Geophysical Research, Vol. 73, p.2,113-2,136.

Hermes, J.J., 1978, The stratigraphy of the Subbetic and southern Prebetic of the Velez Rubio-Caravaca area and its bearing on transcurrent faulting in the Betic Cordilleras of Southern Spain: Proceedings of the Koninklijke Nederlandse Akademie Wetenschappen, Vol. 81, p.1-54.

Hill, K.C. and Hayward, A.B., 1988, Structural constraints on the Tertiary plate tectonic evolution of Italy: Marine and Petroleum Geology, Vol. 5, p.2-16.

Hinz, K., 1973, Crustal structure of the Balearic Sea: Tectonophysics, Vol. 20, p.295-302.

Hirn, A., Steinmetz, L., and Sapin, M., 1977, A long range seismic profile in the Western Mediterranean basin: structure of the upper mantle: Annales Geophysicae, Vol. 33, p.373-384.

Hirn, A., Daignieres, M., Gallart, and Vadell, M., 1980, Explosion seismic sounding of throws and dips in the continental Moho: Geophysical Research Letters, Vol. 7, p.263-266.

Hiscott, R.N., Gradstein, F.M., and Wilson, R.C.L., 1988, Subsidence histories and comparative stratigraphies of some Meozoic basins of the North Atlantic continental margins: Geological Association of Canada Annual Meeting Program with Abstracts, Vol. 13, p.A56.

Hsu, K.J., 1977, Tectonic evolution of the Mediterranean Sea

basins: in Nairn, A.E.M., Kanes, W.H., and Stehli, F.G., (eds.), The Ocean Basins and Margins, Vol. 4A, The Eastern Mediterranean, Plenum Press, New York, p.29-75.

_____, Cita, M.B., and Ryan, W.B.F., 1973, The origin of the Mediterranean evaporites: in Ryan, W.B.F., Hsu, K.J., et al., Initial Reports of the Deep Sea Drilling Project, Vol. 13, p.1,203-1,231.

Huchon, P., Lallemant, S., de Voogd, B., Chamot-Rooke, N., Perrot, J., LePichon, X., Andrier, J.F., Ciais, G., Feignier, B., and Paul, A., 1989, The Eastern Mediterranean crust: new ESP results from 1988 Pasiphae cruise: EOS, Vol. 70, p.307.

Hunziker, J.C., 1974, Rb-Sr and K-Ar age determination and the tectonic history of the Western Alps: Universita di Padova, Istituto Geologia e Mineralogia, Memoir 31, 54pp.

Hutchison, I., von Herzen, R.P., Louden, K.E., Sclater, J.G., and Jemsek, J., 1985, Heat flow in the Balearic and Tyrrhenian Basins, Western Mediterranean: Journal of Geophysical Research, Vol. 90, p.685-701.

Ibarrola, E., 1979, Variation trends in basaltic rocks of the Canary Islands: Bulletin of Volcanology, Vol. 33, p.729-777.

Instituto Geologico y Minero de Espana (IGME), 1980, Mapa Geologico de la Peninsula Iberica, Baleares y Canarias, 1:1,000,000: Madrid, Spain.

International Bathymetric Chart of the Mediterranean (IBCM), 1981, UNESCO Intergovernmental Oceanographic Commission, 1:1,000,000: Leningrad, U.S.S.R., 10 sheets.

Jackson, J.A., 1987, Active normal faulting and crustal extension: in Coward, M.P., Dewey, J.F., and Hancock, P.L., (eds.), Continental Extensional Tectonics: Geological Society of London Special Publication #28, Blackwell Scientific Publishers, Oxford, p.3-17.

Jerez Mir, L., 1971, Bosquejo estratigafico y paleogeografico de la Zona Prebetica en la region de Isso-Elche de la Sierra-Moratalla: Boletin Geologico y Minero, Vol. 81-82, p.117-131.

Julivert, M., Fontbote, J.M., Ribeiro, A., and Conde, L., 1980, Mapa Tectonico de la Peninsula Iberica y Baleares: Instituto Geologico y Minero de Espan~a, Madrid.

Jurdy, D.M., 1979, Relative plate motion and the formation of mariginal basins: Journal of Geophysical Research, Vol. 84, p.6,796-6,802.

Kampschuur, W. and Rondeel, H.E., 1975, The origin of the Betic Orogen, southern Spain: Tectonophysics, Vol. 27, p.39-56.

Kanes, W.H., Saadi, M., Ehrlich, E., and Alem, A., 1973, Moroccan crustal response to continental drift: Science, Vol. 180, p.950-952.

Karasik, A.M., 1974, Plate tectonics and Eurasian basin of the Arctic Sea: in Problems of Geology of the Earth's Polar Regions: Izd. NIIGA, Leningrad, in Russian.

Karig, D.E., Suparka, S., More, G.F., and Hehanussa, P.E., 1979, Structure and Cenozoic evolution of the Sunda Arc in the Central Sumatra region: in Watkins, J.S., Montadert, L., and Dickerson, P.E., (eds.), Geological and Geophysical Investigations of Continental Margins: American Association of Petroleum Geologists Memoir #29, Tulsa, Okla., p.223-237.

Karner, G.D., 1986, Effects of lithospheric in-plane stress on sedimentary basin stratigraphy: Tectonics, Vol. 5, p.573-588.

_____, Grimison, N.L., Chen, W.-P., and Weissel, J.K., 1985, SEASAT derived gravity and geoid anomalies of the Azores-Gibraltar plate boundary: a diffuse zone of ocean-ocean convergence near Gibraltar: EOS, Vol. 66, p.361.

Kastens, K.A., 1981, Structural causes and sedimentological effects of "Cobblestone Topography" in the Eastern Mediterranean: Ph.D. Thesis, University of California, San Diego, 207pp.

_____, Mascle, J., et al., 1987, Proceedings of the Ocean Drilling Project, Initial Report-Part A, Vol. 107: Ocean Drilling Program, College Station, Texas, 1,013pp.

_____, _____, et al., 1988, ODP Leg 107 in the Tyrrhenian Sea: insights into passive margin and back-arc basin evolution: Bulletin of the Geological Society of America, Vol. 100, p.1,140-1,156.

Keen, C.E., Hall, B.R., and Sullivan, K.D., 1977, Mesozoic evolution of the Newfoundland Basin: Earth and Planetary Science Letters, Vol. 37, p.307-320.

Kent, D.V. and Gradstein, F.M., 1985, A Cretaceous and Jurassic geochronology: Bulletin of the Geological Society of America, Vol. 96, p.1,419-1,427.

Kenter, J.A.M., Reymer, J.J.G., and van der Straaten, H.C., 1988, The transition from a passive continental margin to an active margin documented by time-facies profiles and geohistory diagrams: AAPG Bulletin, Vol. 72, p.1,009.

Kidd, R.B., Searle, R.C., Ramsay, A.T.S., Prichard, H., and Mitchell, J., 1982, The geology and formation of King's

Trough, Northeast Atlantic Ocean: Marine Geology, Vol. 48, p.1-30.

_____ and Ramsay, A.T.S., 1987, The geology and formation of the King's Trough Complex in the light of Deep Sea Drilling Project Site 608 drilling: in Ruddiman, W.F., Kidd, R.B. et al., Initial Reports of the Deep Sea Drilling Project, Vol. 94, Pt. 2: U.S. Government Printing Office, Washington, D.C., p.1,245-1,261.

Kieken, M., 1960-62, Les traits essential de la geologie Algierienne: in Durand Delga, M., Bordet, P., et al., Livre a la Memoire du Professeur Paul Fallot, Vol. 1: Memoire Hors-Serie de la Societe Geologique de France, Paris, p.545-614.

_____, 1960-62a, Esquisse Tectonique de l'Algerie, 1:1,000,000: in Durand Delga, M., Bordet, P., et al., Livre a la Memoire du Professeur Paul Fallot, Vol. 1: Memoire Hors-Serie de la Societe Geologique de France, Paris.

Kligfield, R., 1979, The Northern Apennines as a collisional orogen: American Journal of Science, Vol. 279, p.676-691.

Kligfield, R., Hunziker, J., Dallmeyer, R.D., and Schamel, S., 1986, Dating of deformation phases using K-Ar and 40Ar/39Ar techniques: results from the Northern Apennines: Journal of Structural Geology, Vol. 8, p.781-798.

Klitgord, K.D. and Schouten, H., 1982, Early Mesozoic Atlantic reconstructions from sea-floor-spreading data: EOS, Vol. 63, p.307.

_____ and _____, 1986, Plate kinematics of the Central Atlantic: in Vogt, P.R and Tucholke, B.E., (eds.), The Geology of the North America, Vol. M, The Western North Atlantic Region: Geological Society of America-Decade of North American Geology Series, p.351-378.

Knott, S.D., 1987, The Liguride Complex of Southern Italy - a Cretaceous to Paleogene accretionary wedge: Tectonophysics, Vol. 142, p.217-226.

_____, 1988, Structure, sedimentology, and petrology of an ophiolitic flysch terrain, Calabria, south Italy: D. Phil. thesis, Oxford University, 240pp.

Kornprobst, J., 1973, Petrographical study of "acoustic basement" and associated breccia at Site 121-Western Alboran Basin: a comparison with the Betico-Rifean basement: in Ryan, W.B.F., Hsu, K.J., et al., Initial Reports of the Deep Sea Drilling Project, Vol. 13, part 2: U.S. Government Printing Office, Washington, D.C., p.759-761.

Kristoffersen, Y., 1978, Sea floor spreading and the early opening of the Atlantic: Earth and Planetary Science Letters, Vol. 38, p.273-290.

_____ and Talwani, M., 1977, Extinct triple junction south of Greenland and the Tertiary motion of Greenland relative to North America: Bulletin of the Geological Society of America, Vol. 88, p.1,037-1,049.

LaBreque, J.L., Kent, D.V., and Cande, S.C., 1977, Revised magnetic time scale for Late Cretaceous and Cenozoic time: Geology, Vol. 5, p.330-335.

Ladd, J.W., 1974, South Atlantic Sea-floor Spreading and Caribbean Tectonics: Ph.D. Thesis, Columbia University, New York, 251pp.

_____, 1976, Relative motion of South America with respect to North America and Caribbean tectonics: Bulletin of the Geological Society of America, Vol. 87, p. 969-976.

_____ and Sheridan, R.E., 1987, Seismic stratigraphy of the Bahamas: American Association of Petroleum Geologists Bulletin, Vol. 71, p.719-736.

Lancelot, J.R., Reille, J.L., and Wezel, F.C., 1977, Etude morphologique et radiochronologique de zircons detritiques des flyschs "numidien" et "greso-micace": consequences paleogeographiques a l'echelle de la Mediterranee occidentale: Bulletin de la Societe Geologique de France: Vol. 29, p.773-780.

Lancelot, Y. and Seibold, E., 1977, The evolution of the central northeastern Atlantic-summary of the results of DSDP Leg 41: in Lancelot, Y., Seibold, E., et al., Initial Reports of the Deep Sea Drilling Project, Vol. 41: U.S. Government Printing Office, Washington, D.C., p.1,215-1,245.

Larson, R.L. and Pitman, W.C., III, 1972, World-wide correlation of Mesozoic magnetic anomalies and its implications: Bulletin of the Geological Society of America, Vol. 83, p.3,645-3,662.

_____ and Hilde, T.W.C., 1975, A revised time scale of magnetic anomalies for the Early Cretaceous and Late Jurassic: Journal of Geophysical Research, Vol. 80, p.2,586-2,594.

Laubscher, H.P., 1985, Large-scale, thin-skinned thrusting in the Southern Alps: Geological Society of America Bulletin, Vol. 96, p.710-718.

Laubscher, H.P. and Bernoulli, D., 1977, Mediterranean and

Tethys: in Nairn, A.E.M., Kanes, W.H., and Stehli, F.G., (eds.), The Ocean Basins and Margins, Vol. 4A, The Eastern Mediterranean: Plenum Press, New York, p.1-28.

Laughton, A.S., 1971, South Labrador Sea and the Evolution of the North Atlantic: Nature, Vol. 232, p.612-617.

_____, 1972, The Southern Labrador Sea - a key to the Mesozoic and Early Tertiary evolution of the North Atlantic: in Laughton, A.S. et al., Initial Reports of the Deep Sea Drilling Project, Vol. 12: U.S. Government Printing Office, Washington, D.C., p.1155-1179.

_____, 1975, General Bathymetric Chart of the Oceans, Sheet 5.05, 1:10,000,000: Canadian Hydrographic Service, Ottawa, Canada.

_____ and Whitmarsh, R.B., 1974, The Azores-Gibraltar plate boundary: in Kristjansson, J., (ed.), Geodynamics of Iceland and the North Atlantic Area: Reidel Publishing Co., Holland, p.63-81.

_____ and Monahan, D., 1978, General Bathymetric Chart of the Oceans (GEBCO), Sheet 5.04, 1:10,000,000: Canadian Hydrographic Service, Ottawa, Canada.

_____, Roberts, D.G., and Graves, R., 1975, Bathymetry of the Northeast Atlantic, 1:2,400,000: Institute of Oceanographic Services, Wormley, Surrey, 4 Sheets.

_____, _____, and _____, 1975, Bathymetry of the Northeast Atlantic: Mid-Atlantic Ridge southwest to Europe: Deep-Sea Research, Vol. 22, p.791-810.

Lavecchia, G., 1985, Il sovrascorrimento dei Monti Sibillini analisi cinematica e strutturale: Bollettino della Societa Geologica Italiana, Vol. 104, p.161-194.

_____, 1988, The Tyrrhenian-Apennines system: structural setting and seismotectogenesis: Tectonophysics, Vol. 147, p.263-296.

Laville, E. and Petit, J.-P., 1984, Role of synsedimentary strike-slip faults in the formation of Moroccan Triassic basins: Geology, Vol. 12, p.424-427.

Leblanc, D., 1980, L'accident du Nekor et la structure du Rif oriental (Moroc): Revue de Geologie Dynamique et de Geographie Physique, Vol. 22, p.267-277.

_____ and Olivier, P., 1984, Role of strike-slip faults in the Betic-Rifian orogeny: Tectonophysics, Vol. 101, p.345-355.

Lefort, J.P., 1979, Iberian-Amorican arc and Hercynian orogeny in Western Europe: Geology, Vol. 7, p.384-388.

_____, 1980, Un "fit" structurale de l'Atlantique Nord: Arguments geologiques pour correler les marqueurs geophysiques reconnus sur les deux marges: Marine Geology, Vol. 37, p.355-369.

_____, Peucet, J.J., Denuff, J., and Le Herisse, A,, 1985, The Goban Spur Paleozoic basement: in de Graciansky, P.C., Poag, P.C., et al., Initial Reports of the Deep Sea Drilling Project, Vol. 80, Pt. 1: U.S. Government Printing Office, Washington, D.C., p.677-679.

Leg 107 Shipboard Party, 1986, A microcosm of ocean basin evolution in the Mediterranean: Nature, Vol. 321, p.383-384.

Lemoine, M., Bas, T., Arnaud-Vanneau, A., Arnaud, H., Dumont, T., Gidon, M., Bourbon, M., de Graciansky, P.C., Rudkiewicz, J.L., Megard-Galli, J., Tricart, P., 1986, The continental margin of the Mesozoic Tethys in the Western Alps: Marine and Petroleum Geology, Vol. 3, p.179-199.

Le Pichon, X., 1968, Sea-floor spreading and continental drift: Journal of Geophysical Research, Vol. 73, p.3,661-3,697.

_____ and Fox, P.J., 1971, Marginal offsets, fracture zones, and the early opening of the North Atlantic: Journal of Geophysical Research, Vol. 76, p.6,294-6,308.

_____ and Sibuet, J.C., 1971, Western extension of boundary between European and Iberian plates during the Pyrenean orogeny: Earth and Planetary Science Letters, Vol. 11, p.83-88.

_____, Pautot, G., and Weill, J.P., 1972, Opening of the Alboran Sea: Nature Physical Science, Vol. 236, p.83-85.

_____, Francheteau, J., and Bonnin, J., 1973, Plate Tectonics: Elsevier Publishing, New York, 300pp.

_____, Sibuet, J.-C., and Francheteau, J., 1977, The fit of the continents around the North Atlantic ocean: Tectonophysics., Vol. 38, p.169-209.

Letouzey, J., 1986, Cenozoic paleo-stress pattern in the Alpine Foreland and structural interpretation in a platform basin: Tectonophysics, Vol. 132, p.215-231.

Lister, G.S., Etheridge, M.A., and Symonds, P.A., 1986, Detachment faulting and the evolution of passive continental

margins: Geology, Vol. 14, p.246-250.

Livermore, R.A. and Smith, A.G., 1985, Some boundary conditions for the evolution of the Mediterranean region: in Stanley, D.J. and Wezel, F.C., (eds.), Geological Evolution of the Mediterranean Basin: Springer-Verlag, New York, p.83-98.

McCaig, A., 1986, Thick- and thin-skinned tectonics in the Pyrenees: Tectonophysics, Vol. 129, p.319-342.

McGregor, B.A. and Krause, D.C., 1972, Evolution of the sea floor in the Corner Seamounts area: Journal of Geophysical Research, Vol. 77, p.2,526-2,534.

_____, Betzer, P.R., and Krause, D.C., 1973, Sediments in the Atlantic Corner Seamounts: control by topographic, paleo-winds, and geochemically-detected modern bottom currents: Marine Geology, Vol. 14, p.179-190.

McHone, J.G., 1978, Distribution, orientation, and ages of mafic dikes in central New England: Bulletin of the Geological Society of America, Vol. 89, p.1,645-1,655.

McKenzie, D., 1978, Some remarks on the development of sedimentary basins: Earth and Planetary Science Letters: Vol. 40, p.25-32.

_____ and Parker, R.L., 1967, The North Pacific: an example of tectonics on a sphere: Nature, Vol. 216, p.1,276-1,280.

Makel, G.H., Rondeel, H.E., and Vandenberg, J., 1984, Triassic paleomagnetic data from the Subbetic and the Malaguide Complex of the Betic Cordilleras (southeast Spain): Tectonophysics, Vol. 101, p.131-141.

Malinverno, A. and Ryan, W.B.F., 1986, Extension in the Tyrrhenian Sea and shortening in the Apennines as a result of arc migration driven by sinking of the lithosphere: Tectonics, Vol. 5, p.227-245.

Manspeizer, W., Puffer, J.H., and Cousminer, H.L., 1978, Separation of Morocco and eastern North America: a Triassic-Liassic stratigraphic record: Bulletin of the Geological Society of America, Vol. 89, p.901-920.

Martin-Algarra, A., Sanz de Galdeano, C., and Estevez, A., 1988, L'evolution sedimentaire miocene de la region au nord de la Sierra Arana (Cordilleres betiques) et sa relation avec la mise en place du bloc d'Alboran: Bulletin de la Societe Geologique de France, Vol. 4, p.119-127.

Martinis, B. and Pavan, G., 1967, Note illustrative della Carta Geologica d'Italia alla scala 1:100,000, Foglio 157, Mont Sant'Angelo: Servizio Geologico d'Italia, Roma, 56pp.

Masson, D.G. and Miles, P.R., 1984, Mesozoic seafloor spreading between Iberia, Europe, and North America: Marine Geology, Vol. 56, p.279-287.

Mattauer, M. and Henry, J., 1974, Pyrenees: in Spencer, A.M., (ed.), Mesozoic-Cenozoic Orogenic Belts: Data for Orogenic Studies: Geological Society of London Special Publication #4, Scottish Academic Press, Edinburgh, p.3-22.

_____, Tapponnier, P., and Proust, F., 1977, Sur les mecanismes de formation des chaines intracontinentales. L'exemple des chanes atlasiques du Maroc: Bulletin de la Societe Geologique de France, Vol. 19, p.521-526.

Matthews, D.H., Laughton, A.S., Pugh, D.T., Jones, E.J.W., Sunderland, J., Takin, M. and Bacon, M., 1969, Crustal structure and origin of Peake and Freen Deeps, NE Atlantic: Geophysical Journal of the Royal Astronomical Society, Vol. 18, p.517-542.

May, P.D., 1971, Patterns of Triassic-Jurassic diabase dikes around the North Atlantic in the context of pre-drift positions of the continents: Bulletin of the Geological Society of America, Vol. 82, p.1,285-1,292.

Medialdea, T., Surinach, E., Vegas, R., Banda, E., and Ansorge, J., 1986, Crustal structure under the western end of the Betic Cordillera (Spain): Annales Geophysicae, Vol. 4B, p.457-464.

Megias, A.G., 1982, La evolucion del Mar de Alboran y Cadenas Betico-Maghrebides durante el Neogeno: Quinto Congreso Latinoamericano de Geologica, Argentina, Actas, Vol. 2, p.329-340.

Megson, J., 1987, The evolution of the Rockall Trough and implications for the Faeroe-Shetland Trough: in Brooks, J. and Glennie, K., (eds.), Petroleum Geology of North West Europe: Graham and Trotman, London, p.653-665.

Miall, A.D., 1986, The Eureka Sound Group (Upper Cretaceous-Oligocene), Canadian Arctic Islands: Bulletin of the Canadian Society of Petroleum Geologists, Vol. 34, p.240-270.

Monie, P., Maluski, H., Saadallch, A., and Caby, R., 1988, New 39 Ar-40Ar ages of Hercynian and Alpine thermotectonic events in Grande Kabylie (Algeria): Tectonophysics, Vol. 152, p.53-69.

Montadert, L., Winnock, E., Deltiel, J.R., and Grau, G., 1974,

Continental margins of Galicia-Portugal and Bay of Biscay: in Burk, C.A. and Drake, C.L., (eds.), The Geology of Continental Margins: Springer-Verlag, New York, p.323-342.

_____, Roberts, D.G., De Charpal, O., and Guennoc, P., 1979, Rifting and subsidence of the northern continental margin of the Bay of Biscay: in Montadert, L., Roberts, D.G., et al., Initial Reports of the Deep Sea Drilling Project, Vol. 48: U.S. Government Printing Office, Washington, D.C., p.1,025-1,060.

Montenat, C., Bizon, G., and Bizon, J.J., 1975, Remarques sur le Neogene du forage JOIDES 121 et mer d'Alboran (Mediterranee occidentale): Bulletin de la Societe Geologique de France, Vol. 18, p.45-51.

_____, _____, _____, Carbonnel, G., Muller, C., and de Reneville, P., 1976, Continuite ou discontinuite de sedimentation marine mio-pliocene en Mediterranee occidentale: l'exemple du Bassin du Vera (Espagne meridionale): Revue de l'Institut Francais du Petrole, Vol. 31, p.613-663.

Montigny, R., Edel, J.B., and Thuizat, R., 1981, Oligo-Miocene rotation of Sardinia: K-Ar ages and paleomagnetic data of Tertiary volcanics: Earth and Planetary Science Letters, Vol. 54, p.261-271.

Morelli, C. and Nicholich, R., 1980, The structure of the Western Mediterranean basins from marine geophysical data: in Udias, A. and Channel, J., (eds.), Evolution and Tectonics of the Western Mediterranean and Surrounding Areas: Instituto Geografico Nacional Publicacione 201, Madrid, p.1-65.

Morgan, J.W., 1968, Rises, trenches, great faults, and crustal blocks: Journal of Geophysical Research, Vol. 73, p.1,959-1,982.

Morley, C.K., 1987, Origin of a major cross-element zone: Moroccan Rif: Geology, Vol. 15, p.761-764.

Moreau, M.G., Feinberg, H., and Pozzi, J.P., 1985/86, Magnetostratigraphy of a Late Miocene section from the Moroccan Atlantic margin: Earth and Planetary Science Letters, Vol. 76, p.167-175.

Mostardini, F. and Merlini, S., 1986, Appennino centro-meridionale: sezione geologiche e proposta di modello strutturale: AGIP, 73rd Congresso della Societa Geologica Italiana, Roma, 59pp.

Mountrakis, D., 1986, The Pelagonian Zone in Greece: a polyphase-deformed fragment of the Cimmerian continent and its role in

the geotectonic evolution of the Eastern Mediterranean: Journal of Geology, Vol. 94, p.335-347.

Muller, D.W. and Hsu, K.J., 1987, Event stratigraphy and paleoceanography in the Fortuna Basin (southeast Spain): a scenario for Messinian Salinity Crisis: Paleoceanography, Vol. 2, p.679-696.

Mullins, H.T. and Lynts, G.W., 1977, Origin of the northwestern Bahama Platform: review and interpretation: Bulletin of the Geological Society of America, Vol. 88, p.1,447-1,461.

Ness, G., Levi, S., and Couch, R., 1980, Marine magnetic anomaly time scales for the Cenozoic and Late Cretaceous: a precis, critique, synthesis: Reviews of Geophysics and Space Physics, Vol. 18, p.753-770.

Nesteroff, W.D., 1973, The sedimentary history of the Mediterranean area during the Neogene: in Ryan, W.B.F., Hsu, K.J., et al., Initial Reports of the Deep Sea Drilling Project, Vol. 13, part 2: U.S. Government Printing Office, Washington, D.C., p.1,257-1,261.

_____, Wezel, F.C., and Pautot, G., 1973, Summary of lithostratigraphic findings and problems: in Ryan, W.B.F., Hsu, K.J., et al., Initial Reports of the Deep Sea Drilling Project, Vol. 13, p.1,0021-1,040.

Neurdin-Trescartes, J., 1985, Silico-clastic deposits and synsedimentary tectonics in the lower Chelif Basin (Northwestern Algeria): Abstracts, Sixth European Regional Meeting of International Association of Sedimentologists, Lleida, Spain, p.325-328.

Nunns, A.G., 1982, Plate tectonic evolution of the Greenland-Scotland Ridge and surrounding regions: in Bott, M.H.P., Saxov, S., Talwani, M., and Thiede, J., (eds.), Structure and Development of the Greenland-Scotland Ridge: New Methods and Concepts: Plenum Press, New York, p.11-29.

_____ and Peacock, J.H., 1982, Correlation, identification, and inversion of magnetic anomalies in the Norway Basin: Earth Evolution Sciences, Vol. 2, p.130-138.

Ogniben, L., 1964, Arenarie tipo Taveyannaz in Sicilia: Geologica Romana, Vol. 3, p.125-170.

_____, 1969, Schema introduttivo alla geologia del confine calabro-lucano: Memorie della Societa Geologica Italiana, Vol. 8, p.453-763.

_____, 1985, Relazione sul Modello Geodinamico

"Conservativo" dell Regione Italiana, ENEA, Rome, 357pp.

_____, Parotto, M., and Praturlon, A., 1975, Structural Model of Italy: Quaderni de la Ricerca Scientifica, Vol. 90, 502pp.

Olivier, P., 1981-82, L'accident de Jebha-Chrafate (Rif, Maroc): Revue de Geologie Dynamique et de Geographie Physique, Vol. 23, p.97-106.

Olivet, J.L., Pautot, G., and Auzende, J.M., 1973, Structural framework of selected regions of the Western Mediterranean-Alboran Sea: in Ryan, W.B.F., Hsu, K.J., et al., Initial Reports of the Deep Sea Drilling Project, Vol. 13, part 2: U.S. Government Printing Office, Washington, D.C., p.1,417-1,430.

_____, LePichon, X., Monti, S., and Sichler, B., 1974, Charlie-Gibbs Fracture Zone: Journal of Geophysical Research, Vol. 79, p.2,059-2,072.

_____, Bonnin, J., Beuzart, P., and Auzende, J.M., 1984, Cinematique de l'Atlantique nord et central: Rapports Scientifique et Techniques No. 54: CNEXO, Paris, 108pp.

Oversby, V.M., Lancelot, J., and Gast, P.W., 1971, Isotopic composition of lead in volcanic rocks from Tenerife, Canary Islands: Journal of Geophysical Research, Vol. 76, p.3,402-3,413.

Pacquet, J., 1969, Etude Geologique de L'ouest de la Province de Murcie (Espagne): Memoire de la Societe Geologique de France No. 111 (Nouvelle Serie), Paris, 270pp.

Parsons, B. and Sclater, J.G., 1977, An analysis of the variation of ocean floor bathymetry and heat flow with age: Journal of Geophysical Research, Vol. 82, p.803-827.

Pellitier, B.R., 1971, A granodiorite drill core from the Flemish Cap, eastern Canadian continental margin: Canadian Journal of Earth Sciences, Vol. 8, p.1,499-1,503.

Perconig, E., 1960-62, Sur la constitution geologique de l'Andalousie occidentale en particulier du Bassin du Guadilquivir (Espagne meridionale): in Durand-Delga, M., Bordet, P., et al., Livre a la Memoire du Professeur Paul Fallot, Vol. 1: Memoire Hors-Serie de la Societe Geologique de France, Paris, p.229-256.

_____ and Martinez Diaz, C., 1977, Perspectivas petroliferas de Andalucia Occidental: Boletin Geologico y Minero, Vol. 88, p.417-433.

Perrone, V., 1982, Considerazione sulla trasgressione del Miocene inferiore sulla Piattaforma Carbonatica campano-lucana: Rendiconti della Societa Geologica Italiana, Vol. 4, p.369-372.

Perthuisot, V., 1981, Diapirism in northern Tunisia: Journal of Structural Geology, Vol. 3, p.231-235.

Pescatore, T., 1978, Evoluzione tettonica del Bacino Irpino (Italia meridionale) durante il Miocene: Bollettino della Societa Geologica Italiana: Vol. 97, p.783-805.

Peterson, M.N.A., Edgar, N.T., von der Bosch, C., Cita, M.B., Gartner, S., Goll, R., and Nigrini, C., 1970, Site 10: in Peterson, M.N.A., Edgar, N.T., et al., Initial Reports of the Deep Sea Drilling Project, Vol. 2: U.S. Government Printing Office, Washington, D.C., p.117-225.

Peybernes, B. and Souquet, P., 1984, Basement blocks and tecto-sedimentary evolution in the Pyrenees during Mesozoic times: Geological Magazine, Vol. 121, p.397-405.

Phillips, J.D. and Forsyth, D., 1972, Plate tectonics, paleomagnetism, and the opening of the Atlantic: Bulletin of the Geological Society of America, Vol. 83, p.1,579-1,600.

Pieri, M, 1987, Three seismic profiles across the Po Plain: in Bally, A.W., (ed.), Atlas of Seismic Stratigraphy: American Association of Petroleum Geologists Studies in Geology #27, Part 3, Tulsa, Okla., p.90-110.

_____ and Mattavelli, L., 1986, Geologic framework of Italian petroleum resources: American Association of Petroleum Geologists Bulletin, Vol. 70, p.103-130.

Pindell, J.L., 1985, Alleghanian reconstruction and subsequent evolution of the Gulf of Mexico, Bahamas, and proto-Caribbean: Tectonics, Vol. 4, p.1-39.

Pindell, J.L., Cande, S.C., Pitman, W.C., III, Rowley, D.B., Dewey, J.F., LaBreque, J., and Haxby, W., 1988, A plate-kinematic framework for models of Caribbean evolution: Tectonophysics, Vol. 155, p.121-138.

Pirsson, C.V., 1914, Geology of Bermuda Island; the igneous platform: American Journal of Science, Vol. 38, p.189-206.

Pitman, W.C., III and Talwani, M., 1972, Sea-floor spreading in the North Atlantic: Bulletin of the Geological Society of America, Vol. 83, p.619-646.

Platt, J.P., Behrmann, J.H., Cunningham, P.C., Dewey, J.F., Helman, M.L., Parish, M., Shepley, M., Wallis, S., and Weston, P., 1989, Kinematics of the Alpine arc and the motion history of Adria: Nature, Vol. 337, p.158-161.

_____ and Vissers, R.L.M., 1989, Extensional collapse of thickened continental lithosphere: a working hypothesis for the Alboran Sea and Gibraltar Arc: Geology, Vol. 17, p.540-543.

Pratt, R.M., 1963, Great Meteor Seamount: Deep-Sea Research, Vol. 10, p.17-25.

Puigdefabregas, C. and Souquet, P., 1986, Tecto-sedimentary cycles and depositional sequences of the Mesozoic and Tertiary from the Pyrenees: Tectonophysics, Vol. 129, p.173-203.

Purdy, G.M., 1975, The eastern end of the Azores-Gibraltar plate boundary: Geophysical Journal of the Royal Astronomical Society, Vol. 43, p.973-1,000.

Rabinowitz, P.D., Cande, S.C., and Hayes, D.E., 1978, Grand Banks and J-Anomaly Ridge: Science, Vol. 202, p.71-73.

Ramsay, J.G. and Graham, R.H., 1970, Strain variation in shear belts: Canadian Journal of Earth Sciences, Vol. 7, p.786-813.

Raymond, C.A. and LaBreque, J.L., 1987, Magnetization of the oceanic crust: thermoremnant magnetization or chemical remnanent magnetization?: Journal of Geophysical Research, Vol. 92, p.8,077-8,088.

Raymond, D., 1977, Structure et evolution alpine d'un segment interne de l'oregene maghrebin: le Nord-Ouest de la Grande Kabylie (Algerie): Bulletin de la Societe Geologique de France, Vol. 19, p.797-804.

Rehault, J.P., Boillot, G., and Mauffret, A., 1984, The Western Mediterranean Basin geological evolution: Marine Geology, Vol. 55, p.447-477.

Reis, A.C., 1978, The opening of the Bay of Biscay - a review: Earth-Science Reviews, Vol. 14, p.35-63.

Reynolds, D.J., 1984, Structural and dimensional repetition in continetal rifts: M.S. thesis, Duke University, North Carolina, 175pp.

Reynolds, P.H. and Aumento, F., 1974, Deep drill 1972, potassium-argon dating of Bermuda drill core: Canadian Journal of Earth Sciences, Vol. 11, p.1,269-1,273.

Roberts, D.G., Matthews, D.H., and Eden, R.A., 1972, Metamorphic rocks from the southern end of the Rockall Bank: Journal of the Geological Society of London, Vol. 128, p.501-506.

_____, Masson, D.G., and Miles, P.R., 1981, Age and structure of the southern Rockall Trough: new evidence: Earth and Planetary Science Letters, Vol. 52, p.115-128.

_____, Backman, J., Morton, A.C., Murray, J.W., and Keene, J.R., 1984, Evolution of volcanic rifted margins: synthesis of Leg 81 results on the western margin of the Rockall Plateau: in Roberts, D.G., Schnitker, D., et al., Initial Reports of the Deep Sea Drilling Project, Vol. 81: U.S. Government Printing Office, Washington, D.C., p.883-911.

Rod, E., 1962, Fault pattern, northwest corner of Sahara Shield: American Association of Petroleum Geologists Bulletin, Vol. 46, p.529-534.

Roeser, H., 1982, Magnetic anomalies in the magnetic quiet zone off Morocco: in Von Rad, U., Hinz, K., Sarnthein, M., and Siebold, E., (eds.), Geology of the Northwest African Continental Margin: Springer-Verlag, New York, p.60-68.

Rona, P.A. and Richardson, E.S., 1978, Early Cenozoic global plate reorganization: Earth and Planetary Science Letters, Vol. 40, p.1-11.

_____, Brakl, J., and Heirtzler, J.R., 1970, Magnetic anomalies in the northeast Atlantic between the Canary and Cape Verde Islands: Journal of Geophysical Research, Vol. 75, p.7,412-7,420.

Rondeel, H.E. and Simon, O.J., 1974, Betic Cordilleras: in Spencer, A.M., (ed.), Mesozoic-Cenozoic Orogenic Belts: Data for Orogenic Studies: Geological Society of London Special Publication #4, Scottish Academic Press, Edinburgh, p.23-35.

Rosendahl, B.R., 1987, Architecture of continental rifts with special reference to East Africa: Annual Review of Earth and Planetary Sciences, Vol. 15, p.445-503.

Rossi, S. and Sartori, R., 1981, A seismic reflection study of the external Calabrian Arc in the northern Ionian Sea (Eastern Mediterranean): Marine Geophyical Research, Vol. 4, p.403-426.

Ruffman, A. and Van Hinte, J., 1973, Orphan Knoll-a "chip" off the North American "plate": in Hood, P.J., (ed.), Earth Science Symposium on Offshore Eastern Canada: Geological Survey of Canada Paper 71-23, Ottawa, p.407-449.

Ryan, W.B.F., Stanley, D.J., Hersey, J.B., Fahlquist, D.A., and

Allen, T.D., 1970, The tectonics and geology of the Mediterranean Sea: in Maxwell, A.E., (ed.), The Sea, Vol. 4, Part 2, Wiley-Interscience, New York, p.387-492.

Sander, N.J., 1970, Structural evolution of the Mediterranean region during the Mesozoic era: in Alvarez, W. and Gohrbandt, K.H.A., (eds.), Geology and History of Sicily: Petroleum Exploration Society of Libya, Tripoli, p.43-132.

Savelli, C., Beccaluva, L., Beriu, M., Macciotta, G., and Maccioni, L., 1979, K-Ar chronology of the Tertiary "calcalic" volcanism of Sardinia (Italy): Journal of Volcanology and Geothermal Research, Vol. 5, p.257-269.

Savostin, L.A., 1981, Cenozoic Plate Tectonics of the Arctic Region, Northeastern, and Inner Asia and Paleogeodynamic Reconstructions in the Global Scale: Thesis, Sci. Inst. Oceanol. Moscow, 498pp., (in Russian).

_____ and Karasik, A.M., 1981, Recent tectonics of the Arctic Basin and of northeastern Asia: Tectonophysics, Vol. 74, p.111-145.

_____, Sibuet, J.-C., Zonenshain, L.P., Le Pichon, X., and Roulet, M.J., 1986, Kinematic evolution of the Tethys belt from the Atlantic Ocean to the Pamirs since the Triassic: Tectonophysics, Vol. 123, p.1-35.

Scandone, P., 1979, Origin of the Tyrrhenian Sea and the Calabrian Arc: Bollettino della Societa Geologica Italiana, Vol. 98, p.27-34.

_____, Giunta, G., and Liguori, V., 1974, The connection between the Apulia and Sahara continental margins in the Southern Apennines and in Sicily: 24 Congres-Assemblee Plenaire C.I.E.S.M. Committee Geologique et Geophysique Marines, Monte Carlo, 4-6 Dec. 1974.

Schenk, P.E., 1971, Southeastern Atlantic Canada, northwestern Africa, and continental drift: Canadian Journal of Earth Science, Vol. 8, p.1,861-1,881.

Schlager, W. and Ginsburg, R.N., 1981, Bahama carbonate platform-the deep and the past: Marine Geology, Vol. 44, p.1-24.

Schouten, H. and Klitgord, K.D., 1982, The memory of the accreting plate boundary and the continuity of fracture zones: Earth and Planetary Science Letters, Vol. 59, p.255-266.

_____, Srivastava, S.P., and Klitgord, K.M., unpublished manuscript, Iberian plate kinematics: the African connection: 13pp. plus figures.

Schwander, M.M., 1987, The Southern Adriatic Basin, offshore Italy: in Bally, A.W., (ed.), Atlas of Seismic Stratigraphy: American Association of Petroleum Geologists Studies in Geology #27, Part 3, Tulsa, Okla., p.112-115.

Sclater, J.G. and Wixon, L., 1986, The relationship between depth and age and heat flow and age in the western North Atlantic: in Vogt, P.R. and Tucholke, B.E., (eds.), The Geology of North America, Vol. M, The Western North Atlantic Region: Geological Society of America - Decade of North American Geology Series, p.257-270.

_____, Hellinger, S., and Tapscott, C., 1977, The paleo-bathymetry of the Atlantic Ocean from the Jurassic to the present: Journal of Geology, Vol. 85, p.509-522.

Searle, R.C., 1979, Side-scan sonar studies of North Atlantic fracture zones: Journal of the Geological Society of London, Vol. 136, p.283-292.

_____, 1980, Tectonic pattern of the Azores spreading center and triple junction: Earth and Planetary Science Letters, Vol. 51, p.415-434.

_____, 1981, The active part of the Charlie-Gibbs Fracture Zone: a study using sonar and other geophysical techniques: Journal of Geophysical Research, Vol. 86, p.243-262.

_____ and Whitmarsh, R.B., 1978, The structure of King's Trough, Northeast Atlantic, from bathymetric, seismic and gravity studies: Geophysical Journal of the Royal Astronomical Society, Vol. 53, p.259-287.

_____, Monahan, D., and Johnson, G.L., 1982, General Bathymetric Chart of the Oceans (GEBCO), Sheet 5.08, 1:10,000,000: Canadian Hydrographic Service, Ottawa, Canada.

Selli, R., 1962, Il Paleogene nel quadro della geologia dell'Italia centro-meridionale: Memorie della Societa Geologica Italiana, Vol. 3, p.737-789.

Sengor, A.M.C., 1984, The Cimmeride Orogenic System and the Tectonics of Eurasia: Geological Society of America Special Paper #195, Boulder, Colo., 82pp.

Servizio Geologico d'Italia (SGI), 1983, Carta Geologica d'Italia, 1:500,000, 5 sheets.

Seufert, G., 1988, Jurassic sediments and synsedimentary tectonics in the Central High Atlas, Morocco: Bulletin de la Societe Geologique de France, Vol. 4, p.375-390.

Shackleton, R.M. and Ries, A.C., 1984, The relationship between regionally consistent stretching lineations and plate motions: Journal of Structural Geology, Vol. 6, p.111-117.

Shipboard Scientific Party, 1987, Site 608: in Ruddiman, W.F., Kidd, R.B., et al., Initial Reports of the Deep Sea Drilling Project, Vol. 94, Pt. 1: U.S. Government Printing Office, Washington, D.C., p.149-246.

Smith, A.G., 1971, Alpine deformation and the oceanic areas of the Tethys, Mediterranean, and Atlantic: Bulletin of the Geological Society of America, Vol. 82, p.2,039-2,070.

Souquet, P., Peybernes, B., Bilotte, M., and Debroas, E.J., 1977, La Chaine Alpine des Pyrenees: Geologie Alpine, Vol. 53, p.193-216.

Spakman, W., 1986, Subduction beneath Eurasia in connection with the Mesozoic Tethys: Geologie en Mijnbouw, Vol. 65, p.145-153.

Srivastava, S.P., 1978, Evolution of the Laborador Sea and its bearing on the early evolution of the North Atlantic: Geophysical Journal of the Royal Astronomical Society, Vol. 52, p.313-357.

_____ and Tapscott, C.R., 1986, Plate kinematics of the North Atlantic: in Vogt, P.R. and Tucholke, B.E., (eds.), The Geology of North America, Vol. M, The Western North Atlantic Region: Geological Society of America-Decade of North American Geology Series, p.379-404.

Staub, R., 1924, Der Bau des Alpen: Beitr. Geologie Karte Schweiz, Vol. 52, p.272.

Stebbins, J. and Thompson, G., 1978, The nature and petrogenesis of intra-oceanic plate alkaline eruptive and plutonic rocks: King's Trough, Northeast Atlantic: Journal of Volcanology and Geothermal Research, Vol. 4, p.333-361.

Steiger, R.H. and Frick, U., 1973, Isotopic dating of Alboran "basement": in Ryan, W.B.F., Hsu, K.J., et al., Initial Reports of the Deep Sea Drilling Project, Vol. 13, part 2: U.S. Government Printing Office, Washington, D.C., p.762.

Sullivan, K.D., 1983, The Newfoundland Basin: ocean-continent boundary and Mesozoic seafloor spreading history: Earth and Planetary Science Letters, Vol. 62, p.321-339.

_____ and Keen, C.E., 1977, Newfoundland Seamounts: in Baragar, W.R.A., Coleman, L.C., and Hall, J.M., (eds.), Volcanic Regimes of Canada: Geological Association of Canada

Special Paper 16, p.461-476.

Tadili, B., Ramdani, M., Ben Sari, D., Chapochnikov, K., and Bellot, A., 1985, Structure de la croute dans le nord du Maroc: Annales Geophysicae, Vol. 4B, p.99-104.

Talwani, M. and Eldholm, O., 1977, Evolution of the Norwegian-Greenland Sea: Bulletin of the Geological Society of America, Vol. 88, p.969-999.

Tankard, A.J. and Welsink, H.J., 1987, Extensional tectonics and stratigraphy of Hibernia Oilfield, Grand Banks, Newfoundland: American Association of Petroleum Geologists Bulletin, Vol. 71, p.1,210-1,232.

Termier, P., 1903, Les nappes des Alpes orientales et la synthese des Alpes: Bulletin de la Societe Geologique de France, Vol. 3, p.711-765.

Todd, B.J., Reid, I., and Keen, C.E., 1988, Crustal structure across the Southwest Newfoundland Transform Margin: Canadian Journal of Earth Science, Vol. 25, p.744-759.

Torres-Roldan, R.L., 1979, The tectonic subdivision of the Betic Zone (Betic Cordilleras, Southern Spain): its significance and one possible geotectonic scenario for the westernmost Alpine belt: American Journal of Science, Vol. 279, p.19-51.

Treves, B., 1984, Orogenic belts as accretionary prisms: the example of the Northern Apennines: Ofiolit, Vol. 9, p.577-618.

Trumpy, R., 1973, The timing of orogenic events in the Central Alps: in de Jong, K.H. and Schoulten, R., (eds.), in Gravity and Tectonics: John Wiley and Sons, New York, p.229-251.

_____, 1980, Geology of Switzerland: Wepf and Co., Basel, 104pp.

_____, 1982, Alpine paleogeography: a reappraisal: in Hsu, K.J., (ed.), Mountain Building Processes: Academic Press, London, p.149-156.

_____ and Niggli, E., 1980, Central Alps: in Aubouin, J., Debelmas, J., and Latreille, M., (eds.), Geologie des Chaines Alpines Issues de la Tethys: Memoire du Bureau de Recherches Geologiques et Minieres #115, Orleans, p.295-296.

Tucholke, B.E. and Vogt, P.R., 1979, Western North Atlantic: sedimentary evolution and aspects of tectonic history: in Tucholke, B.E., Vogt, P.R., et al., Initial Reports of the Deep Sea Drilling Project, Vol. 43: U.S. Government Printing Office, Washington, D.C., p.791-825.

_____ and Ludwig, W.J., 1982, Structure and origin of the J-Anomaly Ridge, western North Atlantic: Journal of Geophysical Research, Vol. 87, p.9,389-9,407.

_____ and McCoy, F.W., 1986, Paleogeographic and paleobathymetric evolution of the North Atlantic Ocean: in Vogt, P.R and Tucholke, B.E., (eds.), The Geology of the North America, Vol. M, The Western North Atlantic Region: Geological Society of America-Decade of North American Geology Series, p.589-602.

Turcotte, D.L., 1979, Flexure: Advances in Geophysics, Vol. 21, p.51-86.

Uchupi, E., Emery, K.O., Bowin, C.O., and Phillips, J.D., 1976, Continental margin off western Africa, Senegal to Portugal: American Association of Petroleum Geologists Bulletin, Vol. 60, p.809-878.

Udias, A., Lopez-Arroyo, A., and Mezuca, J., 1976, Seismo-tectonics of the Azores-Alboran region: Tectonophysics, Vol. 31, p.259-289.

United Nations Educational, Scientific, and Cultural Organization (UNESCO), 1968, Carte Tectonique Internationale de l'Afrique, 1:5,000,000, 9 sheets.

Vail, P.R., Mitchum, R.M., Jr., Thompson, S., III, 1977, Seismic stratigraphy and global changes of sea level, Part 3: Relative changes of sea level from coastal onlap: in Payton, C.E., (ed.), Seismic Stratigraphy: Applications to Hydrocarbon Exploration, American Association of Petroleum Geologists, Memoir #26, Tulsa, Okla., p.63-81.

Van Bemmelen, R.W., 1966, The structural evolution of the Southern Alps: Geologie en Mijnbouw, Vol. 45, p.405-444.

Van Bemmelen, R.W., 1973, Geodynamic models for the Alpine type of orogengy (test case II: the Alps in Central Europe): Tectonophysics, Vol. 18, p.33-79.

Van den Berg, J., 1979, Paleomagnetism and the Changing Configurations of the Western Mediterranean Area in the Mesozoic and Early Cenozoic: Ph.D. Thesis, University of Utrecht, The Netherlands, (Geologica Ultraiectina #20), 179pp.

Van Hinte, J., 1976a, A Cretaceous time scale: American Association of Petroleum Geologists Bulletin, Vol. 60, p.498-516.

_____, 1976b, A Jurassic time scale: American Association

of Petroleum Geologists Bulletin, Vol. 60, p.489-497.

van Wamel, W.A., 1987, On the tectonics of the Ligurian Apennines (northern Italy): Tectonophysics, Vol. 142, p.87-98.

Vanney, J.R. and Gennesseaux, M., 1985, Mediterranean seafloor features: overview and assessment: in Stanley, D.J. and Wezel, F.C., (eds.), Geological Evolution of the Mediterranean Basin: Springer-Verlag, New York, p.3-32.

Vegas, R. and Banda, E., 1982, Tectonic framework and alpine evolution of the Iberian peninsula: Earth Evolution Sciences, Vol. 4, p.320-343.

Verhoef, J., Collette, B.J., Miles, P.R., Searle, R.C., Sibuet, J.-C., and Williams, C.A., 1986, Magnetic anomalies in the Northeast Atlantic Ocean: Marine Geophysical Research, Vol. 8, p.1-25.

Vidal, J.C., 1977, Structure actuelle et evolution depuis le Miocene de la chaine rifaine (partie sud de l'arc de Gibraltar): Bulletin de la Societe Geologique de France, Vol. 19, p.789-796.

Vogt, P.R., 1971, Asthenosphere motion recorded by the ocean floor south of Iceland: Earth and Planetary Science Letters, Vol. 13, p.153-160.

_____ and Tucholke, B.E. (eds.), 1986, The Geology of the North America, Vol. M, The Western North Atlantic Region: GSA-DNAG Series, 696pp.

_____ and Avery, O.E., 1974, Detailed magnetic surveys in the Northeast Atlantic and Labrador Sea: Journal of Geophysical Research, Vol. 79, p.363-389.

_____, Johnson, G.L., Holcombe, T.L., Gilg, J.G. and Avery, O.E., 1971a, Episodes of sea-floor spreading recorded by the North Atlantic basement: Tectonophysics, Vol 12, p.211-234.

_____, Higgs, R.H., and Johnson, G.L., 1971b, Hypotheses on the origin of the Mediterranean basin: magnetic data: Journal of Geophysical Research, Vol. 76, p.3,207-3,227.

Waters, C., 1986, Evidence for Eocene strike-slip reactivation of Eoalpine compressive structures, Corsica: Abstracts, Tectonic Studies Group, Annual Meeting, Hull, U.K., p.65.

Weijermars, R., 1985, Uplift and subsidence history of the Alboran Basin and a profile of the Alboran Diapir (W. Mediterranean): Geologie en Mijnbouw, Vol. 64, p.349-356.

Welsink, H.J., Srivastava, S.P., and Tankard, A.J., 1988, Tectonic linkage between continental crust of the Grand Banks and oceanic crust during extension: Geological Association of Canada Annual Meeting Program with Abstracts, Vol. 13, p.A133.

Wernicke, B., 1985, Uniform-sense normal simple shear of the continental lithosphere: Canadian Journal of Earth Sciences, Vol. 22, p.108-125.

Wezel, F.C., 1970, Numidian flysch: an Oligocene-Miocene continental rise deposit off the African Platform: Nature, Vol. 228, p.275-276.

_____, 1985, Structural features and basin tectonics of the Tyrrhenian Sea: in Stanley, D.J. and Wezel, F.C., (eds.), Geological Evolution of the Mediterranean Basin: Springer-Verlag, New York, p.153-194.

White, R. and McKenzie, D., 1989, Magmatism at rift zones: the generation of volcanic continetal margins and flood basalts: Journal of Geophysical Research, Vol. 94, p.7,685-7,729.

_____ and Matthews, D.J., 1980, Variations in oceanic upper crustal structure in a small area of the north-east Atlantic: Geophysical Journal of the Royal Astronomical Society, Vol. 61, p.401-435.

Whitmarsh, R.B. and Calvert, A.J., 1986, Crustal structure of Atlantic fracture zones - 1.The Charlie-Gibbs Fracture Zone: Geophysical Journal of the Royal Astronomical Society, Vol. 85, p.107-138.

_____, Ginzburg, A., and Searle, R.C., 1982, The structure and origin of the Azores-Biscay Rise, Northeast Atlantic Ocean: Geophysical Journal of the Royal Astronomical Society, Vol. 70, p.79-107.

Wildi, W., 1983, La chaine Tello-Rifaine (Algerie, Maroc, Tunisie): structure, stratigraphie et evolution du Trias au Miocene: Revue de Geologie Dynamique et de Geographie Physique, Vol. 24, p.201-297.

_____, 1983a, Carte Structurale de la Chaine Tello-Rifaine, 1:2,000,000: Revue de Geologie Dynamique et de Geographie Physique, Vol. 24.

Williams, C.A., 1975, Sea-floor spreading in the Bay of Biscay and its relationship to the North Atlantic: Earth and Planetary Science Letters, Vol. 24, p.440-456.

_____, 1986, An oceanwide view of Palaeogene plate tectonic events: Palaeogeography, Palaeoclimatology, Palaeoecology, Vol. 57, p.3-25.

_____ and McKenzie, D., 1971, The evolution of the north-east Atlantic: Nature, Vol. 232, p.168-173.

Williams, G.D., 1984, Thrust tectonics in the south central Pyrenees: Journal of Structural Geology, Vol. 7, p.11-17.

_____ and Fischer, M.W., 1984, A balanced section across the Pyrenean orogenic belt: Tectonics, Vol. 3, p.773-780.

Williams, H., 1978, Tectonic Lithofacies Map of the Appalachian Orogen, 1:1,000,000: Memorial University of Newfoundland, St. John's, Newfoundland, Canada, 2 sheets.

Winterer, E.L. and Bosellini, A., 1981, Subsidence and sedimentation on a Jurassic passive continental margin (Southern Alps, Italy): American Association of Petroleum Geologists Bulletin, Vol. 65, p.394-421.

_____ and Hinz, K., 1984, The evolution of the Mazagan continental margin: a synthesis of geophysical and geological data with results of drilling during Deep Sea Drilling Project Leg 79: in Hinz, K. and Winterer, E.L., (eds.), in Hinz, K., Winterer, E.L., et al., Initial Reports of the Deep Sea Drilling Project, Vol. 79: U.S. Government Printing Office, Washington, D.C., p.893-919.

Wissman, G. and von Rad, U., 1979, Seismic structure, continental basement, and Mesozoic sediments from the Mazagan Plateau off Morocco: "Meteor" Forschungsargebnisse, Vol. 31., p.1-20.

Working Group for Deep Seismic Sounding in the Alboran Sea (1974), 1978, Crustal seismic profiles in the Alboran Sea-preliminary results: PAGEOPH, Vol. 116, p.167-180.

Zeyen, H.J., Banda, E., Gallart, J., and Ansorge, J., 1985, A wide angle seismic reconnaissance survey of the crust and upper mantle in the Celtiberian Chain of eastern Spain: Earth and Planetary Science Letters, Vol. 75, p.393-402.

Ziegler, P.A., 1988, Evolution of the Arctic-North Atlantic and the Western Tethys: American Association of Petroleum Geologists, Memoir #43, Tulsa, Okla., 198pp.

Zitellini, N., Trincardi, F., Marani, M., and Fabbri, N., 1986, Neogene tectonics of the Northern Tyrrhenian Sea: Giornale di Geologia, Vol. 48, p.25-40.

SHIP AND AEROMAGNETIC SURVEY LINES USED IN THIS STUDY

Surveys conducted by Lamont-Doherty research vessels (R.V. Vema and R.V. Conrad) begin with either V or C followed by a 4 digits. Surveys designated by 5 digits of beginning with A followed by 4 digits are aeromagnetic surveys. All other surveys were obtained by Lamont-Doherty under contract with the National Geophysical Data Center, Boulder, Colorado. Surveys conducted by the R.V. Glomar Challenger under auspices of the Deep Sea Drilling Project and Ocean Drilling Projects are designated by the prefixes GGL or JCH with the 2 following digits designating the drilling leg.

44101	C0912	DD64A	GIB70	KA68E
44102	C0913	DD64B	GIB72	KA68F
44103	C1001	DD64B	GL78A	KA68G
66001	C1101	DDAFZ	GL78B	KA68H
66401	C1310	DDT61	GL78B	KA68J
66601	C1311	DDUT2	IIPOD	KA707
A2320	C1509	DIAFZ	INM02	KA70E
A232A	C1510	DIS29	INM11	KK907
A232B	C1602	DIS31	INM12	KK907
A2490	C1603	DITRV	JCH01	KK94A
A2602	C1612	DIVRD	JCH02	KK9A4
A2652	C1613	DS541	JCH03	KKA01
A2671	C1701	DS542	JCH04	KKA02
A2672	C1702	DS542	JCH14	KKA03
A2731	C1904	EEL02	JCH28	KKC01
A2732	C1906	EQU72	JCH29	KKC02
A2754	C1907	FM017	JCH30	KKD01
A2755	C2103	FM102	JCH37	KKD01
A2756	C2104	FM103	JCH38	KKD03
A2757	C2112	GG226	JCH40	KKD04
A2922	C2116	GGIB1	JCH42	KKT75
A2931	C2212	GGL12	JCH43	KN544
AAKUR	C2213	GGL13	JCH44	KN544
AAL03	C2405	GGL14	JCH48	LY02A
AARC1	C2406	GGL37	JCH49	LY12A
AARC3	C2510	GGL38	JCH50	LY21A
AARC4	C2510	GGL39	JCH53	LY32B
AATL3	C2511	GGL41	JCH54	LY70B
BA75B	CAG71	GGL43	JCH55	LY70C
BA75E	CAT07	GGL45	JCH56	LY70D
BA75F	CH431	GGL46	JCH61	LY71B
BA75G	CH433	GGL47	JCH63	LY72A
BA75G	CH440	GGL48	KA001	LY73F
BA75H	CH611	GGL49	KA008	LY73G
BBD61	CH612	GGL51	KA013	ME464
BBD63	CH820	GGL75	KA406	ME531
BBOW2	CH964	GGL79	KA408	ME532
BBR05	CH992	GGL80	KA415	MET45
BOMDI	CH993	GGL81	KA419	MMIC1
BOMOC	CN151	GGL82	KA507	NIAS3
BOMRA	CN152	GGL94	KA522	NOR01
C0801	CN158	GI715	KA601	NOR05
C0812	CN159	GI716	KA628	OOC67
C0903	DATLS	GI716	KA68D	OPR41

OPR43
SIA01
SIA02
SIA03
SIA04
SIA05
SIA06
SIA07
SIA08
SIA09
SIA10
SIA11
SIB01
SIB02
SIB03
SIB04
SIB05
SIB06
SIB07
SIB08
SIB09
SIB10
SIB11
SIB12
SIB13
SIB14
SIB15
SIB16
SIB17
SIB18
SIB19
SIB20
SIC01
SIC02
SIC03
SIC04
SIC05
SIC06
SIC07
SIC08
SIC09
SIC10
SIC11
SIC12
SIC13
SIC14
SIC15
SIC16
SIC17
SIC18
SIC19
SIC20
SIC21
SIC22
SID01
SID02
SID03
SID04
SID05
SID06
SID07
SID08
SID09
SID10
SID11
SID12
SID22
SID23
SID24
SID25
SID26
SID27
SID28
SID29
SID30
SID31
SID32
SID33
SID34
SID35
SID36
SID37
SID38
SID39
SID40
SID41
SID42
SID43
SID44
SID45
SID46
SID47
SID48
SID49
SID50
SID51
SID52
SID53
SID53
SID55
SID56
SID57
SIE01
SIE02
SIE03
SIE04
SIE05
SIE06
SIE07
SIE08
SIE09
SIE10
SIE11
SIE12
SIE13
SIE14
SIE15
SIE16
SIE17
SIE18
SIE19
SIE20
SIE21
SIE22
SS005
SS006
SS007
SS009
SS009
SS011
SS012
SS013
SS014
SS020
SSA01
SSN13
SUR01
TAG70
TAG71
TT151
TT152
TTH01
TTH02
TTH03
TTR04
TTR28
V1603
V1612
V1614
V1615
V1712
V1713
V1716
V1803
V1913
V2001
V2002
V2012
V2202
V2206
V2207
V2302
V2303
V2304
V2305
V2306
V2413
V2501
V2502
V2503
V2601
V2602
V2603
V2604
V2607
V2701
V2702
V2703
V2706
V2707
V2708
V2709
V2713
V2714
V2801
V2802
V2804
V2805
V2806
V2908
V2909
V2910
V2911
V3003
V3004
V3005
V3006
V3007
V3008
V3009
V3010
V3012
V3013
V3014
V3101
V3106
V3107
V3203
V3204
V3205
V3206
V3207
V3612
V3620
V3621
VA791
VA794
VA795
VA796
VVM72
WI010
WI014
WI404
WI412
WI413
WI421
WI422
WWH61

```
C      ROTATIONS.FOR IS USED IN CONJUNCTION WITH PLOTS.FOR
C      AS A REPLACEMENT FOR ROTPROG.FOR WHICH WAS A
C      MODIFICATION OF ANOMPLOT.FOR AND ANOMROT.FOR
C
C      THE CHANGE TO SEPARATE PROGRAMS WAS MADE NECESSARY
C      BY CHANGES IN THE GRAPHICS SOFTWARE AND HARDWARE
C      IMPLEMENTED IN LATE 1987 AND EARLY 1988 BY THE
C      OXFORD UNIVERSITY COMPUTING SERVICE
C
C      MARC HELMAN  OXFORD UNIVERSITY
C      MODIFIED   FEBRUARY, 1988
C
C      DATA IS READ OFF SEQUENTIAL FILE STORED ON DISK.
C      ***USER MUST BE AWARE OF HOW DATA IS ORGANIZED***
C      IF DATA IS IN LON,LAT FORMAT--RUN SWITCHER FIRST!!
C      SWITCHER CHANGES DATA TO LAT,LON FORMAT
C      ANOMALY FILES--SINGLE ANOMALY PER FILE
C      FZ AND CONT OUTLINE FILES--LAT, LONG PAIRS IN SEGMENTS
C      SEPARATED BY NUMBER PAIRS IN SEGMENT; FILES ENDS IN 0

       IMPLICIT INTEGER*2 (I-N)
       IMPLICIT REAL*4 (A-H,O-Z)
       DIMENSION ALAT(6000),ALON(6000)
       DIMENSION PTLAT(6000),PTLON(6000)
       CHARACTER*35 NAME1,NAME2

  803  CONTINUE
C           FIND OUT TYPE OF DATA TO BE ENTERED
       WRITE (5,*) 'ENTER 1 FOR FZ FILES OR CONTINENT OUTLINES,
      1 0 FOR ANOMALY FILES OR LOCATION DATA'
       READ (5,*)IFZ
C          ENTER ROTATION POLE
       WRITE(5,*) 'ENTER PLAT, PLON, DELT, F8.3'
       READ(5,*)PLAT,PLON,DELT
       WRITE (5,925)PLAT,PLON,DELT
  925   FORMAT(1X,'PLAT= ',F8.3,'PLON= ',F8.3,'DELT= ',F8.3)
       IF (IFZ.EQ.1) GO TO 700
C         READ IN DATA
       WRITE (5,*) 'ENTER FILE W/ ANOMALY OR LOCATION DATA'
       READ (5,900) NAME1
  900  FORMAT(A15)
       OPEN(UNIT=1,NAME=NAME1,TYPE='OLD',READ ONLY)
       I=1
       DO WHILE (.TRUE.)
          READ (1,*,END=910) ALAT(I), ALON(I)
          I=I+1
       END DO
  910   WRITE (5,*) 'FINISHED READING LAT,LONG, DATA'
        CLOSE (UNIT=1)
C          RESET COUNTER AND ROTATE DATA
       ITOTAL = I - 1
       WRITE (5,*) ITOTAL
       WRITE (5,*) 'ENTER NAME OF FILE TO WRITE ROTATED DATA TO'
       READ (5,902) NAME2
       OPEN (UNIT=2,NAME=NAME2,TYPE='NEW')
  929   DO 930 J=1,ITOTAL
       DLAT=ALAT(J)
       DLON=ALON(J)
```

```
        CALL ROTC3(DLAT,DLON,PLAT,PLON,DELT,FLAT,FLON)
        PTLAT(J) = FLAT
        PTLON(J) = FLON
        WRITE (2,100) PTLAT(J),PTLON(J)
 100    FORMAT (2F10.3)
 930    CONTINUE
        CLOSE (UNIT=2)
        WRITE (5,*) 'ENTER 1 TO ROTATE MORE DATA'
        READ (5,*)IGOON
        IF (IGOON.EQ.1) GO TO 803
        IF (IGOON.NE.1) GO TO 975
 700    CONTINUE
C         READ IN DATA
      WRITE (5,*) 'ENTER NAME OF FILE W/ FZ OR CONT OUTLINE DATA'
      READ (5,902) NAME1
 902  FORMAT(A15)
      OPEN(UNIT=1,NAME=NAME1,TYPE='OLD',READ ONLY)
      WRITE (5,*) 'ENTER NAME OF FILE TO WRITE ROTATED DATA TO'
      READ (5,902) NAME2
      OPEN (UNIT=2,NAME=NAME2,TYPE='NEW')
 778  DO 550 J=1,100,1
      READ (1,722) INUM
      WRITE (5,*) INUM
      WRITE (2,722) INUM
 722  FORMAT (I4)
      IF (INUM .EQ. 0) GO TO 703
        DO 560 I=1,INUM
        READ (1,620) ALAT(I), ALON(I)
 620    FORMAT (2F10.3)
 560    CONTINUE
            DO 570 M=1,INUM
            DLAT = ALAT(M)
            DLON = ALON(M)
            CALL ROTC3(DLAT,DLON,PLAT,PLON,DELT,FLAT,FLON)
            PTLAT(M) = FLAT
            PTLON(M) = FLON
            WRITE (2,620) PTLAT(M), PTLON(M)
 570        CONTINUE
 550    CONTINUE
 703    CONTINUE
        CLOSE (UNIT=1)
        CLOSE (UNIT=2)
        WRITE (5,*) 'ENTER 1 TO ROTATE MORE DATA'
        READ (5,*)IGOON
        IF (IGOON.EQ.1) GO TO 803
        IF (IGOON.NE.1) GO TO 975
 975    CONTINUE
 976    CONTINUE
      STOP
      END


C       ROTC3 - SPHERICAL ROTATION PROGRAM
C       ROTC3 ROTATES ALAT,ALON ABOUT POLE PPLAT,PPLON
C       THROUGH DELT DEGREES TO FLAT,FLON

      SUBROUTINE ROTC3(ALAT,ALON,PPLAT,PPLON,DELT,FLAT,FLON)
      IMPLICIT INTEGER*2 (I-N)
```

```
      IMPLICIT REAL*4 (A-H,O-Z)

      RAD=0.017453277
    1 PLAT=PPLAT
      PLONG=PPLON
      DELTL=DELT*RAD
  105 ZLAT=ALAT
      ZLONG=ALON
      RLAT=(90.0-PLAT)*RAD
      IF(PLONG.LT.0) PLONG=PLONG+360.
  103 RLONG=RAD*PLONG
  109 A=COS(RLAT)
      E=SIN(RLAT)
      C=COS(RLONG)
      D=SIN(RLONG)
      RZLAT=(90.-ZLAT)*RAD
      IF(ZLONG.LT.0.) ZLONG=ZLONG+360.
      ZLONG=ZLONG*RAD
      V=SIN(RZLAT)
      W=COS(RZLAT)
      X=SIN(ZLONG)
      Y=COS(ZLONG)
      CTH2=V*Y*E*C+V*X*E*D+W*A
      STH2=SQRT(1-CTH2**2)
      TH2=ATAN(STH2/CTH2)
      IF (CTH2.LT.0) TH2=3.141592+TH2
      CPH2=(V*Y*A*C+V*X*A*D-W*E)/STH2
      SPH2=(-V*Y*D+V*X*C)/STH2
      PH2=ATAN(SPH2/CPH2)
      IF(CPH2) 316,325,317
  316 IF(SPH2) 319,325,319
  317 F(SPH2) 318,325,325
  318 PH2=6.28319+PH2
      GO TO 325
  319 PH2=3.14159+PH2
  325 PH2=PH2+DELTL
      VV=SIN(TH2)
      WW=COS(TH2)
      XX=SIN(PH2)
      YY=COS(PH2)
      CTH1=-VV*YY*E+WW*A
      STH1=SQRT(1-CTH1**2)
      TH1=ATAN(STH1/CTH1)
      IF (CTH1.LT.0) TH1=3.14159+TH1
      CPH1=(VV*YY*C*A-VV*XX*D+WW*C*E)/STH1
      SPH1=(VV*YY*D*A+VV*XX*C+WW*D*E)/STH1
      PH1=ATAN(SPH1/CPH1)
      IF(CPH1) 416,425,417
  416 IF(SPH1) 419,425,419
  417 IF(SPH1) 418,425,425
  418 PH1=6.28319+PH1
      GO TO 425
  419 PH1=3.14159+PH1
  425 TH1=TH1/RAD
      PH1=PH1/RAD
      FLAT=90.-TH1
      IF (PH1.LT.360.) GO TO 435
      PH1=PH1-360.
```

```
      GO TO 450
435   IF (PH1.GT.180.) PH1=PH1-360.
450   FLON=PH1
      RETURN
      END
```

```
C       ROFN3
C
C       PROGRAM TO CALCULATE SUMS OF FINITE ROTATIONS.
C       GIVEN FIRST AND SECOND ROTATIONS, PROGRAM WILL
C       CALCULATE THE COMPOSITE ROTATION.
C
C       SCRIPPS INSTITUTE REFERENCE 70-30
C       JEAN FRANCHETEAU, PALEOMAGNETISM AND PLATE TECTONICS
C
C       PROGRAM BY LADD AUG 71
C
C       MARC HELMAN   UNIVERSITY OF OXFORD
C       MODIFIED   30-NOV-86
C       ANGULAR ROTATION MUST BE LESS THAN 180 DEGREES.

C         GET POLES TO BE COMBINED
    1   WRITE(6,*) ' ENTER FIRST ROTATION: LAT,LONG,ANG F10.3  '
        READ(5,101) A1,P1,T1
  101   FORMAT(3F10.3)
        IF(T1.EQ.0) GO TO 9999
        WRITE(6,*)'ENTER SECOND ROTATION  '
        READ(5,101) A2,P2,T2
C          CONVERT TO RADIANS AND PICK END OF AXIS THAT MAKES
C          ROTATION ANGLE POSITIVE AND LESS THAN 180 DEGREES.
    2   X=3.141592653589793
        CONST=X/180.
        AM1=A1*CONST
        PHI1=P1*CONST
        THET1=T1*CONST
        IF(THET1)21,22,22
   21   THET1=-THET1
        AM1=-AM1
        PHI1=PHI1+X
        GO TO 24
   22   IF(X-THET1)23,24,24
   23   THET1=2.*X-THET1
        AM1=-AM1
        PHI1=PHI1+X
   24   AM2=A2*CONST
        PHI2=P2*CONST
        THET2=T2*CONST
        IF(THET2)31,32,32
   31   THET2=-THET2
        AM2=-AM2
        PHI2=PHI2+X
        GO TO 34
   32   IF(X-THET2)33,34,34
   33   THET2=2.*X-THET2
        AM2=-AM2
        PHI2=PHI2+X
C         CALCULATE COLATITUDE
   34   AM1C=(X/2.)-AM1
        AM2C=(X/2.)-AM2
C         CALCULATE CAYLEY-KLEIN PARAMETERS
   40   OMEG1=COS(THET1/2.)
        XI1=SIN(THET1/2.)*SIN(AM1C)*COS(PHI1)
        ETA1=SIN(THET1/2.)*SIN(AM1C)*SIN(PHI1)
        ZETA1=SIN(THET1/2.)*COS(AM1C)
```

```
      OMEG2=COS(THET2/2.)
      XI2=SIN(THET2/2.)*SIN(AM2C)*COS(PHI2)
      ETA2=SIN(THET2/2.)*SIN(AM2C)*SIN(PHI2)
      ZETA2=SIN(THET2/2.)*COS(AM2C)
C       MATRIX ROTATION
      OMEGT=OMEG1*OMEG2-XI1*XI2-ETA1*ETA2-ZETA1*ZETA2
      XIT=OMEG1*XI2+XI1*OMEG2-ETA1*ZETA2+ZETA1*ETA2
      ETAT=OMEG1*ETA2+XI1*ZETA2+ETA1*OMEG2-ZETA1*XI2
      ZETAT=OMEG1*ZETA2-XI1*ETA2+ETA1*XI2+ZETA1*OMEG2
      IF(OMEGT)3,5,5
    3 OMEGT=-OMEGT
      XIT=-XIT
      ETAT=-ETAT
      ZETAT=-ZETAT
C       INVERT CAYLEY-KLEIN PARAMETERS TO GET COMPOSITE ROTATION.
    5 THETT=2.*ARCOS(OMEGT)
      AMT=(X/2.)-ARCOS(ZETAT/SIN(THETT/2.))
      PHIT=ATAN(ETAT/XIT)
      IF(XIT)41,52,52
   41 IF(ETAT)42,43,43
   42 PHIT=PHIT-X
      GO TO 52
   43 PHIT=PHIT+X
C       INVERT TO DEGREES
   52 CONST=180./X
      AMT=AMT*CONST
      THETT=THETT*CONST
      PHIT=PHIT*CONST
      IF(AMT)7,12,12
    7 AMT=-AMT
      THETT=-THETT
      IF(PHIT)8,8,9
    8 PHIT=PHIT+180.
      GO TO 12
    9 PHIT=PHIT-180.
C       WRITE RESULTS TO SCREEN
   12 WRITE (6,103)
  102 FORMAT (' FIRST  ROTATION ',3F10.3)
      WRITE (6,102) A1,P1,T1
  103 FORMAT (23X,'LAT',6X,'LONG',6X,'ANGLE')
      WRITE (6,104) A2,P2,T2
  104 FORMAT (' SECOND ROTATION ',3F10.3)
      WRITE (6,105) AMT,PHIT,THETT
  105 FORMAT ('   COMPOSITE',5X,3F10.3)
C       PREPARE FOR NEXT SET OF ROTATIONS
      WRITE (6,101)
      WRITE (6,101)
      GO TO 1
C       CLOSE UP AND GO HOME
 9999 CALL EXIT
      END


      FUNCTION ARCOS(W)
    7 IF(W)1,2,2
    1 X=-W
      GO TO 31
    2 X=W
```

```
31    IF(1.-X)8,8,3
8     Y=3.1415926/2.
      GO TO 32
3     S=SQRT(1.-X)
      A=-S*1.570796
      B=S*0.214599*X
      C=-S*0.088979*X**2
      D=S*0.050174*X**3
      E=-S*0.030892*X**4
      F=S*0.017088*X**5
      G=-S*0.006670*X**6
      H=S*0.001262*X**7
      Y=H+G+F+E+D+C+B+A+3.1415926/2.
32    IF(W)4,5,5
4     ASINW=-Y
      GO TO 6
5     ASINW=Y
6     ARCOS=3.1415926/2.-ASINW
9     RETURN
      END
```

```
C       PLOTS.FOR IS USED IN CONJUNCTION WITH ROTATIONS.FOR
C       AS A REPLACEMENT FOR ROTPROG.FOR (A MODIFICATION OF
C       ANOMPLOT.FOR AND ANOMROT.FOR)
C
C       THE CHANGE TO 2 PROGRAMS WAS NECESSITATED BY CHANGES
C       IN GRAPHICS SOFTWARE AND HARDWARE AT OU COMPUTER CENTER
C       IN LATE 1987 AND EARLY 1988
C
C       DATA IS READ OFF SEQUENTIAL FILE STORED ON DISK.
C
C       ***USER MUST BE AWARE OF HOW DATA IS ORGANIZED***
C       IF DATA IS IN LON,LAT FORMAT--RUN SWITCHER FIRST!!
C       SWITCHER CHANGES DATA TO LAT,LON FORMAT
C
C       ***USER MUST BE AWARE OF HOW SCALING IS DONE***
C       BECAUSE OF MANNER IN WHICH PROGRAM WAS CONSTRUCTED
C       USING GHOST-80 GRAPHICS SCALING IS DONE IN 2 PLACES
C       USER MUST KNOW HIS SCALE IN INCHES PER DEGREE OF
C       LONGITUDE AT THE EQUATOR AND AS PROPORTIONAL SCALE
C
C       ONLY GEBCO SCALE (0.4375 " PER DEGREE / 1:10,000,000)
C       GIVES SATIFACTORY RESULTS AT THIS TIME (FEB, 1988)
C       3 PLOT SIZES CAN BE OBTAINED USING VARIATIONS OF SCALE
C           1/3 OF SCALE [0.1458 30,000 ON 10" PAPER]
C           THIS SCALE [0.4375, 10,000 USING 10" PAPER] OR
C           THIS SCALE [0.4375, 30,000 USING 30" PAPER]
C           3X THIS SCALE [0.4375, 10,000 USING 30" PAPER]
C
      REAL WESNS,ALAT,ALON,X,Y
      INTEGER MRCOP
      DIMENSION WESNS(5),MRCOP(10),BC(163)
      DIMENSION ALAT(6000),ALON(6000),PX(6000),PY(6000)
      DIMENSION PTLAT(6000),PTLON(6000)
      CHARACTER*45 NAME1

C        GIVE WARNING ABOUT ROTATIONS
      WRITE (5,*) 'PLOTS IS USED IN CONJUNCTION WITH ROTATIONS
     1  TO PLOT UNROTATED AND ROTATED DATA. IF YOU WANT TO PLOT
     2  ROTATED DATA BUT HAVE NOT YET PERFORMED THE ROTATION YOU
     3  MUST EXIT FROM THIS PROGRAM, RUN ROTATIONS TO ROTATE THE
     4  DATA, AND THEN RUN THIS PROGRAM'
      WRITE (5,*) 'ENTER 1 TO CONTINUE, ANY OTHER NUMBER TO EXIT'
      READ (5,*) ISTART
      IF (ISTART .NE. 1) GO TO 976
      IF (ISTART .EQ. 1) GO TO 1001
 1001 CONTINUE
C        INITIALIZE THE GHOST80 SYSTEM
      CALL PAPER (1)
C        GET GRID INFO
      CALL INFO(WESNS,MRCOP)
C        COMPUTE CONSTANT FOR MERCATOR CORRECTION
      CALL MRCMP(WESNS,MRCOP,YMAX,BC)
      JMAX =  INT( WESNS(4) - WESNS(3) ) + 1
C        USE WEBSTER'S SCALING PROGRAM TO GENERATE SCALE
      SCAX =  ( WESNS(2) - WESNS(1) ) * 111.0
      SCAY = YMAX*2.54*100.0
      YMAXK = SCAY
```

```
      XMAXK = SCAX
      CALL SCALPROG(SCAX,SCAY,RX,RY)
C          DEFINE THE VIEWPORT
      CALL PSPACE (0.1,RX+0.1,0.1,RY+0.1)
C          DEFINE MAPPING SPACE
      CALL MAP (WESNS(1),WESNS(2),0,SCAY)
C        SET THICKNESS FOR BOLD OUTLINE
      CALL THICK(2)
C          DRAW PERIMETER
      IF (MRCOP(1).EQ.1) CALL BORDER
      IF (MRCOP(1).EQ.0) GO TO 100
  100 CONTINUE
C          SET LINE THICKNESS FOR CROSSMARKS AND TICKS
       WRITE (5,*) 'ENTER DESIRED LINE THICKNESS---1,2,3,ETC.;
     1   NOTE FOR OVERSIZE PLOTS (0.4375, 10000 ON LARGE PAPER)
     2   USE 1 TO PREVENT OFFSET OF CROSSMARKS AND TICKS.  NOTE
     3   ALSO THAT THICKNESS IS RESET AUTOMATICALLY TO 2 WHEN
     4   ANNOTATIONS ARE WRITTEN'
      READ (5,10) ILINE
   10 FORMAT (I1)
      CALL THICK(ILINE)
C          PUT IN CROSSMARKS AND TICKS AROUND PERIMETER
       IF (MRCOP(2).NE.1) GO TO 800
       IY1=WESNS(3)
       IY2=WESNS(4)
       IX1=WESNS(1)
       IX2=WESNS(2)
       J=-MRCOP(3) + 1
       BC(1)=0.0
       DO 500 IY=IY1,IY2,MRCOP(3)
       J=J + MRCOP(3)
       YP=BC(J)*2.54*100.0
       DO 600 IX=IX1,IX2,MRCOP(3)
       XP=FLOAT(IX)
       CALL PLOTNC(XP,YP,232)
  600  CONTINUE
  500  CONTINUE
  800  CONTINUE
C          RESET THICKNESS FOR ANNOTATIONS
       CALL THICK(2)
C          ANNOTATE BORDER IN X DIRECTION (LONG)
       IF (MRCOP(4).NE.1) GO TO 801
       DO 501 IX=IX1,IX2,MRCOP(5)
       YPA=YMAXK*1.02
       YPB=YMAXK*(-0.02)
       XP=FLOAT(IX)
       CALL PLOTNI(XP,YPA,IX)
       CALL PLOTNI(XP,YPB,IX)
  501  CONTINUE
  801  CONTINUE
C        ANNOTATE BORDER IN Y DIRECTION (LAT)
       IF (MRCOP(4).NE.1) GO TO 802
       J= -MRCOP(5) + 1
       XMAXD = IX2 - IX1
       BC(1)=0.0
       DO 502 IY=IY1,IY2,MRCOP(5)
       J = J + MRCOP(5)
       YP = BC(J)*2.54*100.0
```

```
      XPA = (IX1 - XMAXD*0.02)
      XPB = (IX1 + XMAXD*1.02)
      CALL PLOTNI(XPA,YP,IY)
      CALL PLOTNI(XPB,YP,IY)
  502 CONTINUE
  802 CONTINUE
  803 CONTINUE
C          SET WINDOW TO PREVENT INCORRECT PLOTTING WHEN PEN
C          MOVES FROM DATA OUTSIDE PLOT AREA TO INSIDE PLOT AREA
      CALL WINDOW (WESNS(1),WESNS(2),0,SCAY)
C          FIND OUT TYPE OF DATA TO BE ENTERED
      WRITE (5,*) 'ENTER 1 FOR FZ FILES OR CONTINENT OUTLINES,
     1 0 FOR ANOMALY FILES OR LOCATION DATA'
      READ (5,*)IFZ
C          SET LINE THICKNESS
       WRITE (5,*) 'ENTER DESIRED LINE THICKNESS---1,2,3,ETC.'
       READ (5,10) ILINE
       CALL THICK(ILINE)
C            CHOOSE COLOR OF PENS TO PLOT WITH
       WRITE (5,*) 'ENTER 0 FOR DEFAULT (BLACK) PEN, 2
     1 FOR RED PEN, 3 FOR GREEN PEN, 4 FOR BLUE PEN'
       READ (5,*) IPEN
       CALL LINCOL (IPEN)
       IF (IFZ.EQ.1) GO TO 700
C        READ IN DATA
       WRITE (5,*) 'ENTER FILE W/ ANOMALY OR LOCATION DATA'
       READ (5,900) NAME1
  900  FORMAT(A45)
       OPEN(UNIT=1,NAME=NAME1,TYPE='OLD',READ ONLY)
       I=1
       DO WHILE (.TRUE.)
          READ (1,*,END=910) ALAT(I), ALON(I)
          I=I+1
       END DO
  910   WRITE (5,*) 'FINISHED READING LAT,LONG, DATA'
        CLOSE (UNIT=1)
C         RESET COUNTER
        ITOTAL = I - 1
        WRITE (5,*) ITOTAL
C         MAKE MERCATOR CORRECTION AND SCALE FOR PLOTTING
  941   DO 940 K = 1,ITOTAL
        PX(K) = ALON(K)
        PYV = BLATI(ALAT(K),WESNS)
        PY(K) = PYV*2.54*100.0
  940   CONTINUE
  970   CONTINUE
C       CHOOSE SYMBOL FOR PLOTTING DATA
           WRITE (5,*) 'CHOOSE PLOTTING SYMBOL: ENTER 235
     1     FOR + IN BOX; 243 FOR . IN BOX; 251 FOR x IN
     2     BOX; ENTER 228 FOR + IN DIAMOND; 244 FOR . IN
     3     DIAMOND; 252 FOR x IN DIAMOND; ENTER 238 FOR
     4     + WITH o IN CENTER; 239 FOR x WITH o IN CENTER;
     5     234 FOR *'
        READ (5,*) ISYM
C            PLOT THIS SUCKER!
        CALL PTPLOT (PX,PY,1,ITOTAL,ISYM)
        WRITE (5,*) 'ENTER 1 TO PLOT MORE DATA'
        READ (5,*)IGOON
```

```
      IF (IGOON.EQ.1) GO TO 803
      IF (IGOON.NE.1) GO TO 975
 700  CONTINUE
C        CHOOSE TYPE OF LINES
      WRITE (5,*) 'ENTER 0 FOR BROKEN LINES'
      READ (5,*) IBROKE
      IF (IBROKE .NE. 0) GO TO 702
      IF (IBROKE .EQ. 0) GO TO 701
 701  WRITE (5,*) 'ENTER 0 FOR EQUAL SEGMENTS'
      READ (5,*) IEQ
      IF (IEQ .EQ. 0) CALL BROKEN (6,6,6,6)
      IF (IEQ .NE. 0) CALL BROKEN (12,6,6,6)
 702  CONTINUE
C        READ IN DATA
      WRITE (5,*) 'ENTER NAME OF FILE W/ FZ OR CONT OUTLINE DATA'
      READ (5,902) NAME1
 902  FORMAT(A45)
      OPEN(UNIT=1,NAME=NAME1,TYPE='OLD',READ ONLY)
 777  DO 510 J=1,100,1
      READ (1,721) INUM
      WRITE (5,721) INUM
 721  FORMAT (I4)
      IF (INUM.EQ.0) GO TO 703
         DO 520 I=1,INUM
         READ (1,610) ALAT(I),ALON(I)
 610     FORMAT (2F10.3)
 520     CONTINUE
            DO 530 K=1,INUM
            PX(K)=ALON(K)
            PYV=BLATI(ALAT(K),WESNS)
            PY(K)=PYV*2.54*100.0
 530        CONTINUE
C           PLOT THIS SUCKER
       CALL PTJOIN (PX,PY,1,INUM,2)
 510   CONTINUE
 703   CONTINUE
       CLOSE (UNIT=1)
       CALL FULL
       WRITE (5,*) 'ENTER 1 TO PLOT MORE DATA'
       READ (5,*)IGOON
       IF (IGOON.EQ.1) GO TO 803
       IF (IGOON.NE.1) GO TO 975
 975   CONTINUE
C           FINISH THIS MESS!
      CALL GREND
 976   CONTINUE
      STOP
      END
```

```
C       SUBROUTINE INFO PROMPTS USER FOR GRID DATA

        SUBROUTINE INFO(WESNS,MRCOP)

        INTEGER MRCOP
        REAL WESNS
        DIMENSION WESNS(5),MRCOP(10)

        WRITE (5,*) ' ENTER WEST,EAST,SOUTH,NORTH BOUNDARIES OF
       1 DESIRED MAP, USE MINUS FOR WEST LONG AND SOUTH LAT'
        WRITE (5,*) 'WEST:'
        READ (5,101) WESNS(1)
        WRITE (5,*) 'EAST:'
        READ (5,101) WESNS(2)
        WRITE (5,*) 'SOUTH:'
        READ (5,101) WESNS(3)
        WRITE (5,*) 'NORTH:'
        READ (5,101) WESNS(4)
  101   FORMAT(F10.0)
        WRITE (5,*) ' ENTER MAP SCALE IN INCHES/DEGREE LONGITUDE
       1    GEBCO SCALE IS 0.4375 '
        READ (5,102) WESNS(5)
  102   FORMAT(F10.0)
        WRITE (5,*) ' ENTER 1 TO DRAW PERIMETER'
        READ (5,103)  MRCOP(1)
  103   FORMAT(I1)
        WRITE (5,*) ' ENTER 1 TO PUT IN TICKS AND CROSSMARKS'
        READ (5,103) MRCOP(2)
        IF (MRCOP(2).NE.1) GO TO 20
        IF (MRCOP(2).EQ.1) GO TO 10
   10   WRITE (5,*) 'ENTER DEGREE SPACING-TICKS,CROSSMARKS-I2'
        READ (5,104) MRCOP(3)
  104   FORMAT(I2)
   20   WRITE (5,*) ' ENTER 1 TO ANNOTATE GRID'
        READ (5,103) MRCOP(4)
        IF (MRCOP(4).NE.1) GO TO 60
        IF (MRCOP(4).EQ.1) GO TO 30
   30   WRITE (5,*) 'ENTER DEGREE SPACING FOR ANNOTATIONS-I2'
        READ (5,104) MRCOP(5)
   60   CONTINUE
        RETURN
        END

------------------------------------------------------------------
C*          FUNCTION BLATI
C       ALL LOCATIONS ARE DETERMINED.  ORIGINAL VERSION
C       ASSIGNED VALUE OF -10000. TO COORDINATES OUT OF
C       PLOTTING AREA.  CALL WINDOW--IN PROGRAM ELIMINATES
C       THE NEED FOR THIS

        FUNCTION BLATI(YLAT,WESNS)
        IMPLICIT INTEGER*2 (I-N)
        IMPLICIT REAL*4 (A-H,O-Z)
        DIMENSION WESNS(5)
        COMMON NDPY(3),LPYR(4),JBSYR,B(163)
        COMMON /MRCATR/CONST,EPSLON
        DATA RAD/57.29578/
```

```
C       COMPUTE LOCATION IN INCHES
        AB=+1.0
        IF(YLAT.LT.0.)AB=-1.0
        FLAT=1+EPSLON*ALOG(1-EPSLON*(SIN((AB*YLAT)/RAD)))
SPHERE=AB*WESNS(5)*RAD*ALOG(TAN((45.0+(AB*YLAT)/2.0)/RAD)*FLAT)
        BLATI=SPHERE-CONST
        RETURN
        END


------------------------------------------------------------
        SUBROUTINE SCALPROG(SCAX,SCAY,RX,RY)

C       SCALING PROGRAM DEVELOPED BY WEBSTER MOHRIAK
C       FOR CHANGING PSPACE SCALING USING GHOST-80 ROUTINES
C       ADAPTED FOR USE IN ROTPROG.FOR AT OXFORD UNIVERSITY

        REAL SCAX,SCAY,RX,RY

C       SCAX AND SCAY ARE DIMENSIONS IN X AND Y DIRECTIONS
C       IN KILOMETERS RELATIVE TO PROPORTIONAL SCALE AT THE
C       EQUATOR OF 1:10,000,000 (1 DEGREE EQUAL TO 111.0 KM)

  10    WRITE(5,15)
  15    FORMAT(1X,' INPUT HORIZONTAL/VERTICAL SCALE(K*1000)',/,1X,
       1' FOR PLOTTING MAP, GEBCO SCALE 10000 (1:10,000,000)',/,1X,
       2' OR 30000 IF PLOTTING ON 30 INCH PAPER')
        READ(5,*) SCA
        TSCA = 1000.0/SCA
        RX= TSCA*SCAX/254.0
        RY= TSCA*SCAY/254.0
        IF (RY.LT.3.0) GO TO 30
        WRITE(5,20)
  20    FORMAT(1X,' RSPACE TOO BIG -- EVEN WITH 30" PAPER ',/,
       1' CHOOSE A SMALLER SCALE ' )
        GOTO 10
  30    CONTINUE
        RETURN
        END


------------------------------------------------------------
C           SUBROUTINE MRCMP
C       CONSTANT FOR USE IN BLATI IS COMPUTED AND PUT INTO NAMED
C       COMMON /MRCATR/CONST,EPSLON. FCONST IS FLATTENING CONSTANT.
C       294.98 IS DEFAULT VALUE.
        SUBROUTINE MRCMP(WESNS,MRCOP,YMAX,BX)
        IMPLICIT INTEGER*2 (I-N)
        IMPLICIT REAL*4 (A-H,O-Z)
        DIMENSION WESNS(5),MRCOP(10),BX(163)
        COMMON NDPY(3),LPYR(4),JBSYR,B(163)
        COMMON /MRCATR/CONST,EPSLON
        DATA WIDTH/30./,RAD/57.29578/

C         NOTE: IF WESNS(5) IS = 0.0, MRCMP RESETS IT = 1.0
        IF (WESNS(5).EQ.0) WESNS(5)=1.
C         MAKE SURE W>E BY ADDING 360 DEGREES TO E
        IF(WESNS(2)-WESNS(1) .LE. 0.)WESNS(2)=WESNS(2)+360.
```

```
C
C       COMPUTE CONST FOR BLATI TO USE.  THIS IS THE MERCATOR
C       DIFFERENCE BETWEEN EQUATOR AND SLAT (WESNS(3))
        FCONST=MRCOP(10)/100.
        IF (MRCOP(10).EQ.0) FCONST=294.98
        F=1.0/FCONST
        EPSLON=SQRT(ABS(2.0*F-F*F))
        AB=1.0
        IF (WESNS(3).LT.0.) AB=-1.0
        FLAT=1+EPSLON*ALOG(1-EPSLON*(SIN((AB*WESNS(3))/RAD)))
CONST=WESNS(5)*RAD*ALOG(TAN((45.0+(AB*WESNS(3))/2.0)/RAD)*FLAT)
        CONST=AB*CONST
        DO 5 I=1,4
    5   IF (AMOD(WESNS(I),1.).NE.0.) GO TO 15
C       FILL B ARRAY
        B(1)=0.0
        K=2
        DO 10 XJ=WESNS(3)+1.0,WESNS(4)
        B(K)=BLATI(XJ,WESNS)
        BX(K) = B(K)
        K=K+1
   10   CONTINUE
C         CHECK WIDTH, HEIGHT OF PLOT
   15   XWIDE=BLATI(WESNS(4),WESNS)
        IF(XWIDE.LE.WIDTH) GOTO 20
C         TOO WIDE FOR PLOTTER
        XLONG=(WESNS(2)-WESNS(1))*WESNS(5)
        TYPE *,' THE PLOTTERS ARE',WIDTH,' INCHES WIDE'
        TYPE *,' THIS PLOT IS ',XWIDE,' INCHES WIDE.'
        TYPE *,' IT IS ',XLONG,' INCHES LONG.'
   20   CONTINUE
        YMAX = XWIDE
         RETURN
         END
```

```
C        STAGEPOLES.FOR
C        PROGRAM TO CALCULATE STAGE POLES FROM FINITE POLES

      CHARACTER*30 NAME1,NAME2
      CHARACTER*3 ID1,ID2,ID(100)
      DIMENSION FLAT(100),FLON(100),DEL(100)

      WRITE(5,*) ' ENTER NAME OF INPUT (FINITE POLE) FILE'
      READ(5,900) NAME1
  900 FORMAT(A)
      OPEN(UNIT=1,NAME=NAME1,TYPE='OLD',READONLY)
      WRITE(5,*) ' ENTER NAME OF OUTPUT (STAGEPOLE) FILE'
      READ(5,900) NAME2
      OPEN (UNIT=2,NAME=NAME2,TYPE='NEW')
      I=0
      READ(1,*)
      DO WHILE (.TRUE.)
      I=I+1
      READ(1,901,END=10)FLAT(I),FLON(I),DEL(I),ID(I)
  901 FORMAT(3F10.3,A5)
      END DO
   10 INUM=I-1
      JNUM=INUM-1
      DO J=1,2
      WRITE(2,902) INUM
  902 FORMAT(I4)
      DELTA=DEL(INUM)
      IF(J.EQ.1) DELTA=-DELTA
      WRITE(2,903) FLAT(INUM),FLON(INUM),DELTA,ID(INUM)
      WRITE(5,903) FLAT(INUM),FLON(INUM),DELTA,ID(INUM)
      DO K=1,JNUM
      N2=INUM-K
      N1=N2+1
      FLAT1=FLAT(N1)
      FLON1=FLON(N1)
      DEL1=DEL(N1)
      ID1=ID(N1)
      FLAT2=FLAT(N2)
      FLON2=FLON(N2)
      DEL2=DEL(N2)
      ID2=ID(N2)
      DEL1=-DEL1
        IF(J.EQ.1)  DEL2=-DEL2
        IF(J.EQ.1)  DEL1=-DEL1
      CALL ROFN3  **see listing in appendix as program**
      (FLAT1,FLON1,DEL1,FLAT2,FLON2,DEL2,FLAT3,FLON3,DEL3)
     WRITE(2,903) FLAT3,FLON3,DEL3,ID2,ID1
  903    FORMAT(3F10.4,2A5)
     WRITE(5,903) FLAT3,FLON3,DEL3,ID2,ID1
     END DO
     END DO
   40 CLOSE(UNIT=1)
     CLOSE(UNIT=2)
     CALL EXIT
     END
```

```
C         SYNFZPLOT.FOR
C
C
C         CALCULATE SYNTHETIC FZ GIVEN STAGE POLES AND
C         RIDGE CREST LOCATIONS

      IMPLICIT INTEGER*2 (I-N)
      IMPLICIT REAL*4 (A-H,O-Z)
      DIMENSION MRCOP(10),WESNS(5),PLAT(50),PLON(50),PDEL(50)
      COMMON NDPY(3),LPYR(4),JBSYR,B(163)
      CHARACTER*30 NAME1,NAME2,NAME3
      CALL INFO(WESNS,MRCOP)
      WRITE(5,*)' ENTER 0 FOR ELIP. COR.,1 FOR NONE'
      READ(5,*) IELIP
      IF(IELIP.EQ.1) MRCOP(10)=32000
C        GET DATA: RIDGE POINTS, STAGEPOLES,
      WRITE(5,*) ' ENTER RIDGE POINT FILENAME'
      READ(5,900) NAME1
      900FORMAT(A)
      OPEN(UNIT=1,NAME=NAME1,TYPE='OLD',READONLY)
      WRITE(5,*) ' ENTER STAGE POLE FILENAME '
      READ(5,900) NAME2
      OPEN(UNIT=2,NAME=NAME2,TYPE='OLD',READONLY)
      WRITE(5,*)' DIVIDE ANGLE BY TWO? YES=2, NO=1'
      READ(5,*) IFAC
      WRITE(5,*) ' ENTER 1 TO WRITE TO FILE,ELSE 0'
      WRITE(5,*) ' IF 1, THEN SPACING OF POINTS IS .1 DEG,
     1 ELSE 1 DEG'
      READ(5,*) IFILE
      IF(IFILE.EQ.1) THEN
      WRITE(5,*)' ENTER FILENAME'
      READ(5,900) NAME3
      OPEN(UNIT=3,NAME=NAME3,TYPE='NEW')
      END IF
      IF(IFILE.EQ.0) INTERVAL=1
      IF(IFILE.EQ.1) INTERVAL=10
      DO J = 1,2
      IOUT=0
      READ(2,*) IPOLE
      DO K = 1,IPOLE
      READ(2,902) PLAT(K),PLON(K),PDEL(K)
  902 FORMAT(3F10.5)
      PDEL(K)=PDEL(K)/FLOAT(IFAC)
      END DO
      READ(1,*) ITOT
      WRITE(5,*) 'ITOT=', ITOT
      DO I = 1,ITOT
      WRITE(5,*)' I=',I
      READ(1,*) SLON,SLAT
      YS=BLATI(SLAT,WESNS)
      XS=BLONG(SLON,WESNS)
      IOUT=1
      END IF
      FLAT=SLAT
      FLON=SLON
      DO K = 1,IPOLE
      LTOT=INTERVAL*ABS(PDEL(K))+1.
      PINC=PDEL(K)/LTOT
      IF(IFILE.EQ.1) WRITE(3,*) LTOT
```

```
DO L=1,LTOT
CALL ROTC3(FLAT,FLON,PLAT(K),PLON(K),PINC,FLAT,FLON)
YL=BLATI(FLAT,WESNS)
XL=BLONG(FLON,WESNS)
IF(IFILE.EQ.1) WRITE(3,*) FLON,FLAT
IF(YL.GE.0.AND.XL.GE.0) THEN
IF(IOUT.EQ.0) THEN
IOUT=1
ELSE
END IF
IF(L.NE.LTOT) IOUT=0
END IF
END DO
END DO
END DO
END DO
WRITE(5,*)' FINISHED'
CLOSE(UNIT=3)
CALL EXIT
END
```

```
C       RATE.FOR
C
C       CALCULATES SPREADING RATE ALONG A SYNTHETIC FLOWLINE
C       FOR A SET OF STAGEPOLES AND STARTING (RIDGE) POINT
C       USING KENT OR LKC TIMESCALE
C
C       CANDE 19-FEB-1986
C
C       MODIFIED  18-OCT-1988
C       MARC HELMAN  UNIVERSITY OF OXFORD
C
        DIMENSION PLAT(100),PLON(100),PDEL(100)
        DIMENSION RAGE(100),AGE1(100),AGE2(100)
        CHARACTER*3 ID2(100),ID1(100),JD(100)
        CHARACTER*50 NAME1,NAME2,NAME3

C          GET NAME OF STAGEPOLE FILE
        WRITE (5,*) ' ENTER NAME OF STAGEPOLE FILE'
        READ (5,900) NAME1
    900 FORMAT (A)
C         OPEN STAGEPOLE FILE
        OPEN (UNIT=1,NAME=NAME1,TYPE='OLD',READONLY)
C         CREATE AND OPEN OUTPUT (RATE) FILE
        WRITE (5,*) ' ENTER NAME OF OUTPUT FILE'
        READ (5,900) NAME2
        OPEN (UNIT=2,NAME=NAME2,TYPE='NEW')
C         GET NAME OF TIMESCALE FILE
        WRITE (5,*) ' ENTER TIMESCALE FILENAME'
C         TIMESCALE FILE USED IS AGEKENT.DAT
        READ (5,900) NAME3
C         SET COUNTER AND READ TIMESCALE FILE
        J=1
        OPEN (UNIT=4,NAME=NAME3,TYPE='OLD',READONLY)
        DO WHILE (.TRUE.)
        READ (4,901,END=50) (JD(J),RAGE(J))
    901 FORMAT (2X,A3,F10.5)
        J=J+1
        END DO
C         CLOSE TIMESCALE FILE AND SET COUNTER
    50     CLOSE (UNIT=4)
        JDTOT=J
C          READ STAGEPOLE FILE
        READ (1,902) ITOT
    902 FORMAT(I4)
        DO I=1,ITOT
        READ(1,903) PLAT(I),PLON(I),PDEL(I),ID2(I),ID1(I)
    903 FORMAT(3F10.3,2X,A3,2X,A3)
        END DO
C          ASSIGN AGES TO STAGEPOLE IDS
        DO I = 1,ITOT
          DO J = 1,JDTOT
            IF(JD(J).EQ.ID2(I)) THEN
            AGE2(I)=RAGE(J)
            GO TO 60
            END IF
          END DO
        WRITE(5,*) ' AGE NOT FOUND FOR ID2=',ID2(I)
        CALL EXIT
```

```
   60   END DO
        DO I = 1,ITOT
          DO J = 1,JDTOT
            IF(JD(J).EQ.ID1(I)) THEN
            AGE1(I)=RAGE(J)
            GO TO 70
            END IF
          END DO
        WRITE(5,*) ' AGE NOT FOUND FOR ID1=',ID1(I)
        CALL EXIT
   70   END DO
C          FIND DISTANCES BETWEEN POINTS
        WRITE(5,*) ' ENTER STARTING FLAT,FLON'
        READ(5,*) FLAT,FLON
        WRITE(5,*) FLAT,FLON
        WRITE(2,902) ITOT
        DO I=1,ITOT
        CALL ROTC3(FLAT,FLON,PLAT(I),PLON(I),PDEL(I),RLAT,RLON)
        CALL CMDST(FLAT,FLON,RLAT,RLON,XXE,XXN,XXD)
        AGEDIF=AGE2(I)-AGE1(I)
        RATE=XXD/AGEDIF
        ERR=RATE*(.05/PDEL(I))
        WRITE(2,906) RATE,ERR,AGEDIF,AGE2(I),AGE1(I),ID2(I),ID1(I)
        WRITE(5,906) RATE,ERR,AGEDIF,AGE2(I),AGE1(I),ID2(I),ID1(I)
   906  FORMAT(5F10.3,2X,A3,2X,A3)
        MFLAT=RLAT
        FLON=RLON
        END DO
C          CLOSE UP UNITS AND FINISH
        CLOSE(UNIT=1)
        CLOSE(UNIT=2)
        WRITE(5,*) ' FINISHED'
        CALL EXIT
        END
```

```
C       ROTC3 -SPHERICAL ROTATION PROGRAM MODIFIED FOR PDP 11
C       COMPUTER FROM PROGRAM ROTC2
C       AUGUST 15,1977---J. LABRECQUE
C       ROTC3 ROTATES A GEOGRAPHIC COORDINATE (ALAT, ALON)
C       ABOUT A POLE (PPLAT, PPLON) THROUGH AN ANGLE (DELT)
C       TO ITS NEW POSITION (FLAT, FLONG)

        SUBROUTINE ROTC3 (ALAT,ALON,PPLAT,PPLON,DELT,FLAT,FLONG)

        IMPLICIT INTEGER*2 (I-N)
        IMPLICIT REAL*4 (A-H,O-Z)

        RAD=0.017453277
    1   PLAT=PPLAT
        PLONG=PPLON
        DELTL=DELT*RAD
  105   ZLAT=ALAT
        ZLONG=ALON
        RLAT=(90.0-PLAT)*RAD
        IF (PLONG.LT.0) PLONG=PLONG+360.
```

```
103   RLONG=RAD*PLONG
109   A=COS(RLAT)
      E=SIN(RLAT)
      C=COS(RLONG)
      D=SIN(RLONG)
      RZLAT=(90.-ZLAT)*RAD
      IF (ZLONG.LT.0.) ZLONG=ZLONG+360.
      ZLONG=ZLONG*RAD
      V=SIN(RZLAT)
      W=COS(RZLAT)
      X=SIN(ZLONG)
      Y=COS(ZLONG)
      CTH2=V*Y*E*C+V*X*E*D+W*A
      STH2=SQRT(1-CTH2**2)
      TH2=ATAN(STH2/CTH2)
      IF(CTH2.LT.0) TH2=3.141592+TH2
      CPH2=(V*Y*A*C+V*X*A*D-W*E)/STH2
      SPH2=(-V*Y*D+V*X*C)/STH2
      PH2=ATAN(SPH2/CPH2)
      IF(CPH2) 316,325,317
316   IF(SPH2) 319,325,319
317   IF(SPH2) 318,325,325
318   PH2=6.28319+PH2
      GO TO 325
319   PH2=3.14159+PH2
325   PH2=PH2+DELTL
      VV=SIN(TH2)
      WW=COS(TH2)
      XX=SIN(PH2)
      YY=COS(PH2)
      CTH1=-VV*YY*E+WW*A
      STH1=SQRT(1-CTH1**2)
      TH1=ATAN(STH1/CTH1)
      IF(CTH1.LT.0) TH1=3.14159+TH1
      CPH1=(VV*YY*C*A-VV*XX*D+WW*C*E)/STH1
      SPH1=(VV*YY*D*A+VV*XX*C+WW*D*E)/STH1
      PH1=ATAN(SPH1/CPH1)
      IF(CPH1) 416,425,417
416   IF(SPH1) 419,425,419
417   IF(SPH1) 418,425,425
418   PH1=6.28319+PH1
      GO TO 425
419   PH1=3.14159+PH1
425   TH1=TH1/RAD
      PH1=PH1/RAD
      FLAT=90.-TH1
      IF (PH1.LT.360.) GO TO 435
      PH1=PH1-360.
      GO TO 450
435   IF(PH1.GT.180.) PH1=PH1-360.
450   FLONG=PH1
      RETURN
      END
```

```
C          SUBROUTINE CMDST                    WALTER BROWN
C
C     COMPUTES THE DISTANCE IN NAUTICAL MILES, USING A FLAT
C     EARTH MODEL, BETWEEN GIVEN TWO GEOGRAPHIC POINTS
C     (QLAT1,QLON1) AND (QLAT2,QLON2).
C     MAKING A FIRST ORDER LATITUDINAL CORRECTION CMDST
C     COMPUTES, IN NAUTICAL MILES, E-W DISTANCE (XXE) ON THE
C     BASIS OF LONGITUDINAL DISPLACEMENT BETWEEN THE TWO POINTS.
C     CMDST ALSO COMPUTES IN NAUTICAL MILES THE N-S DISTANCE
C     COMPONENT (XXN) BETWEEN THE TWO POINTS. THE TOTAL DISTANCE
C     BETWEEN THE POINTS (XXD) IS FROM PYTHAGOREAN THEOREM.
C     XLAT1 /E/ = THE LATITUDE OF THE POINT (XLAT1,XLON1)
C     XLON1 /E/ = THE LONGITUDE OF THE POINT (XLAT1,XLON1)
C     XLAT2 /E/ = THE LATITUDE OF THE POINT (XLAT2,XLON2)
C     XLON2 /E/ = THE LONGITUDE OF THE POINT (XLAT2,XLON2)
C     XXE /R/ = E-W DISTANCE COMPONENT (NAUTICAL MILES)
C       BETWEEN POINTS (XLAT1,XLON1) AND (XLAT2,XLON2).
C     XXN /R/ = N-S DISTANCE COMPONENT (NAUTICAL MILES)
C       BETWEEN POINTS (XLAT1,XLON1) AND (XLAT2,XLON2).
C     XXD /R/ = TOTAL DISTANCE (NAUTICAL MILES) BETWEEN
C       POINTS (XLAT1,XLON1) AND (XLAT2,XLON2).
C
      SUBROUTINE CMDST(XLAT1,XLON1,XLAT2,XLON2,XXE,XXN,XXD)
      IMPLICIT INTEGER*2 (I-N)
      IMPLICIT REAL*4 (A-H,O-Z)
      XXE = COS((XLAT1+XLAT2)*.008726647)*DELON(XLON2-XLON1)*60.
      XXN = (XLAT2-XLAT1)*60.
      XXD = SQRT(XXN*XXN + XXE*XXE)
      RETURN
      END
```

```
C     FUNCTION DELON (Y)
C     FUNCTION DELON (Y) TAKES THE DIFFERENCE IN LONGITUDE (Y)
C     IN DEGREES AND ADDS OR SUBTRACTS 360 TO MAKE THE
C     DIFFERENCE LESS THAN 180.
C
      FUNCTION DELON(RLON)
      IMPLICIT INTEGER*2 (I-N)
      IMPLICIT REAL*4 (A-H,O-Z)
      IF (RLON-180.) 1,1,2
 2    DELON = RLON - 360.
      GO TO 5
 1    IF (RLON+180.) 4,3,3
 4    DELON = RLON + 360.
      GO TO 5
 3    DELON = RLON
 5    RETURN
      END
```

```
C       INITIALIZE GHOST80 SYSTEM
      CALL PAPER (1)
C       DEFINE PLOTTING AREA
      CALL PSPACE (0.2,0.80,0.2,0.60)
C       DEFINE MAP SPACE
      CALL MAP (0.0,10.0,0.0,5.0)
C       SET AXIS ORIGIN
      CALL AXORIG (0.0,0.0)
C       DRAW AXES
      CALL AXES
C       LABEL AXES
      CALL PCSCEN (5.0,-0.5,'TIME  [X 10,000,000 YEARS]')
      CALL CTRORI (90.0)
      CALL PCSCEN (-0.75,2.5,'SPREADING RATE  [CMS/YEAR]')
      CALL CTRORI (0.0)
C      CREATE TITLE FOR PLOT
      WRITE (5,*) 'WRITE TITLE FOR PLOT-1ST LINE'
      READ (5,500) LABEL1
  500 FORMAT (A)
      CALL PLOTCS (1.0,4.5,LABEL1)
      WRITE (5,*) 'ENTER 1 FOR SECOND LINE'
      READ (5,*) ILABEL
      IF (ILABEL .NE. 1) GO TO 501
      WRITE (5,*) 'WRITE TITLE FOR PLOT-2ND LINE'
      READ (5,500) LABEL2
      CALL PLOTCS (2.0,4.1,LABEL2)
  501 CONTINUE
C       SET LINE THICKNESS
      WRITE (5,*) 'ENTER DESIRED LINE THICKNESS---1,2,3,ETC.
     1  FOR PLOTTING'
      READ (5,*) ILINE
      CALL THICK(ILINE)
C       CHOOSE PEN COLOR FOR PLOTTING RATE
      WRITE (5,*) 'ENTER 0 FOR DEFAULT (BLACK) PEN, 2
     1 FOR RED PEN, 3 FOR GREEN PEN, 4 FOR BLUE PEN FOR
     2 FOR PLOTTING RATE'
       READ (5,*) IPEN
      CALL LINCOL (IPEN)
C       PLOT GRAPH OF RATE
      CALL POSITN (X1(I),Y(I))
      DO 10 I = 1,ITOT
      CALL JOIN (X1(I),Y(I))
      CALL JOIN (X2(I),Y(I))
   10 CONTINUE
C       CHOOSE PEN COLOR OF PENS FOR PLOTTING ERRORS
      WRITE (5,*) 'ENTER 0 FOR DEFAULT (BLACK) PEN, 2
     1 FOR RED PEN, 3 FOR GREEN PEN, 4 FOR BLUE PEN FOR
     2 PLOTTING ERRORS'
      READ (5,*) IPEN
      CALL LINCOL (IPEN)
C       CHOOSE TYPE OF LINES FOR PLOTTING ERRORS
      WRITE (5,*) 'ENTER 0 FOR BROKEN LINES IN PLOTTING ERRORS'
      READ (5,*) IBROKE
      IF (IBROKE .NE. 0) GO TO 702
      IF (IBROKE .EQ. 0) GO TO 701
  701 WRITE (5,*) 'ENTER 0 FOR EQUAL SEGMENTS'
      READ (5,*) IEQ
      IF (IEQ .EQ. 0) CALL BROKEN (6,6,6,6)
```

```
      IF (IEQ .NE. 0) CALL BROKEN (12,6,6,6)
  702 CONTINUE
C        PLOT DATA
      CALL POSITN (X1(I),Y3(I))
      DO 20  I = 1,ITOT
      CALL JOIN (X1(I),Y3(I))
      CALL JOIN (X2(I),Y3(I))
   20 CONTINUE
      CALL POSITN (X1(I),Y4(I))
      DO 30  I = 1,ITOT
      CALL JOIN (X1(I),Y4(I))
      CALL JOIN (X2(I),Y4(I))
   30 CONTINUE
C       CLOSE DATA FILE AND GHOST-80 SYSTEM AND PROGRAM
      CALL GREND
      CLOSE(UNIT=1)
      WRITE(5,*) ' FINISHED'
      STOP
      END
```

```
C         INCDEC.FTN
C
C         PROGRAM CALCULATES INCLINATION AND DECLINATION
C         AT ANY GIVEN LATITUDE AND LONGITUDE FROM FIELD
C         PARAMETERS GIVEN BY SUBROUTINE FIELDG
C         TIME ASSUMED TO BE 1970.0,  ALT ASSUMED TO BE 0.

      CHARACTER*20 NAMEP
      NMX=14
      NAMEP='PRMAG1.COF'
      WRITE(5,2133)NAMEP
 2133 FORMAT(' FIELD COEFFICIENTS= ',A)
      RAD=180./3.1415926
      ALT=0.
      TTT=1970.0
      L=1
      OPEN (UNIT=3, TYPE='OLD', NAME=NAMEP, ACCESS='SEQUENTIAL',
     1 READ ONLY, ERR=950)
      DO 20 I = 1,1000
      WRITE(5,*) ' ENTER FLAT,FLON,ALT(KM.), 3F10.3; 0 TO EXIT'
      READ(5,902) XLAT,XLON,ALT
      WRITE(5,*)' TYPE YEAR-F10.3'
      READ(5,902)TTT
  902 FORMAT(8F10.3)
      IF((ABS(XLAT).LT.0.1).AND.(ABS(XLON).LT.0.1)) GO TO 50
      CALL FIELDG(XLAT,XLON,ALT,TTT,NMX,L,X,Y,Z,F)
      L=0
      H=SQRT(X*X+Y*Y)
      FINC=RAD*ATAN(Z/H)
      FDEC=RAD*ATAN(Y/X)
      WRITE(5,*)' ALT= ',ALT,' KM.'
      WRITE(5,903) XLAT,XLON,FINC,FDEC,F
  903 FORMAT(' LAT=',F8.3,' LON=',F8.3,' INC=',F8.3,'
     1  DEC=',F8.3,' TOTAL FIELD=',F8.1)
   20 CONTINUE
  950 WRITE(5,*)' TROUBLE IN OPENING PRMAG.COF '
   50 CLOSE(UNIT=3)
      CALL EXIT
      END

------------------------------------------------------------
C         SUBROUTINE FIELDG (DLAT,DLONG,ALT,TM,NMX,L,X,Y,Z,F)
C         MODIFIED JULY 22,1981
C         FOR DOCUMENTATION OF THIS SUBROUTINE AND SUBROUTINE
C         FIELD SEE: NATIONAL SPACE SCIENCE DATA CENTER'S
C         PUBLICATION COMPUTATION OF THE MAIN GEOMAGNETIC FIELD
C         FROM SPHERICAL HARMONIC EXPANSIONS  DATA USERS' NOTE,
C         NSSDC 68-11, MAY 1968 GODDARD SPACE FLIGHT CENTER,
C         GREENBELT,MD.

      EQUIVALENCE (SHMIT(1,1),TG(1,1))
      COMMON NDPY(3),LPYR(4),JBSYR
      COMMON /COEFFS/TG(18,18), G(18,18), GT(18,18), GTT(18,18),
     1 TLAST, TZERO
      COMMON /FLDCOM/ST,CT,SPH,CPH,R,NMAX,BT,BP,BR,B
      DIMENSION AID(11),SHMIT(18,18)
      DATA A/0./
```

```
      A=6378.16
      FLAT=1.-1./298.25
      A2=A**2
      A4=A**4
      B2=(A*FLAT)**2
      A2B2=A2*(1.-FLAT**2)
      A4B4=A4*(1.-FLAT**4)
C       IF L.LE.0 DON'T READ COEFFICIENTS FILE
      IF (L) 1,1,2
C       IF DATE IS THE SAME AS LAST DON'T UPDATE COEFFICIENTS
    1 IF (TM-TLAST) 17,19,17
C       READ FIELD COEFFICIENTS
    2 READ (3,3) J,K,TZERO,(AID(I),I=1,11)
    3 FORMAT (2I1,1X,F6.1,10A6,A3)
      L=0
    4 FORMAT (2I3,5X6HEPOCH=,F7.1,5X10A6,A3)
      MAXN=0
      TEMP=0.
    5 READ (3,6,END=74) N,M,GNM,HNM,GTNM,HTNM,GTTNM,HTTNM
C     WRITE(5,6)N,M,GNM,HNM,GTNM,HTNM,GTTNM,HTTNM
    6 FORMAT (2I3,6F11.4)
      IF (N.LE.0) GOTO74
      MAXN=(MAX0(N,MAXN))
      G(N,M)=GNM
      GT(N,M)=GTNM
      GTT(N,M)=GTTNM
      IF (M.EQ.1) GOTO5
      G(M-1,N)=HNM
      GT(M-1,N)=HTNM
      GTT(M-1,N)=HTTNM
      GO TO 5
   74 CONTINUE
C     WRITE COEFFICIENTS FOR DEBUGGING PURPOSES
D7    WRITE (5,8)
D8    FORMAT (6H0 NM, 6X1HG, 10X1HH, 9X2HGT, 9X2HHT,
     1 8X3HGTT8X3HHTT//)
D     WRITE(5,239)MAXN
D239  FORMAT(I10)
D     DO 12 N=2,MAXN
D     DO 12 M=1,N
D     MI=M-1
D     IF(M.EQ.1) GO TO 10
D     WRITE (5,9) N, M, G(N,M), G(MI,N), GT(N,M), GT(MI,N),
     1 GTT(N,M), GTT(MI,N)
D9     FORMAT (2I3,6F11.4)
D     GO TO 12
D10   WRITE (5,11) N,M,G(N,M),GT(N,M),GTT(N,M)
D11   FORMAT (2I3,F11.4,11X,F11.4,11XF11.4)
D12   CONTINUE
C*******K.NE.0 IF COEFFICIENTS ARE GAUSS QUASINORMALIZED
C*******K.EQ.0 IF COEFFICIENTS ARE SCHMIDT QUASINORMALIZED
   14 IF (K.NE.0) GOTO17
      SHMIT(1,1)=-1.
      DO 15 N=2,MAXN
      SHMIT(N,1)=SHMIT(N-1,1)*FLOAT(2*N-3)/FLOAT(N-1)
      SHMIT(1,N)=0.
      JJ=2
      DO 15 M=2,N
```

```
      SHMIT(N,M)=SHMIT(N,M-1) *
SQRT(FLOAT((N-M+1)*JJ)/FLOAT(N+M-2))
      SHMIT(M-1,N)=SHMIT(N,M)
 15   JJ=1
      DO 16 N=2,MAXN
      DO 16 M=1,N
      G(N,M)=G(N,M)*SHMIT(N,M)
      GT(N,M)=GT(N,M)*SHMIT(N,M)
      GTT(N,M)=GTT(N,M)*SHMIT(N,M)
      IF (M.EQ.1) GOTO16
      G(M-1,N)=G(M-1,N)*SHMIT(M-1,N)
      GT(M-1,N)=GT(M-1,N)*SHMIT(M-1,N)
      GTT(M-1,N)=GTT(M-1,N)*SHMIT(M-1,N)
 16   CONTINUE
 17   T=TM-TZERO
      DO 18 N=1,MAXN
      DO 18 M=1,N
      TG(N,M)=G(N,M)+T*(GT(N,M)+GTT(N,M)*T)
C       BE CAREFUL THAT SECULAR ACCELERATION TERMS ARE
C       DEFINED AS A*T/2.
      IF (M.EQ.1) GOTO18
      TG(M-1,N)=G(M-1,N)+T*(GT(M-1,N)+GTT(M-1,N)*T)
 18   CONTINUE
      TLAST=TM
 19   DLATR=DLAT/57.2957795
      SINLA=SIN(DLATR)
      RLONG=DLONG/57.2957795
      CPH=COS(RLONG)
      SPH=SIN(RLONG)
      IF (J.EQ.0) GOTO20
C       IF J.NE.0 OUTPUT IS IN GEOCENTRIC COORDINATES
      R=ALT+6371.0
      CT=SINLA
      GO TO 21
C*****CALCULATE GEODETIC CONSTANTS
 20   SINLA2=SINLA**2
      COSLA2=1.-SINLA2
      DEN2=A2-A2B2*SINLA2
      DEN=SQRT(DEN2)
      FAC=(((ALT*DEN)+A2)/((ALT*DEN)+B2))**2
      CT=SINLA/SQRT(FAC*COSLA2+SINLA2)
      R=SQRT(ALT*(ALT+2.*DEN)+(A4-A4B4*SINLA2)/DEN2)
 21   ST=SQRT(1.-CT**2)
C       EVALUATE SPHERICAL HARMONIC TO ORDER AND DEGREE NMAX
C       (NOTE: NMAX IS N+1 OF MATH EXPRESSION, I.E. NMAX 14 =
C       DEGREE 13 TO SATISFY THE COMPUTER DO LOOPS
      NMAX=MIN0(NMX,MAXN)
C       EVALUATE SPHERICAL HARMONICS
      CALL FIELD
      Y=BP
      F=B
      IF (J) 22,23,22
 22   X=-BT
      Z=-BR
      RETURN
C       TRANSFORMS FIELD TO GEODETIC DIRECTIONS
 23   SIND=SINLA*ST-SQRT(COSLA2)*CT
      COSD=SQRT(1.0-SIND**2)
```

```
      X=-BT*COSD-BR*SIND
      Z=BT*SIND-BR*COSD
D     WRITE(5,1212)DLAT,DLONG,TM,X,Y,Z,F
 1212 FORMAT(7F8.1)
      RETURN
      END
```

```
      SUBROUTINE FIELD

      COMMON NDPY(3),LPYR(4),JBSYR
      COMMON/COEFFS/G(18,18), GX(18,18), GT(18,18), GTT(18,18),
     1 TLAST, TZERO
      COMMON/FLDCOM/ST,CT,SPH,CPH,R,NMAX,BT,BP,BR,B
      DIMENSION P(18,18), DP(18,18), CONST(18,18), SP(18),
     1 CP(18), FN(18), FM(18)
      IF (P(1,1).EQ.1.0) GO TO 3
 1    P(1,1)=1.
      DP(1,1)=0.
      SP(1)=0.
      CP(1)=1.
      DO 2 N=2,18
      FN(N)=N
      DO 2 M=1,N
      FM(M)=M-1
 2    CONST(N,M)=FLOAT((N-2)**2-(M-1)**2)/FLOAT((2*N-3)*(2*N-5))
 3    SP(2)=SPH
      CP(2)=CPH
      DO 4 M=3,NMAX
      SP(M)=SP(2)*CP(M-1)+CP(2)*SP(M-1)
 4    CP(M)=CP(2)*CP(M-1)-SP(2)*SP(M-1)
      AOR=6371.2/R
      AR=AOR**2
      BT=0.
      BP=0.
      BR=0.
      DO 8 N=2,NMAX
      AR=AOR*AR
      DO 8 M=1,N
      IF (N-M) 6,5,6
 5    P(N,N)=ST*P(N-1,N-1)
      DP(N,N)=ST*DP(N-1,N-1)+CT*P(N-1,N-1)
      GO TO 7
 6    P(N,M)=CT*P(N-1,M)-CONST(N,M)*P(N-2,M)
      DP(N,M)=CT*DP(N-1,M)-ST*P(N-1,M)-CONST(N,M)*DP(N-2,M)
 7    PAR=P(N,M)*AR
      IF (M.EQ.1) GO TO 9
      TEMP=G(N,M)*CP(M)+G(M-1,N)*SP(M)
      GO TO 10
 9    TEMP=G(N,M)*CP(M)
      BP=BP-(G(N,M)*SP(M))*FM(M)*PAR
 10   BT=BT+TEMP*DP(N,M)*AR
 8    BR=BR-TEMP*FN(N)*PAR
      BP=BP/ST
      B=SQRT(BT*BT+BP*BP+BR*BR)
      RETURN
      END
```

```
C           PROGRAM MODEL2
C           REVISED MARCH 25,1981- J.L. LABRECQUE
C           INCORPORATES GAUSSIAN DIKE INJECTION, CORRECTED
C           LAMINA ROUTINE, THETA VALUES CONSISTENT WITH SCHOUTEN
C           AND MC CAMY DEFINITIONS, INCREASED SPEED, MODEL VALUE
C           OUTPUT FILE OPTION
C           NSCAL.REV CONTAINS REVERSAL TIME SCALE
C
      DIMENSION ITOP(4098),X(4098),XGAM(4098),XINFO(40)
      BYTE NAME(18)
      CHARACTER*20 TSCAL
      COMMON M
      DATA ITOP(18)/0/
      DATA NAME(18)/0/
      M=8
C       DATA IS ENTERED IN DATA FILES EMPLOYING FORMAT 8F10.0
C       DATA RECORD FILE NAME IS INDICATED DURING EXECUTION TIME
C       FIRST DATA RECORD
C       1=1 FOR TOPO,SCALE PLOTS,2 FOR HORIZONTAL SCALE ONLY,
C       3 FOR NO TOPO ,NO SCALE, 4 FOR TOPO,SCALE, LAMINA
C        APPROXIMATION PLOTTED
C       2=XMIN OF TOPO(DISTANCE OF FIRST DATA POINT IN KM)
C       3=XMAX OF TOPO(DISTANCE OF LAST DATA POINT IN KM)
C       4=NUMBER OF LAMINA DESIRED (SET TO 1 FOR SIMPLE FLAT
C        BLOCK MODEL)
C       5=HALF SPREADING RATE IN CM/YR
C       6=DISTANCE OF TIE POINT IN KM
C       7=AGE OF TIE POINT IN MILLIONS OF YRS
C       8=-1 TO REVERSE TOPO, ZERO OTHERWISE
C       SECOND DATA RECORD
C       9=0 FOR PLOT ONLY, =1 FOR MODEL VALUES IN OUTPUT FILE
C          (PROJECTED DATA FO
C       10= STRENGTH OF MAGNETIZATION IN EMU/CM**3
C       11= THICKNESS OF MAGNETIZED LAYER IN METERS
C       12= DIRECTION OF PLOT (0 TO 360. DEGREES)
C       13=INCLINATION OF PRESENT FIELD
C       14= DECLINATION OF PRESENT FIELD
C       15= HORIZONTAL SCALE IN KM PER INCH
C       16= VERTICAL TOPO SCALE IN METERS PER INCH
C       THIRD DATA RECORD
C       17= VERTICAL MAGNETIC ANOMALY SCALE IN GAMMAS PER INCH
C       18= NUMBER OF PAIRS OF REMENANT FIELD PARAMETERS TO BE
C        USED, UP TO 11 DIFFERENT FIELD DIRECTIONS READ (IF
C        PHASE SHIFT IS TO BE INCREMENTED INSTEAD, SET EQUAL TO
C        -10. FOLLOW INSTRUCTIONS IN BRACKETS WHICH FOLLOW)
C       19= FIRST REMANENT FIELD INCLINATION(FIRST VALUE OF
C        THETA IN DEGREES)
C       20= FIRST REMANENT FIELD DECLINATION(NUMBER OF TIMES
C        THETA IS TO BE INCREMENTED)
C       21= SECOND REMANENT FIELD INCLINATION ETC. (THETA
         INCREMENT IN DEGREES)
C       22= SECOND REMANENT FIELD DECLINATION ETC.
C       FOR VARIABLE SPR RATE PROCEED AS FOLLOWS
C       READ IN XINFO(5) GREATER THAN 99991.
C       THEN READ JJ FORMAT 15 JJ IS NO OF VAR SPR RATES
C       NEXT READ AG(1),BG(1),SPR(1),ON FIRST RECORD
C       AG(2),BG(2),SPR(2),ON SECOND CARD AND SO ON FOR
C       JJ CARDS IN ALL
```

```
C       AG(1) MUST BE XINFO(7)     (AGE OF TIE POINT)
C       SPR(J) IS SPR RATE BETWEEN AGE AG(J) AND BG(J)
C       AG(J) MUST BE EQUAL TO BG(J-1)
C       SEQUENCE OF INPUT RECORDS IS  --  XINFO RECORDS,TOPO
C       RECORDS, AND VARIABLE SPREADING RATE RECORDS (OPTIONAL)
C       TOPO INPUT FORMAT IS(' '6(F7.1,16)) FOR PURPOSES OF THIN
C       DIKE APPROXIMATION THE TOPO INTERPOLATION INTERVAL SHOULD
C       NOT EXCEED THE SHALLOWEST TOPO DEPTH
C       FOR THIS PROGRAM THE VALUE (XMAX-XMIN)/SHALLOWEST TOPO
C       POINT SHOULD NOT EXCEED 1, THE UNITS ARE KM/METERS
C       IAL= NUMBER OF INTERPOLATED DATA POINTS 128, 256, 512,
C       OR 1024

      IAL=4096
      CALL ASSIGN(3,'TI:',3)
      CALL ASSIGN(5,'TO:',3)
      WRITE(5,*)' TYPE REVERSAL TIME SCALE FILE NAME'
      READ(5,1932)TSCAL
 1932 FORMAT(A)
      OPEN(UNIT=1,NAME=TSCAL,TYPE='OLD',ACCESS='DIRECT',FORM=
     1'UNFORMATTED',READONLY)
      WRITE(3,133)
 133  FORMAT('$PARAMETER RECORD FILE?')
      READ(3,134)(ITOP(I),I=1,17)
 134  FORMAT(17A2)
      CALL ASSIGN(8,ITOP)
 9111 READ(8,700)(XINFO(I),I=1,24)
      IF(XINFO(18).LT.0)N=21
      IF(XINFO(18).GT.0)N=18+2*XINFO(18)
      IF(N-24)701,701,702
  702 READ(8,700)(XINFO(I),I=25,N)
  700 FORMAT(8(F10.3))
      WRITE(5,*)' XINFO-----'
  701 WRITE(5,700)(XINFO(I),I=1,N)
      IF(XINFO(9).LE.0.)GO TO 1701
      WRITE(5,*)' TYPE OUTPUT FILE NAME-(******.***)'
      READ(3,1702)(NAME(I),I=1,17)
 1702 FORMAT(17A1)
 1701 PI=3.1415926
      BERNG=99999999.
      RAD=57.29577
      D=.025/RAD
      AM=XINFO(10)*1.E05
      AZZ=XINFO(12)/RAD
      THET=XINFO(19)/RAD
      CR=XINFO(21)/RAD
      NP=XINFO(9)
      XKM=1/XINFO(15)
      PDIP=XINFO(13)/RAD+D
      PDEC=XINFO(14)/RAD
      NPOLE=XINFO(18)
      LPT=IAL-40
      XINFO(8)=XINFO(8)+.5
      IF(XINFO(8)) 722,723,723
  722 Z=-XINFO(2)
      XINFO(2)=-XINFO(3)
      XINFO(3)=Z
      XINFO(6)=-XINFO(6)
```

```
723 TERV=(XINFO(3)-XINFO(2))/(LPT-1.)
    CALL TOP1(TERV,IHIGH,ILOW,XINT,LPT,X,ITOP,XINFO)
    CALL REVES(TERV,LPT,X,XINFO)
    CALL LAM1(LPT,XINT,IHIGH,TERV,XGAM,X,ITOP,XINFO)
    Z=-(ILOW+1)/XINFO(16)*XINFO(17)
    NGO=1
    IF(NPOLE) 703,689,689
703 NPOLE=XINFO(20)
    NGO=2
    N=19
    XINFO(19)=BERNG
    XINFO(20)=BERNG
689 DO 5501 IP=1,NPOLE
    GO TO(551,552),NGO
551 N=17+IP*2
    RDIP=XINFO(N)/RAD+D
    RDEC=XINFO(N+1)/RAD
    TANIP=TAN(PDIP)/COS(AZZ-PDEC+D)
    TANIR=TAN(RDIP)/COS(AZZ-RDEC+D)
    PINC=ATAN(TANIP)
    RINC=ATAN(TANIR)
    THETA=RINC+PINC-PI
    IF(THETA.GT.PI)THETA=THETA-2.*PI
    IF(THETA.LT.-1.*PI)THETA=THETA+2.*PI
    CPP=SIN(PDIP)/SIN(PINC)
    CPR=SIN(RDIP)/SIN(RINC)
    CP=CPR*CPP
    GO TO 883
552 THETA=THET+(IP-1)*CR
    CP=1.
 883 WRITE(3,101)
 101 FORMAT(' ENTER SIGMA IN KMS,F10.3')
     READ(3,700) SIG
     PHRL=COS(THETA)
     AL=IAL
     PHIM=-1.*SIN(THETA)
     RCOF=4.*CP*AM*PHRL*PI/AL
     ZCOF=4.*CP*AM*PHIM*PI/AL
     DO 5500 I=1,IAL/2
     XII=I
     S=(2.*PI*(XII-1))/(AL*TERV)
     GAUSS=EXP(-.5*((SIG*S)**2.))
     II=2*I
     IR=II-1
     X(IR)=(XGAM(IR)*RCOF-XGAM(II)*ZCOF)*GAUSS
5500 X(II)=(XGAM(IR)*ZCOF+XGAM(II)*RCOF)*GAUSS
     X(IAL+1)=0.
     X(IAL+2) = 0.
     X(1) = 0.
     X(2)=0.0
     CALL RFFTI(X,IAL)
     YGAM=1/XINFO(17)
     CALL SCALF(XKM,YGAM,0.0,Z)
     Z=0.0
     DO 5600 I=1,LPT
     DIS=(I-1)*TERV
     CALL FPLOT(-2,DIS,X(I))
5600 CONTINUE
```

```
      XDIP=XINFO(N)
      XDEC=XINFO(N+1)
      HETA=THETA*RAD
      BERNG=XINFO(12)
      IF(XINFO(18)) 5602,5603,5603
5603  WRITE(5,5601) XINFO(13),XINFO(14),XDIP,XDEC
5601  FORMAT(' PRESENT INCLINATION=',F4.0,' PRESENT
     1 DECLINATION=',F4.0, ' REMANENT INCLINATION=',F4.0,'
     2 ' REMANENT DECLINATION=',F4.0)
5602  WRITE(5,879)BERNG,XINFO(5),XINFO(10),XINFO(11),CP,HETA,SIG
      CALL FLPLOT (1,0.0,XINFO(17))
      IF(NP)5501,5501,731
 731  OPEN(UNIT=2,NAME=NAME,ACCESS='SEQUENTIAL',TYPE='NEW')
      DO 6 I=1,LPT
      ITOP(I)=X(I)
      X(I)=(I-1)*TERV+XINFO(2)
      IF(XINFO(8)) 16,6,6
  16  X(I)=-X(I)
   6  CONTINUE
      WRITE(2,5531)LPT,XINFO(2),XINFO(3),XINFO(12)
5531  FORMAT(I10,20X,3F10.3)
      WRITE(2,878)(X(I),ITOP(I),I=1,LPT)
      IF(XINFO(18).LT.0)GO TO 1878
      WRITE(2,5601)XINFO(13),XINFO(14),XDIP,XDEC
1878  WRITE(2,879)BERNG,XINFO(5),XINFO(10),XINFO(11),CP,HETA,SIG
      CLOSE(UNIT=2)
 878  FORMAT(' ',F7.1,I6,F7.1,I6,F7.1,I6,F7.1,I6,F7.1,I6,F7.1,I6)
 879  FORMAT(' PLOT AZZIMUTH=',F5.0,' SPR. RATE='F7.2,
     1' MAG. INTENSITY='F7.5,
     2' THICKNESS OF MAGNETIZATION=',F7.0,' CP=',F5.2,'
     3' THETA=',F5.0, SIGMA=',F6.1,//)
 5501 CONTINUE
      ZL=2*XINFO(17)
      CALL FPLOT(1,0.0,ZL)
      STOP ' AU REVOIR SWEETHEART'
      END
```

```
C
C       SUBROUTINE RFFT.FOR
C       COMPUTES THE FINITE FOURIER TRANSFORM OF THE REAL ARRAY
C       XOF LENGTH N (N MUST BE AN INTEGRAL POWER OF 2)
C       THE FOURIER COEFFICIENTS ARE RETURNED AS A COMPLEX
C       ARRAY X OF LENGTH N/2+1

      SUBROUTINE RFFT(X,N)

      REAL X(2)

      NN= N/2
      IS=1
      CALL FOUR1(X,NN,IS)
      NM= NN/2
      S= X(1)
      X(1)= X(1)+X(2)
      X( N+1)= S-X(2)
      X(2)= 0.
      X(N +2)= 0.
      X(NN+2)= -X(NN+2)
      FN= N
      EX= 6.2831852/FN
      J = NN
      WR= 1.
      WI=0.
      WWR= COS(EX)
      WWI= -SIN(EX)
      DO 1 I = 2,NM
      WRR= WR*WWR-WI*WWI
      WI= WR*WWI+WI*WWR
      WR=WRR
      K1J = 2*J-1
      K1I = 2*I-1
      K2J = 2*J
      K2I = 2*I
      A1= .5*(X(K1I)+X(K1J))
      A2= .5*(X(K2I)-X(K2J))
      B1= .5*(-X(K1I)+X(K1J))
      B2= .5*(-X(K2I)-X(K2J))
      S= B1
      B1= B1*WR+B2*WI
      B2= B2*WR-S*WI
      X(K1I)= A1-B2
      X(K2I)=-A2-B1
      X(K1J)= A1+B2
      X(K2J)=  A2-B1
1     J= J-1
      RETURN
      END
```

```
C       SUBROUTINE FOUR1.FOR (DATA,N,ISIGN)
C      THE COOLEY-TUKEY FAST FOURIER TRANSFORM IN FORTRAN.
C      NOTE-- IT SHOULD NOT BE NECESSARY TO CHANGE ANY STATEMENT
C      IN THIS PROGRAM SO LONG AS THE FORTRAN COMPILER USED
C      STORES REAL AND IMAGINARY PARTS ADJACENTLY IN STORAGE.
C      TRANSFORM(K) =
C      SUM (DATA(J)*EXP(ISIGN*2*PI*SQRT(-1)*(J-1)*(K-1)/N)),
```

```
C     SUMMED OVER ALL J AND K FROM 1 TO N.  DATA IS A ONE-
C     DIMENSIONAL COMPLEX ARRAY (I.E., THE REAL AND IMAGINARY
C     PARTS ARE ADJACENT IN STORAGE, SUCH AS FORTRAN IV PLACES
C     THEM) WHOSE LENGTH N=2**K, K.GE.0 (IF NECESSARY, APPEND
C     ZEROES TO THE DATA).  ISIGN IS +1 OR -1.  IF A -1
C     TRANSFORM IS FOLLOWED BY A +1 ONE (OR VICE VERSA) THE
C     ORIGINAL DATA REAPPEAR, MULTIPLIED BY N.  TRANSFORM VALUES
C     ARE RETURNED IN ARRAY DATA, REPLACING THE INPUT.  THE TIME
C     IS PROPORTIONAL TO N*LOG2(N), RATHER THAN THE NAIVE N**2.
C     ACCURACY IS ALSO GREATLY IMPROVED, THE RMS RELATIVE ERROR
C     BEING BOUNDED BY 6*SQRT(2)*LOG2(N)*2**(-B), WHERE B IS THE
C     NUMBER OF BITS IN THE FLOATING POINT FRACTION.
C     WRITTEN BY NORMAN BRENNER MIT LINCOLN LAB.  JULY 1967.
C     THIS IS THE SHORTEST VERSION OF THE FFT KNOWN TO THE
C     AUTHOR.  FASTER PROGRAMS FOUR2 AND FOURT EXIST THAT OPERATE
C     ON ARBITRARILY SIZED MULTIDIMENSIONAL ARRAYS.  SEE-- IEEE
C     AUDIO TRANSACTIONS (JUNE 1967), SPECIAL ISSUE ON FFT.
C

      SUBROUTINE FOUR1.FOR (DATA,N,ISIGN)

      DIMENSION DATA(1)
      IP0=2
      IP3=IP0*N
      I3REV=1
      DO 50 I3=1,IP3,IP0
      IF(I3-I3REV)10,20,20
 10   TEMPR=DATA(I3)
      TEMPI=DATA(I3+1)
      DATA(I3)=DATA(I3REV)
      DATA(I3+1)=DATA(I3REV+1)
      DATA(I3REV)=TEMPR
      DATA(I3REV+1)=TEMPI
 20   IP1=IP3/2
 30    IF(I3REV-IP1)50,50,40
 40    I3REV=I3REV-IP1
       IP1=IP1/2
       IF(IP1-IP0)50,30,30
 50    I3REV=I3REV+IP1
       IP1=IP0
 60    IF(IP1-IP3)70,100,100
 70    IP2=IP1*2
       THETA=6.283185307/FLOAT(ISIGN*IP2/IP0)
       SINTH=SIN(THETA/2.0)
       WSTPR=-2.*SINTH*SINTH
       WSTPI=SIN(THETA)
       WR=1.
       WI=0.
       DO 90 I1=1,IP1,IP0
       DO 80 I3=I1,IP3,IP2
       I2A=I3
       I2B=I2A+IP1
       TEMPR=WR*DATA(I2B)-WI*DATA(I2B+1)
       TEMPI=WR*DATA(I2B+1)+WI*DATA(I2B)
       DATA(I2B)=DATA(I2A)-TEMPR
       DATA(I2B+1)=DATA(I2A+1)-TEMPI
       DATA(I2A)=DATA(I2A)+TEMPR
80     DATA(I2A+1)=DATA(I2A+1)+TEMPI
```

```
      TEMPR=WR
      WR=WR*WSTPR-WI*WSTPI+WR
90    WI=WI*WSTPR+TEMPR*WSTPI+WI
      IP1=IP2
      GO TO 60
100   RETURN
      END
```

```
      SUBROUTINE RFFTI(X,N)

      REAL X(2)

      NN= N/2
      S= X(1)
      X(1)= .5*(X(1)+X( N+1))
      X(2)= .5*(S-X( N+1))
      X(NN+2)= -X(NN+2)
      IS= -1
      NM= NN/2
      FN= N
      EX= 6.2831852/FN
      J = NN
      WR= 1.
      WI=0.
      WWR= COS(EX)
      WWI= -SIN(EX)
      DO 1 I = 2,NM
      WRR= WR*WWR-WI*WWI
      WI= WR*WWI+WI*WWR
      WR=WRR
      K1J = 2*J-1
      K1I = 2*I-1
      K2J = 2*J
      K2I = 2*I
      A1= .5*(X(K1I)+X(K1J))
      A2= .5*(X(K2I)-X(K2J))
      B1= .5*(-X(K1I)+X(K1J))
      B2= .5*(-X(K2I)-X(K2J))
      S= B1
      B1= B1*WR+B2*WI
      B2= B2*WR-S*WI
      X(K1I)= A1-B2
      X(K2I)=-A2-B1
      X(K1J)= A1+B2
      X(K2J)=  A2-B1
1     J= J-1
      CALL FOUR1(X,NN,IS)
      RETURN
      END
```

```
      SUBROUTINE CHART(LOW,XINFO)

      DIMENSION XINFO(40)
      LOGICAL*1 ARRAY1(5)

      XKM=1/XINFO(15)
      YKM=1/XINFO(16)
      N1=XINFO(1)+.5
      XMAX=XINFO(3)
      XMIN=XINFO(2)
    2 Y=-LOW
      CALL SCALF(XKM,YKM,XMIN,Y)
C          PLOTS DISTANCE SCALE
      IMIN=XMIN/10.
      X=(IMIN+1.)*10
      CALL FPLOT(2,X,Y)
      N=(XMAX-XMIN)/10.+1
      CALL FGRID(0,X,Y,10.0,N)
      Y2=-LOW-.25*XINFO(16)
      N=0
      IM=XMAX/100.
   11 X=(IM-N)*100.
      IF(X-XMIN) 23,13,13
   13 CALL FPLOT(-2,X,Y)
      CALL FPLOT(-1,X,Y2)
      XC=100.*XKM/8.
      YC=1.2*XC
      Y3=-LOW-2.3*XC*XINFO(16)
      CALL FCHAR(X,Y3,XC,YC,0.0)
      IX=X
      IF(XINFO(8))133,132,132
  133 IX=-IX
  132 ENCODE (6,10,ARRAY1) IX
   10 FORMAT (I6)
      CALL ANOTAT (6,ARRAY1)
      N=N+1
      GO TO 11
   23 GO TO(24,57,57,24),N1
C        PLOTS TOPO SCALE
   24 X=XMIN
      N=LOW/1000
      CALL FGRID(1,X,Y,1000.,N)
      N=0
   56 Y=-N
      YC=YKM*400
      XC=.8*YC
      X=XMIN-7*XC*XINFO(15)
      CALL FCHAR(X,Y,XC,YC,0.0)
      ENCODE (6,10,ARRAY1) N
      CALL ANOTAT (6,ARRAY1)
      N=N+1000
      IF(N-LOW)56,56,57
   57 Y=-LOW
      CALL FPLOT(1,XMIN,Y)
      RETURN
      END
```

```
C       SUBROUTINE REVES(TERV,LPT,X,XINFO)
C       OLDER TO RIGHT FOR VARIABLE SPR RATE PROCEED AS FOLLOWS
C       READ IN HFSPR GREATER RTHAN  9900.  THEN READ JJ FORMAT
C       I5 JJ IS NO OF VAR SPR RATES NEXT READ AG(1),BG(1),SPR(1),
C       ON FIRST CARD AG(2),BG(2),SPR(2), ON SECOND CARD AND SO
C       ON FOR JJ CARDS IN ALL
C       AG(1) MUST BE AGXKM,  SPR(J) IS SPR RATE BETWEEN AGE
C       AG(J) AND BG(J),  AG(J) MUST BE EQUAL TO BG(J-1)

      SUBROUTINE REVES(TERV,LPT,X,XINFO)
      DIMENSION AG(5),CG(5),SPR(5),XINFO(40),X(2)

      COMMON M
      HFSPR=XINFO(5)
      XKM=XINFO(6)
      AGXKM=XINFO(7)
      IF(HFSPR-9900)500,500,501
  501 READ(M,701)JJ
      CG(1)=0.0
  701 FORMAT(I5)
      DO 502 J=1,JJ
  502 READ(M,702)AG(J ),DUM,SPR(J )
  702 FORMAT(3F10.1)
      DO 507 J=2,JJ
      K=J-1
  507 CG(J)=CG(K)+(AG(J)-AG(K))*SPR(K)
  500 CONTINUE
      N=0
  201 N=N+1
      NA=2*(N-1)+3
      NB=NA+1
      READ(1'N)X(NA),X(NB)
      IF(X(NA)-9997.) 201,202,202
  202 NS=-1
      IR=1
      NN=2*(N-1)
      DO 204 N=3,NN
      NS=-NS
      TIM=X(N)-AGXKM
      IF(HFSPR-9900)503,504,504
  504 DO 521 L=1,JJ
      I=JJ-L+1
      AB=ABS(X(N))
      IF(AB-AG(I)) 521,520,520
  521 CONTINUE
      GO TO 204
  520 DIS=((AB-AG(I))*SPR(I)+CG(I))*10.
      IF(TIM)522,304,304
  522 Z=XKM-DIS
      GO TO 303
  503 DIS=TIM*HFSPR*10.
  304 Z=XKM+DIS
C        SIGN OF X(I) INDICATES A NORMAL (+), OR REVERSED (-)
C        MAGNETIZATION ABSOLUTE VALUE OF X(I) INDICATES ELEMENT
C        OF TOPO MATRIX AT WHICH REVERSAL IS TO TAKE PLACE
  303 IF(Z-XINFO(3)) 199,199,205
  199 IF(Z-XINFO(2)) 204,203,203
  203 IR=IR+1
```

```
      Z=(Z-XINFO(2))/TERV+1.5
      X(IR)=NS*Z
  204 CONTINUE
  205 IR=IR+1
C        1025 INDICATES END OF REVERSAL SEQUENCE
      X(IR)=4097.
      X(1)=-SIGN(1.,X(2))
      XSCAL=1./XINFO(15)
      CALL SCALF(XSCAL,1.,0.0,.8)
      I=0
  307 I=I+1
      IF(X(I)-4097.)3999,4000,4000
 3999 IX=ABS(X(I))
      X1=(IX-1)*TERV
      IF(I-1) 3802,3802,3801
 3801 CALL FPLOT( 2,X1,Y)
 3802 Y=SIGN(.2,X(I))
      CALL FPLOT(-2,X1,Y)
      GO TO 307
 4000 X1=LPT*TERV
      CALL FPLOT(2,X1,Y)
      CALL FPLOT(1,0.0,.8)
      RETURN
      END
```

```
C     SUBROUTINE LAM1(LPT,XINT,IHIGH,TERV,XGAM,X,ITOP,XINFO)
C        CHANGE SIGN OF ITOP ELEMENT WITH RESPECT TO
C        REVERSAL SEQUENCE

      SUBROUTINE LAM1(LPT,XINT,IHIGH,TERV,XGAM,X,ITOP,XINFO)
      DIMENSION XGAM(1),X(1),ITOP(1),XINFO(40)

      DEPTH=XINFO(11) /1000.
      IAL=LPT+40
      PI=3.1415926
      DO 4069 I=1,IAL
 4069 XGAM(I)=0.0
      I=0
      DO 4001 IR=2,LPT
      IX=ABS(X(IR))
      IT=X(IR-1)
 4004 IF(IX-I)4001,4001,4002
 4002 I=I+1
      ITOP(I)=ISIGN(ITOP(I),IT)
      IF(I-LPT)4004,4005,4005
 4001 CONTINUE
 4005 LA=XINFO(4)
      DO 5000 I=1,LA
      DO 4010 IT=1,LPT
      LTOP=IABS(ITOP(IT))
      IF(LTOP-I)4012,4011,4012
 4011 X(IT)=ISIGN(1,ITOP(IT))
      GO TO 4010
 4012 X(IT)=0.0
 4010 CONTINUE
```

```
C          LAST 40 ELEMENTS OF X SET EQUAL TO ZERO
      DO 273 M=1,40
      L=LPT+M
 273  X(L)=0.0
C          FOURIER TRANSFORM LAMINA,APPLY EARTH FILTER,
C          ADD TO TOTAL ANOMALY
      CALL RFFT(X,IAL)
      AL=I-1
      HIGH=IHIGH
      A=(AL*XINT+HIGH)/1000.
      B=A+DEPTH
      M=IAL/2
      WRITE(5,*)A,B,XINT,HIGH,DEPTH,AL
      DO 5009 N=1,M
      Q=N-1
      S=2.*Q*PI/(IAL*TERV)
      NR=2*N-1
      NI=2*N
      FILT=EXP(-A*S)-EXP(-B*S)
      XGAM(NR)=XGAM(NR)+X(NR)*FILT
 5009 XGAM(NI)=XGAM(NI)+X(NI)*FILT
 5000 CONTINUE
      RETURN
      END
```

```
C     SUBROUTINE TOP1(TERV,IHIGH, LOW,XINT,LPT,X,ITOP,XINFO)
      SUBROUTINE TOP1(TERV,IHIGH, LOW,XINT,LPT,X,ITOP,XINFO)
      DIMENSION GDIS(6),IM(6),XINFO(40),ITOP(1),X(1)
      COMMON M

      P2=XINFO(2)
      LIMIT=XINFO(3)*10
      IF(XINFO(8)) 171,170,170
  171 LIMIT=-XINFO(2)*10
      P2=-XINFO(3)
  170 L5=0
      P1=P2
      K=1
      J=0
      INTL=0
C          INTERPOLATION ROUTINE FOR TOPO
   20 I=0
      IF(INTL) 70,70,71
   71 GDS=GDIS(6)
      IMS=IM(6)
   70 READ(M,2)(GDIS(IZ),IM(IZ),IZ=1,6)
    2 FORMAT(' ',6(F7.1,I6))
C          INTERPOLATES TO (IAL-40) POINTS WITH INTERVAL =TERV
      IF(INTL)4,3,4
  3   DO 6 I=1,6
      IF(GDIS(I)-P1)6,5,8
  6   CONTINUE
      IMS=IM(I-1)
      GDS=GDIS(I-1)
      GO TO 70
```

```
  5    ITOP(K)=IM(I)
 17    K=K+1
       IF(LPT-K) 900,117,117
117    P2=P1+(K-1)*TERV
  8    INTL=1
 13    TES=GDIS(I)*10
       END=LIMIT-TES
       IF(P2-GDIS(I)) 12,10,4
  4    I=I+1
       IF(END)900,900,131
131    IF(I-6)13,13,20
 12    IF(I-1)78,78,113
113    GDS=GDIS(I-1)
       IMS=IM(I-1)
 78    G2=IMS+(P2-GDS)*(IM(I)-IMS)/(GDIS(I)-GDS)
       GO TO 30
 10    G2=IM(I)
 30    ITOP(K)=G2
       IF(I-6) 17,17,20
900    XKM=1/XINFO(15)
       YKM=1/XINFO(16)
       IF(XINFO(8)) 333,332,332
333    IHAL=LPT/2
       DO 173 I=1,IHAL
       K=ITOP(I)
       L=LPT-(I-1)
       ITOP(I)=ITOP(L)
173    ITOP(L)=K
C          REDUCTION OF ITOP TO LAMINA NUMBERS
C          FIND HIGHEST,LOWEST POINT OF TOPO
332    LOW=-10
       IHIGH=27000
       DO 559 I=1,LPT
       IF(ITOP(I)-IHIGH)558,558,557
558    IHIGH=ITOP(I)
557    IF(ITOP(I)-LOW)559,559,556
556    LOW=ITOP(I)
559    CONTINUE
C          TOPO PLOTTING ROUTINE
       LLOW=(LOW/1000+1)*1000
       Y5=-LLOW
       N1=XINFO(1)
       GO TO(800,800,906,800),N1
 800   CALL CHART(LLOW,XINFO)
 906   CALL SCALF(XKM,YKM,0.0,Y5)
       GO TO(875,914,914,875),N1
 875   L5=1
       X1=0.0
       DO 904 I=1,LPT
       X1=(I-1)*TERV
       Y=-ITOP(I)
       CALL FPLOT(-2,X1,Y)
 904   CONTINUE
 914   CALL FPLOT(1,0.,Y5)
       LA=XINFO(4)
       XINT=0.
       IF(LA.GT.1) XINT=(LOW-IHIGH)/(LA-1)
       X1=0.0
```

```
      Y=Y5
C           LAMINA PLOTTING ROUTINE
      DO 905 I=1,LPT
      X1=(I-1)*TERV
      GO TO(801,801,801,802),N1
  802 CALL FPLOT(-2,X1,Y)
      L5=1
  801 Z=ITOP(I)-IHIGH
      IF(LA-1)915,915,917
  915 ITOP(I)=1
      GO TO 918
  917 DIFF=LOW-IHIGH
      IF(Z-DIFF)920,930,920
  930 ITOP(I)=LA
      GO TO 918
  920 Y=Z/XINT+1.5
      ITOP(I)=Y
  918 Y=-IHIGH-(ITOP(I)-1)*XINT
      GO TO(905,905,905,804),N1
  804 CALL FPLOT(-2,X1,Y)
  905 CONTINUE
      CALL FPLOT(1,0.,Y5)
      RETURN
      END
```

ANOMALY AGES USED IN AGEKENT.DAT FILE

1	0.	7A	26.38	33R	80.17	M24	155.08
1R	0.73	8	26.86	34	84.00	M25	156.55
J	0.91	9	28.15	CEN	91.00	P26	158.01
2	1.66	10	29.73	M0	118.00	P27	158.37
2A	2.47	11	31.23	M1	122.25	P28	158.87
2AR	3.40	12	32.46	M2	123.03	P29	160.33
3	3.88	12R	32.90	M3	125.35	BSA	165.00
3R	4.77	13	35.29	M4	126.46	FIT	175.00
3A	5.35	15	37.24	M5	127.05		
3AR	5.89	16	38.10	M6	127.34		
4	6.70	17	39.53	M7	127.97		
4R	7.41	18	41.29	M8	128.60		
4A	7.90	18R	42.73	M9	129.43		
4AR	8.50	19	43.60	M10	130.19		
5	8.92	20	44.66	M1N	131.65		
5R	10.42	21	48.75	M11	133.03		
5A	11.55	22	51.95	M12	135.56		
5AA	12.83	23	53.88	M13	137.10		
5B	14.87	24	55.14	M14	138.30		
5C	16.22	25	58.64	M15	139.58		
5D	17.57	26	60.21	M16	141.85		
5E	18.56	27	63.03	M17	143.76		
6	19.35	28	64.29	M18	144.75		
6A	20.88	29	65.50	M19	146.44		
6AR	21.77	30	66.74	M20	148.33		
6B	22.57	31	68.52	M21	149.89		
6C	23.27	32	71.37	M22	152.53		
7	25.50	33	74.30	M23	154.15		